

Final Report on

Standardized Testing Program for Solid-State Hydrogen Storage Technologies

Contract Number: DEFC3602AL67619

Prepared for:

**Department of Energy
Office of Energy Efficiency &
Renewable Energy
Hydrogen & Fuel Cells Program**

**Dr. Ned T. Stetson
DOE Technology Development Manager
Washington, DC**

**Mr. Jesse Adams
DOE Project Officer
Golden, CO**

Prepared by:

**Michael A. Miller, Ph.D. &
Richard A. Page, Ph.D.
Southwest Research Institute®
6220 Culebra Road
San Antonio, Texas 78238-5166**

Teaming Member:

**Ovonic Hydrogen Systems LLC
2983 Waterview Drive
Rochester Hills, MI 48309**

July 30, 2012



Final Report on

Standardized Testing Program for Solid-State Hydrogen Storage Technologies

Contract Number: DEFC3602AL67619

Prepared for:

**Department of Energy
Office of Energy Efficiency &
Renewable Energy
Hydrogen & Fuel Cells Program**

**Dr. Ned T. Stetson
DOE Technology Development Manager
Washington, DC**

**Mr. Jesse Adams
DOE Project Officer
Golden, CO**

Prepared by:

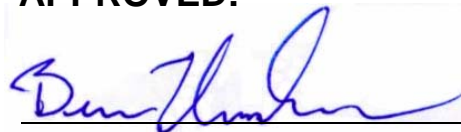
**Michael A. Miller, Ph.D. &
Richard A. Page, Ph.D.
Southwest Research Institute®
6220 Culebra Road
San Antonio, Texas 78238-5166**

Teaming Member:

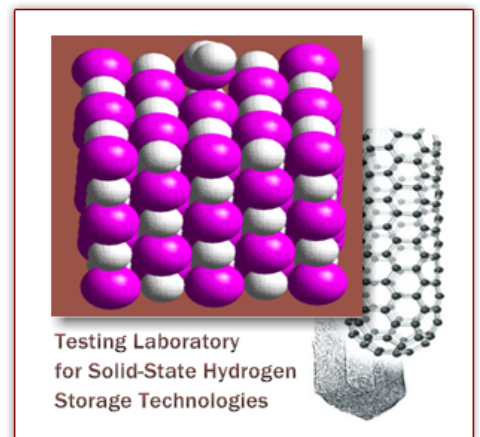
**Ovonic Hydrogen Systems LLC
2983 Waterview Drive
Rochester Hills, MI 48309**

July 30, 2012

APPROVED:



**Ben H. Thacker, Ph.D., Director
Department of Materials Engineering**



EXECUTIVE SUMMARY

Power generation systems based on fuel cells can play a central role in a hydrogen-based transportation infrastructure. In the US and abroad, major research and development initiatives toward establishing a hydrogen-based transportation infrastructure have been undertaken, encompassing key technological challenges in hydrogen production and delivery, fuel cells, and hydrogen storage. However, the principal obstacle to the implementation of a safe, low-pressure hydrogen fueling system for fuel-cell powered vehicles remains storage under conditions of near-ambient temperature and moderate pressure. New concepts and ideas must, therefore, be elicited from the science and engineering community to overcome this major stumbling block through basic and applied research.

The choices for viable hydrogen storage systems at the present time are limited to compressed gas storage tanks, cryogenic liquid hydrogen storage tanks, chemical hydrogen storage (*i.e.*, release of hydrogen from chemical compounds with subsequent on- or off-board regeneration), and hydrogen absorbed or adsorbed in a solid-state material (a.k.a. solid-state storage). More specifically, solid-state storage refers to the storage of hydrogen in materials such as metal hydrides, chemical hydrides, zeolites, and a host of emerging nano-engineered materials. While each of these enabling storage options has specific advantages and disadvantages, the solid-state systems may offer overriding benefits in terms of storage capacity, kinetics and, most importantly, safety.

From a practical viewpoint, on-board hydrogen storage systems are needed that allow a vehicle driving range greater than 300 miles, requiring the vehicle to store a range of 9 ± 4 kg of hydrogen. The potential that solid-state materials for hydrogen storage may one day meet these storage requirements, while also affording improved safety, for a hydrogen-based transportation infrastructure has led to significant interest and monetary investment among academic institutions, governmental agencies, and the commercial sector to accelerate development of materials and containment systems for the storage and delivery of hydrogen at low pressures and practical temperatures.

In the formative years of this endeavor, the fervor among the research community to develop novel storage materials had, in many instances, the unfortunate consequence of making

erroneous, if not wild, claims on the reported storage capacities achievable in such materials, to the extent that the potential viability of emerging materials was difficult to assess. This problem led to a widespread need to establish a capability to accurately and independently assess the storage behavior of a wide array of different classes of solid-state storage materials, employing qualified methods, thus allowing development efforts to focus on those materials that showed the most promise. However, standard guidelines, dedicated facilities, or certification programs specifically aimed at testing and assessing the performance, safety, and life cycle of these emergent materials had not been established.

To address the stated need, the U.S. Department of Energy (DOE), through a competitive solicitation, selected Southwest Research Institute[®] (SwRI) in March of 2002 to establish and operate a national-level research and testing facility to evaluate materials and complete systems that may be used to store hydrogen. Working with industry, academia, and the U.S. government, SwRI set out to develop an accepted set of evaluation standards and analytical methodologies. Under the directive of the DOE, the *Testing Laboratory for Solid-State Hydrogen Storage Technologies* (the Laboratory) was commissioned at SwRI as a focal point for evaluating new materials emerging from the designated Materials Centers of Excellence (MCoE) according to established and qualified standards. Additionally, the Laboratory sought to support parallel efforts underway within the international community, in Europe and Japan, to assess and validate the performance of related solid-state materials for hydrogen storage.

After conducting a thorough review of the current state-of-the-art in measurement equipment and procedures, SwRI designed and constructed laboratory facilities for the analysis of storage materials and full-scale storage systems. An array of analytical instrumentation was carefully selected and, in some cases, custom designed apparatuses were built for hydrogen sorption measurements and were integrated with a state-of-the-art laboratory facility. Critical measurements of hydrogen sorption properties in the Laboratory have been based on three analytical capabilities: 1) a high-pressure Sievert-type volumetric analyzer, modified to improve low-temperature isothermal analyses of physisorption materials and permit *in situ* mass spectroscopic analysis of the sample's gas space; 2) a static, high-pressure thermogravimetric analyzer employing an advanced magnetic suspension electro-balance, glove-box containment, and capillary interface for *in situ* mass spectroscopic analysis of the sample's gas space; and 3) a Laser-induced Thermal Desorption Mass Spectrometer (LTDMS) system for high thermal-resolution desorption and mechanistic analyses.

The Laboratory has adopted a "best practices" approach based on SOP-documented analytical methods to critically evaluate novel storage materials of potential impact to the sought-after storage goals. SOPs have been developed and made available to the storage

community for the submission of samples to the Laboratory, and the validation/qualification of the sorption properties of promising storage materials using the principal methods of analysis. These standards have been qualified based on the positive outcomes of Round-Robin Testing (RRT) exercises.

As a fully qualified laboratory under the purview of the DOE, the Laboratory has played an important role in down-selecting materials and systems that have emerged from the MCoEs and outside entities by:

- Conducting measurements using established protocols to derive performance metrics;
- Providing in-depth analysis and understanding of hydrogen physisorption and chemisorption mechanistic behavior;
- Determining and validating material and system storage capacities;
- Determining material and system kinetics (charging/discharging rates), thermodynamics, and cycle-life durability;
- Contributing to the testing requirements for codes and standards of full-scale systems;
- Providing listing and labeling services, as needed, for full-scale systems such as fire safety performance; and,
- Supporting parallel efforts underway within the international community, in Europe and Japan, to monitor research activities, and assess and validate the performance of related solid-state materials for hydrogen storage.

Promising classes of materials developed under the program for reversible on-board hydrogen storage have emerged from the MCoEs. Between 2005 and 2011, the Laboratory has critically analyzed a total of 46 different storage materials, 26 of these materials were submitted by the MCoEs (as DOE directives), while 20 were submitted by private organization not directly associated with the storage program. The salient results of these analyses can be summarized as follows:

1. Early in this program, pure and catalytically-doped single wall carbon nanotubes (SWNTs) were given highest priority for evaluation due to the need to resolve confounding data previously reported on the apparent storage capacities of these materials. The results provided by the Laboratory helped to guide DOE in focusing research and development efforts on the most promising materials, culminating in a decision not to invest additional resources on pure SWNTs as candidate materials for hydrogen storage. However, catalytically-doped SWNTs were shown to exhibit

potentially useful hydrogen binding interactions, meriting further exploration within the Hydrogen Sorption Center of Excellence (HSCoE).

2. Validated the reported uptake of hydrogen in alloy-doped SWNTs at room temperature via spillover effect, demonstrating 2.78 wt.% hydrogen uptake at 298 K based on LTDMS (desorption) analysis.
3. Established a benchmark for physisorption uptake in low-density, high surface area materials at low temperatures, and independently verified 7.5 wt.% hydrogen uptake in MOF-177 at 77 K (the highest uptake of any known material at that time).
4. Independently validated hydrogen spillover uptake (2.5 wt.%) in platinum-doped carbon-bridged IRMOF-8 (Pt/AC/BC/IRMOF-8) at 298 K, and elucidated stable binding sites for room temperature storage using LTDMS.
5. Validated record-setting hydrogen physisorption in non-crystalline porous polymer network (PPN) materials, demonstrating an uptake 8.5 wt.% at 77 K and 60 bar (the current record holder in gravimetric capacity at low temperature).

The Laboratory was established to ensure that the performance criteria of every element of its activities has conformed to the highest standards and has strived to achieve the most precise, sensitive, and accurate measurements in characterizing hydrogen storage materials and systems for the DOE, academia, and industry. Overall, these goals have been successfully achieved, but not without marked challenges.

As new materials have emerged with unique hydrogen sorption properties, so have new analytical challenges requiring that the previously-established methods be refined along the way. Therefore, continuous improvements to the methods and equipment, along with periodic RRT studies to re-qualify them over the lifetime of the program, have been important activities of the Laboratory and its partners. In fact, the RRT studies conducted in collaboration with the EU (NESSY) demonstrated that several external laboratories had profound and persistent errors in their measurements, most likely caused by improper techniques in calibrating instrumentation. Equally important was the development and qualification of new techniques, not ordinarily familiar to many laboratories, needed to probe the mechanistic features of hydrogen uptake in complex storage materials. The implementation of the LTDMS technique is an example of this need which has proved to be invaluable in confirming and resolving the occurrence of stable binding sites for hydrogen in materials, indicative of room temperature uptake via spillover.

In the search for novel forms of materials for physisorption storage, crystalline materials of well-defined pores and structural motifs have emerged with remarkably-high surface areas and gas storage capacities. MOF-177 has been established as an ideal material to use as a benchmark for hydrogen adsorption measurements owing to its high gravimetric (7.6 wt.%) and volumetric

(48 g/L) uptake capacity, its facile and highly reproducible synthesis, and its well-characterized crystalline structure in terms of atomic connectivity and chemical composition.

Along parallel developments, molecular building units engineered to form three-dimensional porous polymer networks (PPNs), which are completely amorphous, has led to the establishment of a new benchmark in gravimetric performance for hydrogen storage: 8.5 wt.% at 77 K and 60 bar. An important advantage that PPN materials appear to offer over MOFs lies in their remarkable thermal and chemical stability, which can be attributed to their entirely covalent bonding network.

The potential for quasi-chemisorptive strategies predicated on spillover in catalytically-doped nanostructures, such as catalytically-doped MOFs and carbon materials, has pointed to promising opportunities in meeting the DOE on-board storage targets. However, attainment of a broader than present mechanistic understanding of hydrogen spillover in these compounds warrants further pursuit so that rational designs for new materials with much improved kinetics can be synthesized and evaluated in the near future. In particular, open questions pertaining to the thermodynamic constraints and driving forces for spillover relative to the catalyst and substrate, and the nature of binding interactions between hydrogen and substrate (receptor) after dissociative spillover of dihydrogen, still demand definitive answers.

The Laboratory will continue to be available to the hydrogen as well as other gaseous fuel-storage R&D communities in forward years for as long as its operation can be self-supported or sustained by outside funding, or both. It will solicit opportunities to further assist the development and characterization of storage materials and full-scale systems under previously-qualified analytical standards. The near-term goals of the Laboratory for hydrogen storage technologies are to solicit its capabilities and expertise to commercial developers and to the Hydrogen Storage Engineering Center of Excellence (HSECoE), a DOE Center established in 2009 to bridge the gap between the materials research undertaken under the Hydrogen Storage Program and the significant engineering challenges associated with developing lower-pressure, materials-based, hydrogen storage systems for hydrogen fuel cell and internal combustion engine light-duty vehicles.

Complementing a hydrogen-based national infrastructure for transportation, the utilization of abundant domestic sources of natural gas (NG) is also an important component of a national energy plan that reduces the US's dependence on foreign oil. As the principal component of NG, methane is an abundant and currently low-cost fuel that when burned in an internal combustion engine emits less CO₂ per vehicle mile traveled than any other fossil fuel. Like hydrogen storage, the main barriers limiting broad use of NG as a fuel for light-duty passenger vehicles are the ability to store NG on-board safely, in sufficient quantities for a practical operating range, the

availability of economical storage systems relative to the total cost of the vehicle, and the lack of a wide-spread infrastructure of NG fueling stations. Recognizing this opportunity, the Laboratory will seek and solicit opportunities to address these technical challenges through government- and commercially-funded research programs to find and innovate highly porous materials suitable for the adsorptive storage of NG. It should be appreciated that many materials discoveries and physical insights presently applicable to NG adsorptive storage have emerged from DOE's Hydrogen Storage Program, including its complementary program focused on basic sciences. The knowledge base created as a consequence of the extraordinary focus and accomplishments of those programs will be leveraged to help leapfrog technological advancements to be made in adsorptive NG storage.

Drawing from the SwRI's experience in, and the lessons learned from, the development of solid-state materials and systems for on-board storage of hydrogen, it has become abundantly clear that the intrinsic properties of sorbent materials, and in particular that of framework sorbents, measured in the laboratory seldom scale with equal or similar performance at the system level owing to the impact that sorbent engineering - material compaction and, for example, heat-transfer additives - has on the volumetric- and gravimetric energy densities. Consequently, the development of sorbent materials for a storage system cannot be achieved as an insular effort, rather it must be approached at the system level in order to account for and develop a comprehensive understanding of all the engineering factors that collectively affect the net performance of the sorbent material. This system level view for sorbent development constitutes the principal motivation for re-purposing the Laboratory and exercising materials and system engineering to develop NG adsorption storage systems for vehicles.

ACKNOWLEDGEMENTS

Funding for this program was provided by the U.S. Department of Energy (DOE), Office of Energy Efficiency and Renewable Energy, Fuel Cell Technologies Program. The authors wish to acknowledge the contributions from the following advisors of the Hydrogen Storage Program:

Department of Energy:

Sunita Satyapal, Program Manager, Hydrogen & Fuel Cell Technologies Program, DOE Headquarters, Washington DC.

Ned Stetson, Hydrogen Storage Team Lead, Hydrogen & Fuel Cell Technologies Program, DOE Headquarters, Washington, DC.

Jesse Adams, Project Officer, Hydrogen & Fuel Cell Technologies Program, DOE Golden Field Office, Golden, CO.

George Thomas, Sandia National Laboratories (retired), on assignment to DOE Headquarters, Washington DC.

Carole Read, Technology Development Manager, Hydrogen & Fuel Cell Technologies Program, DOE Headquarters, Washington DC.

Robert C. Bowman, Jr., Senior R&D Staff Member, Energy & Engineering Sciences Directorate, Oak Ridge National Laboratory, Oak Ridge, TN.

USCAR Hydrogen Storage Tech Team:

Ford Motor Company –	Diamler-Chrysler Corp. –	Scott Jorgensen, General Motors
Andrea Sudik	Tarek Abdul-Baset	Walt Podolski,
Don Siegel	Scott Freeman	Argonne National Laboratory

CONTENTS

EXECUTIVE SUMMARY	III
ACKNOWLEDGEMENTS	I
1 INTRODUCTION	1-1
2 OVERVIEW OF MATERIALS FOR SOLID-STATE HYDROGEN STORAGE	2-1
2.1 Advances in Chemisorption Materials	2-3
2.2 Nano-Architectures for Hydrogen Physisorption	2-4
2.3 Future Trends in Materials Research	2-8
3 PROGRAM PURPOSE AND OBJECTIVES	3-1
4 INTERNATIONAL COLLABORATION	4-1
5 SUMMARY OF PROGRAM GOALS AND ACCOMPLISHMENTS	5-1
6 PROGRAM ACTIVITIES	6-1
6.1 Overview of Analytical Methods	6-1
6.2 Evaluation of Materials for Hydrogen Storage	6-1
6.2.1 Chemisorption Materials	6-2
6.2.2 Physisorption on Porous Materials	6-4
6.3 Analytical Instrumentation	6-7

6.3.1	Volumetric Analysis	6-7
6.3.2	Gravimetric Analysis	6-11
6.3.3	Laser-Induced Thermal Desorption Mass Spectrometry	6-14
6.4	Small-Scale Laboratory Facility	6-17
6.5	Full-Scale Laboratory Facility	6-22
6.6	Safety Analysis and Implementation	6-24
6.7	Standards Development for Laboratory Operations	6-25
7	SUMMARY AND HIGHLIGHTS OF MEASUREMENT RESULTS (2005-2011)	7-1
7.1	Overall Summary of Results	7-1
7.2	Highlight 1 – Validation of Hydrogen Sorption Capacities in Pure and Catalytically-Doped SWNTs	7-4
7.3	Highlight 2 – Establishment of Analytical and Material Benchmarks for Low-Density, High Surface-Area Storage Materials	7-4
7.4	Highlight 3 – Validation of Hydrogen Spillover Effects in Catalytically-Doped MOFs	7-8
7.5	Highlight 4 – Validation of Record-Setting Hydrogen Physisorption in Non-Crystalline Porous Polymer Network (PPN)	7-10
8	LESSONS LEARNED	8-1
9	PUBLICATIONS, CONFERENCE PRESENTATIONS, AND PATENTS	9-1
10	COLLABORATIONS (DOMESTIC)	10-1
11	PLANNED USE OF LABORATORY	11-1

12 CONCLUSIONS AND FUTURE DIRECTIONS	12-1
13 SWRI PROJECT TEAM	13-1
14 REFERENCES	14-1
Appendix A — (NESSY RRT)	A-1
Appendix B — (NREL REVIEW)	B-1
Appendix C — (BEOS & SLD MODEL)	C-1
Appendix D — (Standard Operating Procedures)	D-1

LIST OF TABLES

Table 1.1:	DOE-prescribed gravimetric and volumetric targets for system-basis storage and fill time of hydrogen on board vehicles (revised in 2009) [13].....	1-5
Table 5.1:	A chronological overview of program goals and accomplishments (2002-2012).	5-1
Table 7.1:	Summary of the hydrogen storage capacities determined by the Laboratory for prospective physisorption, spillover, and chemisorption (color-coded, respectively), including reference materials for RRT studies. The equilibrium pressure at which the peak capacity was observed is given in brackets. Measurement results of proprietary storage materials from private or commercial entities outside the DOE program are omitted.	7-3
Table 7.2:	Summary of high-pressure H ₂ adsorption measurements of MOF-177 (all values ± 1% SD).	7-7

LIST OF FIGURES

- Figure 1-1: Relationship between gravimetric and volumetric energy densities mapped-out for various hydrogen storage modalities as compared with gasoline and a Li ion battery. Drop lines indicate the impending targets set forth by DOE..... 1-3
- Figure 1-2: Formative organization of DOE's Hydrogen Storage Program..... 1-6
- Figure 2-1: Continuum of binding interactions between physisorption and chemisorption modalities. Region between 10 and 60 kJ/mol is most desirable for room temperature hydrogen storage. Inset – Potential energy diagram for molecular physisorption and chemisorption binding interactions. 2-2
- Figure 2-2: Hydrogen physisorption in various nanostructured carbon materials. Left panel – room temperature physisorption of SWNT and porous carbon. Right panel – comparison between low-temperature (77 K) and room temperature physisorption. 2-4
- Figure 2-3: Hydrogen storage on $Ti_{0.86}Al_{0.1}V_{0.04}$ catalyzed SWNTs and other carbon allotropes. Experimental findings indicate the emergence of a new high temperature adsorption site first observed by Dillon and Heben [30, 31] (left panel) and subsequently confirmed by Miller [29] (right panel) based upon thermal desorption mass spectrometry (a.k.a. TPD). Inset of right panel is an expanded scale of the analysis, showing a low-temperature peak for physisorbed hydrogen. 2-6

Figure 2-4:	Illustration of hydrogen spillover in a hypothetical heterostructure. Left - Dihydrogen is adsorbed on a metal nanoparticle (large blue sphere) where it undergoes dissociation on the surface. The chemisorbed atomic hydrogen migrates from the metal particle and spills over onto a receptor (substrate) structure, where then it is free to diffuse and bind to the receptor in ways that is not completely understood. Right – The spillover of dihydrogen is facilitated by engineering at nano-scale dimensions a catalyst support (AC) and bridging compound (light grey) between the supported metal particle and the substrate (in this case MOF).....	2-7
Figure 2-5:	Reaction coordinate for the spillover model, indicating kinetic barriers and thermodynamic starting and final states.	2-8
Figure 2-6:	Trends in synthetic strategies for quasi-chemisorption of hydrogen, past and present.....	2-9
Figure 4-1:	List of participating organizations and principal investigators (PI) for the NESSHY Program.	4-3
Figure 6-1:	a) An idealized representation of Pressure Concentration Temperature (PCT) isotherms for the \square solid solution phase and \square hydride phase. b) The enthalpy of hydride formation $\square H$ is obtained from the slope of a Van't Hoff plot of $\ln(P_{eq})$ as a function of $1/T$ [$\ln P_{eq} = (\square H/(RT))-\square S/R$]......	6-2
Figure 6-2:	Results of fitting Eq. 6.3 to adsorption isotherms of hydrogen on ultra-microporous carbon at 77 and 298 K.	6-6
Figure 6-3:	Isosteric heat of adsorption from Eq. 6.4 as a function of excess concentration.....	6-7
Figure 6-4:	Schematic of the high-pressure volumetric analyzer employed for determining excess sorption isotherms. Inset – Photograph of analyzer (blue), a Hy-Energy, Inc. Model PCT-Pro 2000 (Newark, CA), and high-pressure sample vessel (external components) coupled with a mass spectrometer (not shown) and UHP gas manifold.....	6-9

- Figure 6-5: An illustration of the step-wise procedure for measuring one point on a sorption curve. 6-10
- Figure 6-6: A schematic representation of the step-wise procedure for measuring a PCT curve. The equilibrium pressure is taken as $P(j)$ which may cause errors if the system has not reached equilibrium or if the duration of the first step in the procedure is too long. 6-10
- Figure 6-7: Schematic of high-pressure thermogravimetric apparatus (VTI, Inc., Model GHP) used for sorption measurements. Inset – Photograph of complete system integrated in a glove box (a magnetic suspension microbalance head positioned on top of glove box) and coupled with an external mass spectrometer (white box) via fused-silica glass capillary tubing and UHP gas manifold..... 6-13
- Figure 6-8: Diagram of LTDMS system for measurement of hydrogen chemi- and physisorption binding interactions. Top – Schematic of overall system including laser optics for illuminating sample. Bottom – Internal components for beam steering, sample containment, and heating or cooling. 6-16
- Figure 6-9: (a) Complete LTDMS system attached to an ultra-high purity gas manifold and electronic controls; (b) vacuum chamber, QMS analyzer, and laser driver; (c) optical bench for steering beam of laser through a variable density filter (VDF), acousto-optic tunable filter (AOTF), and collimating lenses before entering the sample vacuum chamber. 6-17
- Figure 6-10: Schematic of gas manifold for internal purification and delivery UHP hydrogen and helium to analytical stations..... 6-20
- Figure 6-11: PLC-based control and monitoring system for the Laboratory’s UHP gas manifold. Upper Left – Control and monitoring system for actuating electropneumatic valves (right) with manual override. Middle – Computer-based automated control, monitoring, and acquisition system. 6-21
- Figure 6-12: Sampling interfaces used to monitor the gas content of the manifold for purity. 6-21

Figure 6-13: Glove box (Ar) and associated evacuation station used to pre-condition and transfer sensitive samples to and from analytical stations.....	6-22
Figure 6-14: Laboratory facility for evaluating full-scale storage systems. Left – Top-view layout of laboratory showing locations of secondary containment bunker wells. Right – Image of laboratory showing primary and secondary containment systems. Storage system is contained inside the primary containment vessel.....	6-24
Figure 6-15: Overall scheme of laboratory operations: interactions, analyses under qualified standards, and reporting process.....	6-26
Figure 7-1: The relative performance of physisorption, spillover, and chemisorption (complex hydride) materials towards achieving the minimum material-based targets for on-board reversible fuel storage.....	7-2
Figure 7-2: (A) Molecular structure of 4,4',4''-benzene-1,3,5-triyl-tribenzoic acid (BTB) linker and (B) crystal structure of MOF-177. An approximately spherical pore is shown as large sphere of 17 Å in diameter. Reproduced from [71].	7-5
Figure 7-3: High-pressure H ₂ isotherms for MOF-177 taken by volumetric (A) and gravimetric (B) methods. As a reference, volumetric data is shown in (C). Filled and open symbols represent adsorption and desorption branch, respectively. Squares symbols are absolute adsorbed amounts. Inset: surface area dependency of H ₂ uptake.....	7-7
Figure 7-4: High-pressure gravimetric sorption isotherm measured for Pt/AC/BC/IRMOF-8 (from INER) at room temperature [46].	7-9
Figure 7-5: LTDMS profile measured for Pt/AC/BC/IRMOF-8 (from U. Mich.) at room temperature [46].	7-10
Figure 7-6: Room temperature (298 K) hydrogen isotherms measured for porous polymer network [PPN-4(Si)] using both the volumetric and gravimetric techniques.....	7-12

Figure 7-7: Low-temperature (77 K) hydrogen isotherms measured for porous polymer network [PPN-4(Si)] using the volumetric technique.....	7-12
Figure 11-1: Correlation between the absolute volumetric and gravimetric energy densities of stored methane at room temperature for a cross-section of current-generation framework sorbents at 35 and 55 bar. The ARPA-E system and material-basis targets are also indicated for comparison.....	11-3
Figure 11-2: Gravimetric energy density normalized by the specific surface area of the framework sorbent as a function of the isosteric heat of methane adsorption. A model trend line for prior-generation framework sorbents is shown to traverse the theoretically-ideal heat of adsorption. Further enhancements in gravimetric energy density are in store for the PCN-6X series MOFs by optimizing methane-framework binding interactions via chemical modifications of framework building units.....	11-4
Figure 11-3: Overview of Laboratory's planned use for development and characterization of materials and systems for fuel storage.....	11-5

1

INTRODUCTION

The inevitability of an early peak in fossil fuel reserves within the ensuing 50 years combined with global carbon emissions exceeding 6 Gt per year, two-thirds of which are emitted from vehicles and heating systems [1, 2], necessitates the adoption of clean and sustainable energy resources. Such resources are ultimately needed to circumvent the socio-economic impact of anthropogenic-induced climate change. As energy use grows with economic development, recent projections of global energy trends to the middle of the current century indicate that unabated energy consumption will demand four times the current level [3]. A growing consciousness for alternative and renewable forms of energy has thus shifted worldwide attention to assessing the potential viability of a hydrogen-based economy as a long-term solution.

Hydrogen as an energy carrier is arguably one alternative to replacing petroleum products for transportation and stationary applications, if it can be produced in large quantities by clean and renewable means. This notion is premised on the fact that molecular hydrogen possesses the largest amount of chemical energy per chemical bond ($142 \text{ MJ mol}^{-1} \text{ kg}^{-1}$), which is three times higher than hydrocarbons ($47 \text{ MJ mol}^{-1} \text{ kg}^{-1}$) [4]. Significant benefits can, therefore, be gained when the energy capacity of hydrogen is combined with more efficient forms of energy consumption for power generation. For example, the maximum efficiency of the internal combustion engine is limited by the Carnot-cycle efficiency of approximately 40 %, though in practical terms conversion from chemical to mechanical via thermal energy is only 25% at best. Alternatively, the direct process of electron transfer from hydrogen to oxygen in the electrochemical reaction of a fuel cell is not limited by the Carnot cycle, and such devices can attain efficiencies ranging 50 to 60 % with an enthalpy and free energy of combustion equal to -286 and $-237 \text{ kJ (mol H}_2\text{)}^{-1}$, respectively [4].

Considering the thermodynamic arguments given above, it is evident that power generation systems based on fuel cells can play a central role in a hydrogen-based transportation infrastructure. In the US and abroad, major research and development initiatives toward establishing a hydrogen-based transportation infrastructure have been started, encompassing key technological challenges in hydrogen production and delivery, fuel cells, and hydrogen storage [5]. However, on-board storage of hydrogen remains the greatest challenge facing the acceptance of hydrogen as an alternative fuel source for automotive propulsion of the future. New concepts and ideas must, therefore, be elicited from the science and engineering community to overcome this major stumbling block through basic and applied research.

From a practical viewpoint, on-board hydrogen storage systems are needed that allow a vehicle driving range greater than 300 miles, requiring the vehicle to store a range of 9 ± 4 kg of hydrogen. Current approaches include compressed hydrogen gas, cryogenic and liquid hydrogen, chemical hydrogen storage, and hydrogen absorbed or adsorbed in a solid-state material (a.k.a. solid-state storage). More specifically, solid-state storage refers to the storage of hydrogen in metal hydrides, nano-structured materials and in chemical storage materials.

To place these approaches into the proper perspective relative to the amount of energy each can accommodate at the current state of development, it is useful to map the relationship between their gravimetric and volumetric energy densities, and compare these with the current use of gasoline. As illustrated in Fig. 1.1, compressed hydrogen requires very high pressures (up to 700 bar) to achieve the storage targets set forth by the US Department of Energy (DOE) [5] and, at the stated pressures, places significant engineering challenges on the design of the containment vessel. While liquid hydrogen achieves these targets for various configurations of vessel design, the complexity of a cryogenic containment vessel may outweigh any benefits gained in energy density. On the other hand, solid-state storage materials based on metal hydrides (*e.g.*, TiH_2) or sodium alanate (NaAlH_4) exhibit high volumetric energy densities but fall short of the gravimetric target due to their weight. For many metal hydrides, the temperature required to remove hydrogen after absorption is typically too high for automotive applications [4]. If, however, light-weight solid-state materials can be developed so that high volumetric capacity is preserved and they can be desorbed at temperatures below 120°C , then such materials have a high potential of achieving the required targets, and would be intrinsically safer than either compressed or liquid hydrogen storage systems [5].

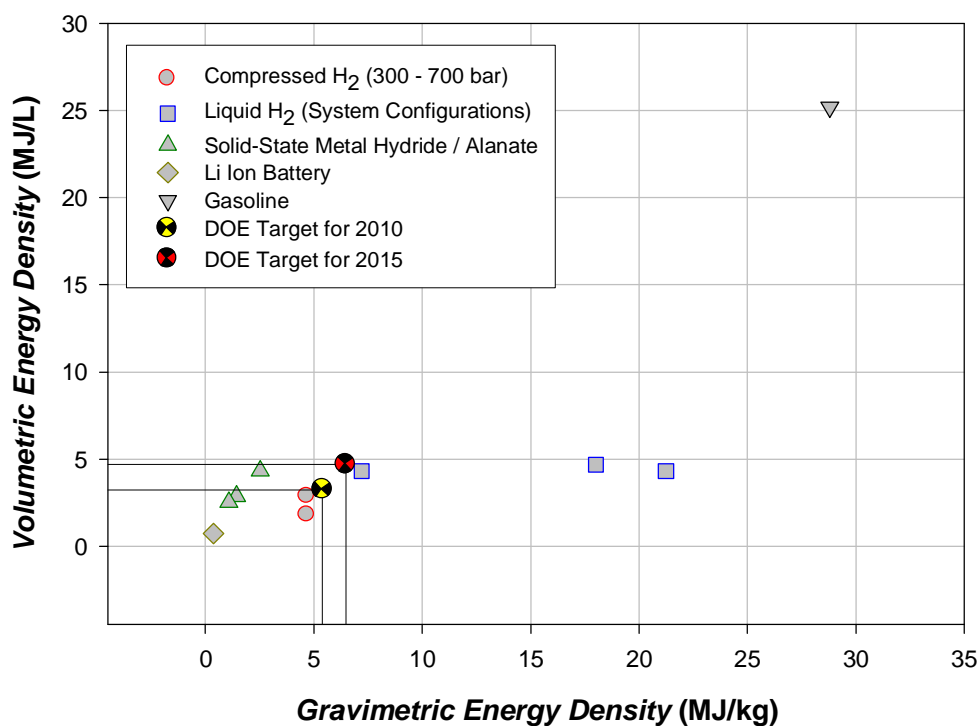


Figure 1-1: Relationship between gravimetric and volumetric energy densities mapped-out for various hydrogen storage modalities as compared with gasoline and a Li ion battery. Drop lines indicate the impending targets set forth by DOE.

The potential that solid-state materials for hydrogen storage may one day meet the storage capacity and safety requirements of a hydrogen-based transportation infrastructure has led to significant interest and monetary investment among academic institutions, governmental agencies, and the commercial sector to accelerate development of materials and containment systems for the storage and delivery of hydrogen at low pressures and practical temperatures. However, traditional materials discovery and development techniques have been slow to yield the necessary breakthroughs for practical utilization, particularly under the narrow thermodynamic and kinetic conditions required of automotive applications. Even the most advanced solid-state material systems to date fall slightly short of the 2017 DOE goal of 5.5 weight percent (wt.%) for vehicular hydrogen storage on a total storage-system basis; the materials basis for gravimetric storage would need to exceed ~8 wt%. In spite of the challenges, significant advancements in, for example, theory-driven design of materials are expected to

foster discoveries of new chemistries and structural motifs that may meet or surpass that goal in the near future if research initiatives are further cultivated.

Over the past decade, promising classes of materials developed and evaluated for hydrogen storage include catalyzed forms of complex hydrides, carbon nanostructures, and sub-nanostructured metal organic framework (MOF) and porous polymer networks (PPNs) [6-9]. Since the conclusion of the present program, new or enhanced structural entities with record-breaking gas sorption properties have been reported [9] and continue to be discovered at a rapid pace.

During the formative years of this endeavor, the fervor among the research community to develop novel storage materials had, in many instances, the unfortunate consequence of making erroneous, if not wild, claims on the reported storage capacities achievable in such materials. The storage capacities reported for many of these advanced materials were controversial and, in many instances, they had become the focus of considerable scrutiny among the scientific community [10, 11]. Despite numerous laboratories working on the development of similar materials, the analytical techniques and protocols employed had varied considerably. Consequently, the measurement results reported in the literature and elsewhere had varied to the extent that the potential viability of emerging materials had been difficult to assess. This problem led to a widespread need to establish a capability to accurately and independently assess the sorption behavior of a wide array of different classes of solid-state storage materials, employing qualified methods, thus allowing development efforts to focus on those materials that showed the most promise. However, standard guidelines, dedicated facilities, or certification programs specifically aimed at testing and assessing the performance, safety, and life cycle of these emergent materials had not been established.

To address the stated need, the U.S. Department of Energy (DOE) selected Southwest Research Institute[®] (SwRI) in March of 2002 to establish and operate a national-level research and testing facility to evaluate materials and complete systems that may be used to store hydrogen [12]. The outcome of independent evaluations would enable hydrogen storage researchers across the nation and the DOE to focus their efforts on those materials that demonstrate the highest potential toward meeting the performance targets required for on-board hydrogen fuel storage in vehicles powered by polymer electrolyte membrane (PEM) fuel cells. For the purpose of comparison, the most contemporary rendition of those targets is summarized in Table 1.

Table 1.1: DOE-prescribed gravimetric and volumetric targets for system-basis storage and fill time of hydrogen on board vehicles (revised in 2009) [13].

Storage Target	Gravimetric Capacity kWh/kg (kg H ₂ /kg system) [wt.% system basis] [†]	Volumetric Capacity kWh/L (kg H ₂ /L system)	System Fill Time for 5 kg H ₂ Store (min)
2010	1.5 (0.045) [4.3]	0.9 (0.028)	4.2
2017	1.8 (0.055) [5.2]	1.3 (0.040)	3.3
Ultimate Fleet	2.5 (0.075) [7.0]	2.3 (0.070)	2.5

[†]Defined as (H₂ wt.) / (H₂ wt + System wt.) * 100

Working with industry, academia, and the U.S. government, SwRI set out to develop an accepted set of evaluation standards and analytical methodologies. Under the directive of the DOE, the *Testing Laboratory for Solid-State Hydrogen Storage Technologies* was commissioned at SwRI [12] as a focal point for evaluating new materials emerging from the designated Materials Centers of Excellence (MCoE) according to established and qualified standards (Fig. 1.2). Additionally, the Laboratory sought to support parallel efforts underway within the international community, in Europe and Japan, to assess and validate the performance of related solid-state materials for hydrogen storage.

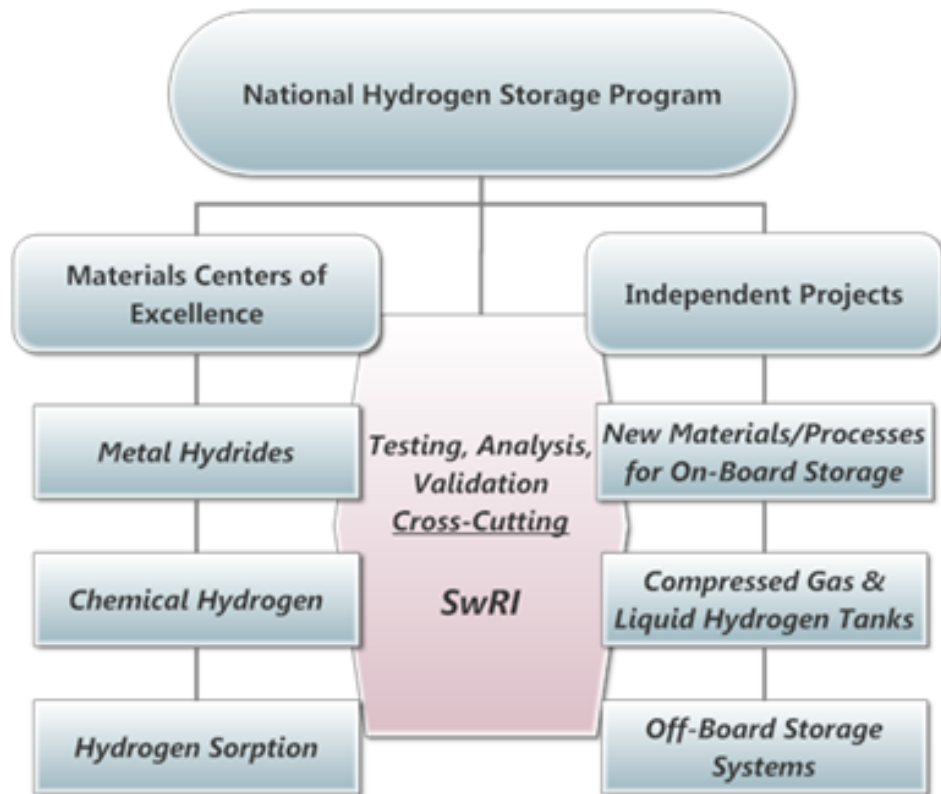


Figure 1-2: Formative organization of DOE's Hydrogen Storage Program.

2

OVERVIEW OF MATERIALS FOR SOLID-STATE HYDROGEN STORAGE

Many transition elements form metallic (interstitial) hydrides, in which hydrogen atoms occupy the interstices of the metal's crystal structure to within the covalent radii of hydrogen molecules. Thus, such hydrides are not compounds but gas-solid solutions. Early development of low-pressure hydrogen storage systems for fuel-cell automotive applications included metallic (interstitial) hydrides as the storage package for molecular hydrogen. While it is true that metals, such as palladium and niobium, and many alloys, such as LaNi_5 , are capable of storing significant quantities of hydrogen (2 – 5 wt.%), research over the past 20 years has revealed some potential problems of a practical nature with these storage technologies. The most difficult problems to overcome are that the most efficient metallic hydrides are expensive, heavy, and bind hydrogen so tightly that the temperature required to desorb it is impractical for most applications [14]; effectively, they are non-reversible when constrained by the thermodynamic regime of a fuel-cell powered vehicle application. These limitations were sufficient cause to halt federal government funding of metallic hydride research in 1996.

Among the various classes of storage materials studied thus far, those in which hydrogen uptake occurs at nearly the same temperature and pressure as hydrogen release are the most practical for on-board storage. Such *reversible* chemistries must be distinguished from those that are not reversible and would require reprocessing of the spent material (*i.e.*, dehydrided) off-board the vehicle storage system. For example, the $\text{Mg}(\text{BH}_4)_2$ and LiBH_4 have theoretical hydrogen capacities of 14.9 and 18.5 wt.%, respectively, but such salts exhibit dehydriding enthalpies of the order 53 kJ/mol (endothermic), and would require an energy-intensive process off-board the storage system to regenerate the spent products (Mg or Li, and B) [15].

A convenient scale for categorizing solid-state materials that exhibit a propensity to absorb hydrogen from the gas phase is to consider the potential-energy barriers associated with binding interactions between hydrogen atoms or molecules and the active constituents of the storage material, as illustrated in Fig. 1.3. While definitive lines tend to be drawn between non-dissociative physisorption of molecular hydrogen and dissociative chemisorption of atomic hydrogen leading to the formation of chemical bonds (covalent or metallic), there is in principle a continuum of binding interactions possible between these two modalities [16].

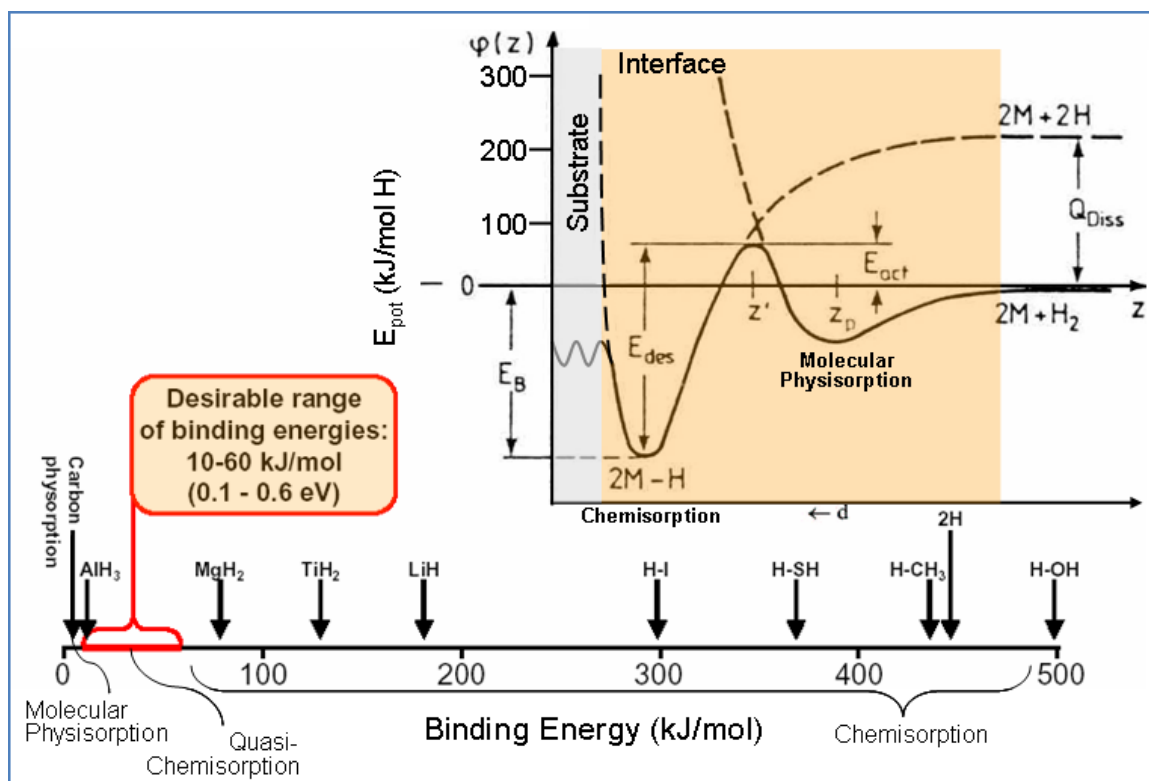


Figure 2-1: Continuum of binding interactions between physisorption and chemisorption modalities. Region between 10 and 60 kJ/mol is most desirable for room temperature hydrogen storage. Inset – Potential energy diagram for molecular physisorption and chemisorption binding interactions.

In porous solids, for example, hydrogen is physisorbed by van der Waals forces between the hydrogen molecule and the surface of the media (shallow potential well in Fig. 2.1). These binding forces are weak (4 kJ/mol at 77 K), and hydrogen physisorption usually takes place at low temperatures. However, the process is non-activated, reversible, and offers fast kinetics of gas uptake and release. To maximize gas uptake, materials with high specific surface area have been commonly used for physisorption of hydrogen and other gases. Since surface area is qualitatively proportional to gas uptake, molecular-scale engineering of crystalline frameworks, such as MOFs, has been rigorously employed to design and synthesize novel storage materials from a vast selection of readily assembled building units [17-24]. The rapidly growing field of

MOF chemistry has enabled a successful strategy for developing highly porous physisorption materials of extraordinary, if not record-setting, surface areas with well defined, ordered, pore spaces. They have been shown to selectively accommodate a high capacity of hydrogen molecules reversibly, though so far only at low temperatures.

The potential for “tuning” material chemistries and structural motifs so that binding interactions for molecular or atomic hydrogen fall in an appropriate region of the energy continuum has been one of the fundamental strategies addressed by many researchers. In the case of porous materials for the storage of molecular hydrogen via physisorption, it is now evident that two strategies – optimization of binding interactions and engineering of optimized structural motifs – are both necessary to achieve the volumetric and gravimetric targets for on-board storage of hydrogen. At or near room temperature, the desirable range for the binding energy of hydrogen, regardless of modality, is between 10 and 60 kJ/mol as noted in Fig. 2.1.

As noted earlier, the binding energies associated with traditional chemisorption materials (*e.g.*, metal hydrides) have been too high for practical use in on-board storage systems, and the kinetics for releasing hydrogen fuel from these materials has been too slow. However, new strategies have been developed for reducing the kinetic barriers limiting the transport of atomic hydrogen within the metallic matrix of these materials (represented by the grey region of Fig. 2.1). In doing so, the temperatures for desorption have been concurrently reduced to near-practical ranges.

Early progress toward overcoming the limitations of conventional materials for hydrogen storage is highlighted below in what can be considered the genesis of advanced storage materials based on either chemisorption or physisorption binding mechanisms. It can be argued that these important discoveries provided the motivation and direction for much of the materials research carried out by the established MCoEs during the course of the Hydrogen Storage Program. Promising materials that emerged from that effort, in turn, led to the Laboratory having to address significant challenges in making accurate measurements for validation.

2.1 Advances in Chemisorption Materials

Significant strides toward improving storage capacity and kinetics have occurred along parallel fronts with the development of new materials and the catalyzation of existing ones. Addition of a catalyst as a homogenous chemical constituent of, or heterogeneous dopant in, the storage material’s matrix is a common denominator across various forms of candidate material technologies, most notably for chemisorptions materials. For example, the seminal investigation by Bogdanovic and Schwickardi [25] led to the identification of a new class of alkali metal hydride that, when doped with a catalyst such as TiCl, significantly enhances the kinetics of

molecular hydrogen desorption and renders the dehydriding process reversible under moderate conditions. These catalytically enhanced hydride materials, based on aluminum hydride (AlH_4^-) and any Group 1 or 2 metal (Na, Li, Mg), are light-weight, store upwards of 5% H_2 by mass [26], and release it below 200 °C, thereby overcoming the limitations of conventional metallic (interstitial) hydrides. The thermodynamic regime within which a few of these materials perform is suitable for automotive applications. However, the kinetics for the absorption and desorption reactions are still slow compared with metallic hydrides.

2.2 Nano-Architectures for Hydrogen Physisorption

Along similar lines as the observations by Bogdanovic and Schwickardi, notable gains in storage capacities have been realized with the advent of catalyzed or doped nano-scale materials for physisorption [27]. As the single most important material of recent times with the potential for commodity availability, single wall carbon nanotubes (SWNTs) were hypothesized to exhibit intrinsic hydrogen storage capacities approaching the chemisorption theoretical limit of approximately 8 wt.% [28]. However, no experimental evidence has emerged to date in support of such high intrinsic capacities for purified forms of SWNTs alone. In fact, Miller *et al.* [29] showed that physisorption uptake of hydrogen in various forms of SWNTs at 298 K typically approaches a limit of 0.5 wt.% at high pressures (80 bar) and approximately 5 wt.% at 77 K (Fig. 2.2).

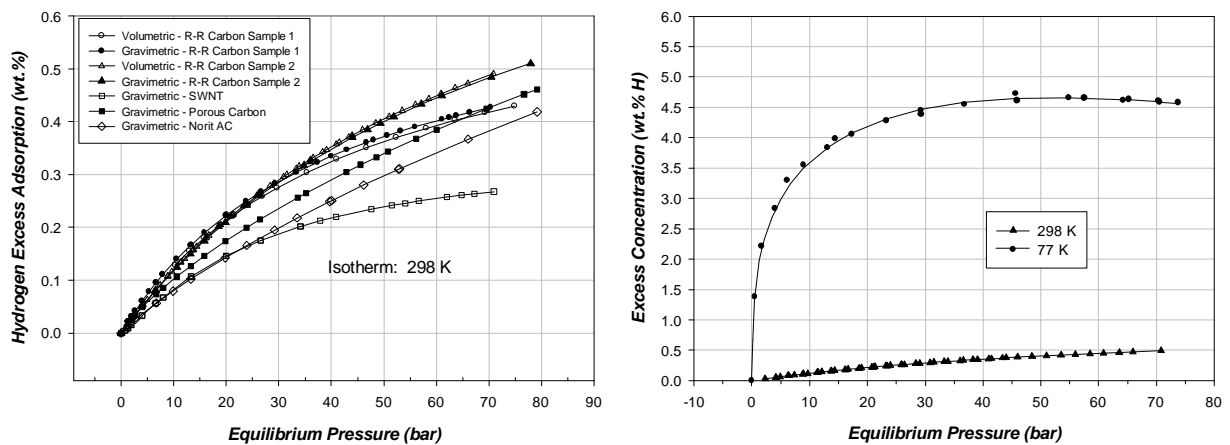


Figure 2-2: Hydrogen physisorption in various nanostructured carbon materials. Left panel – room temperature physisorption of SWNT and porous carbon. Right panel – comparison between low-temperature (77 K) and room temperature physisorption.

For catalyzed forms of SWNTs, wherein SWNTs are doped with a catalytic metal clusters such as Ti or $\text{Ti}_{0.86}\text{Al}_{0.1}\text{V}_{0.04}$ alloy, the landmark, albeit controversial, experimental investigations reported by Dillon and Heben *et al.* [30, 31], among others, suggested that storage capacities approaching the chemisorption theoretical limit can be realized at room temperature. These capacities were also shown to exceed the amount of hydrogen uptake that can be accounted by the metal dopant alone (2.5 wt.%).

Thermal desorption mass spectrometry measurements indicated that doped SWNTs form a high-temperature adsorption site not otherwise observed in SWNTs alone. As depicted in Fig. 2.3, Miller *et al.* [29] also observed a high-temperature adsorption site for $\text{Ti}_{0.86}\text{Al}_{0.1}\text{V}_{0.04}$ catalyzed SWNTs as determined by thermal desorption mass spectrometry, which compared favorably with the results of Dillon and Heben.

A plausible, though speculative, mechanism that may conveniently explain the enhanced hydrogen uptake in catalyzed SWNTs is one borrowed from the mature field of heterogeneous catalysis dealing with supported metal catalysts for hydrogenation. It has long been known that supported metal catalysts, such as Pt or Pd finely dispersed on metal oxides (*e.g.*, Al_2O_3 , WO_3) or carbon supports used in the hydrogenation reactions of organic molecules, reversibly activate the dissociation of molecular hydrogen on the surface of the metal crystallite to yield atomic hydrogen chemically bound to the surface atoms. The desired hydrogenation reaction occurs as these weakly bound hydrogen atoms migrate on the surface and collide with a surface-adsorbed chemical species. Augmenting this mechanism, Khoobiar [32] first reported an additional phenomenon in which hydrogen “spills over” from the catalyst particle to the support through a process of surface interphase migration. Sermon [33] subsequently labeled this hypothetical process for supported metal catalysts as “spillover,” and its mechanism still remains to be properly elucidated. Hydrogen spillover on carbon supports has been experimentally validated via advances in incoherent inelastic neutron scattering (INS) [34].

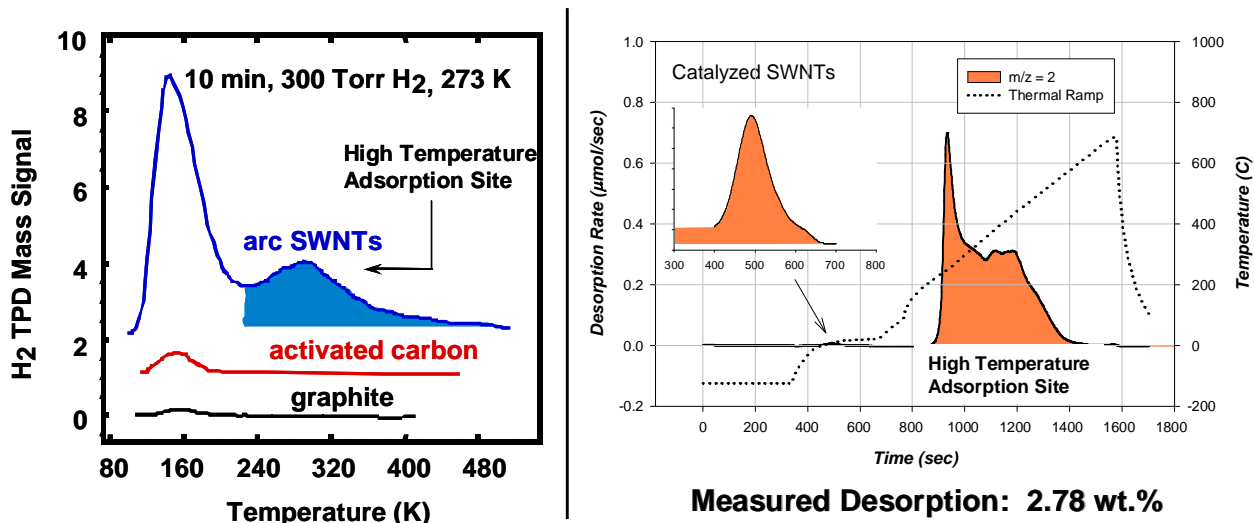


Figure 2-3: Hydrogen storage on $Ti_{0.86}Al_{0.1}V_{0.04}$ catalyzed SWNTs and other carbon allotropes. Experimental findings indicate the emergence of a new high temperature adsorption site first observed by Dillon and Heben [30, 31] (left panel) and subsequently confirmed by Miller [29] (right panel) based upon thermal desorption mass spectrometry (a.k.a. TPD). Inset of right panel is an expanded scale of the analysis, showing a low-temperature peak for physisorbed hydrogen.

Hydrogen spillover can be qualitatively defined as the dissociative chemisorption of hydrogen on metal nanoparticles, and subsequent migration of hydrogen atoms onto adjacent surfaces of a receptor via spillover and surface diffusion [35-37]. Evidence of atomic hydrogen spillover has been observed and reviewed in many studies [38-44]. A stylized representation of the postulated mechanism for spillover is illustrated in Fig. 2.4.

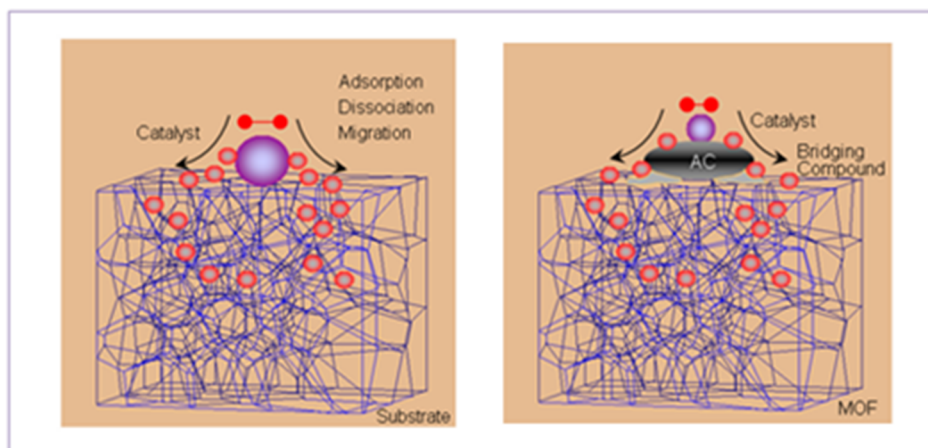


Figure 2-4: Illustration of hydrogen spillover in a hypothetical heterostructure. Left - Dihydrogen is adsorbed on a metal nanoparticle (large blue sphere) where it undergoes dissociation on the surface. The chemisorbed atomic hydrogen migrates from the metal particle and spills over onto a receptor (substrate) structure, where then it is free to diffuse and bind to the receptor in ways that is not completely understood. Right – The spillover of dihydrogen is facilitated by engineering at nano-scale dimensions a catalyst support (AC) and bridging compound (light grey) between the supported metal particle and the substrate (in this case MOF).

The thermodynamic consequences of hydrogen spillover must, however, be carefully considered. A qualitative model to explain mechanistically what is experimentally observed is illustrated in Fig. 2.5. From this model, one can immediately arrive at the central paradox of hydrogen spillover theory: *Is hydrogen spillover, followed by binding of atomic hydrogen to the receptor, thermodynamically plausible in light of an endothermic dissociation barrier?*

This important question stems from the fact that the impeding barrier in the reaction coordinate for the spillover model is the dissociation of molecular hydrogen (4.52 eV). Unless there exist final states – binding configurations of atomic hydrogen with the receptor – lower in energy than the energy state of the starting point (molecular hydrogen), hydrogen spillover would be thermodynamically improbable. To illustrate this point, the spillover model shown in Fig. 2.5 is from a chemist's perspective based upon a classical reaction coordinate diagram.

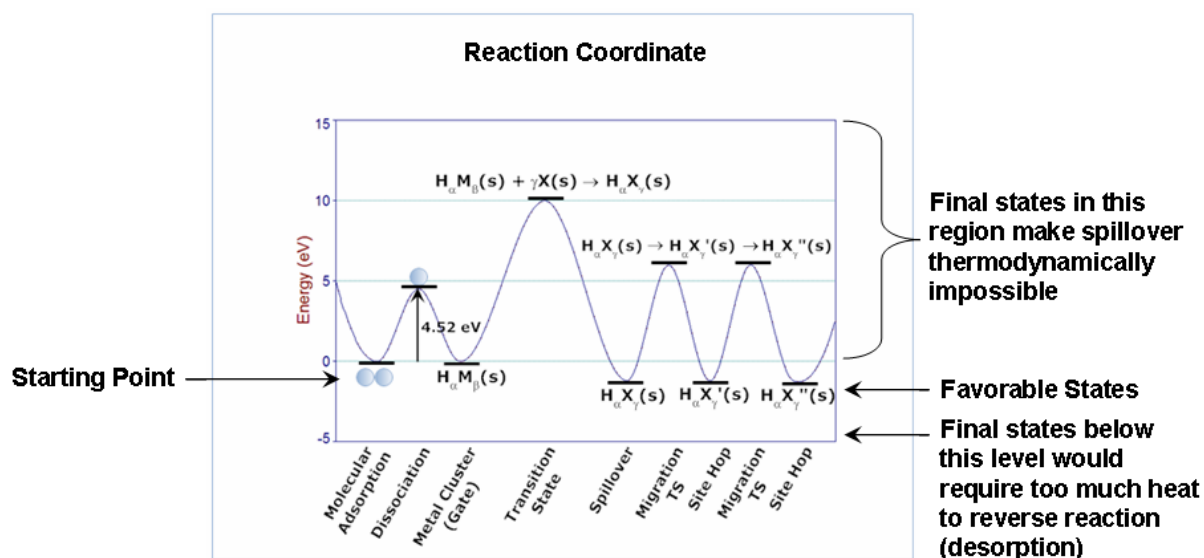


Figure 2-5: Reaction coordinate for the spillover model, indicating kinetic barriers and thermodynamic starting and final states.

The compelling question about what configurations of chemisorbed hydrogen are energetically favorable (Fig. 2.5) was addressed by Lin *et al.* [45] for the structurally simple and, hence, computationally tenable model of metal-doped graphene. *Ab initio* methods showed that, although single hydrogen binding to graphene is quite weak (upper-right region in Fig. 2.1), clusters of hydrogenated graphene that form spatially-separated islands of fully hydrogenated hexagons yield energetically favorable phase configurations.

In the case of MOF-based spillover materials, the organic linkers in MOF heterostructures, in many cases consisting of fused- or unfused aromatic rings, are hypothesized to play the role of receptor sites for hydrogenation, which occur over all three dimensions of these framework materials. It has been shown via *ab initio* calculations that thermodynamically favorable configurations of the hydrogenated linkers do arise following addition of spilt-over hydrogen atoms [46].

2.3 Future Trends in Materials Research

Major breakthroughs in materials suitable for room temperature storage of hydrogen will capitalize on engineering architectures in which the binding energies for molecular hydrogen reside somewhere between physisorption and chemisorption interactions; *i.e.*, 0.1 to 0.6 eV/H₂. This range is defined from this point forward as the “quasi-chemisorption” regime.

A trend has emerged in recent times toward the design of chemical architectures for reversible hydrogen sorption in the quasi-chemisorption regime that is modeled after the Kubas dihydrogen complex originally conceived by Kubas *et al.* [47] in 1984. In such complexes as illustrated in Fig. 2.6, hydrogen is bound to a coordinated metal atom ($M = W, Mo$) specifically through bonding ($H_2 \sigma \rightarrow M$, empty d) and antibonding orbitals (M , filled $d \rightarrow H_2 \sigma^*$) of the metal atom and molecular hydrogen; otherwise known as *metal* $\rightarrow H_2 \sigma^*$ *back-bonding*. The formation of stable coordination compounds of this kind is facilitated by molecular orbitals and spatial curvature in the complex, thus promoting covalent bonding interactions that would otherwise have inadequate orbital overlap. This fundamentally important area of chemistry has evolved into theoretically-postulated Kubas-like atomic coordination complexes in which carbon nanostructures, such as C_{60} fullerenes, are modified with atomically-coordinated hypervalent complexes of various transition metals. Zhao *et al.* [48] has proposed nano-architectures of this kind as potential materials for hydrogen storage, theoretically predicted to evince binding energies in the quasi-chemisorption regime and a storage capacity of 7 wt.% at room temperature.

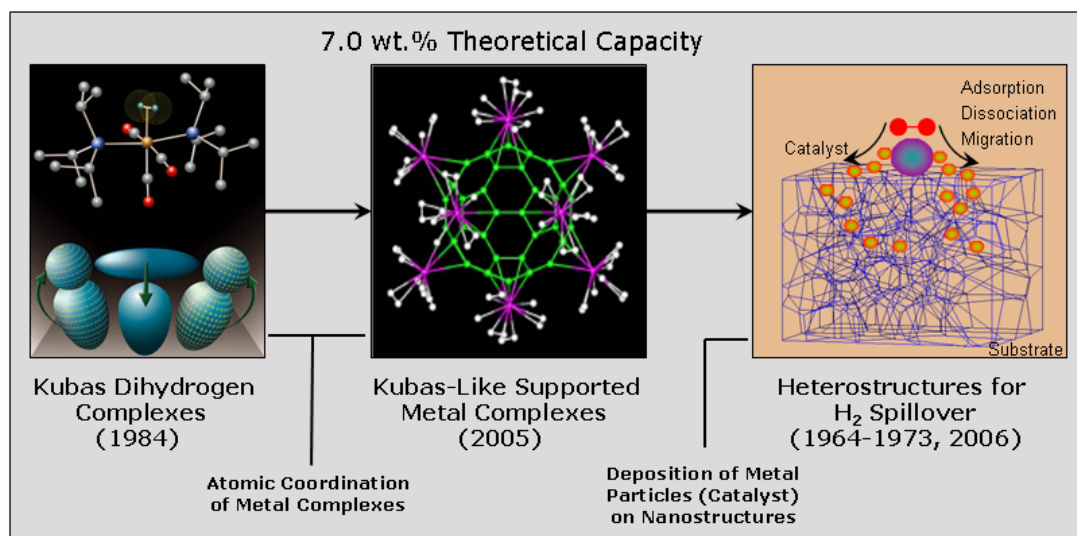


Figure 2-6: Trends in synthetic strategies for quasi-chemisorption of hydrogen, past and present.

These synthetic strategies of current interest being pursued by several investigators of Kubas-like supported metal complexes [49, 50] address an interesting and aesthetic area of chemistry that deserves further thought and experimental validation. However, the fact remains that synthesis of such architectures will be extremely challenging, if not impossible, as thermodynamic and kinetic barriers associated with the reaction coordinate leading to the final structures are brought into question.

An alternative strategy to achieving reversible hydrogen sorption in the quasi-chemisorption energy regime is spillover of atomic hydrogen from a metal particle onto a support having an appropriately scaled binding capacity. The origin of this strategy can be ascribed to the work of Khoobiar and Sermon [32, 33] as previously mentioned. Since the use of particles or clusters do not require atomic coordination or stable covalent bonding structures, well-established precipitation or physical vapor deposition techniques can be employed to prepare the desired heterostructure with sufficient control of geometric features.

Li and Yang [51] showed that isoreticular metal organic frameworks (IRMOF), namely IRMOF-8, doped with a platinum-particle catalyst supported on activated carbon (AC) can undergo hydrogen spillover at room temperature, and further enhancement can be achieved by bridging the supported catalyst to the framework with a carbonized disaccharide (glucose) compound. While the kinetics for hydrogen uptake via spillover has been shown to be exceedingly slow, though reversible, in such architectures, linear isotherms have been measured at room temperature up to 4 wt.% at 100 bar. Miller *et al.* [52] has further shown from laser-induced thermal desorption mass spectrometry experiments that multiple types of binding sites are formed following spillover in these heterostructures at room temperature.

3

PROGRAM PURPOSE AND OBJECTIVES

This program addressed the fundamental need for establishing and operating a national-level reference laboratory whose core mission has been to study and independently verify the intrinsic sorption characteristics of novel and emerging materials for hydrogen storage, including such activities as they pertain to their use in full-scale storage systems. As a fully qualified laboratory under the purview of the DOE, the laboratory has played a central role in down-selecting materials and systems that have emerged from the MCoE and outside entities by:

- Conducting measurements using established protocols to derive performance metrics;
- Providing in-depth analysis and understanding of hydrogen physisorption and chemisorption mechanistic behavior;
- Determining and validating material and system storage capacities;
- Determining material and system kinetics (charging/discharging rates), thermodynamics, and cycle-life durability;
- Contributing to the testing requirements for codes and standards of full-scale systems;
- Providing listing and labeling services, as needed, for full-scale systems such as fire safety performance; and,
- Supporting parallel efforts underway within the international community, in Europe and Japan, to monitor research activities, and assess and validate the performance of related solid-state materials for hydrogen storage.

4

INTERNATIONAL COLLABORATION

An important element of the Laboratory's role, as noted above, was to establish a collaborative relationship with the international community and monitor therein research activities pertaining to the emergence of advanced hydrogen storage materials and measurement techniques. The Laboratory would then support parallel efforts underway outside the US to develop measurement standards, participate in Round-Robin testing of different classes of advanced solid-state hydrogen storage materials under those standards, help validate the performance of promising materials, and collaborate with premier institutions to help answer questions of a fundamental nature.

In 2002, the European Community (EC) Sixth Framework Programme was approved by the European Parliament to create technical centers that would address specific research and technological developments principally related to sustainable development, global change and ecosystems, and sustainable energy systems. Through interactions and discussions with EC representatives of the Programme, and with the concurrence of the DOE, SwRI was invited to contribute to a proposal (EC Proposal No. 518271) that would establish a consortium project under the Programme entitled "Novel Efficient Solid Storage for Hydrogen (NESSHY)." The proposed project was awarded in 2005.

The objectives of this international consortium project is best captured verbatim from the text of the original proposal: "*NESSHY aspires to develop novel materials, storage methods and fabrication processes that provide the energy density and the charge/discharge storage/restitution rates necessary for mobile applications with spin-offs in stationary systems. The final aim of the project is to identify the most promising solid storage solutions for such applications. The envisaged objectives cover porous storage systems, regenerative hydrogen stores (such as the borohydrides) and solid hydrides having reversible hydrogen storage and improved gravimetric storage performance. Initially, two categories of reversible stores will be investigated – light/complex hydrides, such as alanates and imides, and intermetallic systems involving magnesium, although further categories may be included later. In all cases, the performance of different systems will be compared by a standards laboratory (working in collaboration with the US DoE standardisation activity). Further, efforts will be made to understand the mechanisms involved by innovative modelling activities. When promising new materials are identified, industrial and R&D collaborators will be brought in to upscale the material production, develop appropriate demonstration storage tanks and test out the prototype stores in practical conditions.*"

A holistic multidisciplinary approach was adopted by NESSHY, paralleling the goals of the US Hydrogen Storage “Grand Challenge” Program in many respects. It addressed key issues related to hydrogen storage in solid materials, such as the discovery of new materials, the development of novel analytical and characterization tools and measurement techniques, storage methods and fabrication processes, and first principles and phenomenological modeling.

A consortium of 22 different participant organizations comprised NESSHY, including organizations in member countries of the International Partnership for Hydrogen and Fuel Cells in the Economy (IPHE), of which SwRI was the only US entity. A complete list of the participant organizations is provided in Table 4.1.

Beyond monitoring the scientific progress made within the NESSHY program toward the discovery of advanced solid-state storage materials, the Laboratory was directly engaged with NESSHY partners on three technical endeavors requiring critical measurements: a) Round-Robin testing (RRT) of a nano-porous carbon material based on hydrogen physisorption measurements; b) Round-Robin testing of a sodium alanate (NaAlH_4) material based on hydrogen chemisorption measurements; and c) elucidating the fundamental mechanism underlying the purported hydrogen spillover effects in metal-doped carbon foam (graphite oxide) and IRMOF-8 storage materials.

The RRT studies were each coordinated through the European Commission – Joint Research Center (Dr. Pietro Moretto), and an advisory committee consisting of P. Moretto (EC-JRC), M. Fichtner (FZK), B. Dogal (GKSS), O. Gutfleisch (IFW), and M.A. Miller (SwRI) was established to design and plan the RRT study. The EC-JRC was responsible for coordinating the studies, obtaining homogeneous, batch lots of test materials (samples), and distributing random portions of the test materials to the participating laboratories, which were selected from the NESSHY consortium including SwRI.

The principal objectives of the RRT exercise were to assess whether the performance parameters of novel hydrogen storage materials as measured in different laboratories were comparable, identify possible weaknesses in measurement steps, develop best practices guidelines, and provide recommendations for optimizing the measurement techniques and procedures. The final reports summarizing the outcomes for each of the two RRT studies are provided in Appendix A of this report.

Figure 4-1: List of participating organizations and principal investigators (PI) for the NESSHY Program.

No.	Organization / PI	ID	Country
1	University of Salford Dr Ian Morrison Joule Physics Laboratory and Institute for Materials Research	USAL	UK
2	Air Liquide Jerome PERRIN Claude-Delorme Research Center	Air Liquide	France
3	European Commission – Joint Research Centre Pietro Moretto & Dina Filiou European Commission - DG JRC Institute for Energy, Clean Energies Unit	EC-JRC	Netherlands
4	Stockholm University Prof. Dag Noreus Department of Structural Chemistry	SU	Sweden
5	Institutt for Energiteknikk Dr. Jiri Muller Department of Physics Institute for Energy Technology	IFE	Norway
6	University of Fribourg Prof. Andreas Zuttel Physics Department, Science Faculty, Condensed Matter Physics	UniFR	Switzerland
7	University of Birmingham Dr David Book Department of Metallurgy and Materials School of Engineering	BHAM	UK
8	National Centre for Scientific Research, Demokritos Dr. Thanos Stubos INT-RP, Environmental Research Laboratory NCSR	NCSR	Greece
9	Vrije Universiteit Amsterdam Ronald Griessen & Bernard Dam Condensed Matter Physics	VU	Netherlands
10	Laboratoire de Cristallographie du CNRS Daniel Fruchart Directeur de Recherches Laboratoire de Cristallographie du CNRS	CNRS	France
11	DaimlerChrysler AG Dr. Eberhard Schmidt-Ihn	DCAG	Germany
12	GKSS Forschungszentrum Geesthacht GmbH Dr.-Ing. Thomas Klassen Department Powder and NanoTechnology Institute for Materials Research	GKSS	Germany
13	University of Iceland Prof. Hannes Jonsson Department of Chemistry Science Institute, University of Iceland	UICE.SI	Iceland

No.	Organization / PI	ID	Country
14	Johnson Matthey Mr. David Boyd Johnson Matthey Fuel Cells Ltd	JM	UK
15	Forschungszentrum Karlsruhe Dr. Maximilian Fichtner Institut für Nanotechnologie Forschungszentrum Karlsruhe	FZK	Germany
16	Max-Planck Institute Stuttgart Dr. Michael Hirscher Max-Planck-Institut fuer Metallforschung	MPG	Germany
17	Technical University of Denmark Prof. Jens Kehlet Nørskov CAMP, Department of Physics	DTU	Denmark
18	Ankara University Dr. Tayfur Öztürk Professor, Dept of Metallurgical and Materials Engineering	METU	Turkey
19	Instituto Nacional de Engenharia, Tecnologia e Inovacao Dr. Carmen Rangel Materials & Production Technologies/Electrochemistry of Materials Unit	INETI	Portugal
20	Leibniz-Institut für Festkörper- und Werkstoffforschung Dresden e.V. Dr. Oliver Gutfleisch Institut für Metallische Werkstoffe	IFW	Germany
21	Delft University of Technology	DUT	Netherland
22	Southwest Research Institute Dr. Michael A. Miller Southwest Research Institute Materials Characterization and Development Department of Materials Engineering	SwRI	USA

Owing to the controversy surrounding the mechanistic validity and thermodynamic plausibility of hydrogen spillover effects in catalytically-doped high surface-area substrates, such as MOFs and nanoporous carbons, as reported in various accounts (Sections 2.2-2.3), the Laboratory set out to obtain more definitive evidence than was available at that time for the purported effect by teaming with USAL (Drs. Keith Ross and Daniel Bullis), NCSR D (Drs. Theodore Steriotis and Thanos Stubos), and the ISIS synchrotron facility (Drs. Stewart Parker and A.J. Ramirez-Cuesta, Rutherford Appleton Laboratory). The objective of this collaboration was to prepare in sufficient quantities batch lots of candidate spillover materials for performing inelastic (vibrational) neutron scattering (INS) experiments, with the goal of developing a comprehensive understanding of the binding of hydrogen in these systems.

In pursuit of the stated goal, two experiment proposals were submitted to the ISIS review committee that involved studies on two different classes of spillover materials: catalytically-doped carbon foam and IRMOF-8. The Thermal Original Spectrometer with Cylindrical Analyzers (TOSCA) instrument was proposed for INS measurements. Upon acceptance of the two proposals and scheduling of beam time, the team convened at ISIS in July, 2008 and worked collaboratively over the course of one week to setup the experimental apparatuses and make the proposed measurements.

The TOSCA instrument was intended to permit measurement of the inelastic scattering of neutrons from atomic hydrogen when or if produced remotely on catalyst particles and diffused over the carbon or MOF substrate as a function of dihydrogen coverage. However, the extremely weak signal-to-noise ratios inherent in these sorts of difficult measurements due to the necessary presence of bulk dihydrogen did not yield additional insights into the spillover process. In spite of this setback, the experience gained at ISIS enabled the team to identify weaknesses in the experimental design, and propose alternative protocols for improving the sensitivity of the INS measurements in future experiments.

In a separate, though related, endeavor, the Laboratory established a technical collaboration with the Institute of Nuclear Energy Research (INER, Longtan, Taiwan) to help validate hydrogen spillover effects in catalytically-doped IRMOF-8 (containing a bridging compound) using materials synthesized at INER. After acquiring these materials from INER, SwRI hosted a visiting scientist (C.-Y. Wang, INER), trained him on SwRI-developed measurement techniques, and collaboratively made critical measurements to elucidate the sorption behavior of those materials. The results of the measurements were later used by SwRI to support first principles computations as the theoretical basis for reconciling the thermodynamic plausibility of the spillover effect.

5

SUMMARY OF PROGRAM GOALS AND ACCOMPLISHMENTS

The salient goals and major accomplishments of the program – from the inception of the Laboratory through the fruition of storage material validation – are tabulated below (Table 2) in chronological order.

Table 5.1: A chronological overview of program goals and accomplishments (2002-2012).

Year	Goals	Accomplishments
2002		Program Award, April 2002
2002	Review the state-of-the-art in measurement techniques and instrumentation for hydrogen sorption measurements, which may be employed by outside “expert” laboratories.	<ul style="list-style-type: none">• Conducted site visits of four premier laboratories: Air Products (Allentown, PA, Dr. Charles Rowe); Lawrence Livermore National Laboratory (Livermore, CA, Dr. Karl Gross); General Motors Research Corp. (Warren, MI, Dr. Frederick Pinkerton); and, National Renewable Energy Laboratory (Golden, CO, Dr. Michael Heben).• Observed first-hand and discussed with experts the attributes and pitfalls of measurement techniques and instrumentation, which later guided the design of the Laboratory, and selection/augmentation of key equipment.
2002-2004	Design and construct laboratory facilities for the analysis of storage materials and full-scale storage systems	<ul style="list-style-type: none">• Constructed laboratories for analysis of storage materials and full-scale storage systems consisting of the following key components: (a) ultra-high purity H₂ and He high-pressure manifolds with electro-pneumatically-controlled valves; (b) real-time safety monitoring of H₂ leaks with automated emergency shutdown; (c) redundant, in-line purification of manifold gases; (d) SwRI-developed gas sampling system for periodic analysis of manifold- and source-gas purity using mass spectrometry; (e) glove boxes for handling storage materials in helium environment; (f) high-pressure reaction bomb for pre-activation/conditioning of bulk storage materials; (g) mass-flow gas metering and heat-exchange systems for quantifying isothermal or adiabatic sorption properties of full-scale storage systems.

Year	Goals	Accomplishments
2004	Review on-site NREL activities related to synthesis and sorption analysis of catalytically-doped carbon nanotubes	<ul style="list-style-type: none"> Conducted an external, on-site review of NREL activities, in conjunction with the U. Pennsylvania (Dr. Ray Gorte), to verify previous controversial results showing hydrogen uptake in catalytically-doped single wall carbon nanotubes (SWNTs) at room temperature (via spillover), and identify potential sources of poor reproducibility. The outcome of this review was detailed in a report and submitted to DOE (see Appendix B).
2004-2005	Implement array of instrumentation for sorption analysis of storage materials	<ul style="list-style-type: none"> Designed and acquired via a third party a static, high-pressure thermogravimetric analyzer employing a state-of-the-art magnetic suspension electro-balance, glove-box containment, and capillary interface for in situ mass spectroscopic analysis of gas space. Acquired a Sievert-type volumetric sorption analyzer from commercial source and augmented its design to improve low-temperature isothermal analyses of physisorption materials and allow in situ mass spectroscopic analysis of gas space. Developed and installed a Laser-induced Thermal Desorption Mass Spectrometer (LTDMS) system for high resolution thermal desorption analysis of storage materials.
2004-2006	Develop Standard Protocols/Procedures for the sorption analysis of hydrogen storage materials	<ul style="list-style-type: none"> Developed standard operating procedures (SOPs) for the submission of samples to the Laboratory, and the validation/qualification of the sorption properties of promising storage materials using volumetric sorption analysis, gravimetric sorption analysis, and/or thermal desorption mass spectroscopy analysis of storage materials. SOPs received peer review by outside experts and were granted approval for use.
2005	Commission the Testing Laboratory for Solid-State Hydrogen Storage Technologies	<ul style="list-style-type: none"> Completed construction of the Laboratory. Commissioned Laboratory for qualification of SOPs under a Round-Robin testing program.
2006	Conduct Round-Robin testing to qualify SOPs	<ul style="list-style-type: none"> Completed Round-Robin testing on multiple types of carbon samples for physisorption analysis at 77 K and 298 K. Demonstrated excellent complementarity between thermogravimetric and volumetric measurement techniques. Demonstrated excellent agreement in measurements results among those of participating laboratories.
2006	Develop advanced techniques for accurate and reproducible measurement of hydrogen uptake in low-density, porous solids at low temperatures	<ul style="list-style-type: none"> A combined volumetric-gravimetric technique in which a simplified local density (SLD) thermodynamic model was linked to an accurate equation of state and fitting procedure, was formulated as a standard method by which the skeletal density of, and hydrogen uptake in, low bulk-density porous materials (e.g., MOFs) could be accurately measured.
2006	Validate reported uptake of hydrogen in alloy-doped SWNTs at room temperature via spillover effect	<ul style="list-style-type: none"> Demonstrated total hydrogen uptake of 2.78 wt.% in NREL-prepared $Ti_{0.86}Al_{0.1}V_{0.04}$ catalyzed SWNTs at room temperature using LTDMS. Demonstrated agreement with NREL's previously reported results on the same sample (2004).

Year	Goals	Accomplishments
2006	Establish benchmark for physisorption uptake of hydrogen in MOFs at low temperatures	<ul style="list-style-type: none"> • Independently verified 7.5 wt.% excess hydrogen uptake in MOF-177 at 77 K using advanced methods previously established for high surface-area, low density storage materials – the highest uptake ever reported and validate to date. • Established and validated accurate method of quantifying excess and absolute uptake of hydrogen in low-density, highly porous storage materials.
2006-2008	Expand Round-Robin testing internationally through NESSHY program	<ul style="list-style-type: none"> • Established Round-Robin qualification program in partnership with the EU's NESSHY program to quantify hydrogen uptake in ultra-microporous carbon and sodium alanate reference materials.
2007	Determine sorption capacity of full-scale storage vessels	<ul style="list-style-type: none"> • Successfully activated and quantitatively charged a prototype vessel containing a proprietary metal hydride for subsequent evaluation of fire safety performance.
2007-2008	Investigate and validate hydrogen spillover effects in catalytically-doped MOFs	<ul style="list-style-type: none"> • Independently validated hydrogen spillover uptake in platinum-doped carbon-bridged IRMOF-8 at 298 K. • Measured and resolved the stable binding sites of hydrogen in IRMOF-8 (Pt/carbon-bridged) spillover compound by LTDMS to provide mechanistic insight into hydrogen uptake in this compound. • Assessed the thermodynamic plausibility of hydrogen spillover in catalytically-doped MOFs through theoretical computations at the level of Hartree-Fock (HF) and density functional theory (DFT).
2011	Participate in interlaboratory testing of spillover storage materials	<ul style="list-style-type: none"> • Quantified the sorption properties of an unknown storage material at two isothermal conditions and submitted results to NREL. • SwRI measurements were consistent with combined results of other participating laboratories.
2005-2012	Independently verify the intrinsic sorption characteristics of novel and emerging materials for hydrogen storage	<ul style="list-style-type: none"> • Critically analyzed a total of 46 different storage materials: <ul style="list-style-type: none"> ➢ 26 of these materials emerged from the Materials Centers of Excellence (DOE directives) ➢ 20 were submitted from private organization outside the Centers

6

PROGRAM ACTIVITIES

6.1 Overview of Analytical Methods

The methods and instrumentation that have been employed for measuring the capacity, thermodynamic variables, and kinetic properties of hydrogen sorption in solid-state materials are reviewed in this section. Given that the analytical requirements for achieving accurate measurements of these properties are really quite stringent, and that the laboratory facility in which the instrumentation resides plays an integral role in the measurements, a description of the laboratory facility in which all measurements were carried-out is also reviewed.

6.2 Evaluation of Materials for Hydrogen Storage

From the viewpoint of practical storage, three measurements of the interaction between hydrogen and a solid-state substrate are of ultimate importance in determining whether or not a material is useful for storing hydrogen. These measurements are the thermodynamic stability, the kinetics, and the hydrogen capacity of the hydrogen-substrate system. To be able to effectively manipulate these properties, it is essential to understand the fundamental physical mechanisms which govern the interaction between hydrogen and substrate. The most important of these phenomena fall into three general categories: (1) Thermodynamics; (2) Kinetics or Mass Transport; and, (3) Crystal, Microstructure, and Electronic Structure.

Thermodynamics provides a means of understanding the stability of the hydrogen-substrate system; that is, how strong the attraction is for hydrogen to bind with the host substrate and, in the case of an active metal, to possibly form a metal-hydride. Mass transport examines the kinetics of hydrogen transport across surfaces and interfaces, and through the bulk of a material. Finally, the crystal, microstructure, and electronic structure address all three properties, but are particularly important for understanding the absorbed hydrogen capacity.

Up to now, the development and mechanistic study of solid-state hydrogen storage has historically evolved two distinct categories of materials for hydrogen binding: (1) chemisorption, which involves the dissociation of dihydrogen and formation of new bonds with the substrate; and (2) physisorption, in which only non-bonded interactions of dihydrogen with the substrate play a role. More recently, as described in Section 2, the advent of nano-scale materials incorporating composite architectures (*e.g.*, metal nano-particle plus carbon nano-structures), or the synthesis of atomic coordination complexes for Kubas-type covalent

binding of dihydrogen, have blurred these categories. A thermodynamic description of these contemporary materials in a canonical sense is challenging, though significant progress has been made at various levels of theory [47-49].

Setting aside materials in which chemisorption and physisorption processes overlap, it is useful to delineate the experimentally-derived thermodynamic variables (*i.e.*, canonical) for each category because no better unified treatment for analysis of storage materials could be applied. The emphasis for describing the thermodynamic treatments is, furthermore, placed on physisorption processes due to the fact that most storage materials analyzed by the Laboratory were derived from nanostructures intrinsically well-suited for physisorption interactions; that is, porous materials of very high surface area.

6.2.1 Chemisorption Materials

The thermodynamics of the hydrogen-metal systems can be best understood through the use of phase diagrams. Unlike alloy (solid-liquid) phase diagrams, the metal-hydrogen phase composition is dictated by the temperature and pressure of the surrounding hydrogen gas. Equilibrium metal-hydrogen phase diagrams are often constructed from pressure concentration temperature (PCT) measurements. These diagrams consist of isothermal measurements of the equilibrium hydrogen concentration in a metal as a function of the surrounding hydrogen gas pressure [53].

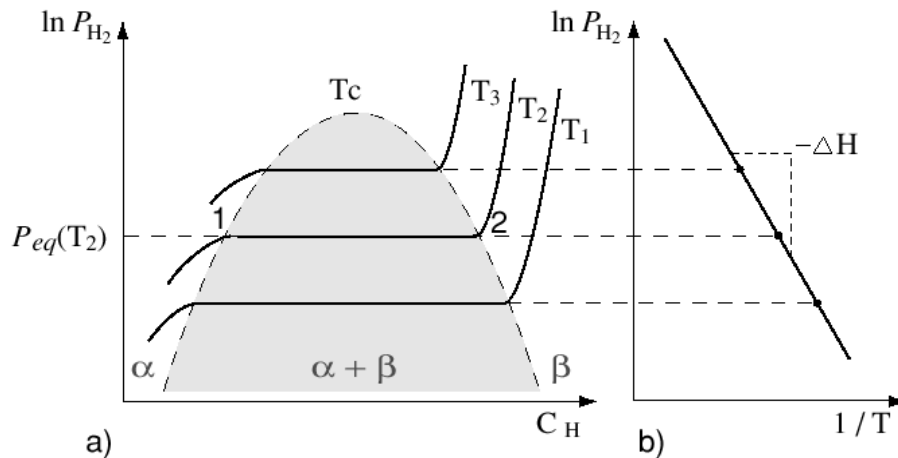


Figure 6-1: a) An idealized representation of Pressure Concentration Temperature (PCT) isotherms for the α solid solution phase and β hydride phase. b) The enthalpy of hydride formation ΔH is obtained from the slope of a Van't Hoff plot of $\ln(P_{eq})$ as a function of $1/T$ [$\ln P_{eq} = (\Delta H/(RT) - \Delta S/R)$].

To develop a basic understanding of the principles behind these thermodynamic measurements, it is useful to start with an idealized representation of a PCT measurement (Fig. 6.1a). Moving along one isotherm, hydrogen begins to dissolve into the host-metal lattice at low concentrations as the surrounding gaseous hydrogen pressure is increased. This region represents a solid solution of hydrogen in the metal which is generally denoted as the α phase. Hydrogen continues to be absorbed with increasing pressure until H-H interactions become important. At this point (1 in Fig. 6.1a), a hydride (denoted β phase) is formed locally by the occupation of particular interstitial lattice sites. The nucleation and growth of the hydride phase may occur at free surfaces, at inter-grain boundaries, or throughout the bulk of the metal, depending on nucleation and diffusion mechanisms. Under idealized equilibrium conditions, the hydrogen gas pressure remains constant as hydrogen is absorbed and the α phase is transformed into the β phase. This behavior is observed as a plateau in the PCT diagram. Thus, the existence of an equilibrium plateau signals the co-existence of the two phases. As the hydride phase grows the total hydrogen content of the sample increases. Eventually all of the α phase is transformed into the β hydride phase (point 2 in Fig. 6.1a). The pressure again rises and the overall hydrogen concentration continues to increase as hydrogen is dissolved as a solid solution in the β hydride phase.

The slope and length of the equilibrium plateau is of particular importance for hydrogen storage applications. A flat plateau enables the reversible absorption and desorption of hydrogen from a metal simply by raising or lowering the surrounding hydrogen pressure above or below the plateau pressure. In raising the pressure, hydrogen is absorbed while forming the β hydride phase. Hydrogen is desorbed by lowering the pressure, transforming the hydride back into the α phase. This change in pressure can be minor (1 to 2 bar for the classic alloy LaNi_5 at 22 °C) compared to the pressures needed to store a significant amount of hydrogen by pressurization (200 bar). The length of the plateau determines how much hydrogen can be reversibly stored in a metal hydride.

The ease with which hydrogen can be reversibly absorbed and desorbed depends on the relative thermodynamic stability of hydrogen in the host metal. Hydrogen absorption to form a solid solution and the formation of a hydride phase can be either an exothermic or an endothermic process. The enthalpy of formation defines a phase's relative stability. This can be determined directly from a series of equilibrium PCT measurements at different temperatures as shown in Fig. 6.1b. Such measurements are the workhorse of metal-hydride hydrogen-storage research. The plateau pressures as a function of temperature are represented as a Van't Hoff plot. Those plots determine the enthalpy ΔH and the entropy ΔS of hydride formation.

6.2.2 Physisorption on Porous Materials

It is important to recognize that statistical thermodynamics and molecular simulations of physisorption are cast in terms of the absolute thermodynamic variables (internal energy, U ; Helmholtz free energy, F ; grand potential, Ω ; enthalpy, H ; and Gibbs free energy, G). These absolute variables are not, however, accessible to experimental measurements of adsorption. The accessible quantities in the experimental measurements of adsorption are the *excess* thermodynamic variables. In considering the mass balance of the two-phase system, the excess adsorption measured by experiment is the total amount of gas present in the gas-solid system minus the amount present in the gas phase. According to the Gibbs definition, the excess adsorption is determined by the difference between the densities of the bulk and adsorbed “fluids” in the adsorbed phase [54]:

$$\Gamma = V_a(\rho_a - \rho_b) \quad (6.1)$$

where V_a is the volume of the adsorbed phase, ρ_a is the density of the adsorbed phase, and ρ_b is the density of the bulk phase. In supercritical fluids adsorbed at high pressures in the range 10-1000 bars, for example, the absolute amount adsorbed approaches a saturation value, whereas the excess amount adsorbed, Eq. 6.1, reaches a maximum then decreases with pressure. This experimentally-accessible measurement was illustrated in Fig. 2.2 for SWNTs at 77 K, and further discussion of the significance of absolute and excess adsorption will be discussed later in the context of establishing a benchmark material for physisorption.

The simplest approach to deriving thermodynamic properties in adsorption is the Langmuir model [55]:

$$n = n_0 \left(\frac{BP}{1 + BP} \right) \quad (6.2)$$

where P is the bulk-gas pressure, n the surface concentration in terms of the number of moles of gas adsorbed per mass of sorbent, and n_0 is the saturation concentration. This model takes into account only the interactions between adsorbate and adsorbent, neglecting the interactions between adsorbate species. Under isothermal conditions, the Langmuir equation increases monotonically as a function of pressure. The saturation concentration and the coefficient B can be obtained from a linear fit of Eq. 6.2 to the measured data. However, this equation is applicable only to homogeneous surfaces and, consequently, does not adequately describe

isotherms obtained on heterogeneous surfaces [56, 57]. In heterogeneous systems, such as porous sorbents, an additional parameter, m , is added to the Langmuir equation as an exponent of the pressure. This extended model is referred to as the Langmuir-Freundlich (L-F) equation.

Neither the Langmuir nor the L-F models can describe, however, the characteristic maximum in excess adsorption isotherms that occurs in the supercritical region. In the very low-pressure, subcritical and sub-atmospheric region, these models are accurate and can be used to derive thermodynamic quantities. In the supercritical region, a virial-type expression consisting of the temperature-independent parameters a_i and b_i must be applied to model the maximum in excess adsorption and estimate the isosteric heats of adsorption [58-60]:

$$\ln P = \ln N + \frac{1}{T} \sum_{i=0}^m a_i N^i + \sum_{i=0}^n b_i N^i \quad (6.3)$$

where P is pressure, N is the adsorbed amount, T is temperature, and m and n represent the number of coefficients required to adequately describe the isotherms. Concentration-dependent isosteric heats of adsorption are calculated from the best-fit parameters using:

$$Q_{st} = -R \sum_{i=0}^m a_i N^i \quad (6.4)$$

where R is the universal gas constant. It should be emphasized that the accuracy of this method relies on the number of isotherm curves considered in the fitting routine. Isotherm curves spaced apart by small temperature intervals would of course be most desirable, providing a more complete description of the thermodynamic surface tying together the isotherms and enabling accurate derivation of the heats of adsorption.

Illustrative calculations of the virial method are shown in Fig. 6.2. In this case, Eq. 6.3 was fitted to two hydrogen adsorption isotherms (77 and 298 K) for an ultra-microporous carbon (Takeda 4A). The fitted parameters a - f were then used in Eq. 6.4 to arrive at the isosteric heats of adsorption shown in Fig. 6.3.

This method has been found to be valid for a great many different types of porous materials with very small pore volumes. It is apparent from Fig. 6.2 that the virial model reproduces the qualitative features of the adsorption isotherms spanning sub- and supercritical pressure regimes.

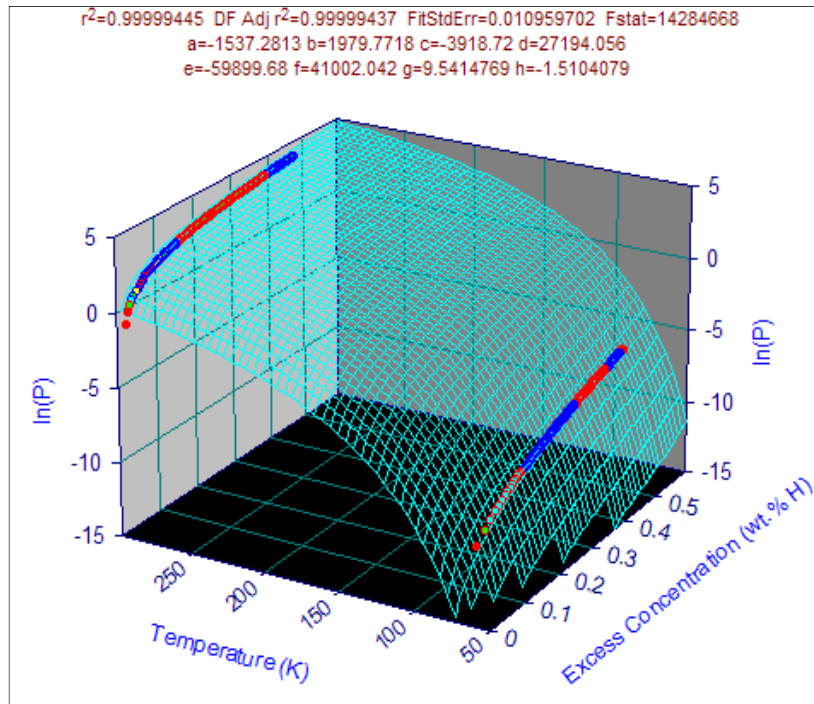


Figure 6-2: Results of fitting Eq. 6.3 to adsorption isotherms of hydrogen on ultra-microporous carbon at 77 and 298 K.

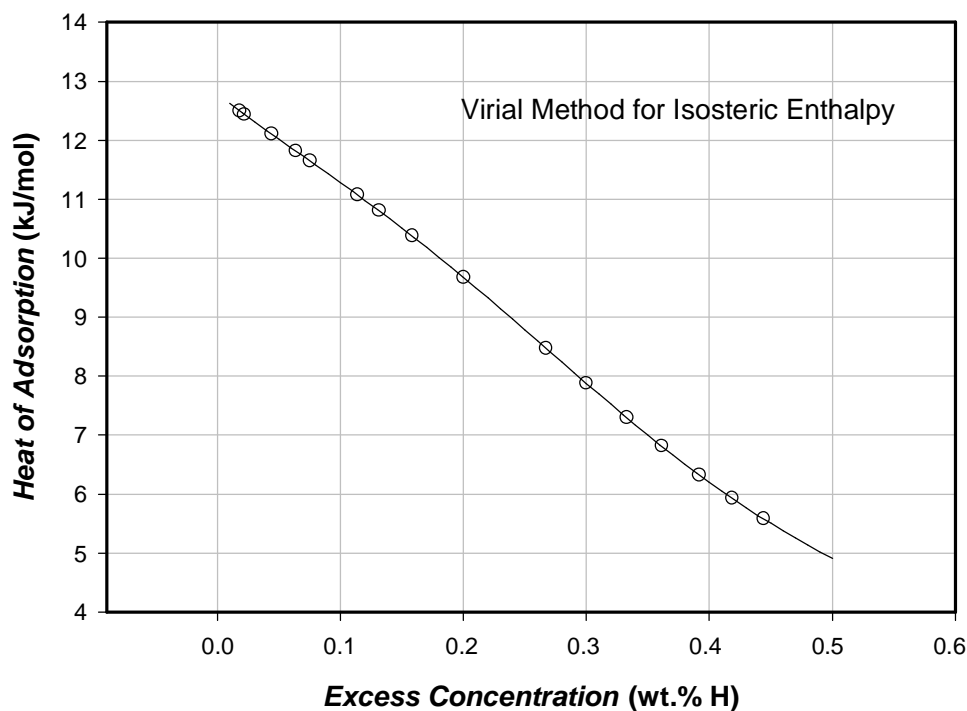


Figure 6-3: Isosteric heat of adsorption from Eq. 6.4 as a function of excess concentration.

6.3 Analytical Instrumentation

In considering the analytical methodologies conventionally practiced for hydrogen sorption measurements, the most suitable technique has been a topic of considerable debate. There are, in general, at least four measurement principles from which to choose: (1) volumetric analysis (Sievert-type apparatus); (2) temperature programmed thermal desorption mass spectrometry (TPD); (3) gravimetric analysis; and, (4) microcalorimetry. A sizeable body of literature has been amassed on each of these techniques over the past several decades for a broad spectrum of different materials [61-63]. While the merits of each measurement principle can be argued, the complementarity among these choices can be demonstrated as long as the constraint boundaries, such as mass, volume, and thermal stability, are not ignored.

6.3.1 Volumetric Analysis

In a volumetric analysis, the mass balance for the determination of the Gibbs excess adsorption is governed by [54, 55]:

$$\Gamma = n - V_f \rho_b \quad (6.5)$$

where n is the total or absolute amount of a pure gas species introduced into the sample cell, V_f is the free volume of the gas phase, sometimes referred to as the “void” volume or “dead” space of the system, and ρ_b is the density of the bulk gas. One of the principal challenges in volumetric analysis is to determine what actually constitutes the free volume of the system or, more specifically, what constitutes the void volume of a porous material. If a gas for which $\Gamma = 0$ were available, one could readily determine V_f from Eq. 6.5 as $V_f = n/\rho_b$. For this purpose, it is often assumed that helium is a non-absorbing gas, although it is now known that, depending on the conditions, quite significant amounts of helium are adsorbed in many porous materials. Whether or not helium adsorbs is actually unimportant in the determination of V_f . The choice of gas for this calibration is in essence a choice of the dividing surface for the Gibbs excess. The adoption of standard practices for the choice of gas and reference state conditions for measuring the void volume of the material is the most appropriate and unified approach to comparing different experimental measurements of excess adsorption. It should be recognized that even if the adsorption excess for a gas is zero, the estimate obtained by a calibration gas depends on the size of the gas molecule, and on the temperature and pressure used to determine V_f . The important point here is that correct determinations of the Gibbs excess can be realized as long as the same probe molecule is used for calibration at the same temperature and pressure.

The experimental apparatus consists essentially of a high-vacuum pumping system, a sample chamber, a gas measuring system, pressure gauges or manometers, and a hydrogen reservoir. For sorption measurements at high pressures, an all-metal apparatus, equipped with metal bellows valves and high precision pressure transducers, must be employed. A schematic of a high-pressure volumetric analysis system that has been employed in the Laboratory is shown in Fig. 6.4.

All components of this device are constructed of Type 316L stainless steel tubing with VCR[®] fittings to avoid carbon segregation and hydrogen embrittlement at elevated temperatures. This design allows experiments to be safely performed at up to 400 °C with 200 atm of hydrogen pressure. Metal fritted-filter VCR gaskets are usually used between sections of internal tubing to bleed hydrogen to (or from) the instrument reservoirs during a measurement. In this way, the supply pressure is increased (decreased) slowly over the duration of the experiment, providing a more even distribution of measuring points along the sorption curve. The internal reservoirs are pre-calibrated for exact volume and maintained at constant temperature, thus fixing volume and temperature as known quantities with pressure as a measured quantity.

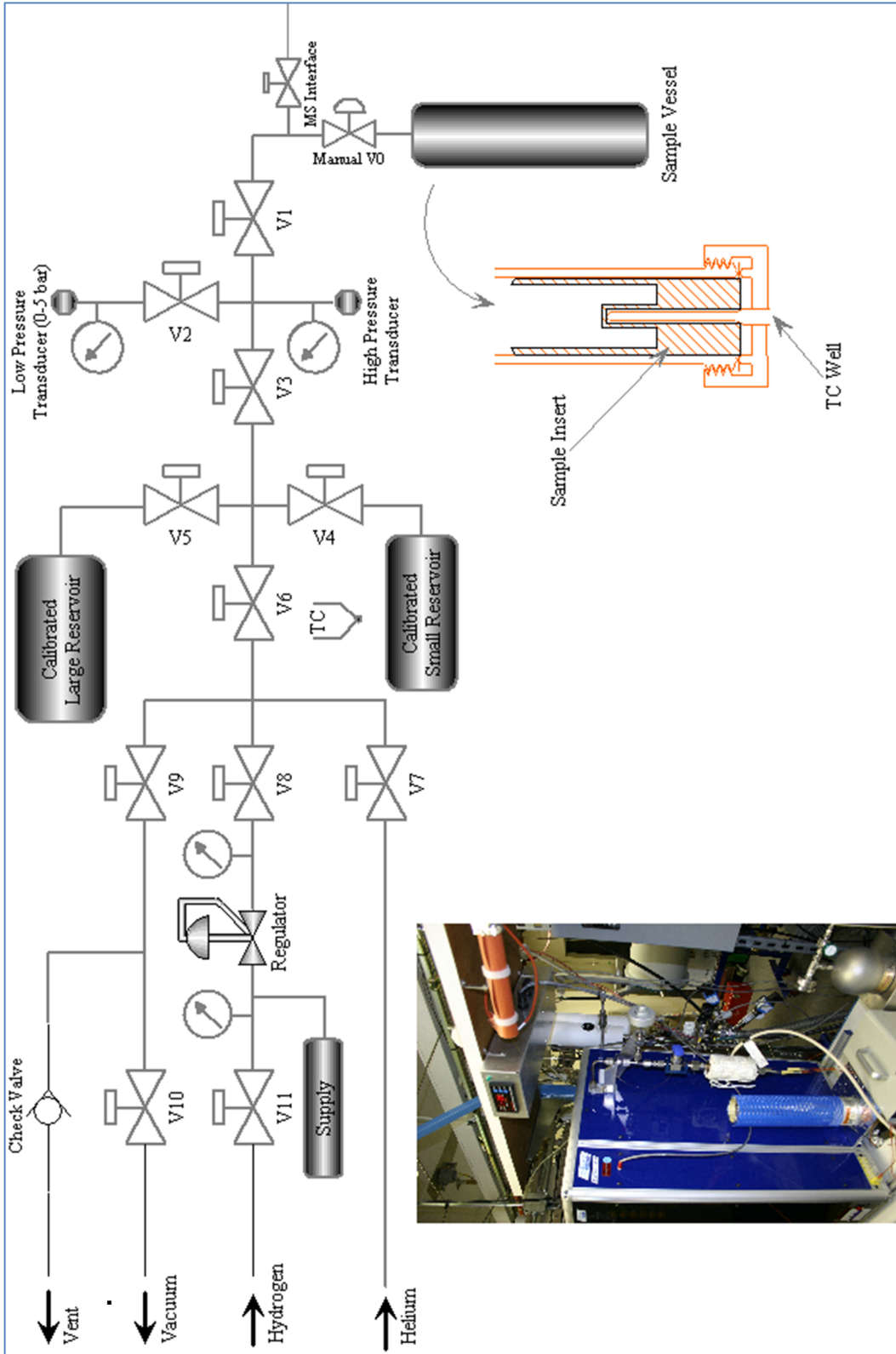


Figure 6-4: Schematic of the high-pressure volumetric analyzer employed for determining excess sorption isotherms. Inset – Photograph of analyzer (blue), a Hy-Energy, Inc. Model PCT-Pro 2000 (Newark, CA), and high-pressure sample vessel (external components) coupled with a mass spectrometer (not shown) and UHP gas manifold

Measurement of one point (j) on a sorption plot proceeds in two steps, as is illustrated in Fig. 6.5 and 6.6. First, valve E2 is closed, then E1 is opened and the supply pressure P_{Rj} is recorded. In the second step, E1 is closed, then E2 is opened. The change in pressure in the sample plus reservoir chambers due to sorption is immediately recorded over specified time intervals. This pressure change as a function of time measurement provides a means of evaluating the kinetics at each point on the sorption plot. When the change in pressure finally slows to a specified limit, the equilibrium pressure P_j is recorded, and the instrument proceeds to the next cycle.

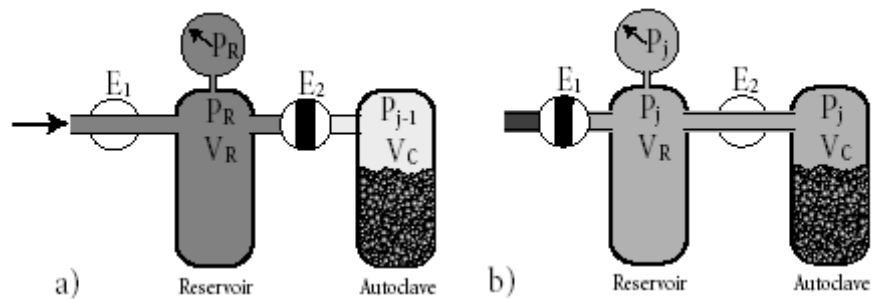


Figure 6-5: An illustration of the step-wise procedure for measuring one point on a sorption curve.

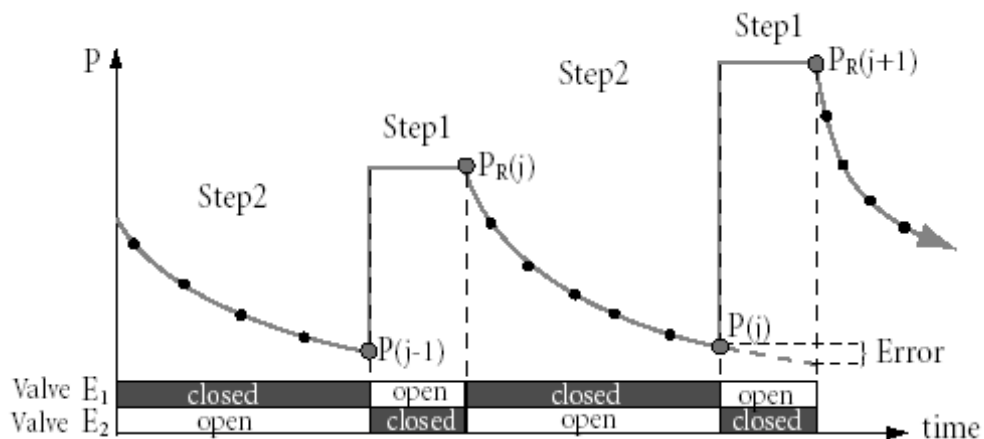


Figure 6-6: A schematic representation of the step-wise procedure for measuring a PCT curve. The equilibrium pressure is taken as $P(j)$ which may cause errors if the system has not reached equilibrium or if the duration of the first step in the procedure is too long.

6.3.2 Gravimetric Analysis

The gravimetric method measures excess adsorption as the apparent increase in weight of the sample corrected for the buoyancy force exerted by the bulk gas. In this case, accurate determination of the sample density and correction for the buoyant forces exerted by the bulk gas are central to the overall accuracy of the technique. The relationship between the theoretical Gibbs excess (Eq. 6.1) and the experimentally-measured value is given by:

$$W_a - W_{sb} \left(1 - \frac{\rho_b}{\rho_{sb}} \right) - W_s \left(1 - \frac{\rho_b}{\rho_s} \right) = V_{ad} (\rho_{ad} - \rho_b) \equiv \Gamma$$

W_a = Apparent Weight
 W_{sb} = Weight of Sample Basket
 W_s = Weight of Sample
 V_{ad} = Volume of Adsorbed Phase
 Γ = Gibbs Excess Adsorption
 ρ_b = Density of Bulk - Phase Gas
 ρ_{sb} = Density of Sample Basket
 ρ_s = Density of Sample
 ρ_{ad} = Density of Adsorbed Phase

(6.6)

Similar to the volumetric method, a non-interacting calibration gas, such as He, can be used to determine the sample density or, in more precise terms, the He density of the sample, ρ_s . The He calibration also permits one to correct the apparent weight of the sample to derive the actual weight according to a simple equation of state (SEOS):

$$W_{corr} = W_a + \left(|m_{He}| \times P_s \times \frac{M_{H_2}}{M_{He}} \right)$$

W_{corr} = Corrected Weight
 W_a = Apparent Weight
 m_{He} = Slope of Helium Isotherm
 P_s = Pressure
 M = Molecular Weight

(6.7)

While Eq. 6.7 is quite suitable for many materials with limited porosity, a more robust method is needed to accurately measure the Gibbs excess for microporous materials of low density, and the buoyant forces exerted on such materials at elevated pressures. Under these circumstances, the accuracy of the gravimetric excess is directly tied to how accurately the density of the bulk gas and the skeletal density of the storage material can be computed in the

left-hand-side of Eq. 6.6 for any given pressure and temperature condition. For this purpose, an extremely accurate state function for hydrogen has been implemented under the present program, given the Bender equation of state (BEOS) [54, 64, 65], which is presented in the Appendix C along with a table of the empirically-derived coefficients. By combining Eq. 6.6 with the fugacity expression for the BEOS, and the equation for the chemical potential of the bulk gas in equilibrium with the adsorbed layer, it is possible to further determine, via a fitting procedure of the measured data, the density of the sample, ρ_s , the volume of the adsorbed layer, V_{ad} , and the adsorption potential, U (see Appendix C).

The thermogravimetric apparatus employed in the Laboratory is shown schematically in Fig. 6.7. Components of the analyzer requiring placement or removal of the sample are enclosed in a controlled environment (Ar glove box), to avoid exposing air- and moisture sensitive samples to the laboratory environment. A magnetically suspended electrobalance with 1 μg mass resolution is used to measure mass changes during an isothermal sorption experiment. The sample is housed and pressurized in a 316L stainless steel reaction vessel compatible to pressures ranging from ultra-high vacuum (UHV, 10^{-7} Torr) to 200 bar. Additionally, the sample and environment in the reaction vessel are physically isolated from the microbalance's electronic components using a contactless magnetic coupling for vertical force measurements.

The measurement cycle for the thermogravimetric apparatus is to hold the pressure on the sample constant, after each step change in system pressure, during uptake or desorption until steady-state, mass equilibration is achieved. This approach ensures that the driving chemical potential is held constant, whereas the pressure and, hence, chemical potential is allowed to relax in the volumetric method. Real-time analysis of the individual mass relaxation in response to a step change in system pressure gives valuable insight into the dynamics of the sorption process.

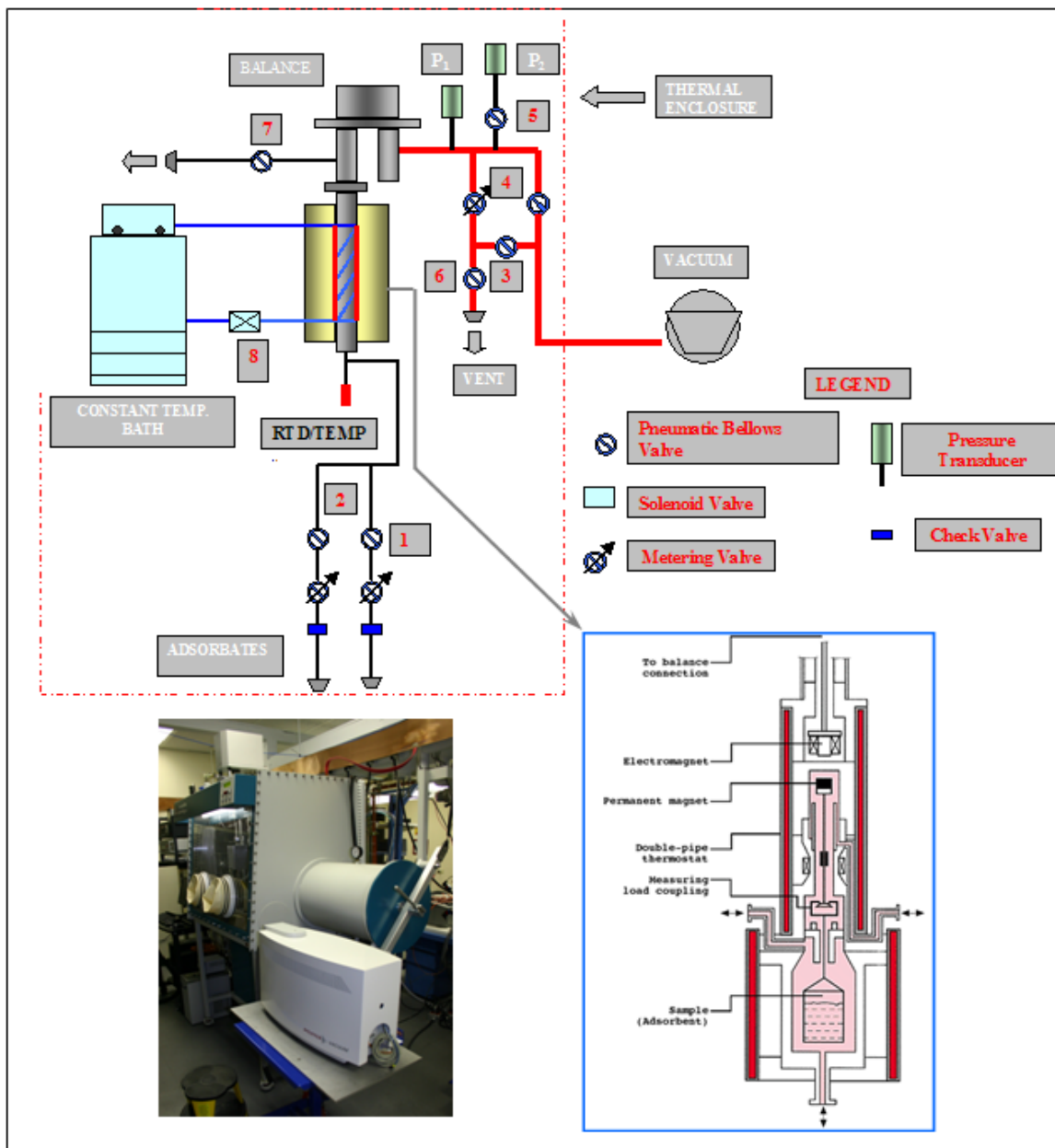


Figure 6-7: Schematic of high-pressure thermogravimetric apparatus (VTI, Inc., Model GHP) used for sorption measurements. Inset – Photograph of complete system integrated in a glove box (a magnetic suspension microbalance head positioned on top of glove box) and coupled with an external mass spectrometer (white box) via fused-silica glass capillary tubing and UHP gas manifold.

6.3.3 Laser-Induced Thermal Desorption Mass Spectrometry

Thermal desorption mass spectrometry (TDMS), a.k.a. temperature programmed desorption (TPD), provides yet another dimension – both in terms of sensitivity and mechanistic understanding – to making hydrogen storage measurements on most any material [66-68]. The objectives of a TDMS experiment are to elucidate and resolve the stable binding interactions of hydrogen within the material, quantify very precisely the total amount of hydrogen that is bound, and determine whether any other chemical species are desorbed from the material due to chemical instabilities or intrinsic transformations. The key advantages over the volumetric and gravimetric techniques are very high detection sensitivity, thus requiring very small sample sizes (< 5 mg), and speciation via interpretation of mass spectral fragmentation patterns. Given that TDMS is, by its very nature, a vacuum-based technique, the gas-space pressure surrounding the sample must at some point be reduced after dosing with hydrogen to a level of vacuum compatible with the minimum vacuum requirements of the mass spectrometer. Therefore, high-pressure dosing of the sample at equilibrium is not possible.

The Laser-induced Thermal Desorption Mass Spectrometry (LTDMS) technique developed under the present program can be set apart from conventional TDMS techniques principally on the basis of how the sample is thermally interrogated. Conventional TDMS techniques have historically made use of resistive heating elements to control and drive the temperature of the sample [67, 68], whereas LTDMS is based on direct illumination of the sample with a laser light source. The latter enables efficient coupling between the internal degrees of freedom (*e.g.*, lattice vibrations) of the material and photons from, in the present case, an ytterbium fiber laser (1080 nm), providing very-high thermal resolution. Since the sample is interrogated directly, background levels of gas desorbed from the system components are virtually eliminated. By contrast, desorption of gas from resistive heating elements is often problematic in conventional TDMS experiments. Furthermore, in the low temperature regime of hydrogen desorption, acousto-optic modulation of the laser light source can be used to carefully control the power delivered to the sample, and to afford the thermal resolution required to differentiate a manifold of binding energies associated with stable, though weak, interactions between the material and atomic or molecular hydrogen. Hydrogen yields are determined with a quadrupole mass spectrometer and a 90° off-axis secondary electron multiplier (SEM) detector.

The LTDMS apparatus, illustrated in Fig. 6.8 and 6.9, consists of an ultra-high vacuum (UHV) sample chamber equipped with a quartz sample holder, cryogenic sample-cooling loop, a piezoelectric variable dosing valve, and a cold-cathode/pirani combination gauge (Pfeiffer, Asstar, Germany; Model PKR-251). All surfaces of the stainless-steel sample chamber are passivated with Ni/Cr-oxide electropolish (SUMMA[®] passivation, Huntington,

Mountain View, CA). The sample chamber is interfaced to a quadrupole mass spectrometer (Balzers, Asslar, Germany; Model QMS-400) employing electron-impact ionization and a SEM detector, which is positioned 90° off-axis from the quadrupole beam-line to eliminate the impact of neutral species on the SEM, which leads to improved detection sensitivity. The system is differentially pumped using two turbomolecular pumping (TMP) stations attached to the sample chamber (60 L/s) and QMS (150 L/s). Differential pressures that develop between the sample chamber and the QMS are handled by a dual gate-valve interface in which one can select either a low-conductance orifice when pressures in the sample chamber are considerably higher than QMS vacuum, while operating within the linear range of the SEM, or an unobstructed path to the QMS. Sample heating under programmed control is afforded with the output beam of an ytterbium fiber laser (1080 nm, 30 W CW; IPG Photonics Corp., Oxford, MA). A computer-controlled optical assembly adjacent to the sample chamber delivers a collimated laser beam of appropriate power to the sample through an optical window using a feedback-control algorithm via a micro-thermocouple embedded in the sample. Beam intensity from the laser for sample temperatures greater than 100 K is controlled within the optical assembly through a combination of current control of the laser's pump diodes and rotation of a variable-density filter (VDF). For low-temperature studies (below 100 K), the beam is steered through an acousto-optic filter (AOTF) providing beam power up to 2 W with very high differential resolution.

For calibration, a NIST-traceable capillary leak device is used to deliver hydrogen at a steady-state, leak rate (8.4×10^{-9} mol/s) into the sample chamber while acquiring hydrogen ion intensities. A calibration factor Eq. 6.8 is calculated from the average intensity of the steady-state leak rate after subtracting the background, which is then applied to the hydrogen ion trace for the sample. Integration of any part of the desorption-versus-time trace for the sample enables accurate quantification of the amount of hydrogen desorbed.

$$CF = \frac{L_{H_2}}{(I_{H_2} - I_0)}$$

$$L_{H_2} = \text{Calibrated Leak Rate (moles/sec)} \tag{6.8}$$

$$I_{H_2} = \text{Average QMS Signal Intensity During Leak}$$

$$I_0 = \text{Average QMS Background Signal (no leak)}$$

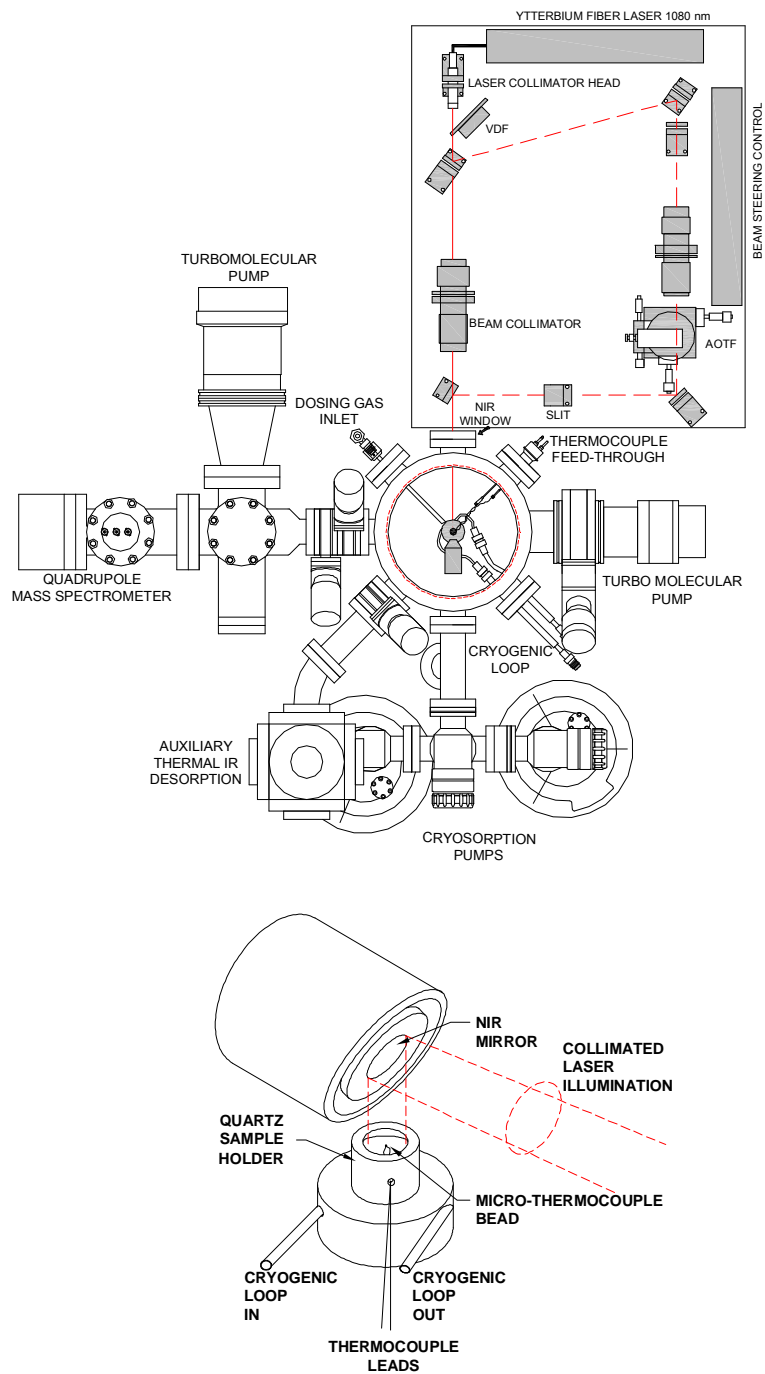


Figure 6-8: Diagram of LTDMS system for measurement of hydrogen chemi- and physisorption binding interactions. Top – Schematic of overall system including laser optics for illuminating sample. Bottom – Internal components for beam steering, sample containment, and heating or cooling.

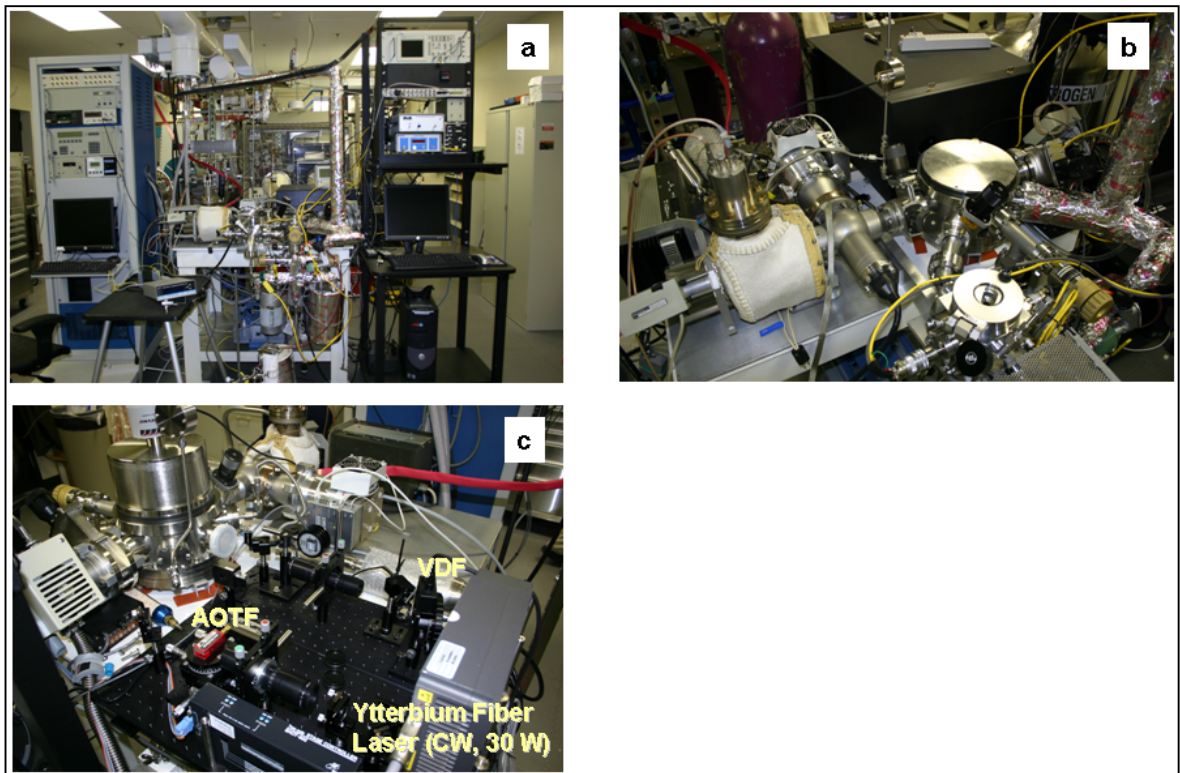


Figure 6-9: (a) Complete LTDMS system attached to an ultra-high purity gas manifold and electronic controls; (b) vacuum chamber, QMS analyzer, and laser driver; (c) optical bench for steering beam of laser through a variable density filter (VDF), acousto-optic tunable filter (AOTF), and collimating lenses before entering the sample vacuum chamber.

6.4 Small-Scale Laboratory Facility

The laboratory facility in which the analytical systems described above are housed plays an integral role in measuring the sorption properties of hydrogen storage materials. In particular, even very small quantities (ppm) of contaminants in hydrogen and helium source gases can lead to erroneous results because the quantities of sample materials available for study are typically < 100 mg. Absolute purity of source gases has, therefore, been a persistent concern. Commercial sources of high-purity hydrogen and helium (99.9995%) are readily available, though they do not, in many cases, meet the analytical standards required of hydrogen storage measurements. In this regard, the design and function of the facility must be capable of addressing the stringent requirements for delivering ultra-high purity (UHP) source gases to each analytical station at high pressures, in a safe manner, and with less than ppb levels of contaminants (*e.g.*, O₂, CO₂, CO, H₂S, SO₂, NO_x).

Overall, the design philosophy and functional goals of the Laboratory, and its sub-assemblies, can be summarized as follows:

- Safety first:
 - Hazards effects mitigation
 - Two-level redundant sensor and alarm systems
 - Emergency ventilation system
 - Control system redundancies and user interlocks
 - Stand-alone emergency power (i.e., diesel generator)
- Ultra-high purity (UHP) source gases, materials, and assembly procedures
- UHP manifold with pneumatic actuation
- Continuous process gas exhaust for all instrumentation and support equipment
- PLC-driven manual and automated computer control system for UHP manifold processes
- Gas sampling and purity monitoring systems
- Manifold-based, point-of-use redundant gas purification
- Array of high-pressure, vacuum compatible analytical capabilities
- Independent mass spectrometry for volumetric and gravimetric analyzers
- Independent sample activation capabilities contained in an inert environment
- Glove box (Argon environment) for handling and manipulating storage materials

There are in essence three important functions the facility must perform: (1) internal purification of commercial gas sources; (2) delivery of UHP gas to analytical stations; and (3) periodic monitoring of gas purity. Internal purification involves the use of passive purifiers under high pressures to “scrub” the commercial gas sources of any contaminants down to ppb levels through a gas manifold which, of itself, must not contribute to additional contaminants. Passive purifiers consist of high-pressure modules containing fixed-bed media of Na- and K-metal nanoparticles supported on amorphous carbon. Suitable materials used to construct the manifold for delivery of UHP gas consists of 316L stainless-steel tubing. The manifold’s internal surfaces are electropolished to improve its passivity and minimize the adsorption of condensable species.

Combining these functions with the implementation of safety measures to mitigate the potential hazards associated with handling a pressurized, flammable gas leads to a rather complex manifold system as illustrated in Fig. 6.10. To manage this system and its safety features, a PLC-driven gas manifold control system (Fig. 6.11) is used to direct gas pathways for purging, evacuation, and emergency shutdowns, and to monitor pressure, vacuum, and temperature of the manifold.

Once UHP levels of the gas source are achieved within the manifold, it is equally important to establish a method of monitoring and verifying this purity level. For this purpose, the manifold illustrated in Fig. 6.10 is further configured with a sub-manifold consisting of fused-silica capillary lines which are used to sample the gas content of the pressurized manifold through specially designed ports (1 μm laser-drilled orifice through a VCR nipple) positioned at various locations. The sampled gas in the capillary sub-manifold is directed to, and analyzed by, a QMS interfaced with a 6-channel gas stream selector (Pfeiffer, Omnistar QMS plus GSS-300 gas sampling system). The termination of this sampling system is shown in Fig. 6.12. Also shown here is an auxiliary sampling vessel used to analyze the gas purity of the commercial gas source prior to connecting the source bottle to the gas manifold.

Finally, an important aspect of handling and manipulating materials for hydrogen storage is to ensure that they are not in any way contaminated by air or moisture. Chemical hydrides, for example, are extremely pyrophoric and must be specially handled in an inert, glove box. All nano-structured materials studied under this program were known to be unstable in the presence of moisture and were susceptible to contamination by air. To overcome these difficulties, the laboratory facility is equipped with a centrally located Ar glove box (Fig. 6.13), inside of which materials are pre-conditioned, weighed, and transferred to appropriate vessels for subsequent analysis.

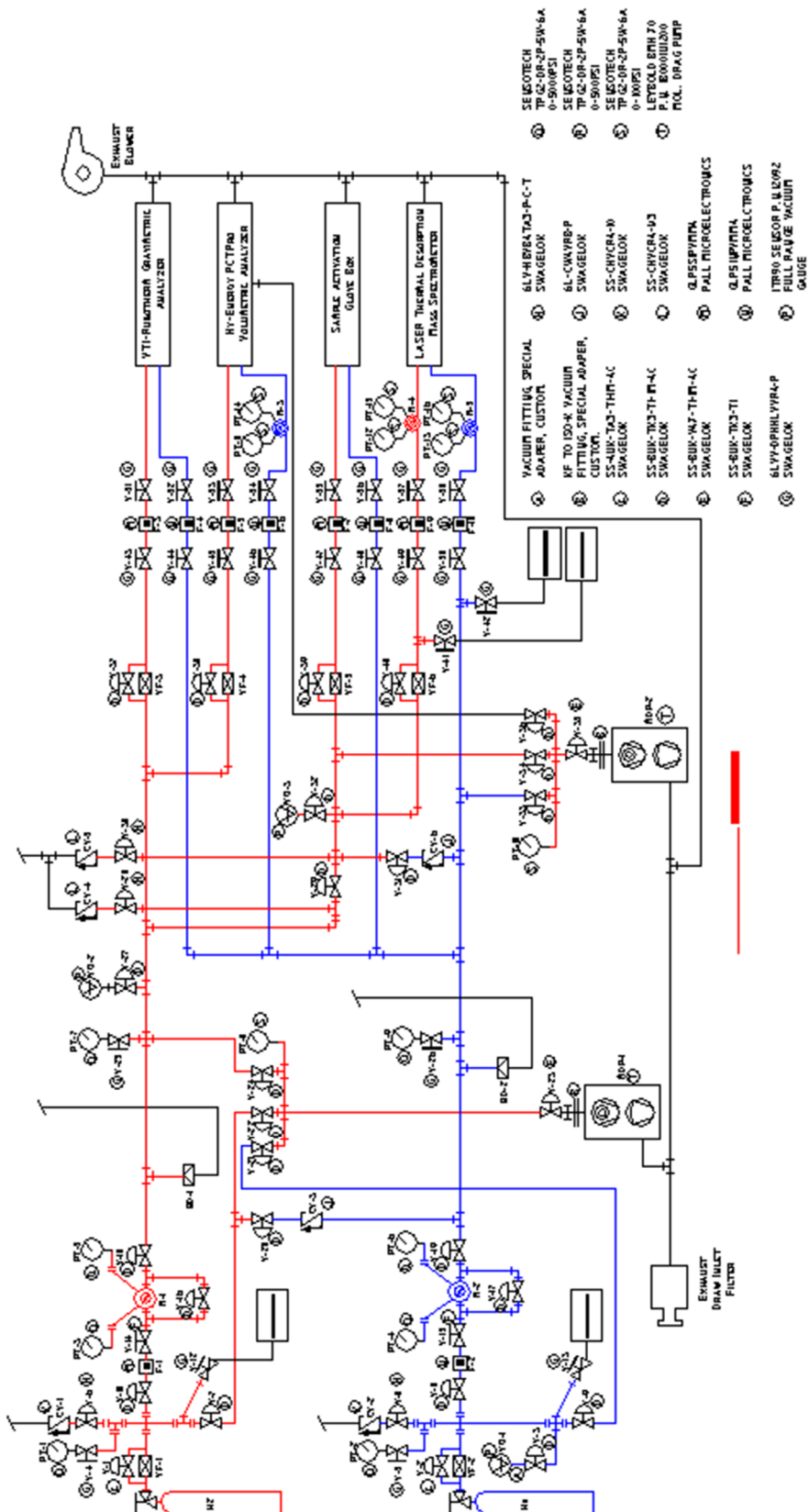


Figure 6-10: Schematic of gas manifold for internal purification and delivery UHP hydrogen and helium to analytical stations.

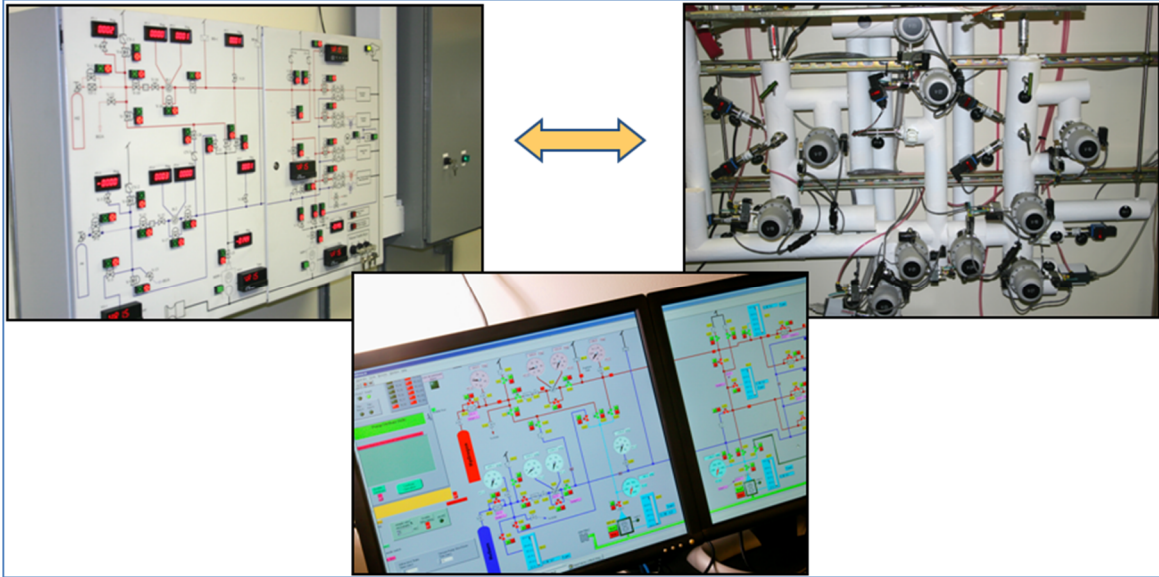


Figure 6-11: PLC-based control and monitoring system for the Laboratory's UHP gas manifold. Upper Left – Control and monitoring system for actuating electropneumatic valves (right) with manual override. Middle – Computer-based automated control, monitoring, and acquisition system.

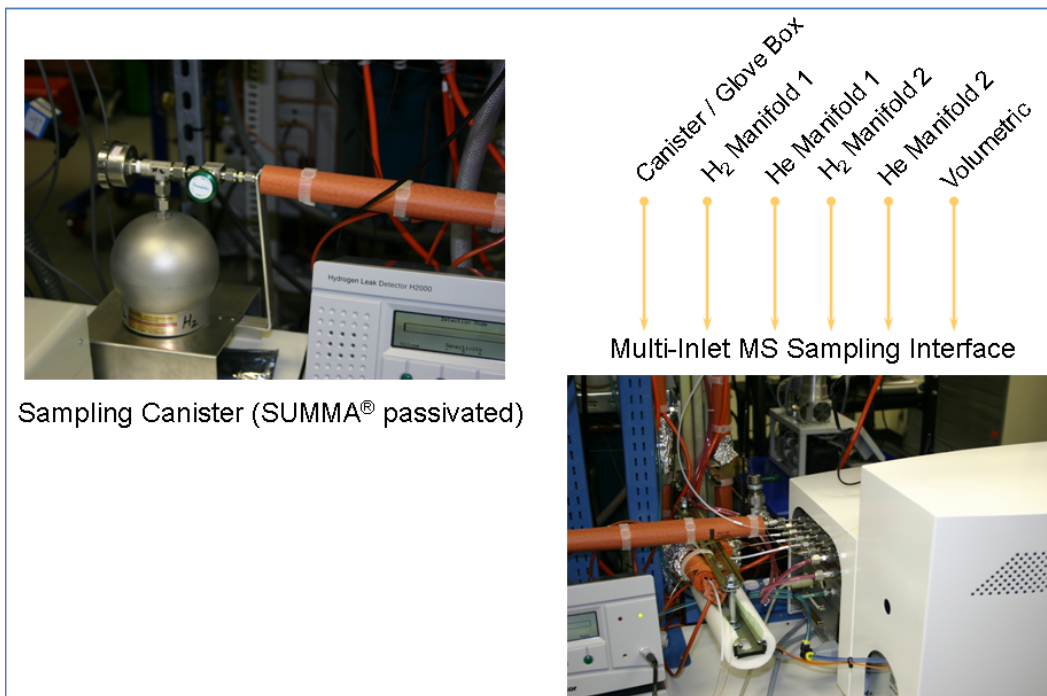


Figure 6-12: Sampling interfaces used to monitor the gas content of the manifold for purity.

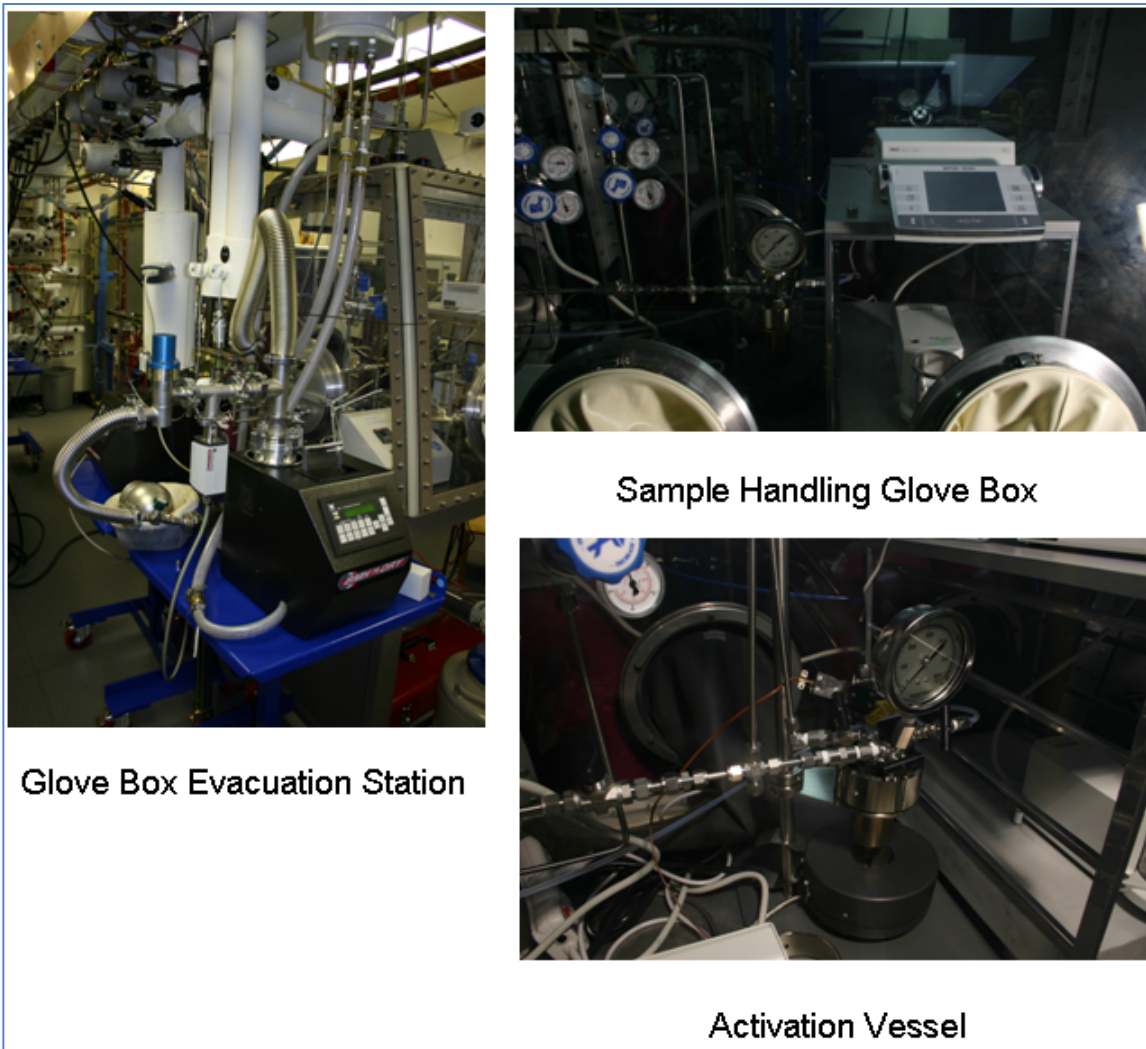


Figure 6-13: Glove box (Ar) and associated evacuation station used to pre-condition and transfer sensitive samples to and from analytical stations.

6.5 Full-Scale Laboratory Facility

The intrinsic properties of storage materials, and in particular that of framework sorbents, measured in the small-scale research laboratory seldom, if ever, scale with equal or similar performance at the system level. Consequently, the development of materials for a storage system cannot be achieved as an insular effort, rather it must be approached at the system level in order to account for and develop a comprehensive understanding of all the engineering factors that collectively affect the net performance of the storage material while accessing usable

hydrogen from the storage system. Therefore, an ability to assess the engineering requirements for full-scale storage systems (≥ 5 kg H₂ per fill), and the effects that storage material engineering (*i.e.*, densification, packing structure, additives, embedded heat exchangers) may have on the net in-tank properties under real-world testing conditions was needed.

A full-scale laboratory (Fig. 6.14) was designed and constructed at SwRI, in close proximity to the small-scale laboratory described above, to characterize complete storage system performance for vehicles. The analytical objectives of this facility were to: (1) conduct (a) adsorption/desorption cycling experiments to assess lifetime performance; (2) determine refueling time; (3) assess the resistance to exogenous contaminants; (4) quantify the specific energy contained in the storage system and its degradation over the system's life cycle; and (5) perform impact, vibration, and fire resistance tests on the storage system under qualified national and international standards.

The principal safety features of the full-scale laboratory consisted of both primary and secondary containment systems for the storage system, as indicated in Fig. 6.14, and a dedicated, remotely operated laboratory building monitored continuously for hydrogen release. The secondary containment consists of three "bunker" wells, constructed from 24-inch diameter, schedule 40 steel pipes placed in three vertical, 48-inch diameter by 15-foot deep holes. The annulus of the secondary containment was filled with 4,000 psi concrete during construction. A 15' x 15' x 0.5' (thick) reinforced pad was then poured around the vertical containments as a working platform. This design was determined to provide adequate containment in the event of an energetic event during testing of storage systems.

A fully-instrumented storage system is placed in a primary containment system. This primary system typically consists of a flanged, thick-walled stainless-steel vessel that is designed on a case-by-case basis to accommodate gas and vacuum-line inlets/outlets, heat exchanger outlets/inlets, and feedthroughs for monitoring sensors (*e.g.*, thermocouples, gas analysis, strain sensors). The storage system is first sealed in the primary containment system, and the test package is then lowered into one of the three secondary containments.

Storage system performance metrics can be determined adiabatically, but in most cases isothermal conditions are achieved during testing using a high-capacity heat exchanger located outside the laboratory facility. The storage capacity of the system and its mass balance are quantified using Coriolis mass-flow meters, which are capable of achieving the fast-fill rates of the testing protocol (~ 1 kg H₂ /min), yet are sensitive enough to quantify hydrogen desorption from the storage system during cyclic tests.

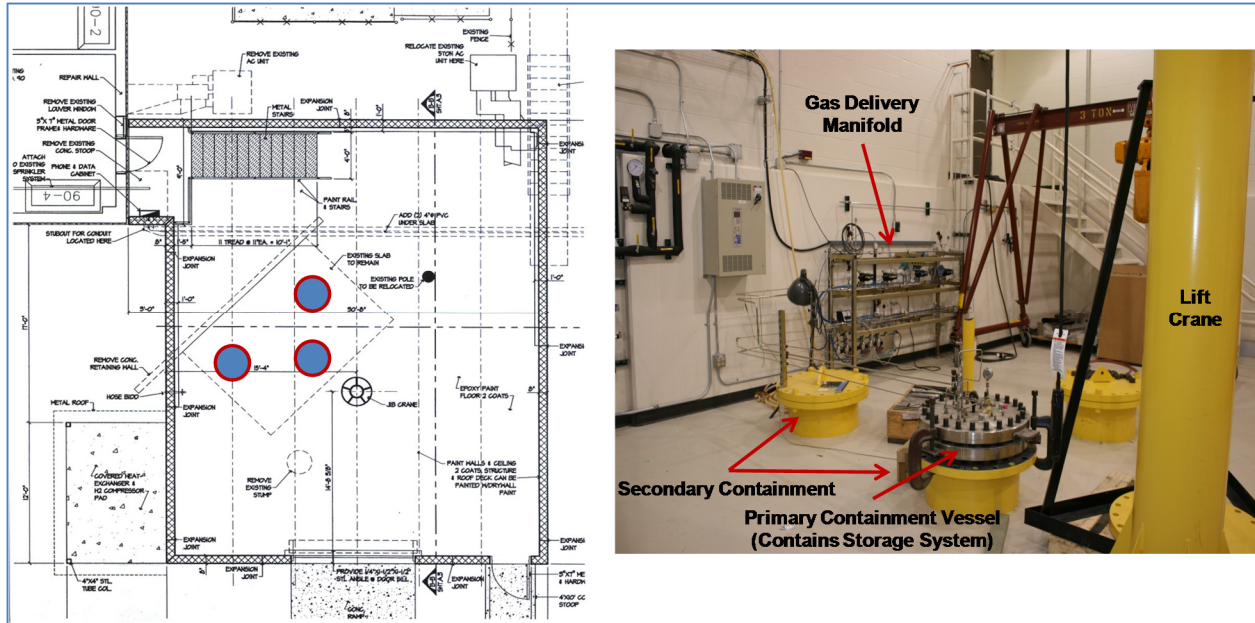


Figure 6-14: Laboratory facility for evaluating full-scale storage systems. Left – Top-view layout of laboratory showing locations of secondary containment bunker wells. Right – Image of laboratory showing primary and secondary containment systems. Storage system is contained inside the primary containment vessel.

6.6 Safety Analysis and Implementation

In an effort to systematically anticipate and eliminate potential hazards and failures that can affect the well-being and safety of workers, and potentially cause adverse effects on laboratory and facility system hardware, SwRI has employed several industrial rules and has followed the guidelines offered in the 1996 DOE Handbook, Chemical Process Hazards Analysis, DOE-HDBK- (February 1996).

The primary two rules referenced are the OSHA Process Safety Management (PSM) rule (29 CFR1910.119) and EPA’s Risk Management Plan (RMP) rule (40 CFR 68) Process Safety Management (PSM). Within these reference materials reside the basis for a comprehensive and thorough Process Hazards Analysis (PrHA). SwRI’s PrHA consisted of several methods. The common elements of these methods included analysis pre-planning through accident history cases, appointing appropriate PrHA team membership (management to technicians, subcontractors), developing a systematic process to identify and control hazards, understanding engineering controls and interrelationships, looking at the influence of facility location with

regard to adjacent activities and processes, studying the impact of human factors and quantification of failure effects on resources. The outcome of the PrHA has been used to modify safety-system hardware in the laboratory facilities, or implement new ones, as well as incorporate procedures and system checks into the SOPs and test protocols.

An external safety review of the laboratory facilities was initially conducted to fulfill the goals of the PrHA. A review team consisting of members from DOE's Hydrogen Safety Review Panel, formed in 2004 to integrate safety procedures into hydrogen-related DOE projects, was invited to conduct a site visit and critical audit of safety systems, protocols, and potential vulnerabilities associated with the laboratory facilities and its analysis activities. The members of the panel who participated in the external review were:

Addison Bain, NASA (ret.), Chair, Hydrogen Safety Review Panel.

Harold Beeson, Project Manager, NASA, White Sands, Member, Hydrogen Safety Review Panel Member.

Richard Kallman, City of Santa Fe Springs, Hydrogen Safety Review Panel Member.

The review panel issued a list of recommended improvements in safety based on their findings, which were considered by SwRI and corrective actions were taken accordingly, where needed. Some of the key safety features of the Laboratory's final configuration include:

- A continuous, flow-monitored central exhaust line for venting hydrogen safely outside the laboratory.
- Hydrogen sensors at various locations in and outside the laboratory interfaced with an emergency ventilation system. The lower trigger, 10% of the lower flammability limit (LFL) for hydrogen, will cause an alarm to be sounded. At 20% of LFL, the monitoring system shuts-off all valves in laboratory and activates a high-speed exhaust system.
- Velocity fuses are present on both the hydrogen and helium lines as they enter the laboratory. These valves fail closed when excessive flow conditions occur and cannot be reopened until pressure is equalized on both the inlet and outlet sides.
- A high-sensitivity hand-held hydrogen detector (Sensistor, Inc., Model H2000) to check fitting connections and other high-pressure components for possible leaks. A base unit for the same detector also continuously monitors various locations of the laboratory which serves as an early warning alarm.

The Laboratory has employed a “best practices” approach based on SOP-documented analytical methods to critically evaluate novel storage materials of potential impact to the sought-after storage goals. The principal objectives of developing such standard protocols have been to: (1) assure that laboratory operations are performed in a safe manner; (2) provide for precision hydrogen sorption measurements performed in a repeatable manner; and (3) provide for a clear understanding of the methods used within the facility.

Validating the sorption behavior of storage materials and uncovering the mechanisms involved have been approached through close collaboration with researchers among the MCoE (e.g., the HSCoE), the international community, and SwRI’s Internal Research & Development Program (Fig. 6.15). To address the best practices objectives of the Laboratory, SOPs have been developed for the submission of samples to the Laboratory, and the validation/qualification of the sorption properties of promising storage materials using volumetric sorption analysis, gravimetric sorption analysis, and/or thermal desorption mass spectrometry analysis. These standards were initially qualified based on the positive outcome of Round-Robin Testing, which demonstrated that the Laboratory results (*i.e.*, isotherm sorption curves) fell well within the variance of the predominantly-grouped trend of measurements among the participating laboratories. The latest revisions of the SOPs are given in Appendix D.

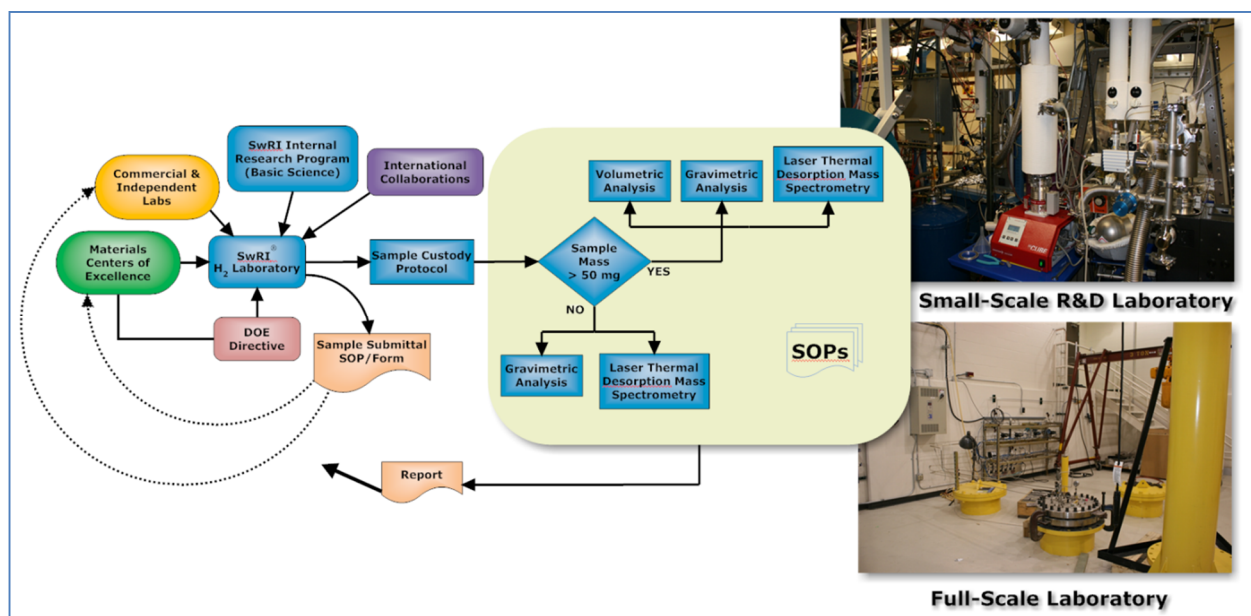


Figure 6-15: Overall scheme of laboratory operations: interactions, analyses under qualified standards, and reporting process.

7

SUMMARY AND HIGHLIGHTS OF MEASUREMENT RESULTS (2005-2011)

7.1 Overall Summary of Results

Promising classes of materials developed under the program for reversible on-board hydrogen storage have emerged from the MCoE (Fig. 1.2), thus compelling a rigorous and independent evaluation of their storage capacity, thermodynamics, and kinetics. Occasionally, entirely new chemistries or structural motifs were discovered that yielded unexpected properties which were further studied or validated. Notably, metal organic frameworks (MOFs), spillover compounds of MOFs, and non-crystalline porous polymer networks (PPN), are examples of materials exhibiting surprisingly favorable storage properties which approach the sought-after material targets for on-board storage.

To place the overall results into the proper perspective relative to the storage targets on a materials basis, the hydrogen capacities validated by the Laboratory are plotted in Fig. 7.1 against the temperature at which the peak sorption capacity was observed, delineated by three modalities of hydrogen uptake: physisorption, spillover, and chemisorption. The numerical data are further summarized in Table 7.1.

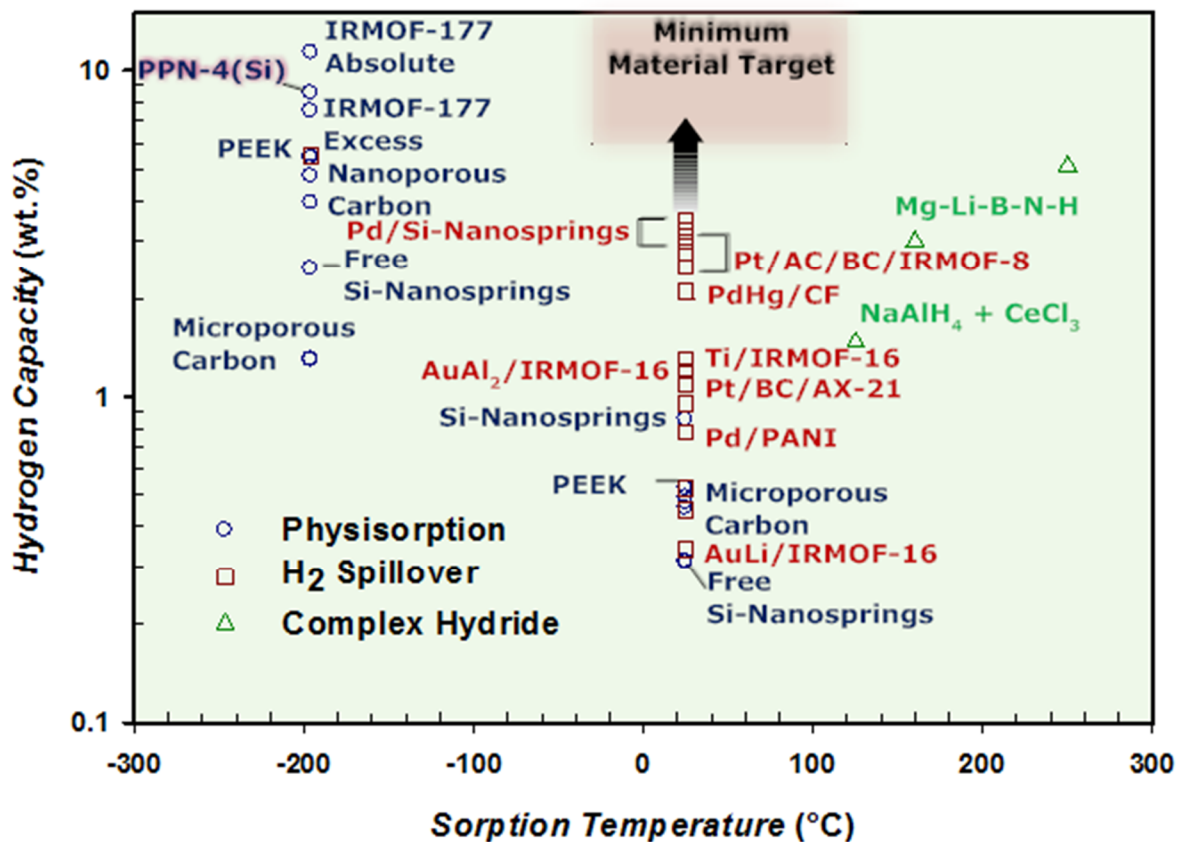


Figure 7-1: The relative performance of physisorption, spillover, and chemisorption (complex hydride) materials towards achieving the minimum material-based targets for on-board reversible fuel storage.

Table 7.1: Summary of the hydrogen storage capacities determined by the Laboratory for prospective physisorption, spillover, and chemisorption (color-coded, respectively), including reference materials for RRT studies. The equilibrium pressure at which the peak capacity was observed is given in brackets. Measurement results of proprietary storage materials from private or commercial entities outside the DOE program are omitted.

Storage Material	Source	Peak Excess Gravimetric Capacity (wt.% H)		Absolute Volumetric Capacity (g/L) 77 K
		298 K	77 K	
MOF-177	UCLA	0.42 [67 bar]	7.50 [70 bar]	47 [70 bar]
CO ₂ -Activated PEEK-Derived Carbon	Duke University	0.52 [80 bar]	5.39 [55 bar]	29 [70 bar]
PEEK-Derived Carbon	SUNY	0.31 [81 bar]	5.50 [49 bar]	38 [71 bar]
Microporous Carbon	NREL	0.49 [80 bar]	4.75 [45 bar]	28 [70 bar]
Porous Polymer Network [PPN-4(Si)]	TAMU	0.97 [92 bar]	8.48 [60 bar]	28 [86 bar]
Carbosieve SIII	U. Tenn.	0.47 [79 bar]	ND	ND
Nanostructured Carbon (SWNT)	RRT-USA	0.43 [75 bar]	2.81 [71 bar]	ND
Microporous Carbon	RRT-USA	0.49 [71 bar]	4.37 [58 bar]	ND
Microporous Carbon	RRT-EU	0.46 [80 bar]	1.29 [13 bar]	ND
Nanoporous Carbon	Mich. Tech.	ND	3.94 [24 bar]	ND
Nanoporous Carbon / PZT	Mich. Tech.	ND	3.84 [24 bar]	ND
Pt/SWNT	NREL	2.78 [Desorb]	ND	ND
Pt/AC/BC/IRMOF-8	INER	2.50 [75 bar]	ND	ND
Pt/BC/AX-21	U. Mich.	1.10 [74 bar]	ND	ND
Pd/Carbon Foam	NCSR (EU)	2.1 [88 bar]	ND	ND
Pd/Polyaniline (PANI)	UNLV	0.80 [73 bar]	ND	ND
Ti-IRMOF-16	SwRI	1.30 [80 bar]	ND	ND
AuAl ₂ -IRMOF-16	SwRI	1.10 [80 bar]	ND	ND
Pd/Si-Nanosprings	WSU, GoNano, Inc.	3.00-3.46 [66 bar]	ND	ND
RRT – Spillover Sample [†]	NREL	0.52 [82 bar]	5.48 [40 bar]	ND
Mg-Li-B-N-H [‡]	USF	5.1 [243 K, 75 bar]	ND	ND
NaAlH ₄ + CeCl ₃	RRT-EU	1.47 [398 K, 43 bar]	ND	ND

Table 7.1 Notes: PEEK = polyether ether ketone; SWNT = single wall carbon nanotube; PZT = piezoelectric transducer immersed in microporous carbon; Pt/AC/BC/IRMOF-8 = Pt supported on activated carbon and combined with a bridging compound (BC), which is then combined with the “receptor” IRMOF-8 (an isorecticular metal organic framework); X-IRMOF-16 = IRMOF-16 in which the void space of the MOF framework is intercalated with X; RRT = Round-Robin Testing; [†]Reference sample known to exhibit hydrogen spillover effects, but whose composition was not revealed; [‡]A complex, ternary hydride consisting of MgH₂/LiBH₄/LiNH₂.

Upon completing and qualifying a state-of-the-art laboratory facility in 2005, SwRI proceeded to evaluate materials of major importance to the program and whose validation of hydrogen uptake was regarded as high-priority within the DOE solid-state storage community. The most important outcomes of that endeavor are highlighted below.

7.2 Highlight 1 – Validation of Hydrogen Sorption Capacities in Pure and Catalytically-Doped SWNTs

Early in this program, pure and catalytically-doped single wall carbon nanotubes (SWNTs) were given highest priority for evaluation by the Laboratory due to the need to resolve confounding data previously reported on the apparent storage capacities of these materials. The results provided by the Laboratory helped to guide DOE in focusing research and development efforts on the most promising materials, culminating in a decision not to invest additional resources on pure SWNTs as candidate materials for hydrogen storage [69, 70]. However, as was discussed in Section 2.2, catalytically-doped SWNTs were shown to exhibit potentially useful hydrogen binding interactions and, therefore, merited further exploration within the HSCoE (Appendix B).

7.3 Highlight 2 – Establishment of Analytical and Material Benchmarks for Low-Density, High Surface-Area Storage Materials

In contrast to the stagnant levels of performance of pristine carbon materials, synthetic framework materials like MOFs have evolved in measured performance much more rapidly than zeolites or even nanoporous carbon materials principally due to the relative ease with which topology and other properties can be engineered into their structural motifs, starting from a large selection of structural building units and employing systematic methods for synthesis. Both the volumetric and gravimetric energy densities of a cross section of different framework materials have steadily increased as a consequence of a concerted effort to design structural motifs that result in higher specific surface areas and stronger van der Waals binding interactions between hydrogen molecules and the building units of the framework than the materials that preceded them.

It was previously reported that MOF-177 (Fig. 7.1) could store 7.5 wt% hydrogen with a volumetric capacity of 32 g L^{-1} at 77 K and 70 bar [7]. These results were exciting because, at the time, this MOF represented the highest hydrogen uptake of any porous material and clearly showed that in principle the DOE targets could be achieved, albeit at 77 K. In light of these developments and the extensive work being done on MOFs, this work sought to establish MOF-177 as a benchmark for researchers in the field.

The importance of this effort can be appreciated from the fact that measurements of hydrogen storage in highly porous, low density materials, particularly at low temperatures, had traditionally suffered from unreliable methods and erroneous results. Accordingly, independent measurements of hydrogen uptake were performed between the Laboratory and UCLA (Yaghi group) to verify hydrogen uptake measurements reported for MOF-177 [71].

MOF-177 has been deemed an ideal material to use as a benchmark for hydrogen adsorption measurements for the following reasons: (1) it has high gravimetric and volumetric uptake capacity; (2) its synthesis is simple and highly reproducible; and (3) it has a crystalline structure that is well-characterized in atomic connectivity and chemical composition. In this collaboration, two independent investigations were undertaken to assess the H₂ saturation uptake on MOF-177 samples using volumetric and gravimetric techniques. The validity of MOF-177 as a benchmark material was shown (Table 7.1) based on the complementarity between volumetric (7.5 ± 0.1 wt%) and gravimetric (7.3 ± 0.1 wt%) H₂ adsorption measurements at 77 K, which were in agreement with a previous report (volumetric data, 7.5 ± 0.1 wt%) [5]. The complete isotherm curves are shown in Fig. 7.2, and experimental details can be found in [71].

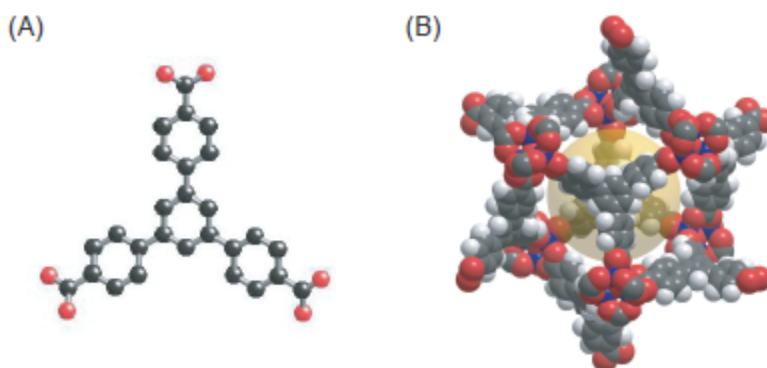


Figure 7-2: (A) Molecular structure of 4,4',4''-benzene-1,3,5-triyl-tribenzoic acid (BTB) linker and (B) crystal structure of MOF-177. An approximately spherical pore is shown as large sphere of 17 Å in diameter. Reproduced from [71].

To estimate the absolute amount of gas adsorbed, the thickness of the adsorbed layer must be known. However, this variable, and its spatial profile, cannot be measured experimentally. Instead, the absolute adsorption can only be estimated theoretically using, for example, Monte Carlo simulations [72]. Although the surface excess mass is a useful concept, from the viewpoint of hydrogen storage, the total amount that a material can store has been found to be more relevant to use for hydrogen as a fuel. However, at high temperatures and pressures (*i.e.*, above the critical temperature and pressure of hydrogen), the density profile of the adsorbed

phase becomes more diffused and, therefore, it is not possible to distinguish between the adsorbed and bulk phases. In this situation the surface excess is the only experimentally accessible quantity, and there is not a reliable method to estimate the absolute adsorbed amount with high accuracy, although many efforts have been devoted to resolve this issue [73]. Therefore, the absolute amount of hydrogen adsorbed is estimated using a simple equation [74, 75]:

$$N_{\text{abs}} = N_{\text{ex}} + \rho_{\text{bulk}} V_{\text{pore}} \quad (7.1)$$

where N_{abs} is the absolute adsorbed amount, N_{ex} is the surface excess amount, ρ_{bulk} is the bulk density of H_2 , and V_{pore} is pore volume for MOF-177. For crystalline materials such as MOFs, the hydrogen-accessible pore volume can be determined from Monte Carlo simulation or estimated from classical void-filling computations of the unit cell using the kinetic diameter of hydrogen (2.6 Å).

From an engineering perspective, an integrated storage tank on a vehicle would be bounded by a lower limit in pressure of 1.5 bar to accommodate the inlet pressure requirements of a fuel cell (Note: the DOE target is 3.0 bar, but a slight upward temperature swing may be used below this limit to extract additional hydrogen at the required pressure). Since the absolute adsorbed amount would constitute the total extractable hydrogen from the tank, it has been proposed that an alternative metric for achieving the DOE target should be defined on the basis of the total amount of delivered H_2 (e.g., an absolute adsorbed amount ranging from 1.5 to 100 bar), instead of a simple surface excess mass of H_2 .

Table 7.2: Summary of high-pressure H₂ adsorption measurements of MOF-177 (all values ± 1% SD).

Analysis	Surface Area ^a (m ² /g)	Surface Excess Amount (Pressure)			Absolute Adsorbed Amount (Pressure)			Method
		(wt.%)	(g/L)	(bar)	(wt.%)	(g/L)	(bar)	
SwRI 1	5640 (4750)	7.6	32	(66)	11.2	48	(72)	Volumetric
SwRI 2	5640 (4750)	7.4	32	(57)	11.5	49	(72)	Volumetric
UCLA	5250 (4630)	7.3	31	(52)	11.1	48	(75)	Gravimetric
UM ^b	5640 (4750)	7.5	32	(69)	11.4	49	(78)	Volumetric

^aLangmuir model (BET model). ^bData from ref. [5]

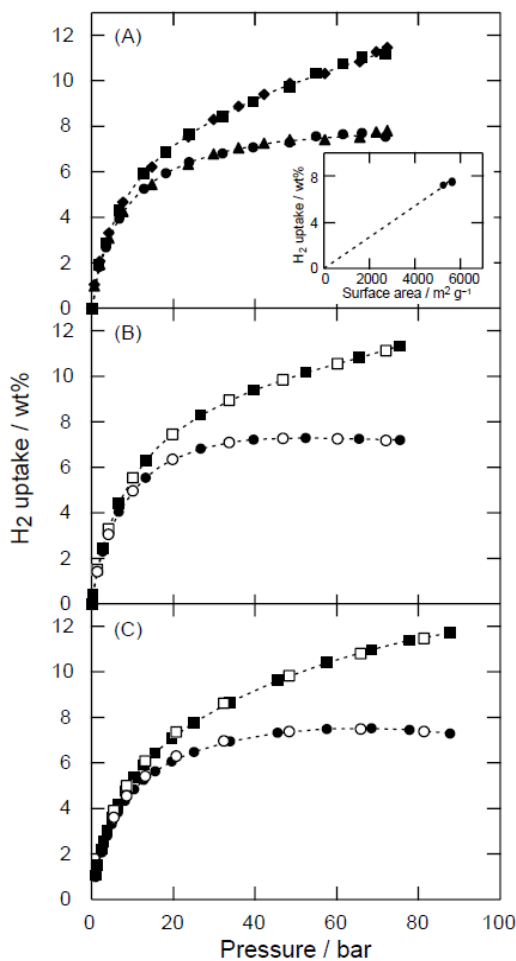


Figure 7-3: High-pressure H₂ isotherms for MOF-177 taken by volumetric (A) and gravimetric (B) methods. As a reference, volumetric data is shown in (C). Filled and open symbols represent adsorption and desorption branch, respectively. Squares symbols are absolute adsorbed amounts. Inset: surface area dependency of H₂ uptake.

7.4 Highlight 3 – Validation of Hydrogen Spillover Effects in Catalytically-Doped MOFs

Yang and coworkers [76] previously reported excess uptake of hydrogen at room temperature via spillover in catalytically-doped amorphous and crystalline substrates. The best results obtained by these researchers involved a platinum (Pt) catalyst supported on activated carbon (AC), which in turn was coupled to an isoreticular metal organic framework (IRMOF-8) via a bridging compound (BC) composed of amorphous carbon.

The mechanism proposed for these Pt/AC/BC/IRMOF-8 heterostructures can be summarized concisely: (1) adsorption of dihydrogen on the Pt surface; (2) dissociation of dihydrogen and chemisorption of atomic hydrogen on the surface; (3) migration of atomic hydrogen onto the AC support; and finally (4) chemisorptive spillover onto the IRMOF-8 substrate. Spillover was reported to be facilitated by the amorphous-carbon bridging compound between the Pt/AC complex and the IRMOF-8 substrate. It has been postulated [77] that modification of any of the elements of these heterostructures (*e.g.*, choice of IRMOF) could lead to improved storage under near ambient conditions. While this mechanism may be endothermic ($BDE(H_2) = 4.5 \text{ eV}$) [78], higher than expected uptake was observed to occur reversibly at room temperature.

In order to assess critically the viability of hydrogen-storage materials predicated upon spillover, the Laboratory sought to independently validate the effect in Pt/AC/BC/IRMOF-8 and develop a better understanding of the underlying spillover mechanism. Accordingly, small batches of this compound were synthesized and then provided to the laboratory by two independent groups, U. Michigan and INER, each of whom used similar procedures for their synthesis.

The seminal results of Yang were successfully validated by the Laboratory using gravimetric analysis. Fig. 7.3 illustrates the room-temperature isotherms for the Gibbs excess adsorption measured from Pt-doped carbon-bridged IRMOF-8 (sample prepared by INER). These results were remarkably similar to those previously published [76], confirming linear hydrogen uptake to 2.5 wt.% at 75 bar. It is important to note that both laboratories observed exceedingly slow uptake kinetics to the extent that equilibration times for each pressure point in the isotherm was typically greater than five hours. Moreover, these observations were consistent with a hydrogen spillover mechanism as proposed earlier if one considers that the rate-limiting step may be attributed to the migration of atomic hydrogen away from catalytic centers while encountering sufficiently stable binding configurations in the framework.

Additional insights into the nature of specific binding interactions within the doped IRMOF-8 compound (sample prepared by U. Michigan) were gained from the LTDMS spectrum [46]. As illustrated in Fig. 7.4, it was evident from these measurements that multiple binding sites for hydrogen occur in the framework between 263 and 298 K, which were clearly higher in

energy than the physisorption peak occurring at 163 K. These results provided the first direct evidence for energetically favorable binding interactions in a doped MOF compound at room temperature.

Complementing the experimental results, *ab initio* calculations were also carried out at the level of Hartree-Fock (HF) and density functional theory (DFT) to elucidate the thermodynamics for the addition of dihydrogen to the organic linker (i.e., receptor) in IRMOF-8, naphthalene-2,6-dicarboxylate (NDC). The DFT calculations predicted the first addition of H₂ to be mildly endothermic, corresponding to the disruption of the quasi-aromatic naphthalene system, across the 1 and 4 positions. The second addition across the 2 and 3 positions were computed to be exothermic as there is not aromatic penalty to be paid. Overall, the theoretical results have suggested the thermochemical plausibility of the spillover mechanism and offer upper limits for chemisorptive uptake in these materials [46].

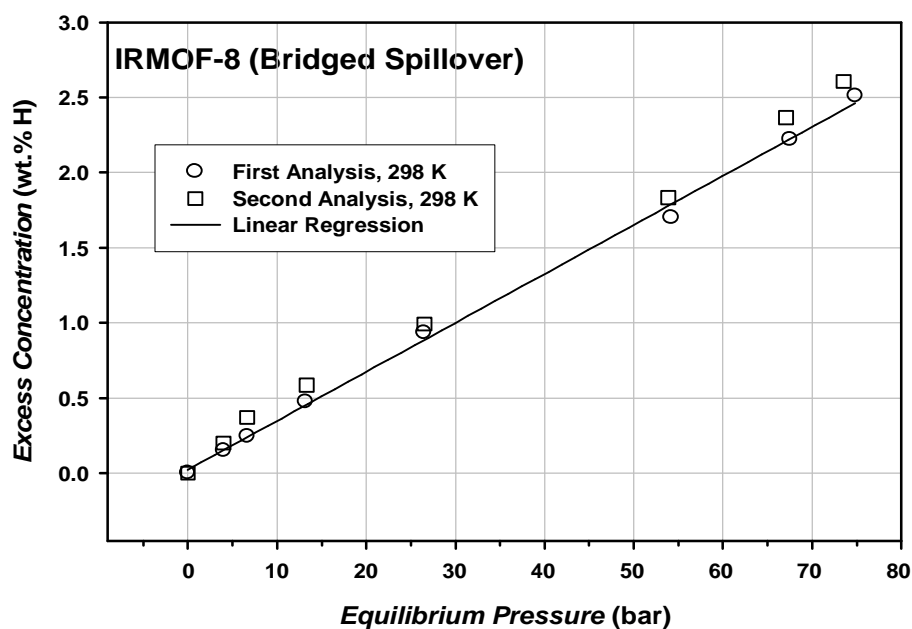


Figure 7-4: High-pressure gravimetric sorption isotherm measured for Pt/AC/BC/IRMOF-8 (from INER) at room temperature [46].

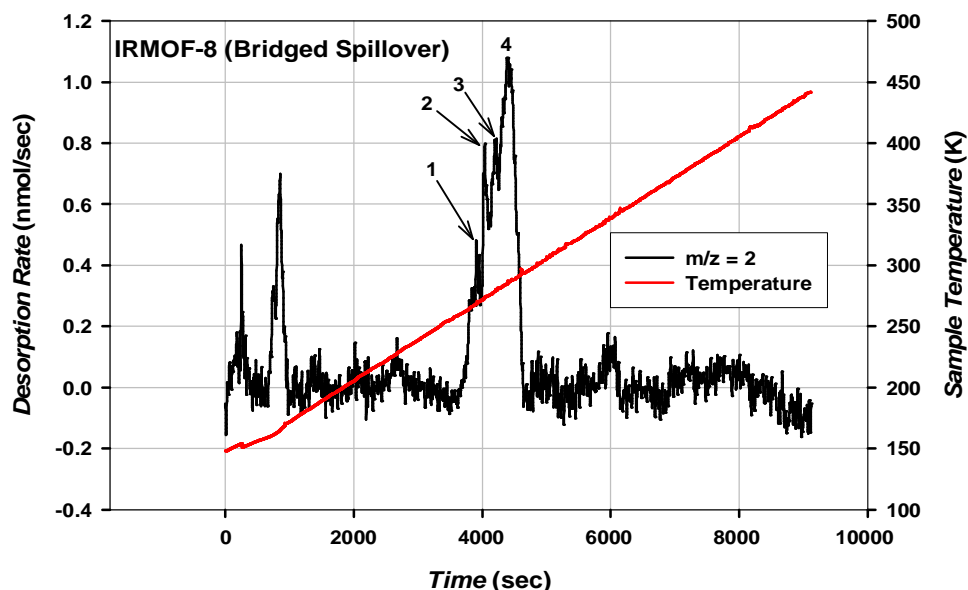


Figure 7-5: LTDMS profile measured for Pt/AC/BC/IRMOF-8 (from U. Mich.) at room temperature [46].

7.5 Highlight 4 – Validation of Record-Setting Hydrogen Physisorption in Non-Crystalline Porous Polymer Network (PPN)

A significant amount of experimental and modeling effort was dedicated to the analysis of a PPN based on tetrakis(4-bromophenyl)silane building units [PPN-4(Si)] developed by H-C Zhou's group at TAMU [79]. This material was previously shown to exhibit exceptionally-high BET specific surface areas (6,470 m²/g) with a correspondingly-high gravimetric excess capacity (8.5 wt% at 60 bar) at 77 K: the highest surface area and hydrogen uptake reported to date for a physisorption material.

As in the previous cases for highly active, high surface-area physisorption materials, high-pressure volumetric analysis of PPN-4(Si) was encumbered by this material's propensity to absorb helium, thus invalidating the use of a helium calibration for determining the skeletal density of the sample (or free volume of the system). Therefore, accurate measurement of the true Gibbs excess concentration and subsequent determination of the absolute volumetric capacity would lead to erroneous results.

To overcome the challenge of helium adsorption, the high-pressure gravimetric technique was employed at room temperature as a complementary method to derive the skeletal density of the material and the volume of the adsorbed layer. In this approach, one assumes in the formal

definition of the Gibbs excess that the free energy of the adsorbed fluid is equal to the bulk-gas free energy plus a surface potential term. When this definition is equated to the measured Gibbs excess for the gravimetric mass balance, a simplified local density (SLD) model can be derived.

In the SLD model, the Bender equation state (BEOS) is first used to accurately calculate hydrogen gas densities and the gas fugacity. The combined expressions for the SLD model and BEOS were used in a fitting algorithm to derive the hydrogen skeletal density and the pore volume of the sample by treating these characteristic properties as fitting parameters [54, 71].

The room temperature gravimetric hydrogen isotherms for the Gibbs excess are compared in Fig. 7.5 with analyses using the volumetric technique at room temperature. The two results were shown to correlate very well after correcting the volumetric measurements for the SLD-derived skeletal density.

The same SLD-derived skeletal density was used to correct low-temperature hydrogen isotherms. After taking into consideration thermal gradient effects, the corrected hydrogen isotherm curves derived from the analyses are represented in Fig. 7.6. The maximum Gibbs-excess concentration at 77 K was 8.5 wt%, which occurred at 60 bar and is higher than the benchmark material, MOF-177 (Table 7.1). Moreover, these results were determined to be consistent with those previously reported by the TAMU team, thus validating the exceptional performance of PPN-4(Si).

Additionally, the absolute volumetric capacity was estimated using the SLD-derived skeletal density and adsorbed volume (i.e., pore volume). A value of ~28 g/L absolute volumetric capacity was calculated at 85 bar (77 K). Since the material is completely amorphous, the absolute data cannot be verified theoretically using void-space routines and the kinetic diameter of hydrogen (or helium) for comparison.

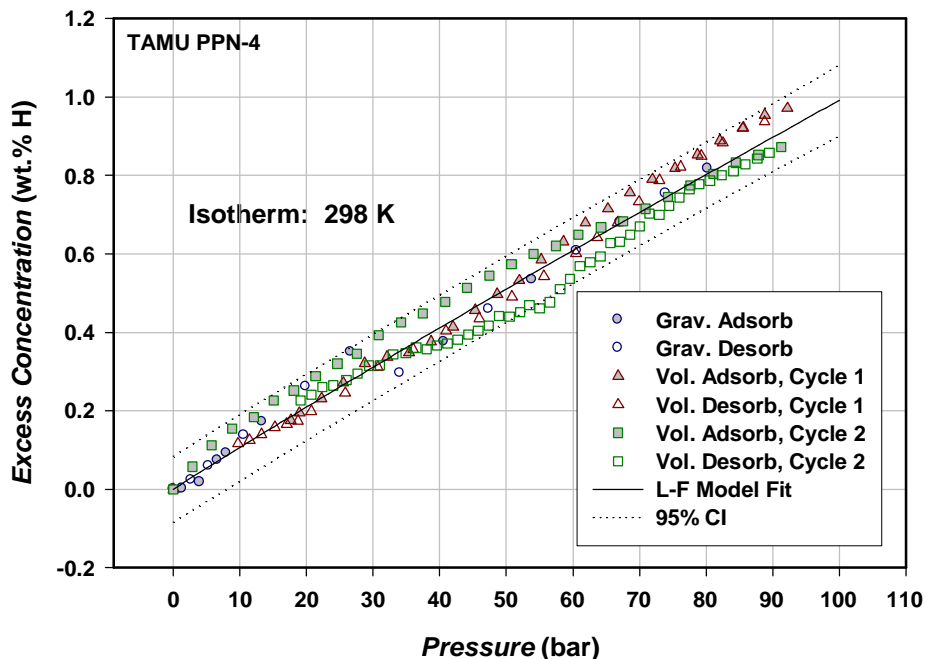


Figure 7-6: Room temperature (298 K) hydrogen isotherms measured for porous polymer network [PPN-4(Si)] using both the volumetric and gravimetric techniques.

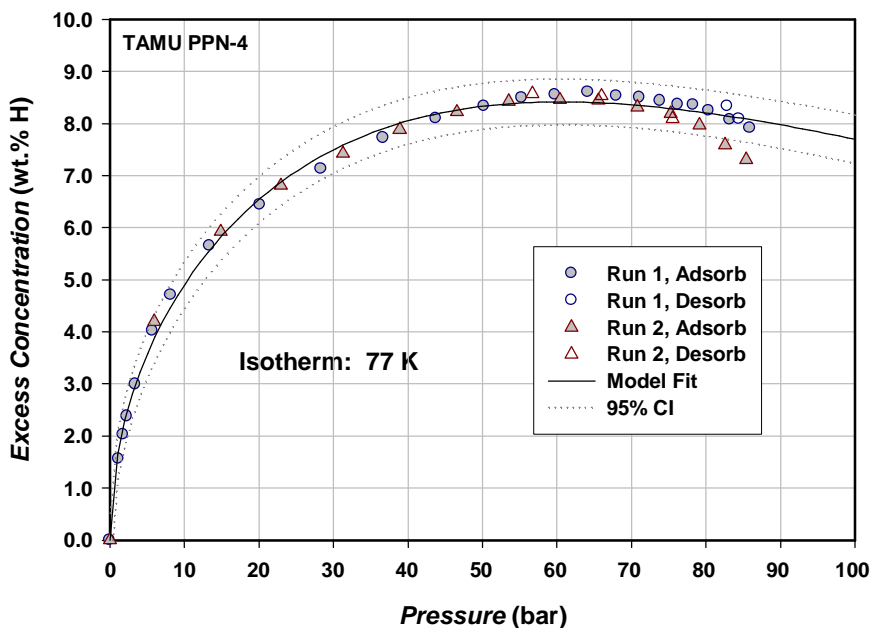


Figure 7-7: Low-temperature (77 K) hydrogen isotherms measured for porous polymer network [PPN-4(Si)] using the volumetric technique.

8

LESSONS LEARNED

The Laboratory was established to ensure that the performance criteria of every element of its activities conformed to the highest standards and has strived to achieve the most precise, sensitive, and accurate measurements in characterizing hydrogen storage materials and systems for the DOE, academia, and industry. To ensure that these goals could be achieved, Round-Robin testing in collaboration with several other participant laboratories in the US has proved to be an exceedingly valuable exercise before qualifying the Laboratory for official operation. Beyond this initial qualification, additional RRT studies were completed during the lifetime of the program and have been essential in demonstrating the long-term conformance to accurate standards and gaining credibility among the storage community.

The three central analytical capabilities for hydrogen sorption measurements – gravimetry, monometry, and laser thermal desorption mass spectrometry – have been validated according to prescribed standard protocols developed under this program. However, a significant amount of effort has been dedicated to refining both hardware and procedures to accommodate small sample weights and improve accuracy and precision in the measurements over the broad temperature regimes typical of physisorption and chemisorption hydrogen uptake. In particular, nano-structured materials for physisorption, such as SWNTs and MOFs, initially presented several analytical challenges relative to accuracy and precision when attempting to quantify hydrogen uptake at low temperatures (77 K) using high-pressure volumetric analysis (monometry).

Two important goals, or lessons learned, toward the design of a high quality volumetric sorption experiment at low temperature were to minimize the ratio of the free volume to the sample volume, and to minimize fluctuations in the thermal gradients that arise in the free gas space of the system. It was found that as a consequence of near-critical-point and supercritical effects, small thermal perturbations in the free-volume gas space from the external system caused uninhibited fluctuations of volume or density in the system, which were reflected as pressure fluctuations by the pressure transducers of the instrument. Therefore, in the particularly sensitive phase region near the critical point, it has been important to reduce this ratio to such an extent that the susceptibility of the free volume to density fluctuations is significantly limited, and the consequent pressure fluctuations fall below the resolution of the transducers. Related to these effects, the degree of compaction of the sample also has been found to be an important factor in

achieving sorption isotherms consistent with what would be theoretically predicted. Hence, special consideration has been given to optimizing the configuration of the sample vessel and the manipulation of the sample itself so that these effects are minimized in low temperature volumetric analyses, and so reproducible, accurate results can be derived from measurement of nano-structured materials.

Measurement of the Gibbs excess of adsorption for nano-structured materials at high pressures using static thermogravimetric analysis (gravimetry) was principally challenged by suitable methods for correcting the buoyancy of the sample in a dense gas. Compensating this effect by calibrating the system with helium has been found to be problematic for samples of very high surface area as they tend to adsorb helium. Three buoyancy correction techniques have therefore been adopted to accommodate the unique requirements of measuring hydrogen sorption in nano-structured materials. These techniques evince different levels of sophistication depending on whether helium can be used as a calibration gas: (1) a simple equation of state (SEOS), which employs helium as a calibration gas; (2) reference material correction, which uses an inert material (e.g., pure Si) and hydrogen gas; and, (3) the Bender equation of state (BEOS), which uses a highly refined form of the Bender equation to calculate the bulk density of hydrogen over a very broad pressure and temperature regime. Combining BEOS with the simplified local density model (SDL) via a fitting procedure and the gravimetric technique has proven to be the most accurate and reliable method of determining the skeletal density of the sample and the volume of the adsorbed layer. The central lesson has been that the quality and accuracy of volumetric technique are significantly enhanced by deriving these critical parameters using the gravimetric technique.

Contrary to the *status quo* opinion among a number of researchers in the storage community during the formative years of the program, the LTDMS technique (a.k.a., TPD) has proven to be invaluable in three respects: (1) high sensitivity, thus enabling measurements on small sample weights (< 50 mg); (2) high thermal resolution, providing a means of delineating multiple binding interactions between hydrogen and the storage material; and, (3) identification of desorbed species, allowing for the detection of internal conversion processes, such as the formation of water, in the material. For example, the high sensitivity and thermal resolution of the technique were central to detecting and validating high-energy binding sites in spillover materials involving carbon (e.g., SWNTs) and MOFs as receptors. In the case of spillover compounds using carbon foam as a support (receptor), the LTDMS technique showed conclusively that water was liberated from this storage material as a side reaction of spillover owing to the catalytically-mediated internal conversion of oxygen functional groups with spilt hydrogen. These findings provided a sound explanation for the large variances observed in gravimetric and volumetric sorption measurements.

9

PUBLICATIONS, CONFERENCE PRESENTATIONS, AND PATENTS

1. M.A. Miller and R.A. Page, “National Testing Laboratory for Solid-State Hydrogen Storage Technologies,” NHA National Hydrogen Conference, Washington, DC, March 29 – April 1, **2005**.
2. M.A. Miller and N. Sridhar, “Measurement and Prediction of Material Performance Subject to Hydrogen Exposure,” Hydrogen Gas Embrittlement Workshop, ASTM T.G. 01.06.08, ASTM Meeting, Reno, NV, May 17, **2005**.
3. M.A. Miller, “Development and Application of Standard Methods for Quantifying Hydrogen Sorption in Nanostructured Materials,” Taiwan Symposium on Hydrogen Storage in CNMs, Institute of Nuclear Energy Research (INER), Taipai, Taiwan, Oct. 18-19, **2005**
4. M.A. Miller and G.N. Merrill, “Laser Desorption Mass Spectrometry and Atomistic Modeling of Hydrogen Physisorption on Alloy-Doped Nanostructures,” *Federation of Analytical Chemistry and Spectroscopy Societies (FACSS)*, 33rd Annual Meeting, Sept. 24-28, **2006**.
5. M.A. Miller, K.E. Coulter, and J.H. Arps, “Nanoengineered Material for Hydrogen Storage,” US Patent Application 11/615,572, Filed December 22, **2006**.
6. M.A. Miller and K.E. Coulter, “High Aspect Platelets as Synthetic Platforms for Nano-Engineered Hydrogen Storage Materials,” NHA Annual Hydrogen Conference, March 19-22, **2007**.
7. H. Furukawa, M.A. Miller, and O.M. Yaghi. “Independent Verification of the Saturation Hydrogen Uptake in MOF-177 and Establishment of a Benchmark for Hydrogen Adsorption in Metal-Organic Frameworks.” *J. Mater. Chem.* 17, 3197, **2007**.
8. M.A. Miller and G.N. Merrill, “The Potential Role of Surface Plasmons in Molecular Adsorption and Transformation,” 63rd Southwest Regional Meeting of the American Chemical Society, Lubbock, TX, Nov 4-7, **2007**.
9. G.N. Merrill and M.A. Miller, “Ab Initio Investigations of Hydrogen Chemisorption on Isorecticular Metal Organic Frameworks,” 63rd Southwest Regional Meeting of the American Chemical Society, Lubbock, TX, Nov 4-7, **2007**.

10. M.A. Miller, R.E. Page, and G.N. Merrill, "Platelet Heterostructures for Solid-State Hydrogen Storage," European Commission's 18-Month Meeting on Novel Efficient Solid-Storage of Hydrogen (NESSHY), Dübendorf, Switzerland, June 18-20, **2007**.
11. M.A. Miller and G.N. Merrill, "The Role of Surface Plasmons in Molecular Adsorption: A Theoretical and Experimental Study of Gold and Titanium Compounds," *J. Phys. Chem. C* **112**, 6939-6946, **2008**.
12. Bourlinos, A.; Steriotis, T.; Stubos, A.; Miller, M.A. "Carbon Material for Hydrogen Storage," US Patent Application, Filed November 17, **2008**.
13. M.A. Miller, C-Y Wang, and G.N. Merrill, "Experimental and Theoretical Investigation into Hydrogen Storage via Spillover in IRMOF-8," *J. Phys. Chem. C* **2009**, *113*, 3222-3231.
14. L. Wang, F.H. Yang, R.T. Yang, and M.A. Miller, "Effect of Surface Oxygen Groups in Carbons on Hydrogen Storage by Spillover," *Ind. Eng. Chem. Res.* **2009**, *48*, 2920-2926.
15. M.G. Norton, D.N. McIlroy, G. Corti, and M.A. Miller, "Silica Nanosprings – A Novel Nanostructured Material for Hydrogen Storage," *Proceedings of the Clean Technology Conference* **2009**, Houston, TX.
16. Cheng-Yu Wang, Cheng-Si Tsaoa, Ming-Sheng Yua, Pin-Yen Liao, Tsui-Yun Chung, Hsiu-Chu Wu, Michael A. Miller, and Yi-Ren Tzeng, "Hydrogen Storage Measurement, Synthesis and Characterization of Metal-Organic Frameworks via Bridged Spillover", *J. Alloys and Compnds* **2010**, *492*, 88-94.
17. D.N. McIlroy, Y. Zhan, L. Wang, B. Hare, G. Corti, T. Cantrell, M. Beaux II, T. Prakash, F.M. Ytreberg, and M.A. Miller, "Nanoscale Geometry and Spillover on Room Temperature Storage of Hydrogen on Silica Nanosprings," *Energies* **2012**, *5*.

10

COLLABORATIONS (DOMESTIC)

National Renewal Energy Laboratory (NREL), Lin Simpson (HSCoE Director), Michael Heben (currently at U. Toledo), Anne Dillon, and Philip Parilla.

- Peer review of analytical methods for sorption analysis.
- Synthesis and critical evaluation of the sorption properties of pure SWNTs, metal-catalyzed SWNTs, and other carbon materials.
- Coordination and participation in Round-Robin testing.

University of California, Los Angeles (UCLA), Omar Yaghi, Hiroyasu Furukawa.

- Establishment of benchmark for hydrogen adsorption in MOFs.
- Established and validated accurate methods of quantifying excess and absolute uptake of hydrogen in low-density, highly porous storage materials.

University of Michigan, Ralph T. Yang.

- Elucidated range of hydrogen binding sites in spillover storage materials.
- Studied effects of surface oxygen groups in carbon material on hydrogen storage by spillover.

Rice University, Robert Hauge. [External Collaboration]

- Development of platelet catalyst for carbon nanotube growth.
- Hydrogen storage properties of platelet-grown carbon nanotubes.

University of Texas, San Antonio (UTSA), Grant N. Merrill.

- Determined the thermodynamic plausibility for hydrogen spillover effects in MOFs using first principles calculations.
- Synthesis and hydrogen sorption properties of metal-cluster-intercalated MOFs

University of Idaho (UI), David N. McIlroy, Giancarlo Corti. [External Collaboration]

- Synthesis of silica nanosprings and metal-doped silica nanosprings.
- Hydrogen sorption and spillover properties of silica nanosprings.

11

PLANNED USE OF LABORATORY

The Laboratory will continue to be available to the hydrogen as well as other gaseous fuel-storage R&D communities in forward years for as long as its operation can be self-supported or sustained by outside funding, or both. It will solicit opportunities to further assist the development and characterization of storage materials and full-scale systems under previously-qualified analytical standards. The near-term goals of the Laboratory for hydrogen storage technologies are to solicit its capabilities and expertise to commercial developers and to the Hydrogen Storage Engineering Center of Excellence (HSECoE), a DOE Center established in 2009 to bridge the gap between the materials research undertaken under the Hydrogen Storage Program and the significant engineering challenges associated with developing lower-pressure, materials-based, hydrogen storage systems for hydrogen fuel cell and internal combustion engine light-duty vehicles.

Complementing a hydrogen-based national infrastructure for transportation, the utilization of abundant domestic sources of natural gas is also an important component of a national energy plan that reduces the US's dependence on foreign oil. An increased reliance on domestic natural gas will support America's energy security and provide a reduction in greenhouse gas (GHG) emissions by cutting emissions of particulate matter by 95%, carbon monoxide by 90 to 97%, carbon dioxide by 25%, and other hydrocarbon emissions by 50 to 75% [80]. These reductions can be achieved by replacing diesel and gasoline vehicles with clean-burning adsorbed natural gas vehicles provided a natural gas fueling infrastructure for low-pressure storage can be established.

As the principal component of natural gas (NG), methane is an abundant and currently low-cost fuel that when burned in an internal combustion engine emits less CO₂ per vehicle mile traveled than any other fossil fuel [80]. Like hydrogen storage, the main barriers limiting broad use of NG as a fuel for light-duty passenger vehicles are the ability to store NG on-board safely, in sufficient quantities for a practical operating range, the availability of economical storage systems relative to the total cost of the vehicle, and the lack of a wide-spread infrastructure of NG fueling stations [81]. Recognizing this opportunity, the Laboratory will seek and solicit opportunities to address these technical challenges through government- and commercially-funded research programs to find and innovate highly porous materials suitable for the adsorptive storage of NG.

The current state-of-the-art involves compressing NG in a costly carbon-composite pressure containment vessel (Type IV) at ~ 250 bar and room temperature. Deployment of this technology is further inhibited by the costly compression technologies that are needed to attain such pressures at the forecourt of fueling stations [81]. It is therefore evident that significant well-to-wheels cost savings would be realized if an on-board storage system technology can be developed that provides a comparable operating range as a 250 bar system, but at much lower pressures.

In an effort to address these technical challenges, government- and commercially-funded research programs have been undertaken internationally to find and innovate highly porous materials suitable for the adsorptive storage of NG. These initiatives were initially motivated by the U.S. Department of Energy (DOE), who in 2000 established the storage targets for materials-based adsorbed methane at 7.15 MJ/L [82], far less than the ambitious targets set forth by a recent ARPA-E initiative (12.5 MJ/L). However, it should be appreciated that many materials discoveries and physical insights presently applicable to NG adsorptive storage have emerged from DOE's Hydrogen Storage Program, including its complementary program focused on basic sciences. The knowledge base created as a consequence of the extraordinary focus and accomplishments of those programs can be leveraged to help leapfrog technological advancements to be made in adsorptive NG storage. In particular, important advances made in the molecular engineering and synthesis of ultra-high surface area framework materials, the fundamental understanding of the interplay among structural motifs, surface area, pore volume, and molecule-sorbent binding interactions (i.e., isosteric heat), as well as the development and modeling of full-scale system concepts, are immediately relevant to achieving the energy density targets for NG storage systems.

Adsorptive NG storage has traditionally employed zeolites and porous carbon materials. These material systems can be discounted from further consideration for NG storage because, based on historical data, they are unlikely to transcend their typical methane uptake capacities of < 4 MJ/L for zeolites and $\sim 2 - 6$ MJ/L for most porous carbons [83]. In contrast to these stagnant levels of performance, synthetic framework materials have evolved in measured performance much more rapidly than zeolites or even nanoporous carbon materials principally due to the relative ease with which topology and other properties can be engineered into their structural motifs, starting from a large selection of structural building units and employing systematic methods for synthesis.

As illustrated in Fig. 11.1, both the volumetric and gravimetric energy densities (material basis) of a cross section of different framework materials have steadily increased as a consequence of a concerted effort to design structural motifs that result in higher specific surface

areas and stronger van der Waals binding interactions between sorbate molecules and the building units of the framework than the materials that preceded. Both of these physical characteristics are critical to achieving the materials-basis targets for gravimetric capacity.

However, binding interactions must fall within an optimum range in order to maximize reversible storage at or close to room temperature. The optimum heat of adsorption has been determined to be 18.8 kJ/mol. The relationship between the absolute gravimetric energy density (normalized by the specific surface area) and the isosteric heat of methane adsorption for the current state-of-the-art in framework sorbents (e.g., MOFs) follows a trend illustrated in Fig. 11.2. It follows that further improvements in methane adsorption under ambient conditions may be realized by tweaking the binding energies of these physisorption storage materials.

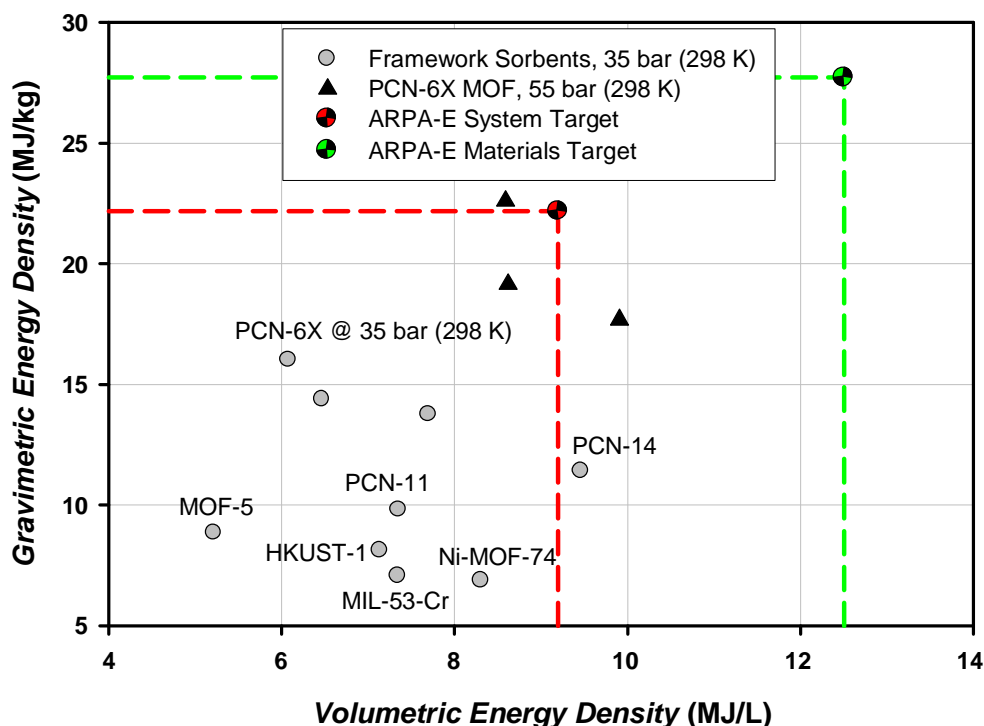


Figure 11-1: Correlation between the absolute volumetric and gravimetric energy densities of stored methane at room temperature for a cross-section of current-generation framework sorbents at 35 and 55 bar. The ARPA-E system and material-basis targets are also indicated for comparison.

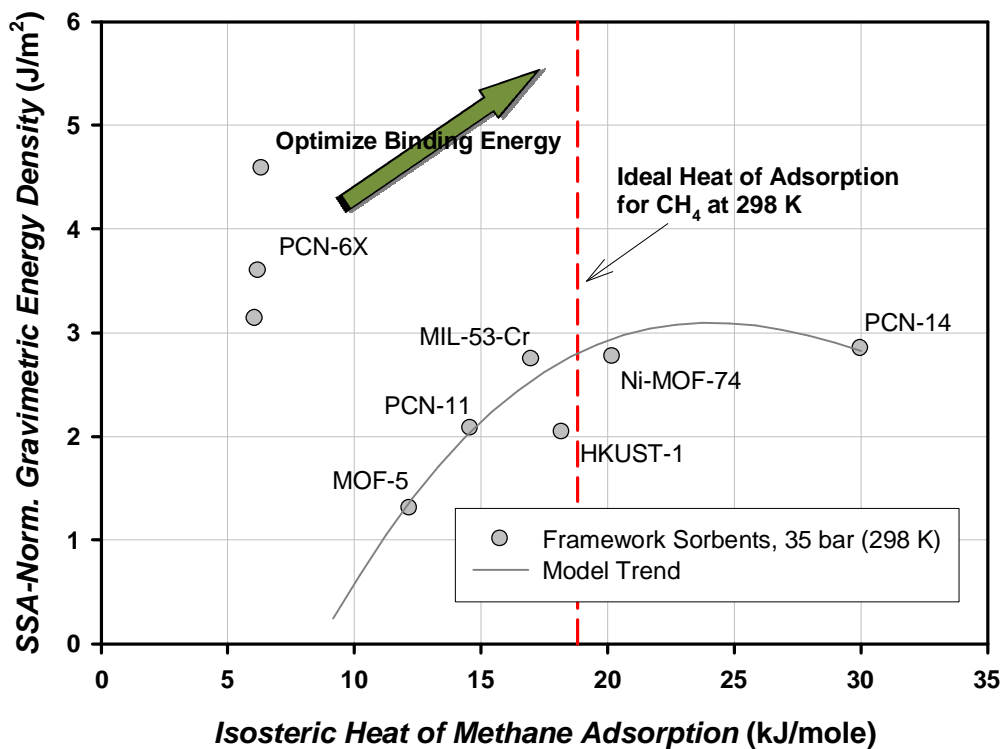


Figure 11-2: Gravimetric energy density normalized by the specific surface area of the framework sorbent as a function of the isosteric heat of methane adsorption. A model trend line for prior-generation framework sorbents is shown to traverse the theoretically-ideal heat of adsorption. Further enhancements in gravimetric energy density are in store for the PCN-6X series MOFs by optimizing methane-framework binding interactions via chemical modifications of framework building units.

Drawing from the team’s experience in, and the lessons learned from, the development of solid-state materials and systems for on-board storage of hydrogen, it has become abundantly clear that the intrinsic properties of sorbent materials, and in particular that of framework sorbents, measured in the Laboratory seldom scale with equal or similar performance at the system level. Consequently, the development of sorbent materials for a storage system cannot be achieved as an insular effort, rather it must be approached at the system level in order to account for and develop a comprehensive understanding of all the engineering factors that collectively affect the net performance of the sorbent material while accessing usable NG from the storage system. This system level view for sorbent development constitutes the principal motivation for re-purposing the Laboratory and exercising materials and system engineering to develop NG adsorption storage systems for vehicles, as illustratively outlined in Fig. 11.3.

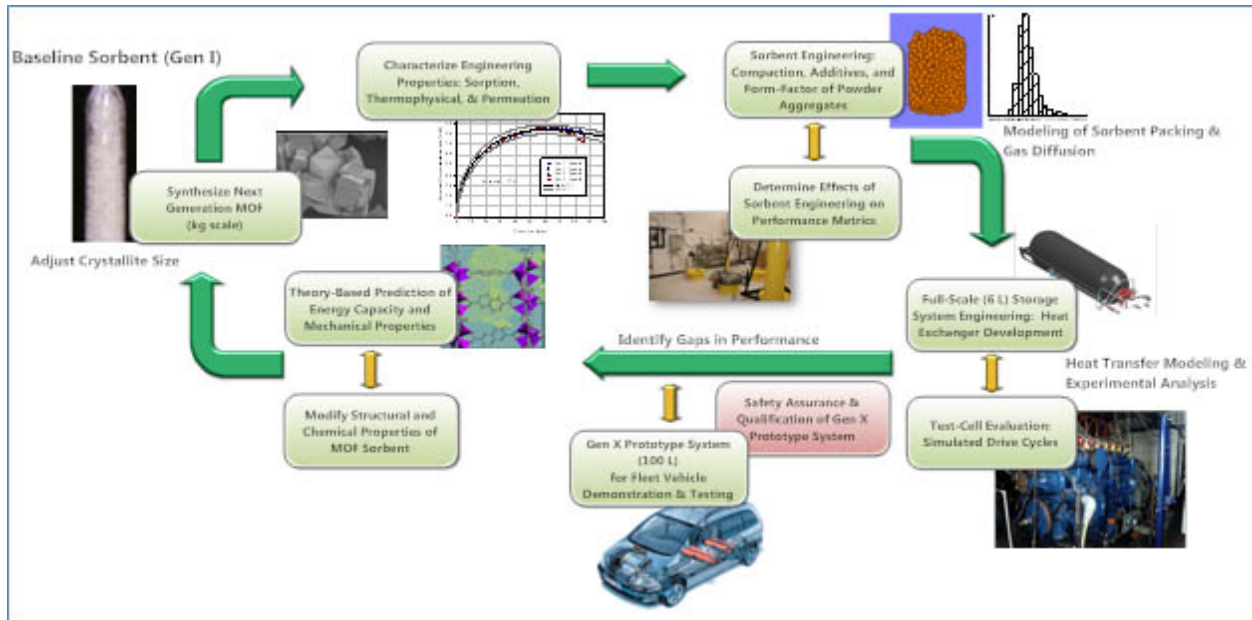


Figure 11-3: Overview of Laboratory's planned use for development and characterization of materials and systems for fuel storage.

12

CONCLUSIONS AND FUTURE DIRECTIONS

This program has addressed the fundamental need for establishing a qualified laboratory whose core mission has been to study and independently verify the intrinsic sorption characteristics of novel and emerging materials for solid-state hydrogen storage, while further providing analysis of select materials in full-scale storage systems. Accordingly, the Laboratory has worked with DOE, the materials centers of excellence, and outside institutions, to develop qualified standards for analysis and provide independent assessment and validation of storage material performance based on those standards. The outcome of that activity has enabled a consortium of hydrogen storage researchers and the DOE to focus their efforts on those materials that demonstrate the highest potential toward meeting the targets required for on-board hydrogen fuel storage in vehicles powered by polymer electrolyte membrane (PEM) fuel cells. These goals have been successfully achieved, but not without marked challenges.

The analytical requirements for making accurate and precise measurements of hydrogen sorption on diverse classes of storage materials evidently were quite rigorous, and the variables associated with the synthesis and preparation of materials suitable for study were often convoluted. Therefore, the potential for drawing erroneous conclusions from experiment could be very high unless careful steps were taken to ensure that the analytical methodologies employed provided sufficient precision and accuracy and, in particular, that the variables inherent in the processing of materials were clearly understood.

To ensure that the laboratory facility could meet the stated expectations of the hydrogen storage community, it was imperative to demonstrate that the adopted standards and analytical methods provided accurate and reliable measurements. This goal was facilitated by conducting Round-Robin testing (RRT) on a range of reference storage materials and verifying that the Laboratory's results were consistent with those of the participant laboratories within the variance of the principal data group. In fact, the RRT studies conducted in collaboration with the EU (NESSY) demonstrated that several external laboratories had profound and persistent errors in their measurements, most likely caused by improper techniques in calibrating instrumentation.

As new materials have emerged with unique hydrogen sorption properties, so have new analytical challenges requiring that the previously-established methods be refined along the way. Therefore, continuous improvements to the methods and equipment, along with periodic RRT

studies to re-qualify them over the lifetime of the program, have been important activities of the Laboratory and its partners. Equally important has been the development and qualification of new techniques, not ordinarily familiar to many laboratories, needed to probe the mechanistic features of hydrogen uptake in complex storage materials. The implementation of the LTDMS technique is an example of this need which has proven to be invaluable in confirming and quantifying the occurrence of stable binding sites for hydrogen in materials, indicative of room temperature uptake via spillover.

In the search for novel forms of materials for physisorption storage, crystalline materials of well-defined pores and structural motifs have emerged with remarkably high surface areas and gas storage capacities. Indeed, MOF-177 has been established under the present program as an ideal material to use as a benchmark for hydrogen adsorption measurements owing to its high gravimetric (7.6 wt.%) and volumetric (48 g/L) uptake capacity, its facile and highly reproducible synthesis, and its well-characterized crystalline structure in terms of atomic connectivity and chemical composition. While nanoporous carbons, such as those derived from PEEK, also exhibit promising characteristics, the overall comparisons have strongly suggested that the development of MOF-based storage materials is a more promising venue to meeting the much sought-after storage targets as long as the engineering requirements for densification of the sorbent in a real-world low-temperature storage tank can be achieved.

Along parallel developments, the engineering and self-assembly of a novel class of storage materials from molecular building units forming three-dimensional porous polymer networks (PPNs), which are completely amorphous, has led to the establishment of a new benchmark in performance for hydrogen storage: 8.5 wt.% at 77 K and 60 bar. An important advantage that PPN materials appear to offer over MOFs lies in their remarkable thermal and chemical stability, which can be attributed to their entirely covalent bonding network. PPNs can in fact be handled in an open-air laboratory environment without impacting their performance. Studies in the future should examine post-synthetic methods of improving the volumetric capacity of these materials, which currently falls short of the MOF-177 benchmark, by examining what effects high-pressure mechanical compaction (*i.e.*, pelletizing) may have on the gravimetric and volumetric capacity of PPNs.

The potential for quasi-chemisorptive strategies via spillover in catalytically-doped nanostructures, such as Pt/AC/BC/IRMOF-8, has pointed to promising opportunities in meeting the DOE on-board storage targets. However, attainment of a broader than present mechanistic understanding of hydrogen spillover in these compounds warrants further pursuit so that rational designs for new materials with much improved kinetics can be synthesized and evaluated in the

near future. Based on the recent results of PdHg/CF, for example, it is evident that much has yet to be learned about what structural motifs are conducive to spillover and why.

Overall, the immediate scientific questions to answer for the collective class of spillover materials can be summarized concisely: (1) What are the thermodynamic constraints and driving forces for spillover relative to the catalyst and substrate? (2) What is the nature of binding interactions between hydrogen and the substrate after dissociative spillover of dihydrogen from the catalyst? (3) What role does catalyst composition and structure play on surface adsorption, chemisorption, and dissociative spillover of dihydrogen? (4) Are there ideal structural motifs (receptors) that exhibit high reversible uptake while overcoming kinetic and diffusion constraints?

Insofar as chemisorption materials are concerned within the context of the Laboratory's investigations, a renewed interest in complex hydrides can be attributed to the realization that ternary composites of MgH₂/LiBH₄/LiNH₂ have exhibited unexpected improvements in thermodynamics, reversibility, and chemical stability. Exhaustive pressure-composition-isotherm measurements conducted in the Laboratory have indicated that hydride phase formation is significantly limited by kinetics even after this ternary hydride is cyclically conditioned to achieve consistent reversibility. Although this system desorbs hydrogen at lower temperatures than the individual components, the desorption temperature at which significant quantities of hydrogen can be evolved (523 K) is still too high for practical use. Further improvements in kinetics and thermodynamics are therefore needed.

13

SWRI PROJECT TEAM

This program was undertaken with the support of a cohesive team of scientists and engineers whose contributions were invaluable to accomplishing the technical goals of the program. The authors are grateful for the generous contributions from:

Carol A. Ellis-Terrell, Research Scientist – *Hydrogen sorption analyses, sample preparation, materials synthesis.*

Thomas L. Booker, Engineering Technologist – *Design, assembly, and maintenance of laboratory systems, LTDMS analysis.*

Forrest S. Campbell, Principal Engineering Technologist – *Design, assembly, and maintenance of laboratory control systems.*

The late John Campbell, Senior Engineering Technologist – *Design and assembly of analytical tools, including LTDMS.*

Jose Martinez, Technician (currently with Thermo-Fisher, Inc.) – *Hydrogen sorption analyses and sample preparation.*

Victor D. Aaron, Senior Engineering Technologist – *Laboratory safety oversight and hazards monitoring systems.*

14

REFERENCES

1. Lackner, K.S. *Science* **2003**, *300*, 1677-1678
2. Schrag, D.P. *Science* **2007**, *315*, 812-813.
3. Chow, J.; Kopp, R.J.; Portney, P.R. *Science* **2003**, *302*, 1528-1531.
4. Léon, A. *Hydrogen Technology*, Aline Léon (Ed.), Springer-Verlag Berlin Heidelberg, **2008**.
5. Satyapal, S.; Petrovic, J.; Read, C.; Thomas, G.; Ordaz, G. *Catalysis Today* **2007**, *120*, 246-256.
6. Li, H., Eddaouddi, M., O’Keeffe, M., Yaghi, O.M., (1999), *Nature*, 402:276.
7. Wong-Foy, A.G., Matzger, A.J., Yaghi, O.M., (2006), *JACS*, 128:3495.
8. Dillon, A.C., Jones, K.M., Bekkedahl, T.A., Kiang, C.H., Bethune, D.S., and Heben, M.J., (1997), *Nature*, 377:386.
9. Yuan, D.; Zhao, D.; Sun, D.; Zhou, H.C. *Angew. Chem. Int. Ed.* **2010**, *49*, 5357-5361.
10. Hirscher, M., Becher, M., Haluska, M., et al. (2001), *Appl. Phys. A.: Mater. Sci. Process*, 129:72.
11. Hirscher, M., Becher, M., Haluska, M., et al. (2002), *J. Alloys Compd.*, 330-332:654.
12. Page, R.A.; Miller, M.A. FY2003 Annual Progress Report for the Department of Energy Hydrogen Program, November **2003**, available at: www.hydrogen.energy.gov/annualprogress03.html.
13. http://www1.eere.energy.gov/hydrogenandfuelcells/storage/pdfs/targets_onboard_hydro_storage.pdf
14. Léon, A. *Hydrogen Technology*, Aline Léon (Ed.), Springer-Verlag Berlin Heidelberg, **2008**.
15. Satyapal, S.; Petrovic, J.; Read, C.; Thomas, G.; Ordaz, G. *Catalysis Today* **2007**, *120*, 246-256.
16. Lochan, R.C.; Head-Gordon, M. *Phys. Chem. Chem. Phys.* **2006**, *8*, 1357-1370.
17. Rosi, N. L.; Eckert, J.; Eddaouddi, M.; Vodak, D. T.; Kim, J.; O’Keeffe, M.; Yaghi, O. M. *Science* **2003**, *300*, 1127; Rowsell, J. L. C.; Eckert, J.; Yaghi, O. M. *J. Am. Chem. Soc.* **2005**, *127*, 14904.
18. Rowsell, J. L. C.; Millward, A. R.; Park, K. S.; Yaghi, O. M. *J. Am. Chem. Soc.* **2004**, *126*, 5666.
19. Rowsell, J. L. C.; Yaghi, O. M. *J. Am. Chem. Soc.* **2006**, *128*, 1304.
20. Wong-Foy, A. G.; Matzger, A. J.; Yaghi, O. M. *J. Am. Chem. Soc.* **2006**, *128*, 3494.
21. Dincă, M.; Dailly, A.; Liu, Y.; Brown, C. M.; Neumann, D. A.; Long, J. R. *J. Am. Chem. Soc.* **2006**, *128*, 16876. Dybtsev, D. N.; Chun, H.; Yoon, S. H.; Kim, D.; Kim, K. *J. Am.*

- Chem. Soc.* **2004**, *126*, 32; Kaye, S. S.; Long, J. R. *J. Am. Chem. Soc.* **2005**, *127*, 6506; Lin, X.; Jia, J.; Zhao, X.; Thomas, K. M.; Blake, A. J.; Walker, G. S.; Champness, N. R.; Hubberstey, P.; Schröder, M. *Angew. Chem. Int. Ed.* **2006**, *45*, 7358.
22. Pan, L.; Sander, M. B.; Huang, X.; Li, J.; Smith, M.; Bittner, E.; Bockrath, B.; Johnson, J. K. *J. Am. Chem. Soc.* **2004**, *126*, 1308; Kesanli, B.; Cui, Y.; Smith, M. R.; Bittner, E. W.; Bockrath, B. C.; Lin, W. *Angew. Chem. Int. Ed.* **2005**, *44*, 72; Chen, B.; Ockwig, N. W.; Millward, A. R.; Contreras, D. S.; Yaghi, O. M. *Angew. Chem. Int. Ed.* **2005**, *44*, 4745; Kabbour, H.; Baumann, T. F.; Satcher, J. H. Jr.; Saulnier, A.; Ahn, C. C. *Chem. Mater.* **2006**, *18*, 6085; Forster, P. M.; Eckert, J.; Heiken, B. D.; Parise, J. B.; Yoon, J. W.; Jhung, S. H.; Chang, J.-S.; Cheetham, A. K. *J. Am. Chem. Soc.* **2006**, *128*, 16846; Sun, D.; Ma, S.; Ke, Y.; Collins, D. J.; Zhou, H.-C. *J. Am. Chem. Soc.* **2006**, *128*, 3896; Ma, S.; Sun, D.; Ambrogio, M.; Fillinger, J. A.; Parkin, S.; Zhou, H.-C. *J. Am. Chem. Soc.* **2007**, *129*, 1858.
 23. Latroche, M.; Surlé, S.; Serre, C.; Mellot-Draznieks, C.; Llewellyn, P. L.; Lee, J.-H.; Chang, J.-S.; Jhung, S. H.; Férey, G. *Angew. Chem. Int. Ed.* **2006**, *45*, 8227; Dailly, A.; Vajo, J. J.; Ahn, C. C. *J. Phys. Chem. B* **2006**, *110*, 1099; Jia, J.; Lin, X.; Wilson, C.; Blake, A. J.; Champness, N. R.; Hubberstey, P.; Walker, G.; Cussena, E. J.; Schröder, M. *Chem. Commun.* **2007**, 840.
 24. Li, H.; Eddaoudi, M.; O'Keeffe, M.; Yaghi, O. M. *Nature* **1999**, *402*, 276; Yaghi, O. M.; O'Keeffe, M.; Ockwig, N. W.; Chae, H. K.; Eddaoudi, M.; Kim, J. *Nature* **2003**, *423*, 705.
 25. Bogdanovic, B.; Schwickardi, M. *J. Alloy Comp.* **1997**, *253-254*, 1-9.
 26. Sandrock, G.; Gross, K., *et al.* *J. Alloy Comp.* **2002**, *330-332*, 696-701.
 27. Baker, R.T.K.; Rodriguez, N.; Mastalir, A.; Wild, U.; Schlogl, R.; Wootsch, A.; Paal, Z. *J. Phys. Chem. B* **2004**, *108*, 14348-14355.
 28. Li, J.; Yip, S. *J. Chem. Phys.* **2003**, *119*, 2376-2385.
 29. Miller, M.A.; Page, R.A. FY2006 Annual Progress Report for the Department of Energy Hydrogen Program, November **2006**, available at: www.hydrogen.energy.gov/annualprogress06.html.
 30. Dillon, A.C.; Jones, K.M.; Bekkedahl, T.A.; Kiang, C.H.; Bethune, D.S.; Heben, M.J. *Nature* **1997**, *386*, 377-379.
 31. Heben, M.J.; Dillon, A.C.; Alleman, J.L.; Gilbert, K.E.H.; Jones, K.M.; Parilla, P.A.; Gennett, T.; Grigorian, L. *Materials Research Society Fall Meeting Symposium* **2001**, Z10.2.
 32. Khoobiar, S. *J. Phys. Chem.* **1964**, *68*, 411-412.
 33. Sermon, P.A.; Bond, G.C. *Cat. Rev.* **1973**, *8*, 211.
 34. Mitchell, P.C.H.; Ramirez-Cuesta, A.J.; Parker, S.F.; Tomkinson, J. *J. Phys. Chem. B* **2003**, *107*, 6838-6845.
 35. Robell, A. J.; Ballou, E. V.; Boudart, M. *J. Phys. Chem.* **1964**, *68*, 2748.
 36. Srinivas, S. T.; Rao, P. K. *J. Catal.* **1994**, *148*, 470.
 37. Pajonk, G. M. *Appl. Catal. A* **2000**, *202*, 157.

38. Sinfelt, J. H.; Lucchesi, P. J. *J. Am. Chem. Soc.* **1963**, *85*, 3365.
39. Conner, W. C., Jr.; Falconer, J. L. *Chem. Rev.* **1995**, *95*, 759.
40. Mitchell, P. C. H.; Ramirez-Cuesta, A. J.; Parker, S. F.; Tomkinson, J.; Thompsett, D. *J. Phys. Chem. B* **2003**, *107*, 6838.
41. Mitchell, P. C. H.; Ramirez-Cuesta, A. J.; Parker, S. F.; Tomkinson, J. *J. Mol. Struct.* **2003**, *781*, 651-653.
42. Pamitar, A. P.; Yates, J. T., Jr. *J. Phys. Chem. C* **2007**, *111*, 2959.
43. Chen, L.; Cooper, A. C.; Pez, G.P.; Cheng, H. S. *J. Phys. Chem. C* **2007**, *111*, 18995.
44. Lachawiec, A. J., Jr.; Yang, R. T. *Langmuir* **2008**, *24*, 6159.
45. Lin, Y.; Ding, F.; Yakobson, B.I. *Phys. Rev. B* **2008**, *78*, 041402(R).
46. Miller, M.A.; Wang, C-Y; Merrill, G.N. **2009** *J. Phys. Chem. C*, *113*, 3222.
47. Kubas, G.J.; Ryan, R.R.; Swanson, B.I.; Vergamini, P.J.; Wasserman, H.J. *J. Am. Chem. Soc.* **1984**, *106*, 451-452.
48. Zhao, Y.; Kim, Y.H.; Dillon, A.C.; Heben, M.J.; Zhang, S. *Phys. Rev. Lett.* **2005**, *94*, 155504.
49. Kubas, G.J. *Science* **2006**, *314*, 1096-1097.
50. Welch, G.C.; San Juan, R.R.; Masuda, J.D.; Stephan, D.W. *Science* **2006**, *314*, 1124-1126.
51. Li, Y.; Yang, R.T. *J. Am. Chem. Soc. Comm.* **2006**, *128*, 12410-12411.
52. Miller, M.A.; Page, R.A. FY2007 Annual Progress Report for the Department of Energy Hydrogen Program, November **2007**, available at: www.hydrogen.energy.gov/annualprogress07.html.
53. Dantzer P. Metal-Hydride Technology: A critical review, 279 (1997), Topics in Applied Physics **73**. *Hydrogen in Metal III*. Editor H. Wipf. Springer-Verlag, **1997**.
54. Puziy, A. M.; Herbst, A.; Poddubnaya, J.G.; Harting, P., *Langmuir* **2003**, *19*, 314-320.
55. Bénard, P.; Chahine, R. *Langmuir* **2001**, *17*, 1950-1955.
56. Zhou, L.; Zhang, J.; Zhou, Y. *Langmuir* **2001**, *17*, 5503-5507.
57. Sips, R. *J. Chem. Phys.* **1950**, *18*, 1024.
58. Dincă, M.; Dailly, A.; Liu, Y.; Brown, C. M.; Neumann, D. A.; Long, J. R. *J. Am. Chem. Soc.*, **2006**, *128*, 16876.
59. Czepirski, L.; Jagiełło, *J. Chem. Eng. Sci.*, **1989**, *44*, 797.
60. Jagiello, J.; Badosz, T. J.; Putyera, K.; Schwarz, J. A. *J. Chem. Eng. Data*, **1995**, *40*, 1288.
61. Brinks, H.W.; Fossdal, A.; Bowman, R.C., Jr.; Hauback, B.C. *J. Alloys Compd.* **2006**, *417*, 92-95.
62. Tibbetts, G.G.; Meisner, G.P.; Olk, C.H. *Carbon* **2001**, *39*, 2291-2301.
63. Poirier, E.; Chahine, R.; Tessier, A.; Bose, T.K. *Rev. Sci. Instrum.* **2005**, *76*, 055101.

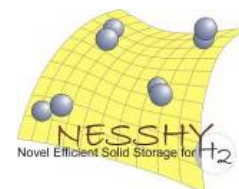
64. Rangarajan, B.; Lira, C.T.; Subramanian, R. *AIChE J.* **1995**, *41*, 838.
65. Benedict, M.; Webb, G.B.; Rubin, L.C. *J. Chem. Phys.* **1940**, *8*, 334.
66. White, J.M. *J. Phys. Chem.* **1983**, *87*, 915-924.
67. Yates, J.T., Jr. *The Thermal Desorption of Adsorbed Species in Methods of Experimental Physics*, R.L. Park, Ed., Academic Press, New York, **1981**.
68. Redhead, P.A. *Vacuum* **1962**, *12*, 203.
69. M.A. Miller, R. Gorte, Carbon Nanotube Sorption Science: External Peer Review of NREL Activities, Report to US DOE, Office of Hydrogen, Fuel Cells, and Infrastructure Technologies, March 1, 2004.
70. Go/No-Go Decision: Pure Undoped Single Wall Carbon Nanotubes for Vehicular Hydrogen Storage, Discussion Document US DOE, October 2006.
71. Furukawa, H.; Miller, M.A.; Yaghi, O.M. *J. Mat. Chem.* **2007**, *17*, 3197-3204.
72. Frost, H.; Düren, T.; Snurr, R. *J. Phys. Chem. B* **2006**, *110*, 9565.
73. Murata, K.; El-Merraoui, M.; Kaneko, K. *J. Chem. Phys.* **2001**, *114*, 4196.
74. Neimark, A. V.; Ravikovitch, P. I. *Langmuir* **1997**, *13*, 5148.
75. Actual pore volume after H₂ adsorption may be smaller than the accessible pore volume, V_{pore}. However, in the Gibbs definition of the dividing surface, the adsorbed phase is a surface and, therefore, it does not have a volume. Considering that, in terms of H₂ storage, the important parameter is not thickness of adsorbed layer, but rather the number of H₂ molecules in the pore (which includes bulk region); a rough estimation of absolute amounts adsorbed is an important issue.
76. Li, Y.; Yang, R. T. *J. Am. Chem. Soc.* **2006**, *128*, 12410-12411.
77. Wang, L.; Yang, F.H.; Yang, R.T.; Miller, M.A. *Ind. Eng. Chem. Res.* **2009** *48* (6), 2920-2926.
78. *NIST Chemistry WebBook, NIST Standard Reference Database Number 69*, Linstrom, P. J.; Mallard, W. G., Eds., June **2005**, National Institute of Standards and Technology, Gaithersburg MD, 20899 (<http://webbook.nist.gov>).
79. Yuan, D.; Lu, W.; Zhao, D.; Zhou, H-C *Adv. Mater.* **2011**, DOI: 10.1002/adma.201101759.
80. *A Full Fuel-Cycle Analysis of Energy and Emissions Impacts of Transportation Fuels Produced from Natural Gas*, 12/1999. U.S. Dept. of Energy - Argonne National Laboratory.
81. *National Transportation Statistics Table 1-14: U.S. Automobile and Truck Fleets by Use* US Department of Transportation, Research and Innovative Technology Administration.
82. Burchell, T.; Rogers, M. *SAE Tech. Pap. Ser.* **2000**, 2001-2205.
83. (a) Menon, V. C.; Komarneni, S. *J. Porous Mater.* **1998**, *5*,43. (b) Lozano-Castello, D.; Alcaniz- Monge, J.; Casa-Lillo, M.A.; Cazorla-Amoros, D.; Linares-Solano, A. *Fuel* **2002**, *81*, 1777.

A

APPENDIX (NESSY RRT)



EUROPEAN COMMISSION
DIRECTORATE-GENERAL
JOINT RESEARCH CENTRE
Institute for Energy



REPORT

Results of the 2nd Round Robin Test exercise: Hydrogen sorption properties of a sodium alanate

Reporting author: Pietro Moretto

Round Robin Test Organizers:

P. Moretto, C. Zlotea, E. Weidner (JRC-IE),
O. Zabara and W. Lohstroh (KIT-INT)

Contributors:

A. Amieiro (Johnson Matthey)
M. Miller (SwRI)
S. Wang (GRINM)
B. Hauback and S. Sartori (IFE)
O. Gutfleisch, I. Llamas Jansa, C. Rongeat (IFW)
N. Eigen, J. Bellosta von Colbe (GKSS)
A. Borgschulte (EMPA)

Executive summary

This report describes the Round Robin Test (RRT) performed on hydrogen sorption properties of a sodium alanate (NaAlH_4) material. The RRT has been conducted in the frame of the European FP6 IP project NESSHY (Novel and Efficient Solid State HYdrogen storage systems). The main objectives of this and the other RRT exercises of NESSHY aimed at guaranteeing that the performance parameters of novel hydrogen storage materials as measured in different laboratories are comparable, identifying possible weaknesses in the measurement steps, developing best practices proposals, and recommending a general check list in the reporting of data.

To our knowledge, the present RRT exercise is the first ever formally organised in the world on the material class of the complex hydrides. Participants were provided with a well characterised a CeCl_3 -added NaAlH_4 material and a detailed measurement protocol. They were asked to perform Pressure-Composition-Isotherms at different temperatures in both absorption and desorption modes at 125°C (at least) and 140°C , desorption kinetics curves at two different temperatures (125°C and 150°C) and an evaluation of the enthalpy of dissociation for both alanate phases. Ten NESSHY partners participated to this RRT exercise and 7 reported (partially) results, one could only provide TGA data, one was experimentally unsuccessful, one never replied to reminders. This report presents a comparison of the experimental isothermal data delivered by participants together with a basic statistic evaluation of the scattering of the results.

The full H_2 capacity has been found to vary in the [3.0 – 4.5] wt% and in the [2.0 – 4.5] wt% range at respectively 125°C and 140°C . The absorption plateau pressure of NaAlH_4 varies between 5.0 and 6.0 MPa with an average of 5.2 MPa and a standard deviation of 0.4 MPa at 125°C . At 140°C the absorption plateau pressure results in the 6.0 - 7.5 MPa range.

Similar data dispersion can be also found in the literature and must be considered as representative of the average uncertainty related to all the materials sharing with sodium alanate the same slow kinetics and environmental sensitivity.

Despite the fact that the scope of this inter-laboratory comparison was an assessment of the accuracy of pcT curve measurements and not the identification of individual causes of data dispersion, a detailed analysis of participant reports allowed for the identification of tentative source of errors: the partial deterioration of the material in presence of rest oxidising atmosphere and a too short time allowed for reaching equilibrium of individual pcT curve points.

Due to the limited amount of participants, it is not possible to perform an advanced statistical analysis. Nevertheless, the measurement and reporting protocol can be proposed as minimal requirement for a best practice guideline.

The kinetic curves show total capacity values ranging from 2.5 to 3.6 wt% and kinetic constant values which can differ of an order of magnitude. The kinetics curves cannot

be quantitatively compared because the some of the partners did not follow the protocol and results of some others were affected by experimental limitations such as too high back pressure or not well calibrated expansion volumes. The result confirms that the assessment of the kinetic parameters is still far from being quantitative.

Summary

1. Objectives	5
2. The Round Robin Test exercise	6
2.1. Round Robin organisation	6
2.2. Material handling	7
2.3. List of participants	7
2.4. Confidentiality of Round Robin Test results	8
2.5. The test protocol	8
2.6. Statistical analysis of results	8
3. Previous works, guidelines and standards	10
3.1. Previous RRT exercises	10
3.2. Existing guidelines and standards	11
4. The material	14
5. The RRT reporting	15
5.1. Overview of the data reported	15
5.2. Experimental parameters of the participants	15
6. Results	17
6.1. pcT curves	17
6.2. Comparison of dissociation enthalpies	20
6.3. Comparison of kinetics curves	21
7. Discussion	24
7.1. pcT curves	24
7.2. Kinetics curves	26
8. Conclusions	28
8.1. Acknowledgments	29
9. References	30

ANNEXES

1. Measurement Protocol	32
2. Detailed Results Partner 1NA	36
3. Detailed Results Partner 2NA	38
4. Detailed Results Partner 4NA	40
5. Detailed Results Partner 7NA	42
6. Detailed Results Partner 9NA	48
7. Detailed Results Partner 9NA	50
8. Detailed Results Partner 10NA	57

1. OBJECTIVES

Due to the increasing effort of the research in the hydrogen storage field, reliable methods of measurement are required to determine the hydrogen uptake in the laboratory, not only to verify previous claims in the literature and to facilitate the comparison between results, but also to prepare a sound and accurate set of data for engineering of up-scaled storage systems.

Since the measurement tests are subject to unavoidable random errors, the accuracy plays an important role as it expresses the precision of a method and the closeness to the accepted reference value. Two measurements concepts are used to express the precision of a test method: repeatability and reproducibility [ASTM 1999]. Repeatability deals with variability between independent tests obtained within a single laboratory. Reproducibility concerns variability between single test results obtained in different laboratories.

While the effort of improving repeatability of a test method remains at the level of individual laboratory, the reproducibility of a test method can be estimated by an inter-laboratory study, which can take the form of a Round Robin Test, and generally brings appreciable variability of the results.

The present study reports the results of a Round Robin Test exercise on measurements of the hydrogen sorption parameters of a NaAlH_4 material containing 4%mol of CeCl_3 . As in the previous RRT exercise, on physisorption of carbon-base material, the overall objectives of the work have been:

- to guarantee that the performance parameters of novel hydrogen storage materials as measured in different laboratories are comparable,
- to identify possible weaknesses in some measurement steps,
- to develop, if possible, a best practice proposal,
- to propose recommendations for optimizing the absorption isotherm measurements
- to propose a check list of reporting absorption isotherm data

In addition to the previous RRT exercise, focussing on thermodynamic quantities only, the present one had the ambition to evaluate also the comparability of kinetic parameters.

2. THE ROUND ROBIN TEST EXERCISE

The overall goal of the Round Robin Test (RRT) exercises is the evaluation of the variability between test method results as obtained by different laboratories on random portions of a homogenous material. Unavoidable random errors may be introduced by factors such as the operator, the equipment used, the calibrations of the equipment or the environment. A RRT is therefore measuring the precision of a test method including all the previous factors as sources of variability. General information on RRT exercises and detail standard procedures can be found in the ASTM standard “*Standard Practice for Conducting an Interlaboratory study to determine the Precision of a Test Method*” [1].

2.1. Round Robin organisation

The organisation of the present RRT has followed that of the previous RRT and can be summarise in the following steps:

- a) The decision on the material classes to be used in the RRT exercises was taken at the 1st Annual NESSHY Governing Board meeting (Amsterdam, 13-15.12.2006).
- b) The choice of the NaAlH_4 material and the producer were chosen at the 18th month NESSHY Governing Board meeting (Zurich, 17-19.06.2007), when also the acquisition protocol was finalised by the advisory group.
- c) Invitation to NESSHY partners to participate was sent (January 2007).
- d) The material has been produced at KIT- INT and delivered to JRC (March 2007).
- e) Portions of homogenous material have been sent by JRC to all participants (July 2007) together with the test protocol. The time allocated for performing the measurements as described in the protocol was originally 6 months from the moment of the reception of the material. A unique participant number was assigned to each partner and were used for communication.
- f) The original deadline for data reporting by partners was December 2007, corresponding to month 24 of the project. To allow delayed participants to contribute and guarantee a statistically meaningful number of participants, it has been extended a first time to March 2008, then to December 2008 and finally up to one week before the 3rd progress review meeting (Crete, 06.2009).

g) Eventually the experimental results have been summarised and analysed in this report, which is not only based on raw RRT data but on additional information obtained later from the participants, in an attempt to explain discrepancies.

2.2. *Material handling*

Approximately 100 g of the material to be measured has been produced in batches of ~25g each at the INT (KIT in Karlsruhe, D) and shipped to JRC (Petten, NL) in plastic bottle placed under argon overpressure in a steel container with vacuum-tight closures. At JRC samples of approximately 5 g have been randomly extracted from the KIT bottle and shipped to partners in the same way. Dates of shipping and of reception have been recorded and archived.



Figure 1 - Holder used for distribution of sample to participants

2.3. *List of participants*

Nine laboratories have accepted to participate to the Round Robin Test, out of which seven have reported (partially) measurements as required by the measurement protocol. The names of the participating laboratories together with the origin countries and the contact persons are listed in Table 1.

2.4. Confidentiality of Round Robin Test results

In order to assure the confidentiality of the Round Robin Test results, anonymous code names have been used instead of real name of laboratories in the following sections.

No.	Laboratory	Country
1	Johnson Matthey	United Kingdom
2	JRC	The Netherlands
3	SwRI	USA
4	GRINM	China
5	IFE	Norway
6	KIT - INT	Germany
7	IFW	Germany
8	GKSS	Germany
9	EPMA	Swiss
10	METU	Turkey

Table 1 The list of the 10 NESSHY partners which participated to the RRT on NaAlH_4 .

2.5. The test protocol

The test method has been developed by an advisory group set-up with volunteering experts of the present material: W. Lohstroh (KIT-INT) and N.Eigen (GKSS) plus the involved JRC staff (C. Zlotea and P. Moretto).

The entire test protocol, as it was sent to all partners, is given in Annex 1.

2.6. Statistical analysis of results

The ASTM *Standard Practice for Conduction an Interlaboratory Study to Determine the Precision of a Test Method* [1] is a very useful document to organise and analyse a RRT exercise. In the case of the previous exercise on carbon base material for example the Interlaboratory Consistency, has been calculated according to the ASME standard. Unfortunately the number of participants who answered to the present RRT

in NaAlH₄ base material is not enough to allow a thoroughly statistical evaluation as described in the standard. As quoted in it: “9.1.2 An Interlaboratory Study should include 30 or more laboratories but this could not be practical. 9.1.2 Under no circumstances should the final statement of precision of a test method be based on acceptable test results for each material from fewer than 6 laboratories”.

Since the data of the present RRT come from approximately 4 to 7 laboratories, it has been possible to perform only the most basic statistical evaluation. The analysis is applied to the plateau pressure and total hydrogen capacity values of the Pressure Composition Isotherms and consists only of the basic statistical parameters *Mean* and *Standard Deviation*:

Mean:

$$\bar{x} = \frac{\sum x}{n} \quad (1)$$

where x is the value of interpolated PCI curve at fixed pressures and n is the total number of partners.

Standard deviation:

$$s = \sqrt{\frac{\sum (x - \bar{x})^2}{n - 1}} \quad (2)$$

3. PREVIOUS WORKS, GUIDELINES AND STANDARDS

3.1. Previous RRT exercises

RRT exercises in the hydrogen sorption field are often performed in the frame of a project, involving few partners and with a limited scope, so that very rarely results are published in scientific literature. An example of these can be found in the validation of sorption measurement techniques contained in a report of Channing Ahn et al., to the 2005 Annual Merit Review Proceedings of the DoE [2]. To our knowledge the RRT exercise has never been published and the mention of it in the above mentioned report is related to the demonstrated capacity of a specific participant to fit well within the dispersion of the results.

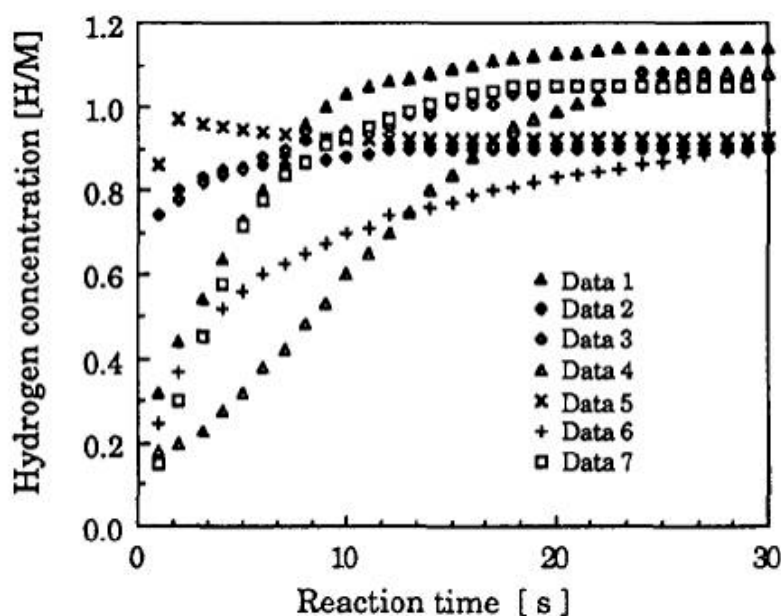


Figure 2 A comparison of the experimental data taken under identical experimental conditions for the $\text{LaNi}_{4.8}\text{Al}_{0.1} - \text{H}$ system by different research group (from [3]).

RRT exercises have been organised in Japan in the frame of the development of the Japanese sorption standards (see next paragraph). A record of this can be found in an article specifically on the accuracy of gas phase sorption measurements by Wang and vSuda [3]. The intention of the article is the reduction of errors in isothermal kinetic measurements and it presents results from a Japanese RRT exercise (Figure 2). It is specific to AB_5 hydrides (or, at least, intermetallic hydrides) rather than hydrogen storage compounds as a whole and classifies the sources of error in kinetic

measurements of this type as: (1) the thermal effects caused by the heat of reaction, (2) the system volume to sample mass ratio, (3) the sample history, (4) the experimental conditions, (5) the particle surface state and (6) the particle size.

We have not been able to identify any previous RRT specifically dedicated to complex light hydrides, what brings us to conclude that the present RRT exercise is the first ever formally organised in the world.

3.2. *Existing guidelines and standards*

The present RRT exercise did not have as an objective the validation of a specific standard and any reference to already existing documents has been avoided in the formulation of the protocol. However, since one of the overall goals of the WP7 of NESSHY is the contribution to the development of international standard, in this paragraph we want to report on the already existing guidelines and standards related to the measurements of hydrogen capacity and other properties by chemisorption processes.

International standards, such as ISO' ones, dedicated to chemisorption do not exist. To our knowledge the Japanese Standard Association is the only national association which has issued an Industrial Standards (JIS) dedicated to hydrogen absorption measurements¹. The first set of these standards dates back to 1989 to 1995 period and have been updated in 2007.

- JIS H 7003:2007 - Glossary of terms used in hydrogen absorbing alloys. It specifies the principal terms and definitions relating to hydrogen absorbing alloys and their applications.
- JIS H 7201:2007 - Method for measurement of pressure-composition-temperature (PCT) relations of hydrogen absorbing alloys. It specifies the general measuring method for obtaining the pressure-composition-temperature relations of hydrogen absorbing alloys by the Sievert's method.
- JIS H 7202:2007 - Method for measurement of hydrogen absorption/desorption reaction rate of hydrogen absorbing alloys. It specifies the general measuring method for obtaining the hydrogen absorption/desorption reaction rate of hydrogen absorbing alloys.

¹ We would be very grateful to any reader who can indicate additional existing national standard.

- JIS H 7203:2007 - Method for measurement of hydrogen absorption/desorption cycle characteristic of hydrogen absorbing alloys. It specifies the method for measuring the hydrogen absorption/desorption cycle characteristic of hydrogen absorbing alloys by means of cyclic reaction of hydrogen gas and hydrogen absorbing alloys.
- JIS H 7204:1995 - Method for measuring the heat of hydriding reaction of hydrogen absorbing alloys. It specifies the method for measuring the heat of hydriding reaction of hydrogen absorbing alloys with a calorimeter.

An additional standard sets the hydrogen quality class. In the case of sorption measurement purity equal or better than class 3 should be used: >99.99%.

Two of these standards are of interest for the present RRT, respectively the JIS H 7201:2007 for the pcT acquisitions and the JIS H 7202:2007 for the kinetics experiment. However, the Japanese standards focus specifically on ‘alloys’ and the measuring procedures are optimised for relatively ‘mild’ experimental conditions, especially in term of temperatures and pressures (for example, the recommended set-up for kinetics experiment works up to 3 Mpa and 473 K only). Nevertheless it is interesting that a formula for the optimal quantity of samples for a given available reactor volume is given.

DoE guidelines (by K. Gross)

The Department of Energy of the US Government is developing document with best practices. The document, for the moment available only on line [4], gives a very comprehensive introduction and physics and chemistry background information. Interesting is the part dedicated to the characterisation of kinetics properties, introduced by the following caveat:

“Kinetics is a measure of the rate of hydrogen sorption or desorption of a material and may not be exclusively dependent on intrinsic material properties. Sample size, heat transfer effects and other parameters that are highly dependent on the experimental method can affect kinetic measurements and conclusions. Minimizing the effects of external influences on kinetics is very difficult and requires a great deal of knowledge and preparation. Thus, extreme caution should be used in ascribing measured kinetics to fundamental sorption mechanisms or an intrinsic property of a given material. Sample preparation, catalyst and additives, particle size, heat transfer capabilities, among other things can strongly influence the kinetics.” [4, page 14]

In paragraph 4.3 information and examples are given for matching experimental setup to the purpose, differentiating among measurements for material development, system performance and fundamental studies.

A very recent and complete literature review on measurements accuracy and errors analysis and control can be found in [5] which is a reduced version of deliverable D7.04 of NESSHY, published as EUR Report 23242 EN.

4. THE MATERIAL

At the start of the NESSHY project it has been decided that one of the three RRT exercise's had to be dedicated to a light complex hydride, because of the importance of the class in the present R&D effort. NaAlH_4 is representative of the whole class and has been studied extensively in the past years. Production and activation process are relatively well understood and tested and its production can be up-scaled to a mass per batch which is enough for a RRT exercise of this scale. In term of RRT objectives, NaAlH_4 is a complex material, characterised by performances which make of it an interesting candidate for 'difficult' benchmarking, such as very slow kinetics, the presence of two plateaus and high air and moisture degradations. In addition, also project FuncHy, whose participants are also part of NESSHY, intended to perform a similar RRT. Consequently it was agreed to perform only one common exercise.

The specific material to be used in the exercise has been NaAlH_4 with 4 mol% CeCl_3 as catalyser (promoter), because of its characteristic of relative "quick" kinetics and stability of capacity with cycling [6]. In addition, it shows a stable kinetic performance after a few cycles only which is an advantage over the more classical additive TiCl_3 [7].

NaAlH_4 (Albemarle, 96%) and CeCl_3 (Aldrich, 99,9%) were used as received. The powder with composition $\text{NaAlH}_4 + 4\text{mol}\% \text{CeCl}_3$ was ball milled for 20h in a planetary mill (Fritsch P6, 600 rpm) using a WC vial and balls (ball to powder ratio 1:50). Several batches of material (~ 25 g) have been produced, independently tested and finally mixed together prior to distribution to the partners.

5. THE RRT REPORTING

In this section we give an overview of the data reported by the participants and all detailed information available on experimental parameters

5.1. Overview of the data reported

A synoptic of the data available is given in Table 2.

Partner	PCI - 125°C	PCI - 140°C	PCI - other T	Technique ^{***}	Kinetics 125°C	Kinetics 140°C	Sample Mass [10 ⁻³ kg]	Volume of reaction chamber [ml]	H2 purity
1NA	✓ [*]	✓ [*]		n.r.			0.791	12.486	
2NA	✓	✓		V	✓	✓	0.327	168 in abs 1024 in des	4.0
4NA	✓	✓	111°C	V	✓	✓	2.280 for kinetics 2.0 (for pcT)	2017 in des	
7NA ^{**}	-	✓		G V D	✓	-	0.816 for G 0.127 for D		5N
8NA	✓	-		V	-	-	0.6735	2.2	5.7
9NA	✓	-		V	✓	✓	0.103	5.0	6.0
10NA	✓	✓	150°C 160°C	V	✓	✓	n. r.		

* The pcT curve has been acquired only up to the first plateau

** The pcT curve at 140°C and the kinetic curves by gravimetry, at 125°C by dynamics method.

*** V = volumetric, G = gravimetric, D = dynamic, n.r. = not reported

Table 2 - The reported isotherm data and the type of technique used.

5.2. Experimental parameters of the participants

The activation procedure consisted in 3 cycles of full desorption at 150°C under vacuum and full absorption at 125°C at 100 bar.

Partners were asked to report the density of the sample used for the measurements.

Partner	Density [g/cm³]	Evaluation method
1NA	2.554 -3.029	He pycnometry at RT (*)
2NA	0.95	He pycnometry at RT
4NA	n. a.	
7NA	n. a.	
8NA	1.25 (NaAlH₄) 1.397 (NaAlH₄ + 4% CECL₃)	Calculated from theoretical densities
9NA	1.0 ± 0.15	He pycnometry at RT
10NA	n. a.	

(*) No report but He mentioned in the excel sheet.

Table 3 Density measurement Theoretical density of pure NAH: 1.3 g/cm³ [8]

Important experimental parameters for gas sorption measurements such as the real equation of state (EoS) used, the equilibrium time for each pcT point and the temperature stability can be found, when available, in the appendixes dedicated to the individual participants.

6. RESULTS

In this section the results of the Round Robin Test from all partners are summarised and compared anonymously.

6.1. Pressure composition isotherm curves

Figure 3 and Figure 4 show respectively desorption and absorption data at 125°C. Desorption curves are presented before absorption because it corresponds to the time line of the experiment.

Figure 6 and Figure 5 show respectively absorption and desorption data at 140°C.

The pcT measurement results can be summarised as follows:

- NaAlH₄ absorption plateau: [5.0 - 6.0] MPa and [6.0 - 7.5] MPa ranges respectively at 125°C and 140°C.
- NaAl₃H₆ absorption plateau: [2.5 - 4.0] MPa and [4.5 - 6.0] MPa ranges respectively at 125°C and 140°C.
- Full H₂ capacity: approximately [3.0 - 4.0] wt% and [3.5 - 4.5] wt% respectively at 125°C and 140°C.

Average Plateau pressure	NaAlH ₄		NaAl ₃ H ₆	
	Absorption	Desorption	Absorption	Desorption
125°C [MPa]	5.21 10 ⁶	2.76 10 ⁶	3.65 10 ⁵	1.03 10 ⁵
(σ)	(4.3 10 ⁵)	(3.3 10 ⁵)	(6.5 10 ⁴)	(8.0 10 ⁴)
Relative σ	8.3%	12.0%	21.8%	35.0%
140°C [MPa]	6.75 10 ⁶	4.01 10 ⁶	5.36 10 ⁵	1.08 10 ⁵
(σ)	(5.5 10 ⁵)	(2.3 10 ⁵)	(7.1 10 ⁴)	(4.1 10 ⁴)
Relative σ	8.2%	5.7%	13.3%	38.1%

Table 4 Average values of the plateau pressures

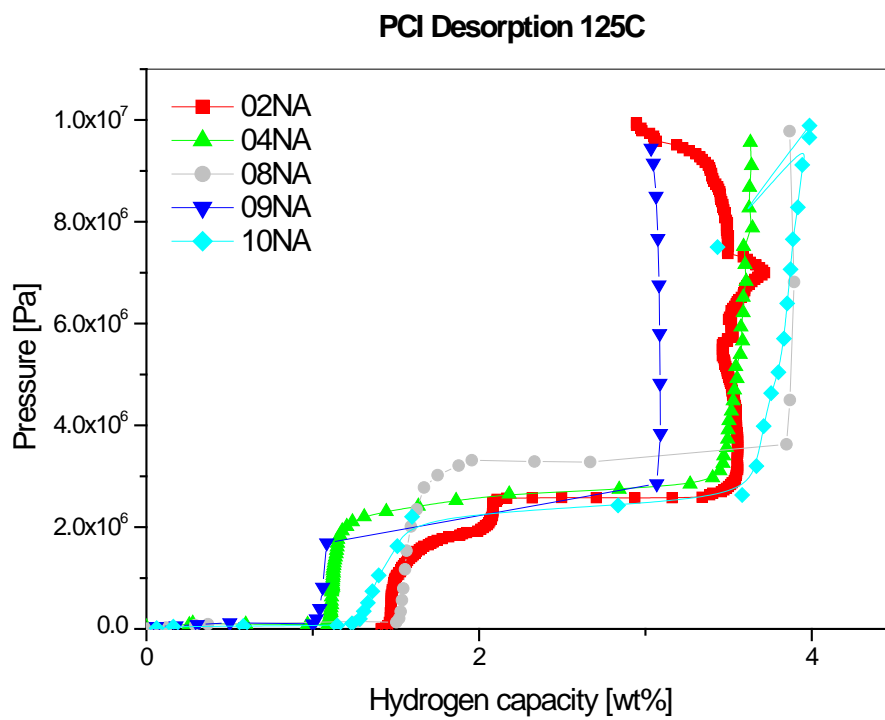


Figure 3 - Desorption curves at 125°C

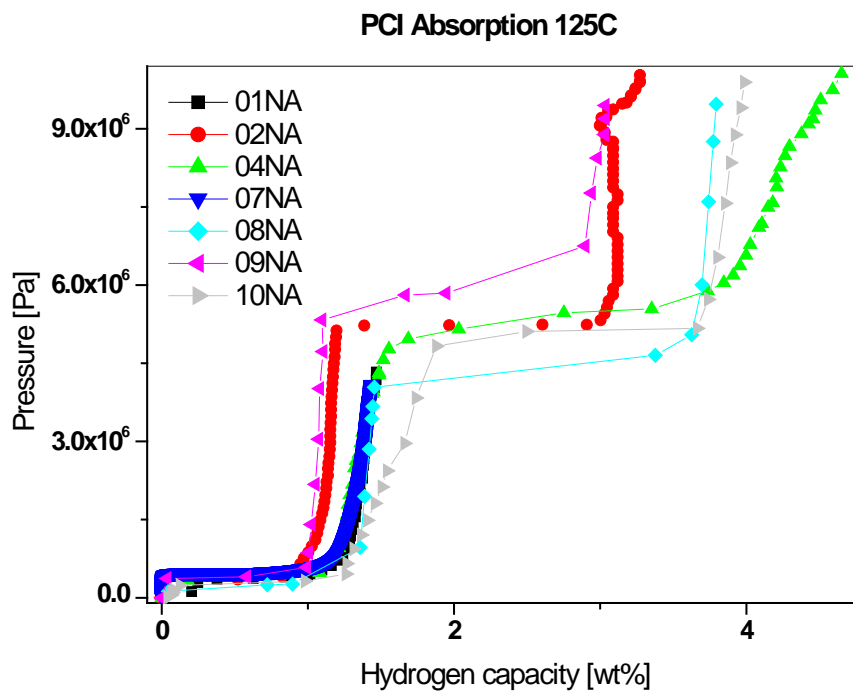


Figure 4 - Absorption curves at 125°C

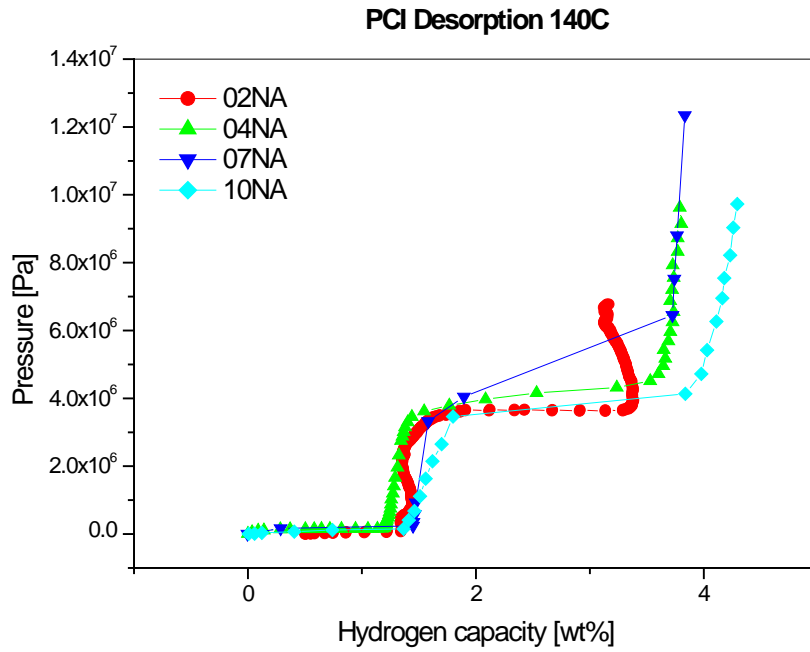


Figure 5 - Desorption curves at 140°C

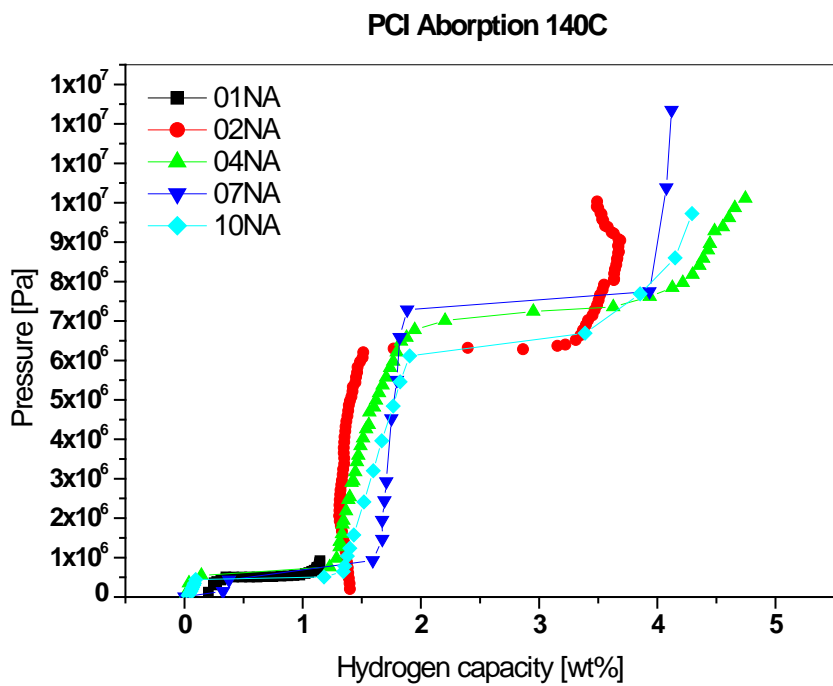


Figure 6 - Absorption curves at 140°C

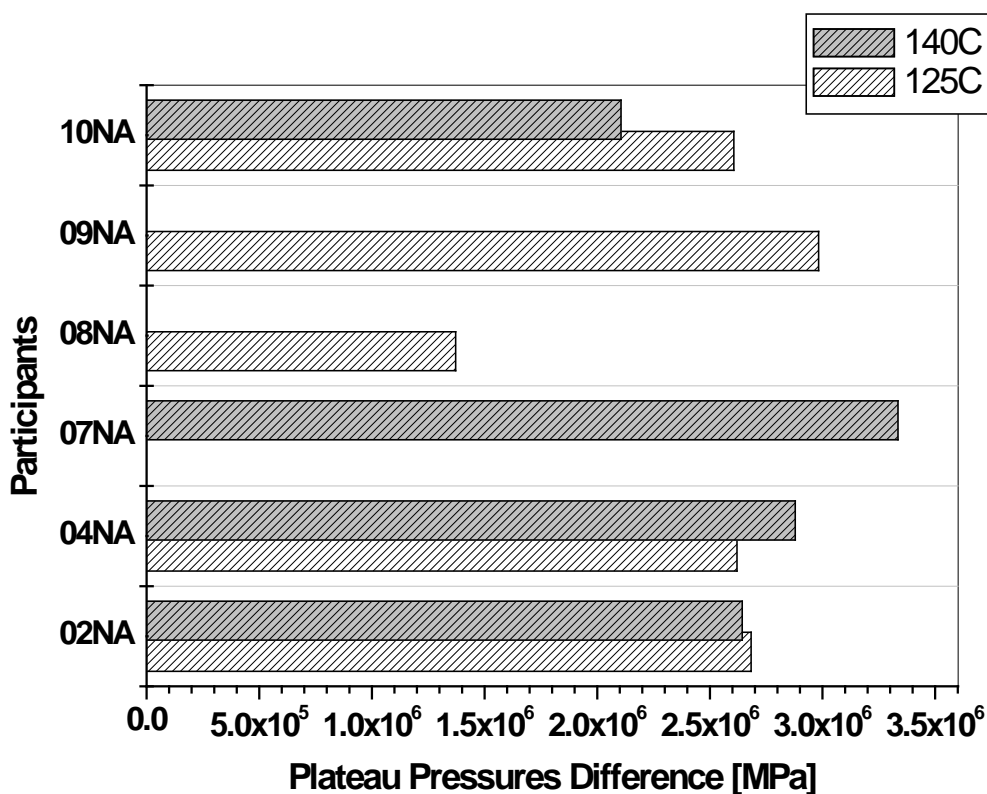


Figure 7 - Difference between the plateau pressures of absorption and desorption.

6.2. Enthalpies of formation

The RRT protocol asked to evaluate the enthalpy of dissociation of the two dissociation reactions, stating that a minimum of 2 isotherms curves were required, but that a minimum of 3 isotherms were recommended. Very few partners reported some values of the enthalpy of formation or dissociation.

Participant 1NA evaluated the thermodynamic parameters for Na_3AlH_6 from the absorption curves: $\Delta H = -32.61 \text{ kJ/molH}_2$ and $\Delta S = -93.10 \text{ J/(K molH}_2)$.

participant 7NA calculated the thermodynamic parameters in Na_3AlH_6 formation via van't Hoff plot build from the measurements of dynamic pcT curves,: $\Delta H = -34.4 \text{ kJ/molH}_2$ and $\Delta S = -98.2 \text{ J/(K molH}_2)$.

The Enthalpies of dissociation for partner 4NA and 10NA has been calculated by the authors of this report based respectively on 3 and 4 isotherms, and corresponds to -66.3 and -48.7 kJ/molH₂ for Na_3AlH_6 and to -49.2 and -42.0 kJ/molH₂ for NaAlH_4 .

Figure 7 compares the reported with a literature data.

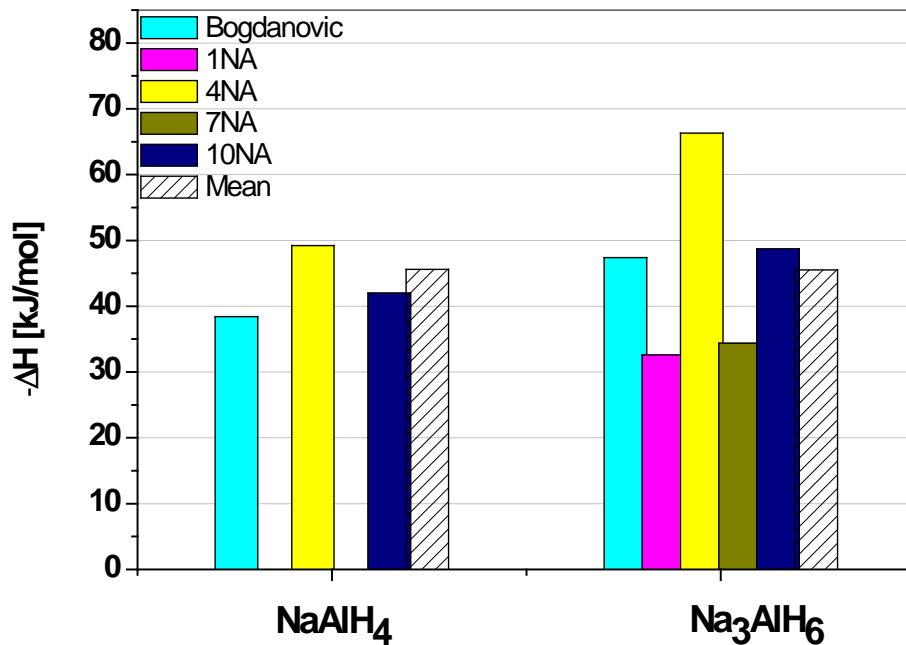


Figure 8 - The calculated dissociation enthalpy of NaAlH₄ and Na₃AlH₆

6.3. Kinetics curves

Figure 8 to Figure 11 show kinetics curves (both in linear and logarithmic time scale) at respectively 125°C and 150°C. Participant 7NA used thermogravimetry, while all the others used a volumetric apparatus.

The kinetics experiments of participant 4NA have not been performed under full isothermal conditions. In the first 500 sec the reaction chamber was linearly heated from room temperature. Participant 9NA's back pressure approached a value of approximately 1 bar at the end of desorption, what probably did not allowed for full desorption. The kinetics curves of participant 2NA show an abnormally high desorption value, which could be tentatively attributed to a problem in the volume calibration.

The kinetic curves show different total capacity values and kinetic constant which can differ of an order of magnitude.

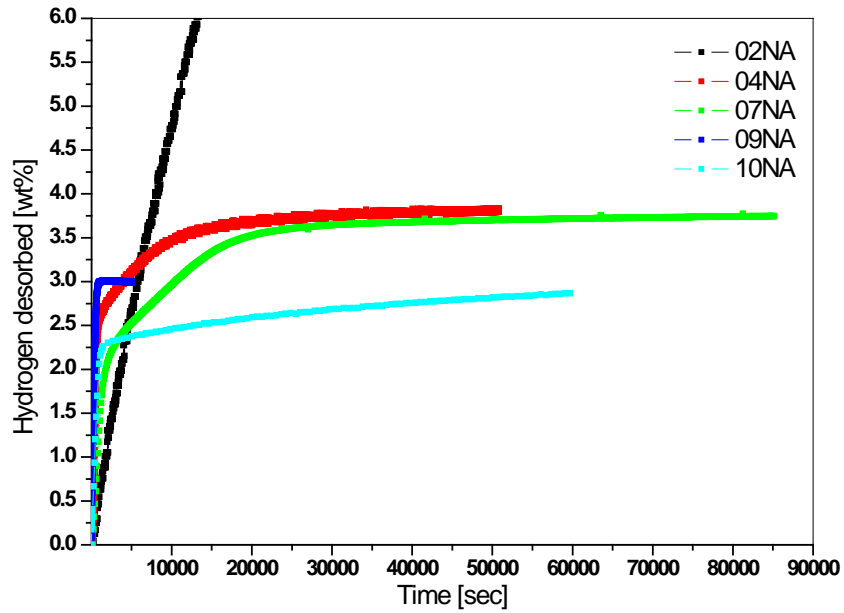


Figure 9 - Kinetics curves at 125°C (The insert shows the first 3000 seconds details).

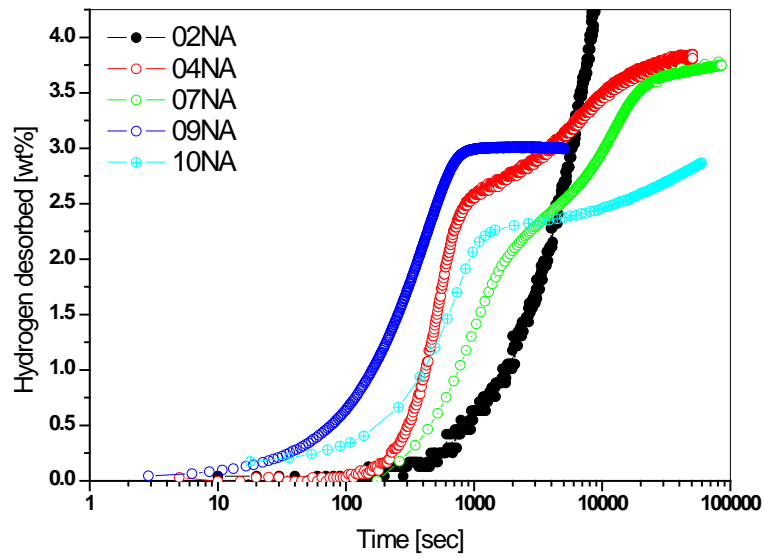


Figure 10 - Kinetics curves at 125°C (logarithmic time scale).

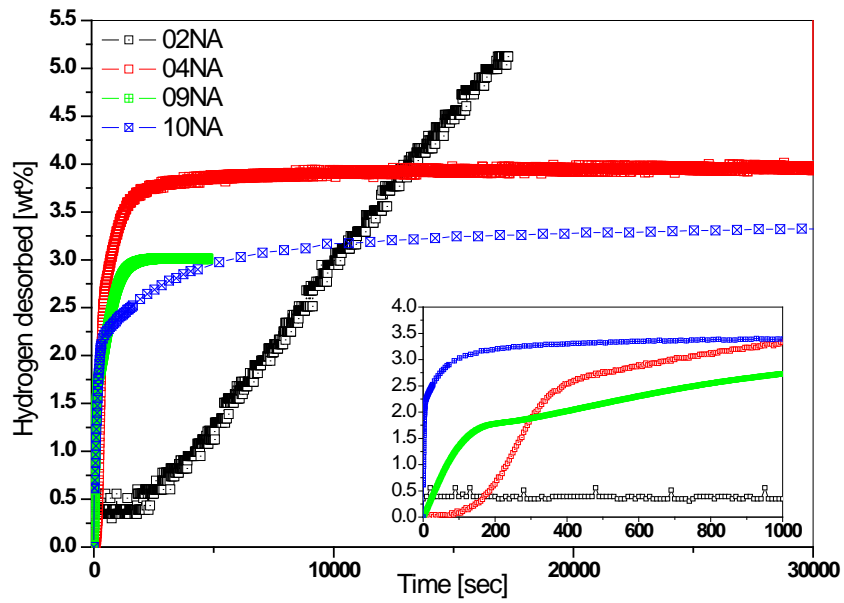


Figure 11 - Kinetics curves at 150°C (The insert shows the first 3000 seconds details).

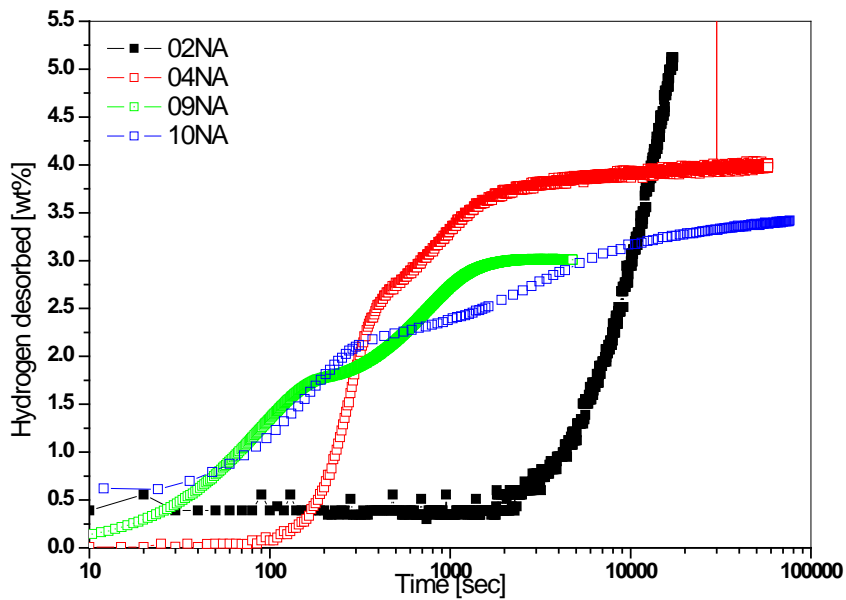


Figure 12 - Kinetics curves at 150°C (logarithmic time axis).

7. DISCUSSION

7.1. *pcT curves*

Various sources of error could be the cause of the discrepancy remarked among the *pcT* curves. We briefly discuss the plausibility of these causes.

Material deterioration during distribution and temporary storage

Samples have been shipped to each partner under exactly the same preparation and sampling conditions. To check that the handling and shipping procedure did not deteriorated the material, FZK partners compared an as-produced sample (thus not shipped) with the sample received back from JRC. The results of the two samples were identical. The distribution stage cannot be the cause of results discrepancy.

On the contrary, the storage and handling conditions in each laboratory could have been a cause of deterioration. Participant 8NA report a change in the colour of the powder experiment and identifies as possible cause of the measured low hydrogen capacity the loading of the sample in the equipment (or to impurities present in the hydrogen distribution line). Participant GKSS did not deliver any results because they found the sample almost not absorbing.

Un-homogeneity of the as-produced material

The material has been produced in various batches but carefully mixed before distribution. Two randomly chosen samples have shown exactly the same performance parameters.

Not achievement of full desorption

If the first desorption *pcT* curve at 125°C does not achieved a full desorbed state, possibly due to experimental limitations in obtaining low pressure values required to de-hydrogenate Na_3AlH_6 , the total hydrogen capacity value will result lower than the theoretical value. This aspect is typical of every hydrogen capacity measurement when starting sample is in the hydrogenated state. If no action is adopted to insure that full de-hydrogenation, the same total capacity value will be measured also at the end of the subsequent absorption experiment. This however would not be case, if an activation step is performed between the desorption and the absorption measurements. This is in fact the case for participant 2NA. The desorption experiment did not succeed to completely de-hydrate the material. Following one cycle of activation under the conditions prescribed in the protocol however (appendix 1, desorption at 150°C in vacuum), the material was fully desorbed and the absorption curve reach

higher hydrogen capacity. Therefore, the desorption curve has been a posteriori correct to start at the maximal capacity found during absorption (Figure 17). The other participants did not performed additional activation steps between desorption and absorption, so that it cannot be absolutely excluded that some results are to some extent affected by this error.

Time-to-equilibrium during pcT

The material is characterised by very slow kinetics of the materials. If not enough time is given to allow for chemical equilibrium at each pressure point, the result is a reduced total capacity and an increased plateau pressure. Unfortunately not all the participants have reported the adopted time-to-equilibrium. Participant 9NA has performed a parametric study with the acquisition time (2, 4, 10, 13 and 37 hour). A choice of 2 hours for the time to equilibrium does not allow for the achievement of the full capacity. From 4 hours upwards however, the final capacity did not increase further (Figure 12).

Some participants reported time-to-equilibrium values for each pcT point. The individual values are reported in the appendixes. It can be seen that in some case time of less than one hours have been used, which very probably were not enough to allow for equilibrium. It would be expected that the pcT curves affected by this too short equilibrium time would show a higher value of Δp_{ab-de} , the pressure difference between the ab- and the de-sorption plateaus (condition farer from equilibrium). However, the values of Δp_{ab-de} (Figure 7) do not show a trend when compared to time-to-equilibrium.

A look at the kinetic curves of the individual pcT points reveals that, even for very long time to equilibrium, the equilibrium is not achieved for some of the pcT curve points. However, these points belong to the steepest part of the pcT curve, where the uptake is negligible, so that the fact that a chemical equilibrium is not achieved does not affect the general curve behaviour. A comparison of the individual point kinetics curves could help in identifying difference usually not visible in the graphic representation of the pcT curves. Unfortunately it has not been possible to obtain the individual curves from the participants.

Leakage

The maximum in storage capacity has been measured as 4.5wt% at 125°C by participant 4NA. Considering however that the curve does not show a vertical asymptote as expected in the NaAlH₄ phase zone, it could be concluded that the data at high pressure are affected by a small leak.

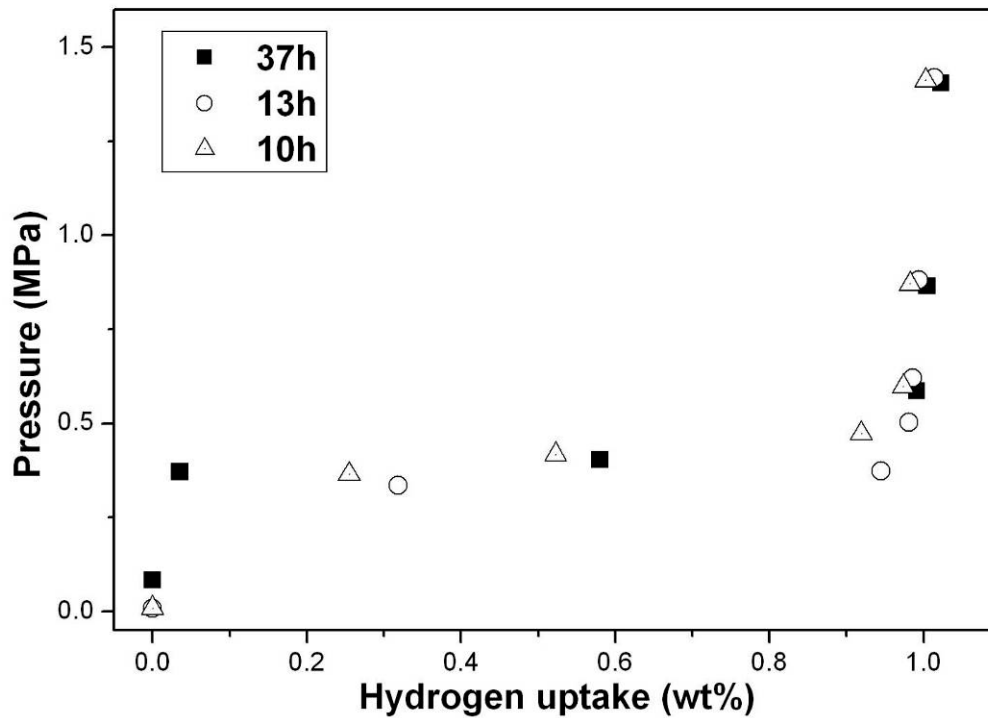


Figure 13 - Effect of the time-to-equilibrium on the measured hydrogen capacity

7.2. Kinetics curves

Already visually it is evident that the individual kinetics results differ almost orders of magnitudes. This has in first instance to do with the limitation of the experimental set-up of some partners. While gravimetric apparatuses can be performed desorption in dynamic vacuum, volumetric equipments have to measure pressure evolution during desorption in a closed vessel, with consequent pressure build up during experiment and the risk of a pressure build up so high to hinder the final desorption. In the case of sodium alanate, already a pressure of 1 – 2 bar would completely suppress the second desorption step corresponding to the decomposition of Na_3AlH_6 .

- Participant 7NA has performed an isothermal gravimetric experiment with dynamic vacuum, so that the results are not affected by the consequence of the build up of pressure occurring in static vacuum systems during desorption. From this point of view, its results should be considered as reference data set. However, it must be taken into account that the gravimetric set-up is

characterised by a worse sample temperature control than the volumetric technique especially under vacuum condition.

- Participant 4NA experiments are not isothermal. The first part of desorption occurred with a linear temperature ramp from room temperature.
- Participant 2NA and 10NA performed a volumetric experiment with a total volume enough big to keep pressure well below 1 bar. However, 10NA is not desorbing the whole hydrogen capacity while 2NA curve does not show any saturation. In both case not accurate calibration of the instrument could be an explanation.
- Participant 9NA has a final pressure probably too high for full desorption. Nevertheless at 150°C it is possible to see a well developed low pressure desorption step.

As reported in Section 3.2, a major and well known source of errors occurring during an experiment of isothermal sorption aiming at the assessment of kinetics time constants is related to the development of heat of reaction. If this heat is not properly accounted for in an optimised experimental set-up, the reaction is not performed isothermally and the results from different apparatus cannot be compared. Also in a qualitative comparison mode, experiment from the same apparatus could be misleading when materials with notably different heat of reaction (or different sampling quantities) are compared.

Nothing can be concluded on this issue from this RRT exercise. The differences encountered are to be explained with the very different way the experiments have been executed. The possible effect of the heat of reaction can obviously not be excluded, but is overshadowed by other more critical factors.

8. CONCLUSIONS

This round robin test was the most challenging among the three organised, the major obstacles to an accurate pcT acquisition consisting in the very slow kinetics and the very sensibility to air and moisture exposure. In fact, many participants have reported only partial data, some preferring the quicker kinetics at 140 °C to the acquisitions at 125°C. In one case, the participant has not been able to perform the experiment probably due to massive deterioration of the sample.

As expected, the data are characterised by a considerable dispersion of data. The full H₂ capacity has been found to vary in the [3.0 – 4.0] wt% and [3.5 – 4.5] wt% range at respectively 125°C and 140°C. The absorption plateau pressure of NaAlH₄ varies between 5.0 and 6.0 MPa with an average of 5.2 MPa and a standard deviation of 0.4 MPa at 125°C. At 140°C the absorption plateau pressure results in the 6.0 - 7.5 MPa range. The relative error for the 2nd plateau are 8% at both 125°C and 140°C (absorption) and for the 1st plateau 22% at 125°C and 13% at 140°C (absorption). As expected due to smaller absolute numbers, the Na₃AlH₆ plateau results shows much relative errors. Desorption values result higher, above 35% in the case of the Na₃AlH₆.

Similar data dispersion can be also found in the literature and must be considered as representative of the average uncertainty related to all the materials sharing with sodium alanate the same slow kinetics and environmental sensitivity.

The scope of this inter-laboratory comparison was an assessment of the accuracy of performance of the pcT curves by the various participants, and not the identification of individual causes of data dispersion. However, from a detailed analysis of participant reports two tentative discrepancy causes could be identified: too short time-to-equilibrium allowed for during pcT and Material deterioration during temporary storage and/or loading in the measuring instrument.

The kinetic curves show total capacity values ranging from 2.5 to 3.6 wt% and kinetic constant values which can differ of an order of magnitude. The kinetics curves cannot be quantitatively compared because the some of the partners did not follow the protocol and results of some others were affected by experimental limitations such as too high back pressure or not well calibrated expansion volumes. The result confirms the literature findings, i.e. that the assessment of the kinetic parameters is still far from being quantitative. However, the reason for this failure lays in the case of this RRT not so much in the control of the reaction heat, but more in the different approach to the kinetic experiment.

The analysis and discussion reported above clearly demonstrate how important is the recording and reporting of many experimental details for a thoroughly interpretation of the results and the identification of source of errors. In this sense, the acquisition and reporting protocol developed for this RRT exercise can be used as best practice for the experiments.

Differently to the first RRT exercise, the material selected for this exercise cannot be advised as standard material, being affected by to high sensitivity to environmental conditions and therefore prone to possible chemical instability of difficult control.

8.1. Acknowledgments

The Round Robin exercise organisers would like to thank all RRT participants and in particular the members of the RRT advisory group which prepared the measurement protocol, Nico Eigen (GKSS) and Wiebke Lohstroh (KIT-INT),

A special thank goes to Maximilian Fichtner, Oleg Zabara and Wiebke Lohstroh, which produced the material used in the RRT.

9. REFERENCES

- 1 Standard Practice for Conducting an Interlaboratory study to determine the Precision of a Test Method, ASTM International, E691-99, 1999.
- 2 Channing Ahn et al., Enhanced Hydrogen Dipole Physisorption, 2005 Annual Merit Review Proceedings of the US Department of Energy, http://www.hydrogen.energy.gov/pdfs/review05/stp_34_ahn.pdf
- 3 Wang X. -L., Suda S., "Consistent determination of the intrinsic kinetic properties between hydrogen and hydriding alloys" *Journal of Alloys and Compounds* 231 (1995) 660-665
- 4 K. J. Gross and K. Russell Carrington, Recommended Best Practices for the Characterization of Storage Properties of Hydrogen Storage Materials, National Renewable Energy Laboratory Contract No. 147388, V31, 12 December 2008 available at: <http://www1.eere.energy.gov>
- 5 D. P. Broom, The accuracy of hydrogen sorption measurements on potential storage materials, *International Journal of Hydrogen Energy*, 32 (2007) 4871-4888
- 6 B. Bogdanovic, M. Felderhoff, A. Pommerin, F. Schüth, N. Spielkamp, A. Stark, Cycling properties of Sc- and Ce-doped NaAlH₄ hydrogen storage materials prepared by the one-step direct synthesis method, *J. Alloy and Compounds*, 471 (2008) 383-386
- 7 B. Bogdanović, U. Eberle, M. Felderhoff, F. Schüth, Complex aluminum hydrides, *J Scripta Materialia*, 56 (2007) 813-816
- 8 Mosher et al., Design, fabrication and testing of NaAlH₄ based hydrogen storage systems, *J. Alloy and Compounds*, 446-447 (2007) 707-712

ANNEXES

1. Measurement Protocol	32
2. Detailed Results Partner 1NA.....	36
3. Detailed Results Partner 2NA.....	38
4. Detailed Results Partner 4NA.....	40
5. Detailed Results Partner 7NA.....	42
6. Detailed Results Partner 9NA.....	48
7. Detailed Results Partner 9NA.....	50
8. Detailed Results Partner 10NA.....	57

1. MEASUREMENT PROTOCOL

NESSHY ROUND ROBIN TEST ON HYDROGEN ABSORPTION MEASUREMENTS – NaAlH₄

Your participation RRT number: xxxx

Material

NaAlH₄ + 4mol.% CeCl₃ produced by Institut für Nanotechnologie, Forschungszentrum Karlsruhe.

Safety and handling

The sample is sent in a SS special leak tight container under Argon atmosphere. The sample **must** be transported and handled under protective atmosphere without any exposure to air and moisture. Health hazards and safety prescriptions can be found in the Material Safety Data Sheet attached to this protocol.

Loading / Outgassing / Flushing procedure

The sample **must** be loaded in the experimental set up under protective atmosphere without exposure to air. Before the experiment starts, an **outgassing / flushing** procedure is required and repeated at least three times. The outgassing can be performed using primary vacuum or better. The flushing procedure can be carried out with inert or hydrogen gas.

Activation procedure before any experiment

Prior to any experiment, an activation procedure is required consisting of 3 desorption / absorption cycles. The activation procedure must be recorded and reported.

- ☞ The desorption should be performed at 150 °C under vacuum,
- ☞ The absorption at 125 °C and 100 bar.

Indicatively, the time scale for the absorption is around 5-6 hours.

☞ Partners that cannot perform the activation procedure and the re-absorption of the material at indicated hydrogen pressure may only perform and report the first desorption kinetic curve at 125 °C.

Experiments

A - Sorption characterisation

Purpose of this part is the inter-laboratory comparison of both thermodynamic and kinetic hydrogen sorption properties measured by volumetric and/or gravimetric methods.

P-C isotherms shall be acquired up to the maximal pressure the equipment can reach or, alternatively, up to the maximal uptake, in the following way:

- ☞ **One desorption and one absorption isotherm at a temperature of 125 °C.**

Optionally, a second set of desorption and absorption isotherms is to be measured at 140 °C under similar hydrogen pressure conditions.

Please note! The activation procedure described above must be repeated after each P-C isotherm measurements.

Desorption Kinetic properties shall be acquired isothermally, in the following way:

- ☞ **One desorption kinetic curve at temperature of 125 °C,**
- ☞ **One desorption kinetic curve at temperature of 150 °C.**

The absorption after kinetics measurements can be performed at 125°C and 100 bar.

The instrumental calibrations for the measurements as well as the choice of the method for the evaluation of the sample density to be used for the calculations is left to the individual laboratories, and the detailed description of this procedure and its pertinent data will have to be provided.

B – Dissociation enthalpy evaluation

Goal of this second part is the inter-laboratory comparison of the enthalpy of dissociation of the two step reversible dissociation reactions measured by volumetric and/or gravimetric methods.

To this purpose, at least two isotherms are required, although a minimum of 3 isotherms are recommended. The choice of these temperatures, as well as the plateau pressure values to be used for the calculation is left to the individual laboratories.

Reporting results

Please send back to JRC at least the following set of data:

❖ Sorption characterisation

- ☞ Sample storage place and time before experiment, oxygen and moisture levels of the inert atmosphere of the glove box (if available),
- ☞ The description and record of the activation procedure experiments,
- ☞ Sample weight for each experiment is left to individual laboratories,
- ☞ The density used for the calculations, together with a detailed description of the procedure adopted for this measurement,
- ☞ The full P-C isotherms and kinetics data in ASCII datasheets, in term of Sorption Concentration (wt. % H₂ per NaAlH₄ + 4mol.% CeCl₃) as function of the pressure (Pa) for all measured temperatures (if available, also isotherm and kinetic graphs, in any form),
 - Details of every individual isotherm points: the sorption concentration (wt. % Hydrogen) versus time for every pressure step (if available),
 - The temperature records for all the isothermal points, together with the maximum accepted temperature variation during the isotherm measurements,
 - The minimum time and time out for the pressure equilibration of each isotherm individual points,
 - The buoyancy correction for the gravimetric method (if used),
- Experimental set-up data: such as the reaction chamber volume, the molar balance formula (in case of volumetric method) together with the gas law used (compressibility factors etc.), purity of the hydrogen gas, the precision of pressure gauge (if available) etc,
- ☞ A description of the outgassing experiment (if available, also the pressure record during outgassing),
- ☞ All pertinent events that arise during any phase of the test and may affect the measurements.

❖ **The dissociation enthalpy** (if calculated)

- ☞ All the experimental data at the basis of the dissociation enthalpy calculation in ASCII datasheet: the isotherms used (see the previous report guideline for sorption characterisation),
- ☞ The Van't Hoff plots : the temperature and the plateaux pressure values for the enthalpy calculation,
- ☞ All pertinent events that arise during any phase of the test and may affect the measurements.

In case a laboratory best practice or protocol has been followed, please send also a copy of it.

Confidentiality of data

Your participant number is 1HYS. Please use this number for all the communication during the execution of the RRT and when reporting the results. For example, do not name your result files with the name of our laboratory, but with your participant number.

2. DETAILED RESULTS PARTNER 1NA

Partner 1NA performed only pcT curves in absorption and desorption up to the end of the first plateau.

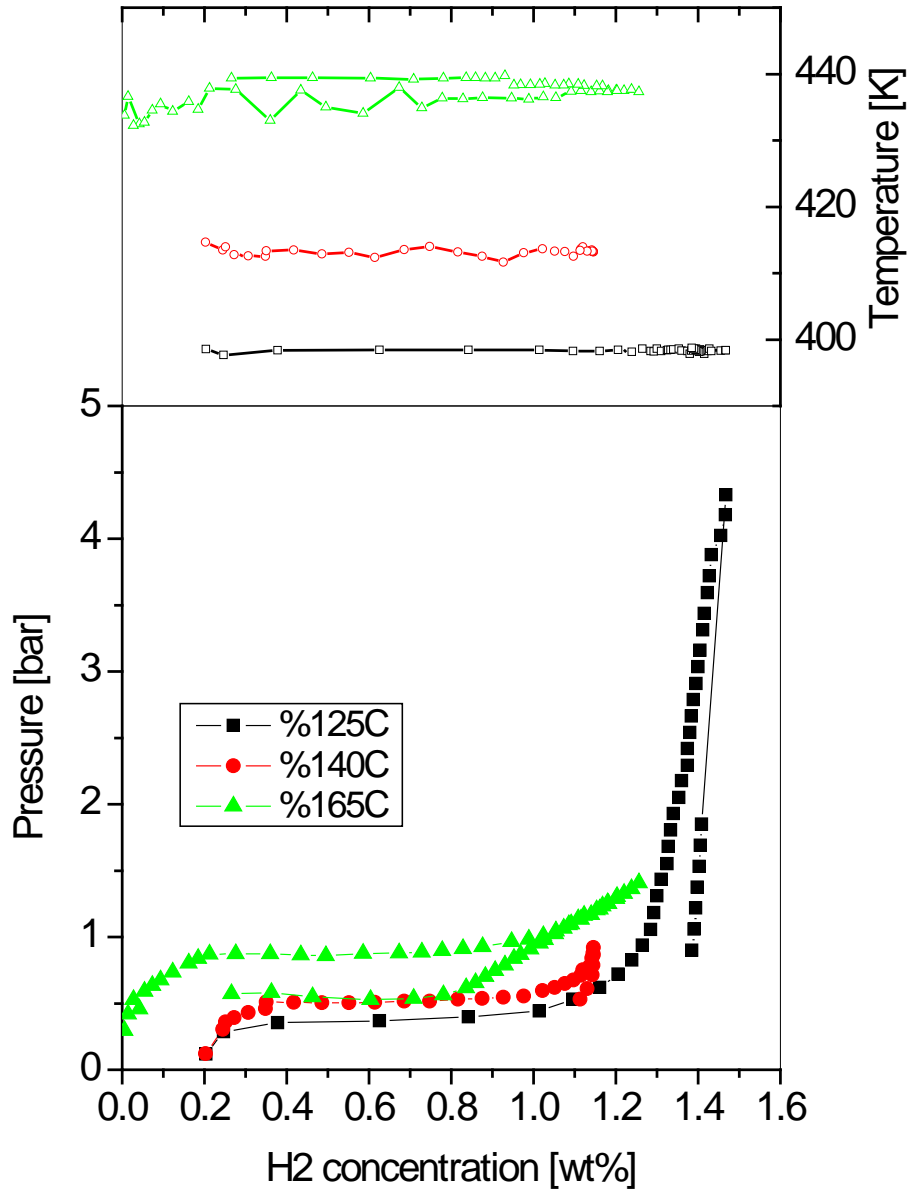


Figure 14 – Partner 1NA pcT at three temperatures (only first plateau). Thermal stability is also shown. No indication of position of measurement.

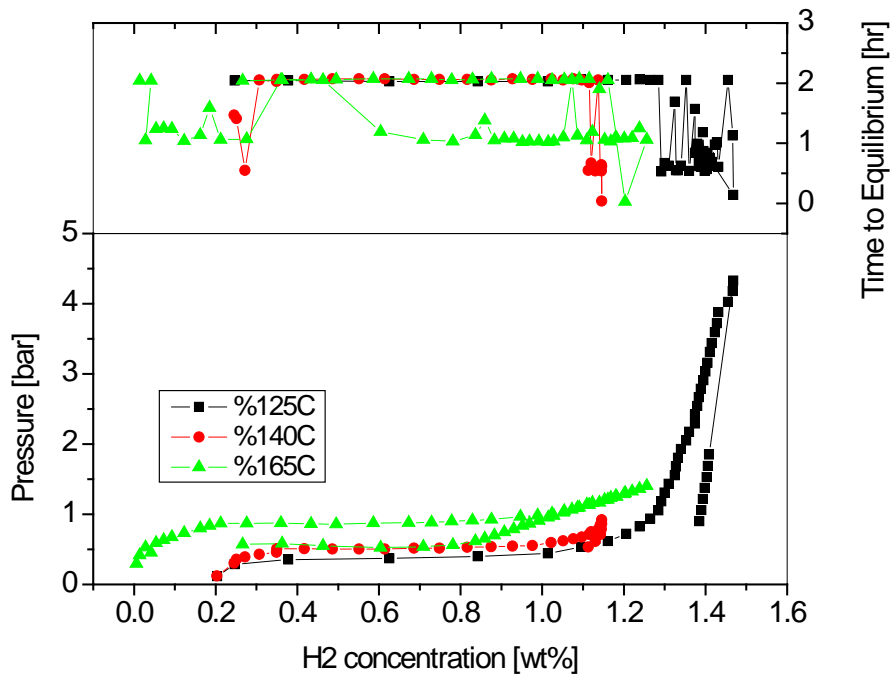


Figure 15 - Time to equilibrium for individual pcT isotherm points. Times to equilibrium range between 0.5 to 2 hours. No indication from participant on the method adopted.

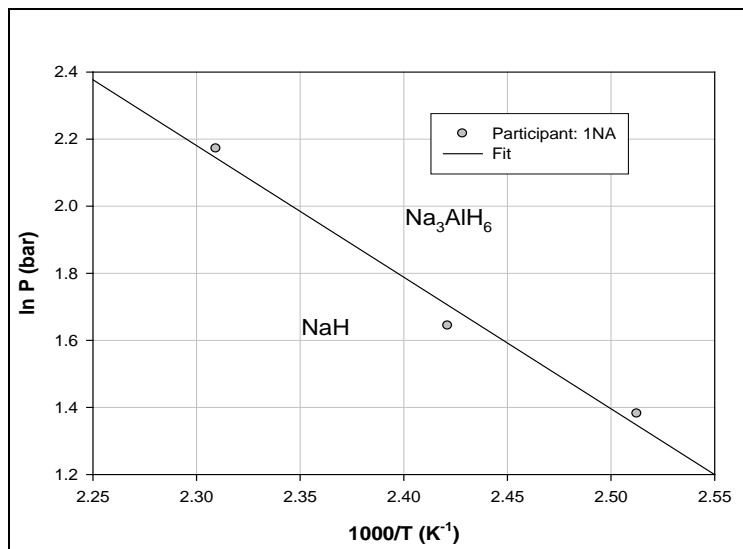


Figure 16 – Partner 1NA van T'Hoff plot for Na_3AlH_6

3. DETAILED RESULTS PARTNER 2NA

While all the other laboratories has acquired a desorption and absorption curve after each other, participant 2NA performed the absorption after a second set of activation steps (Figure 17). Considering the stability of the material, this should not influence sensibly the results. The equipment used by 2NA was not able to perform a full desorption, due probably to limited capability in the sub-atmospheric pressure control. As a consequence, the raw desorption pcT curve does not show the low pressure plateau. The desorption curves were corrected by shifting the max hydrogen capacity to that value found at the absorption curve.

It is not clear however, the cause of the non linear behaviour of the pcT curves after the 2nd plateau, well in the NaAlH₄ phase. The temperature history (Figure 17 and Figure 18– middle) shows a decrease of the temperature stability in that area. The variation, however, are less than $\pm 0.5^{\circ}\text{C}$ and cannot account for the non-linear curve evolution. 2NA has also reported acquisition time for each pcT curve (Figure 17 and Figure 18– top).

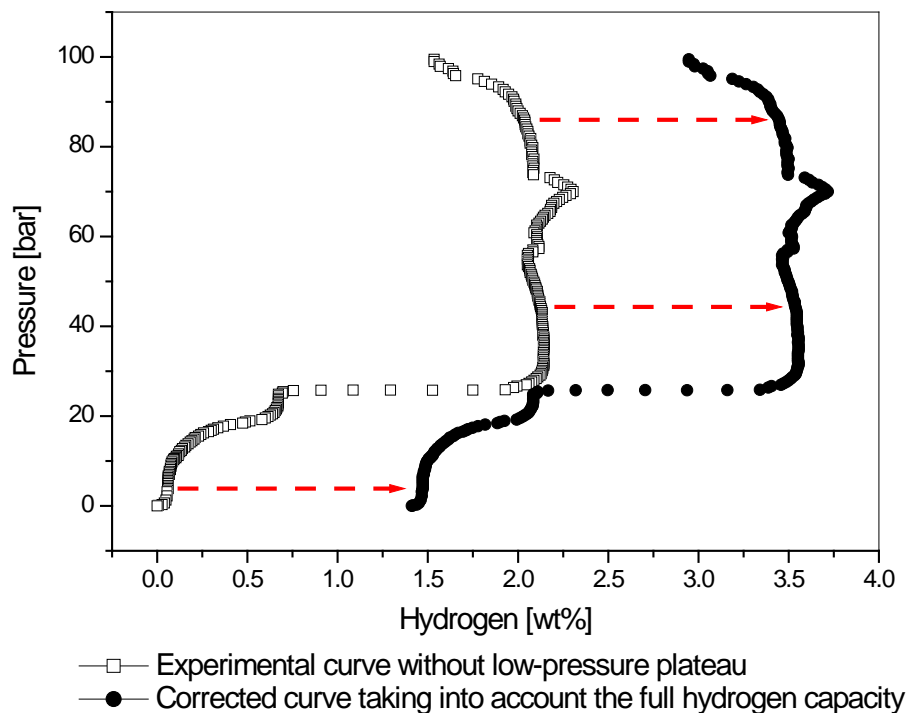


Figure 17 - Participant 2NA: the original desorption curve has been corrected by shifting it to correspond to the maximal hydrogen capacity found during absorption, in order to take into account the uncompleted desorption as first step.

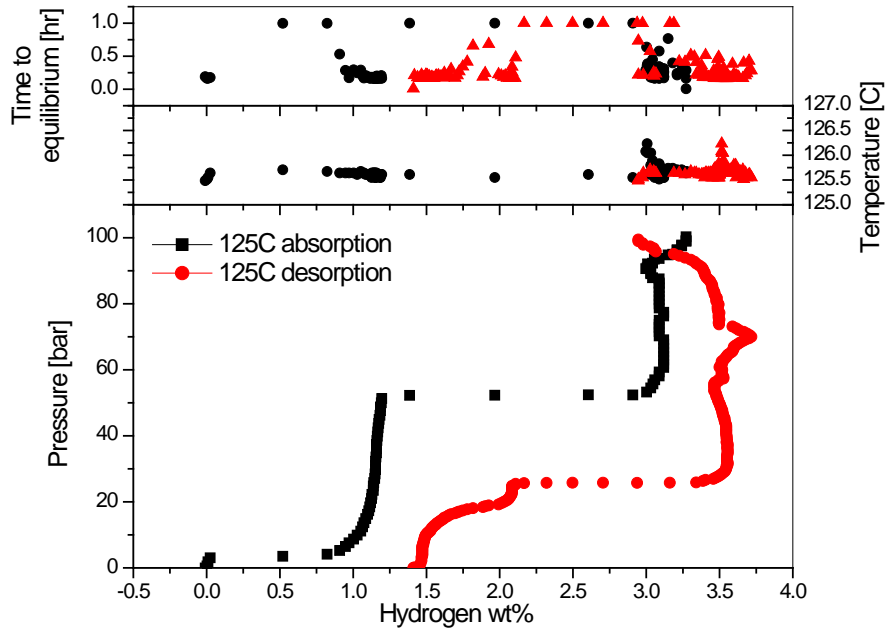


Figure 18 - Participant 2NA: pcT curves at 125°C (bottom), temperature history (middle) and time spent for each pcT point (top)

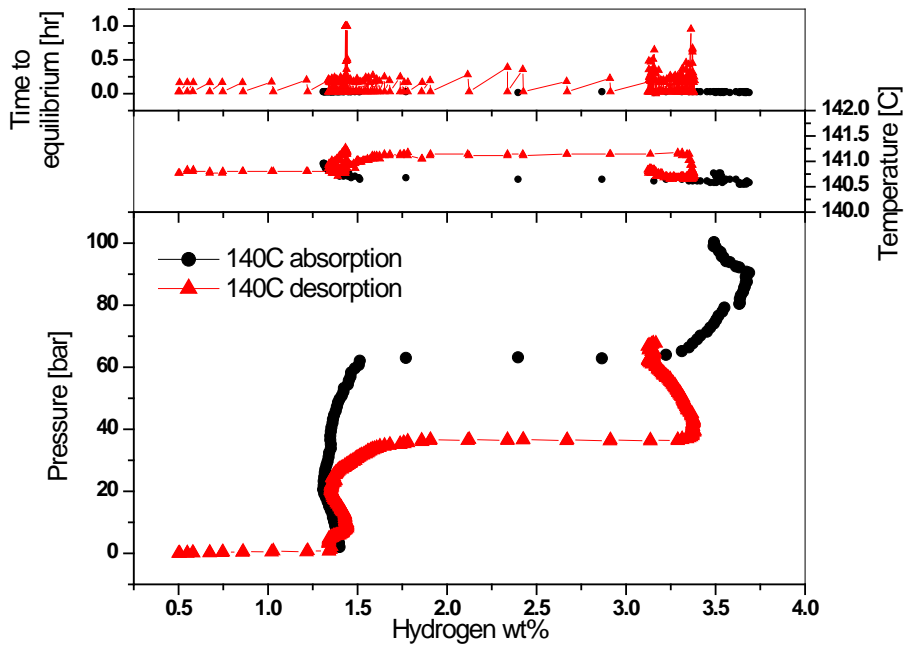


Figure 19 - Participant 2NA: pcT curves at 140°C (bottom), temperature history (middle) and time spent for each pcT point (top)

4. DETAILED RESULTS PARTNER 4NA

Thermal stability has been indicated as ± 0.1 °C for all isotherms.

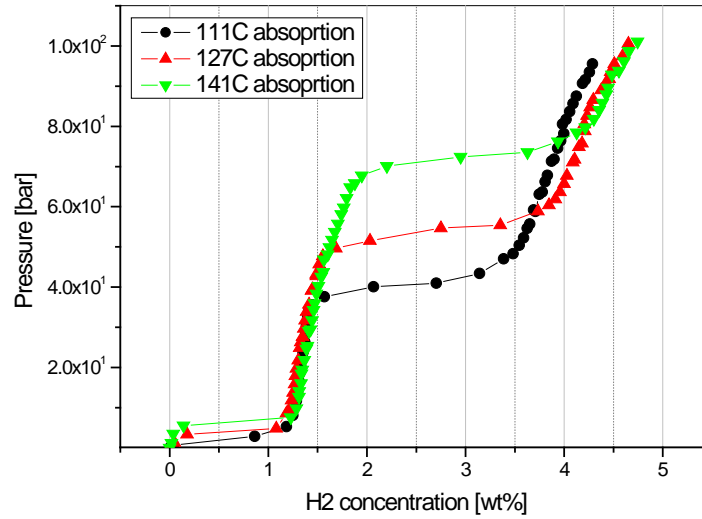


Figure 20 - Partner 4NA - pCT absorption curves

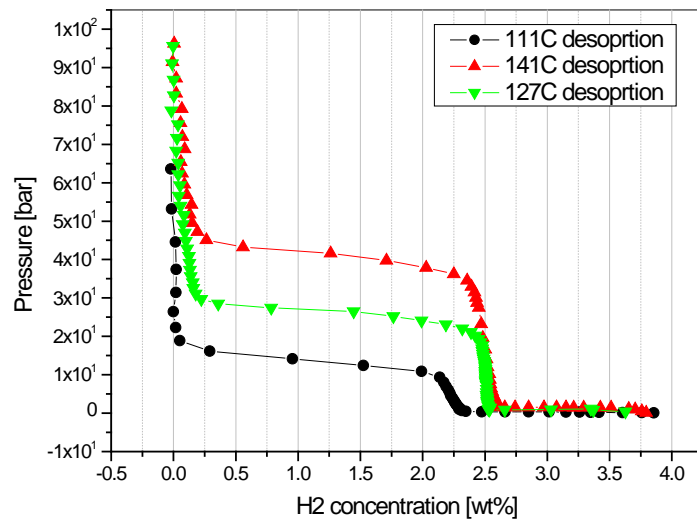


Figure 21 - Partner 4NA - pCT desorption curves

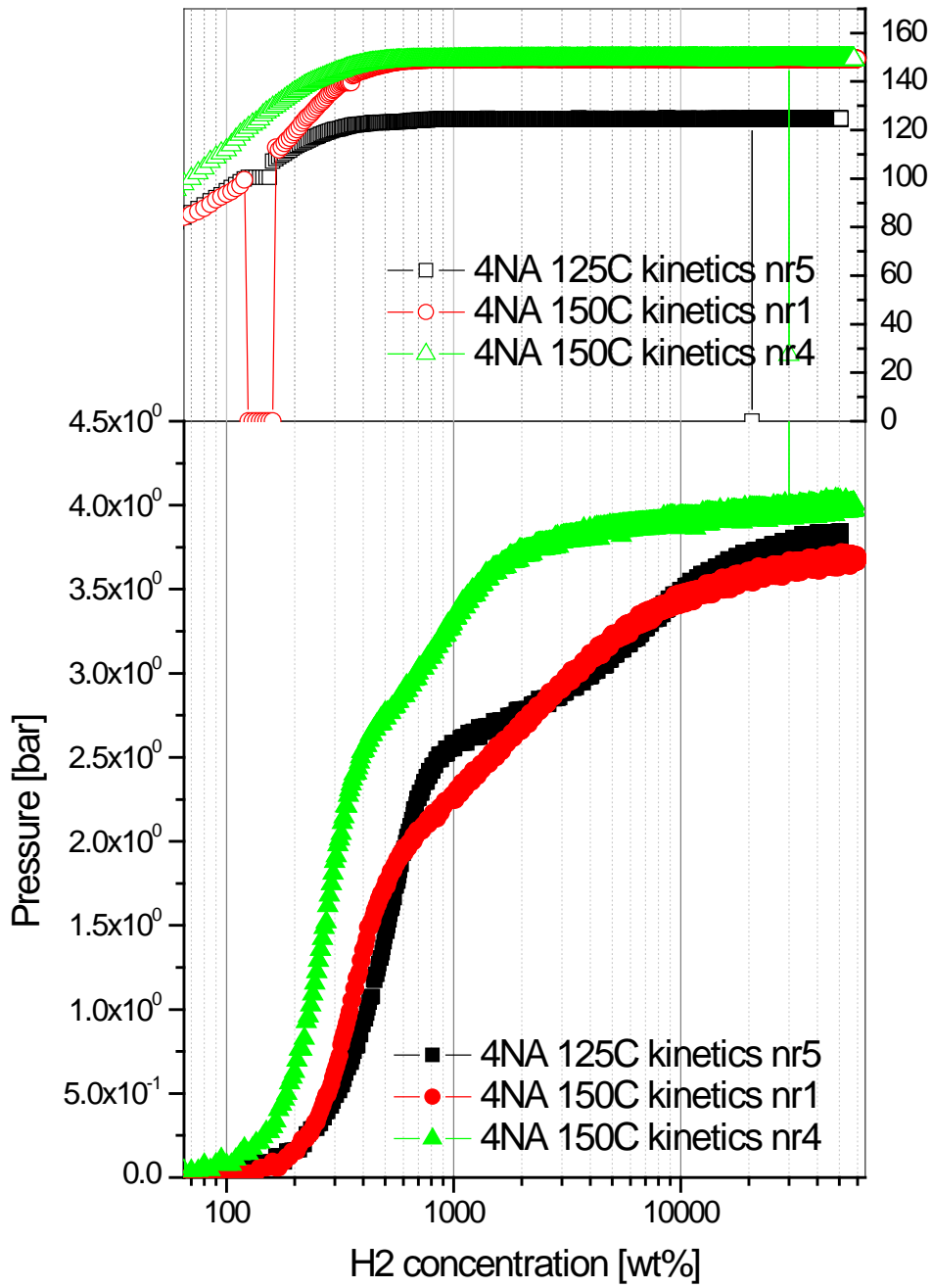


Figure 22 - Partner 4NA kinetics. Thermal history is also shown.

5. DETAILED RESULTS PARTNER 7NA

Participant 6 performed dynamic pcT according to A mass flow controller was used to determine the amount of hydrogen supplied into the system. The amount of hydrogen absorbed by the sample n_{abs} was calculated from the following equation

$$n_{abs} = \frac{P^* V_g}{RT^*} - \frac{PV_{sys}}{RT}$$

with $V_g = ft$

where P^* and T^* are the standard pressure and temperature, R gas constant, V_g the volume of hydrogen supplied into the system, f flow rate (const.), t the reaction time, V_{sys} the system volume, P and T the pressure and temperature in the system, respectively. The pcT measurements were made in the pressure range up to 40 bar and at the temperatures of 125 °C, 140 °C, and 150 ° (Fig. 4). The plateaux of pcT curves were measured at the pressures ranging from 4 to 10 bar where the compressibility factor of hydrogen is below 1.006 at 25 °C. The compressibility factor of hydrogen was not used in the calculation of n_{abs} .

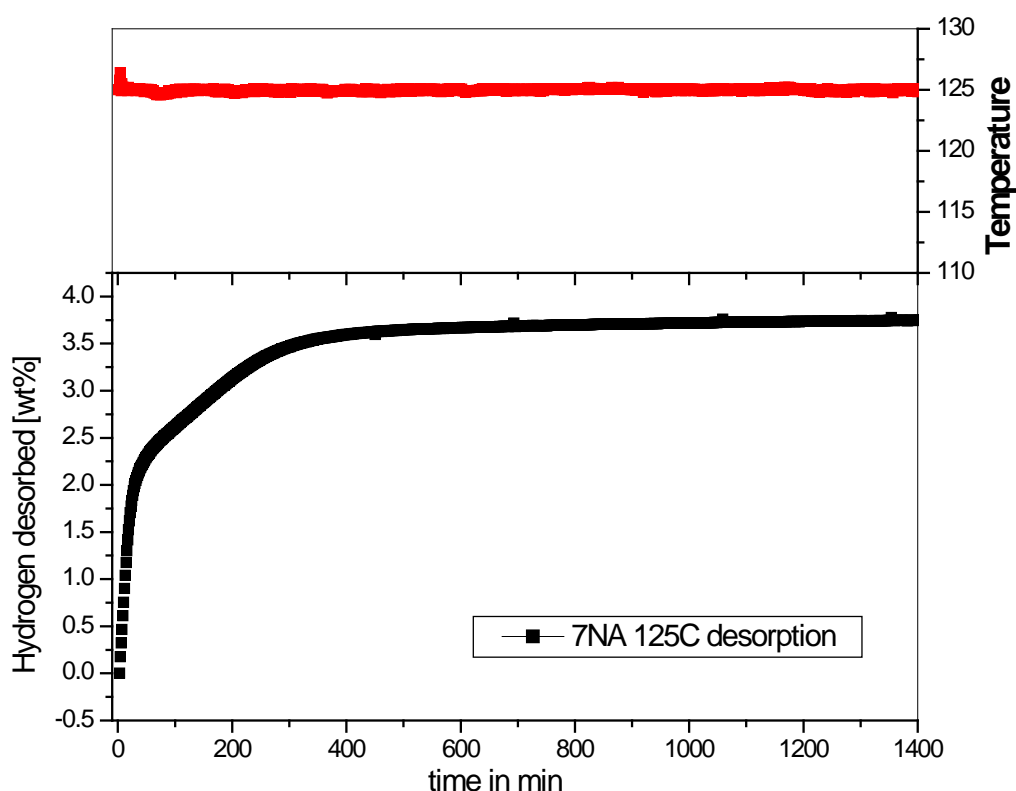


Figure 23 - The 3rd desorption under vacuum at 125°C measured by thermogravimetry. Due to the fast initial kinetics, there is an uncertainty of ~0.7 mass%.

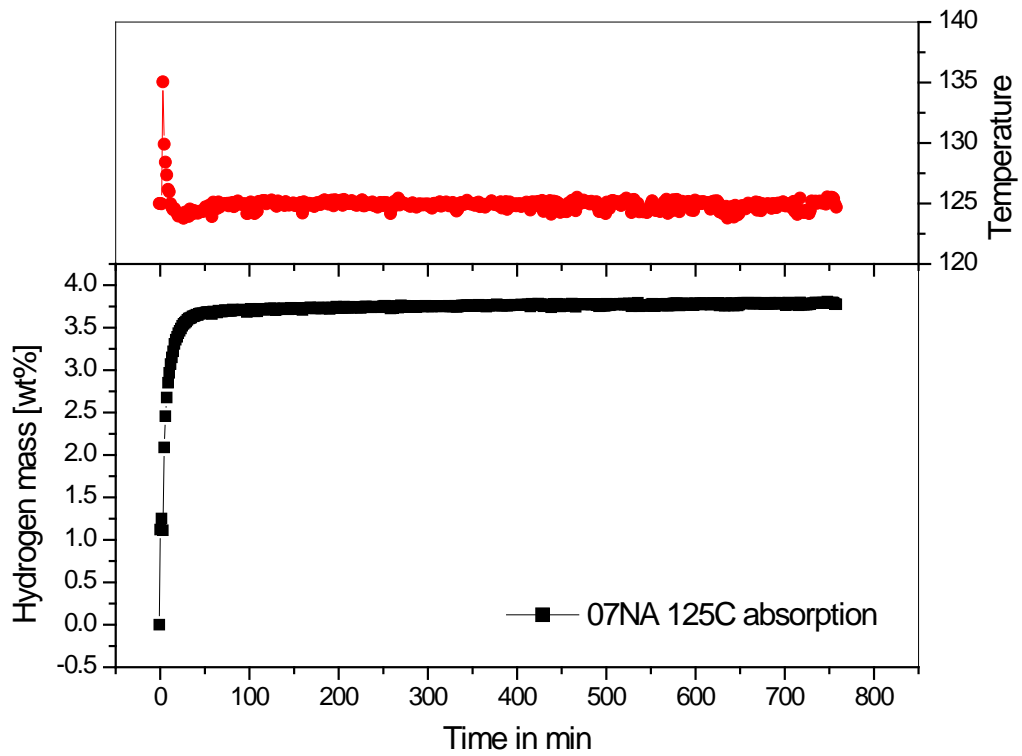


Figure 24 - The 3rd absorption at 125°C and 100 bars measured by thermogravimetry. Due to the fast initial kinetics, there is an uncertainty of ~0.7 mass%.

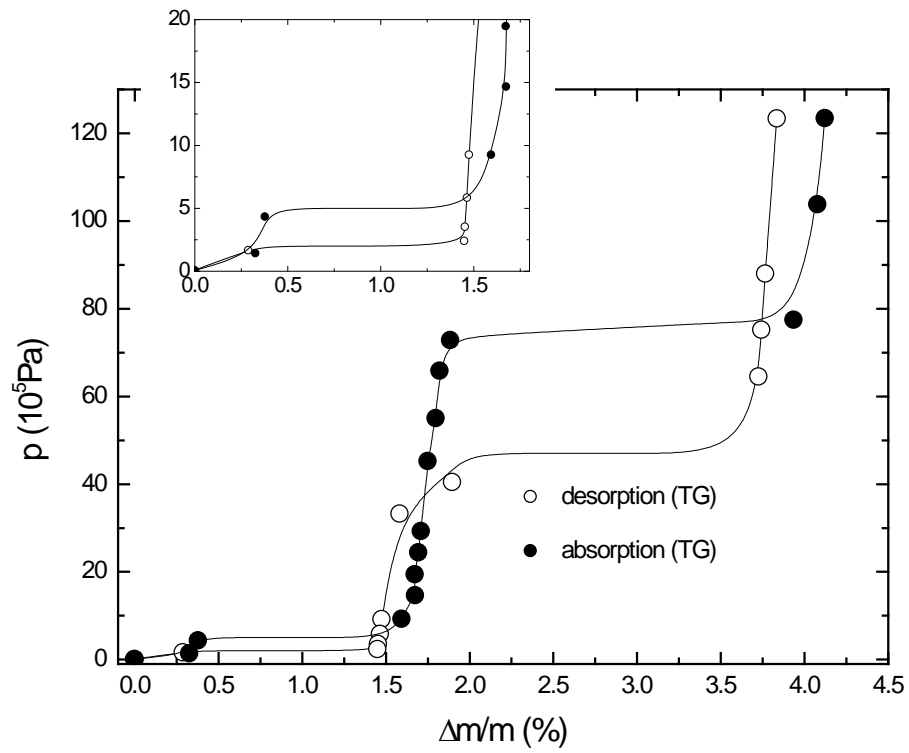


Fig. 3 pcT of NaAlH₄ at 140°C measured by thermogravimetry. Lines are guides to the eyes.

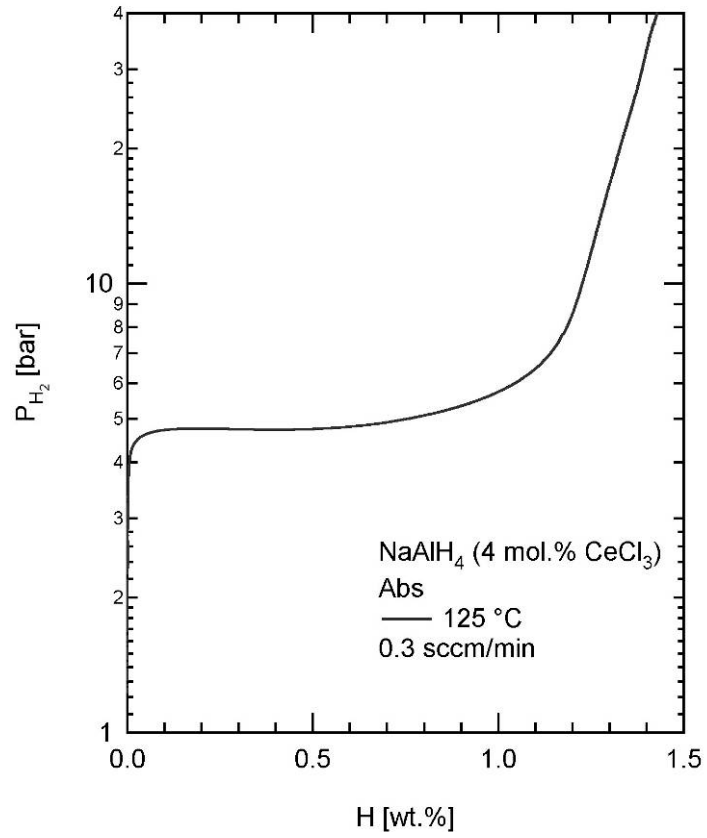


Figure 25 - Dynamic pcT at 125°C measured under the constant flow rate of 0.3 sccm/min.

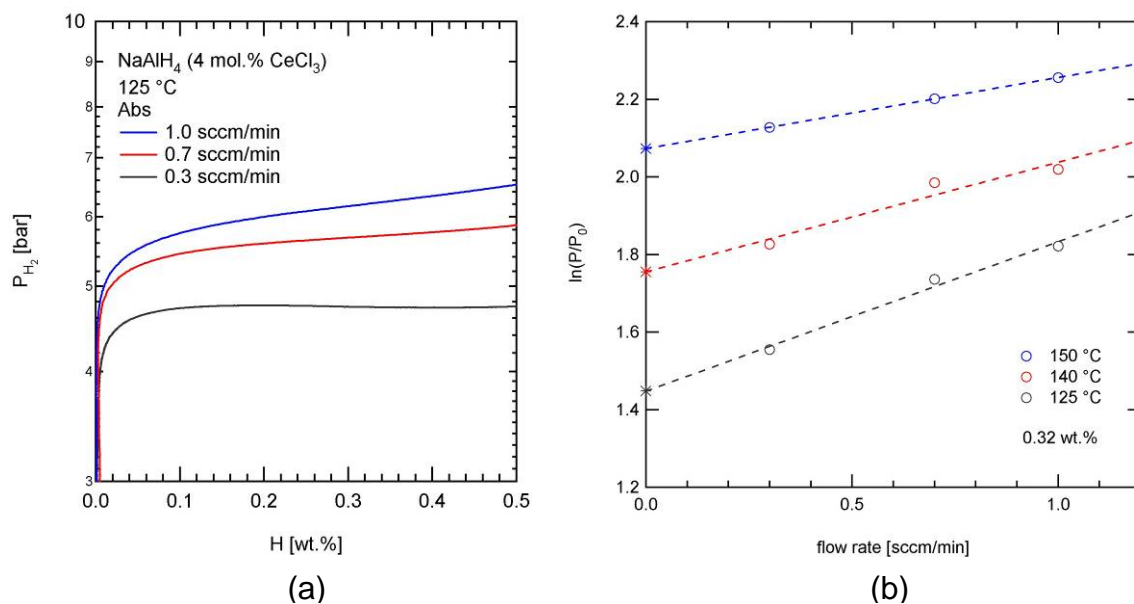


Figure 26 - (a) The flow dependence of the plateau pressures at $125^\circ C$ measured at the different flow rates of 0.3, 0.7 and 1.0 sccm/min. (b) The flow dependence of the pressures at the H concentration of 0.32 wt.% and the temperatures of $125^\circ C$, $140^\circ C$, and $150^\circ C$. The equilibrium pressures in Na_3AlH_6 formation were determined by extrapolating the pressures to the zero flow rate (intercepts).

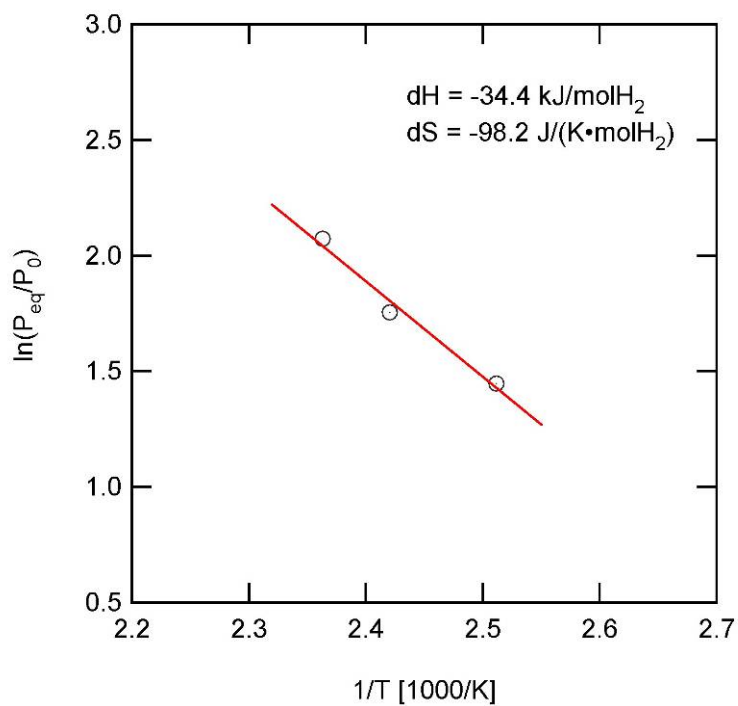


Figure 27 - van't Hoff plot equivalent to the formation of Na_3AlH_6 . $\Delta H = -34.4 \text{ kJ/molH}_2$ and $\Delta S = -98.2 \text{ J/(K}\cdot\text{molH}_2)$ were obtained.

6. DETAILED RESULTS PARTNER 9NA

Temperature records were not reported, however the temperature stability in the sample is declared as ± 0.2 °C.

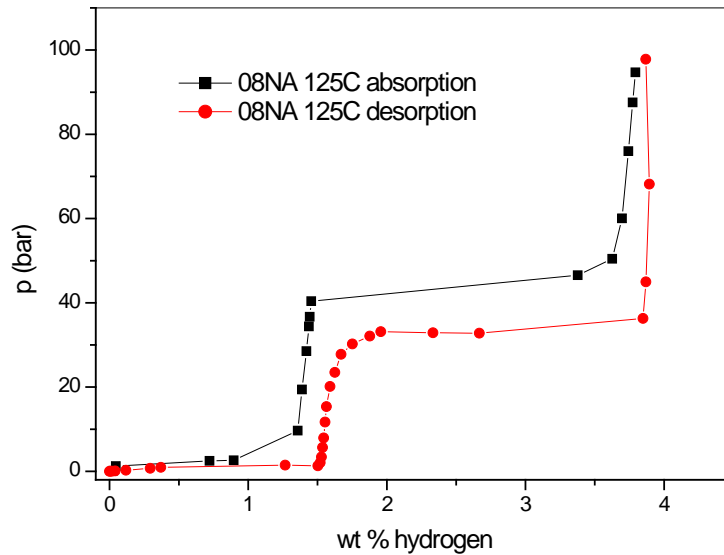


Figure 28 – p-cT of participant 08NA.

The activation procedure consisted of 3 desorption / absorption cycles. During desorption, the system was first kept closed until an equilibrium pressure was reached, then it was set to vacuum at 50 °C (T_1). The temperature was then raised from 50 to 150 °C (T_2) and the sample kept under vacuum. For the absorption the system was kept at 125 °C and 100 bar (refilling when the pressure was decreasing).

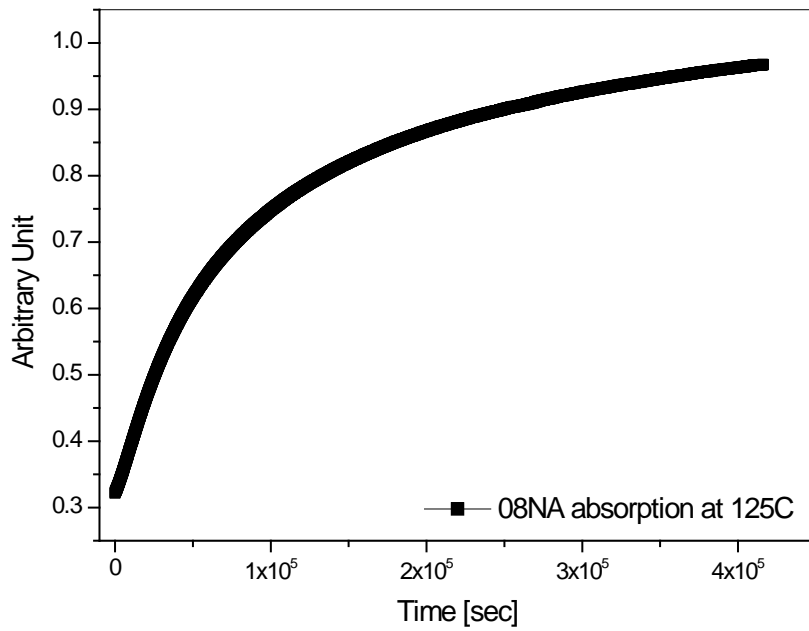


Figure 29 – Participant 08NA, example of activation curve: 2nd absorption at 125°C

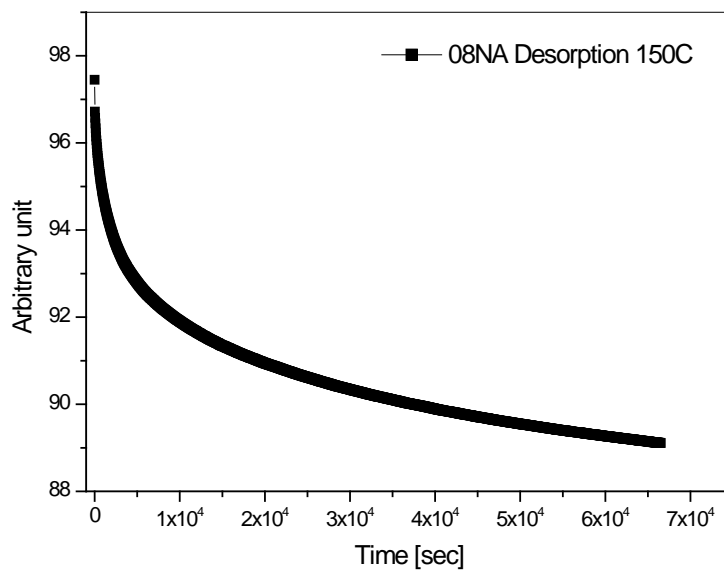


Figure 30 – Participant 08NA, example of activation curve: 2nd desorption at 125°C

7. DETAILED RESULTS PARTNER 9NA

The maximum uptake for both isotherms is 3.0 wt% at 9.5 MPa. This value is lower than we might expect from such a material. One possible explanation is coming from examination of sample after unloading from the instrument. A small fraction of the sample is found to be white after all experimental campaign indicating an oxidation and therefore a strong reduction of the hydrogen capacity. The oxidation might have occurred either during the first loading of the sample in the inert atmosphere or during measurements (activation, PCI's, kinetics) by the use of slightly contaminated gases.

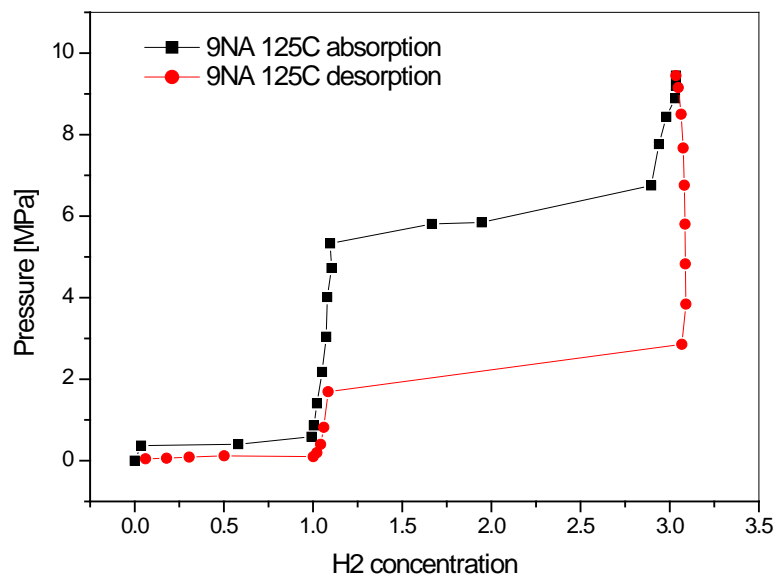


Figure 31 - 9NA pcT at 125°C

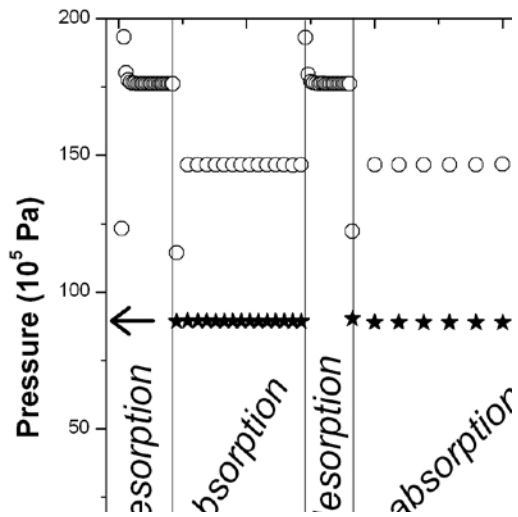


Figure 32 - 9NA Activation cycles

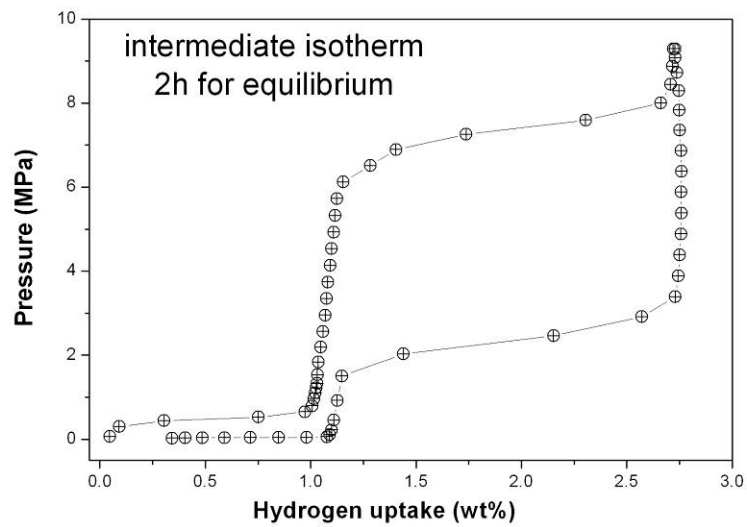


Figure 33 - Intermediate absorption/desorption isotherm at 125 °C (398 K) with 2h time allowed for equilibrium. The maximum uptake is 2.72 wt% at 9.5 MPa.

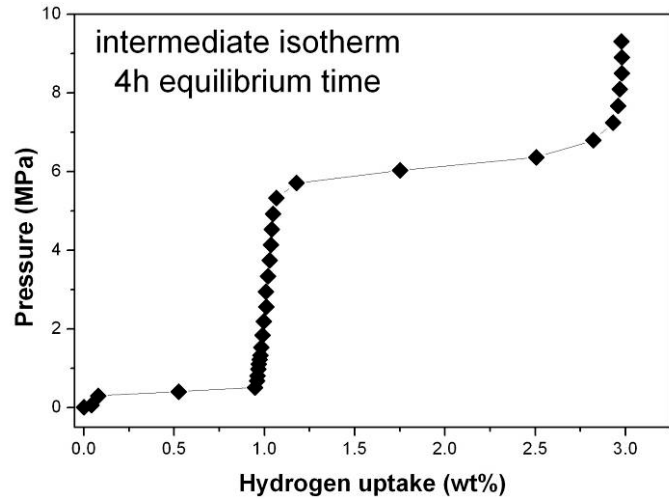


Figure 34 - Intermediate absorption isotherm at 125 °C (398 K) with 4h time allowed for equilibrium. The maximum uptake is 3.0 wt% at 9.5 MPa.

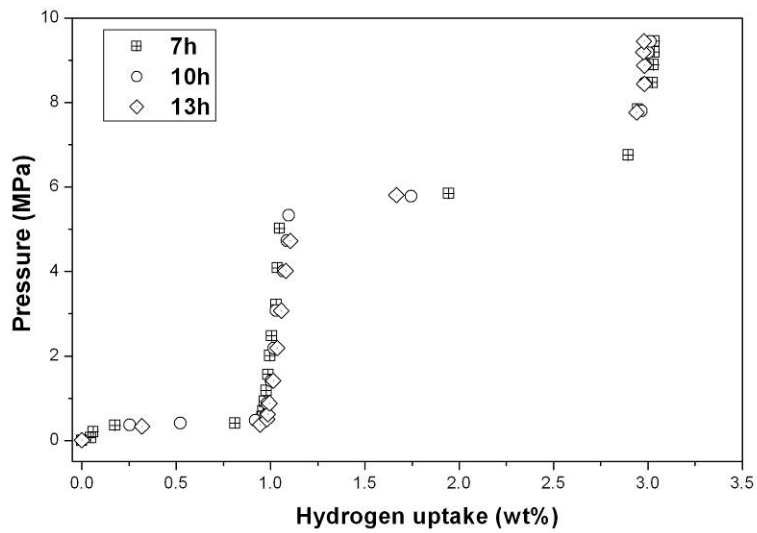


Figure 35 - Comparison of three absorption isotherms at 125 °C (398 K) with 7h, 10h and 13h time for equilibrium.

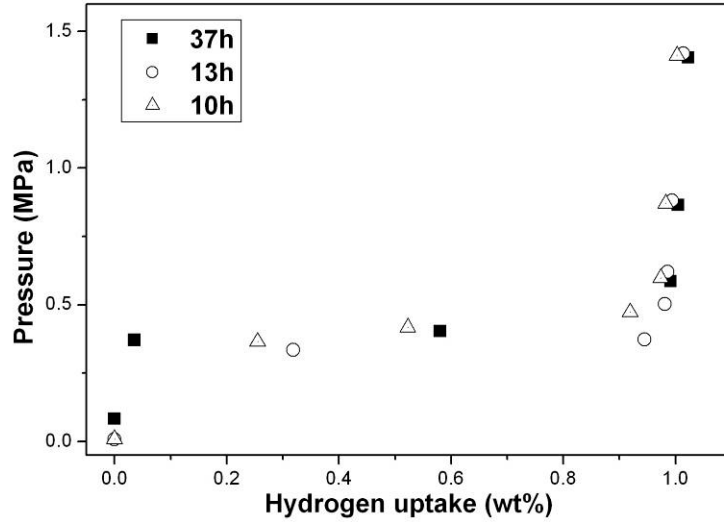


Figure 36 - Comparison of three absorption isotherms at 125 °C (398 K) with 10h, 17h and 37h time for equilibrium. Only the first plateau is shown here for comparison.

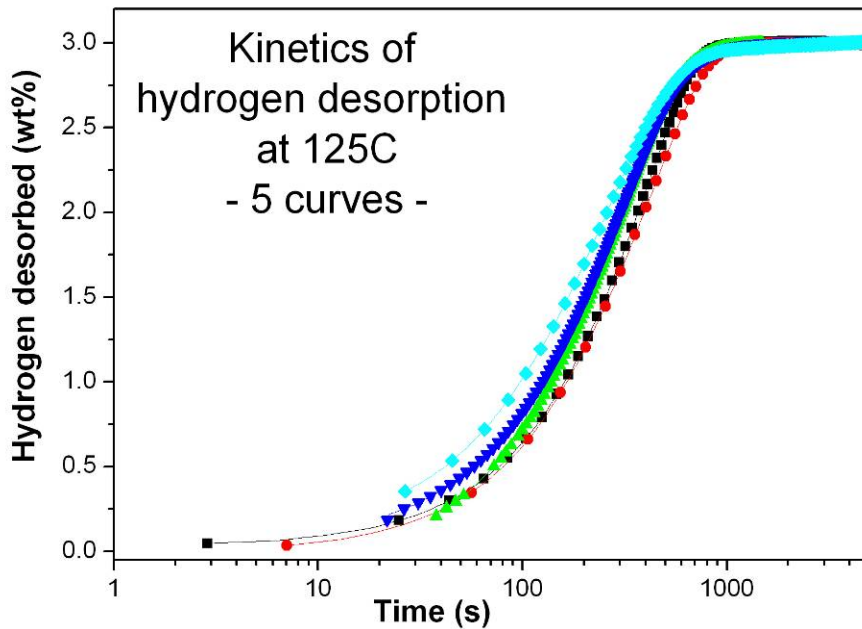


Figure 9. Five recorded kinetic curves of hydrogen desorption at 125 °C. Figure 9 displays the five hydrogen desorption kinetic curves recorded 125 °C. They have the same shape and the small time shift is probably due to the determination of the time origin.

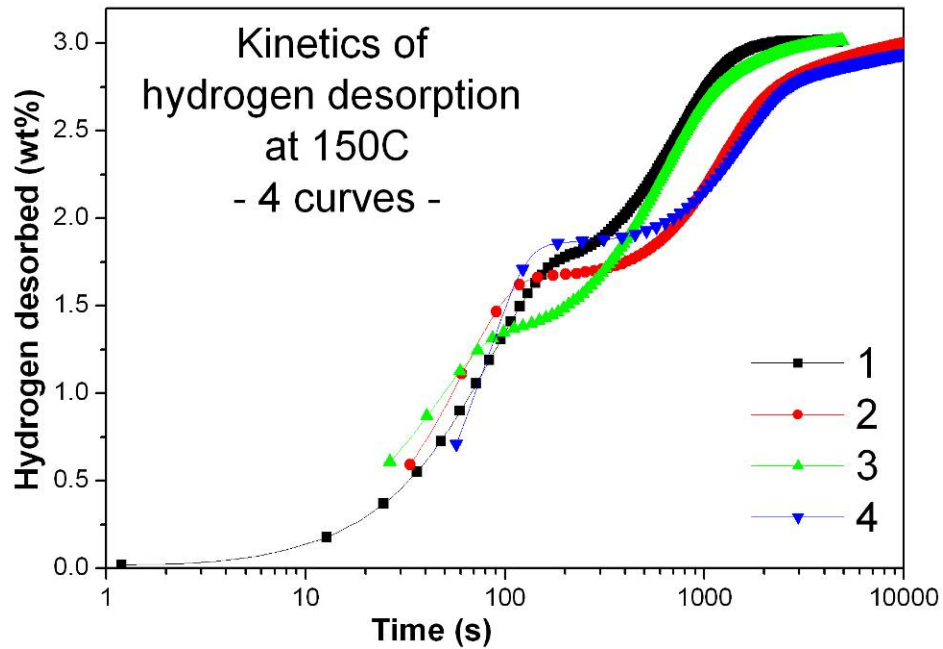


Figure 10. Kinetic curves of hydrogen desorption at isothermal conditions of 125 and 150 °C. Figure 10 shows the four hydrogen desorption kinetic curves recorded 150 °C. All curves show 2 step desorption reaction. They do not overlap each other and the strong time dependence might be accounted for by the history of the sample. The curves 1, 2 and 4 have been recorded after 2 or 3 activation cycles performed between experiments. The curve 3 was recorded just after performing PCI measurement. Unfortunately, due to limited time the kinetic behaviour at 150 °C could not be confirmed by further measurements.

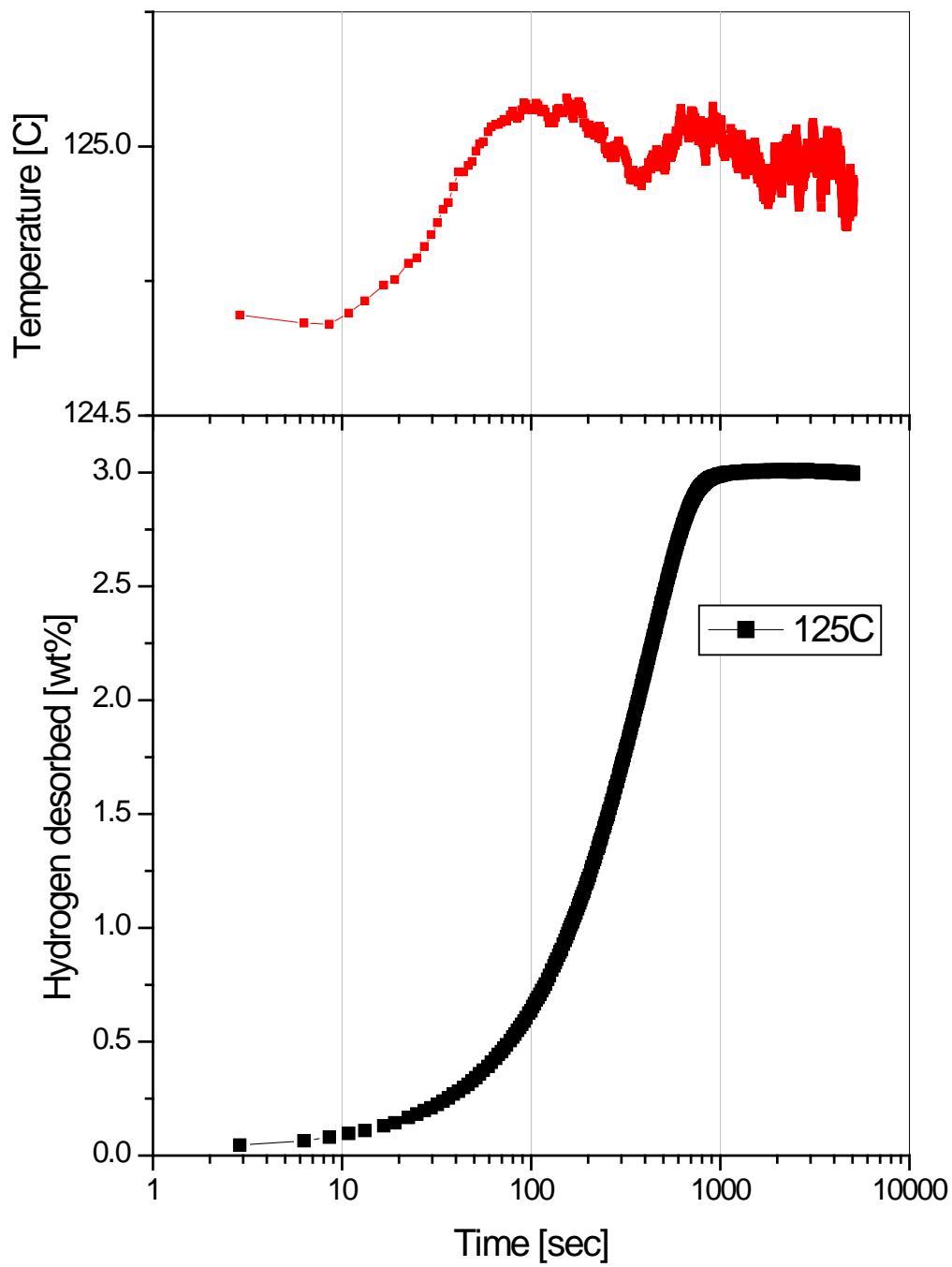


Figure 37 - 9NA kinetics at 125°C

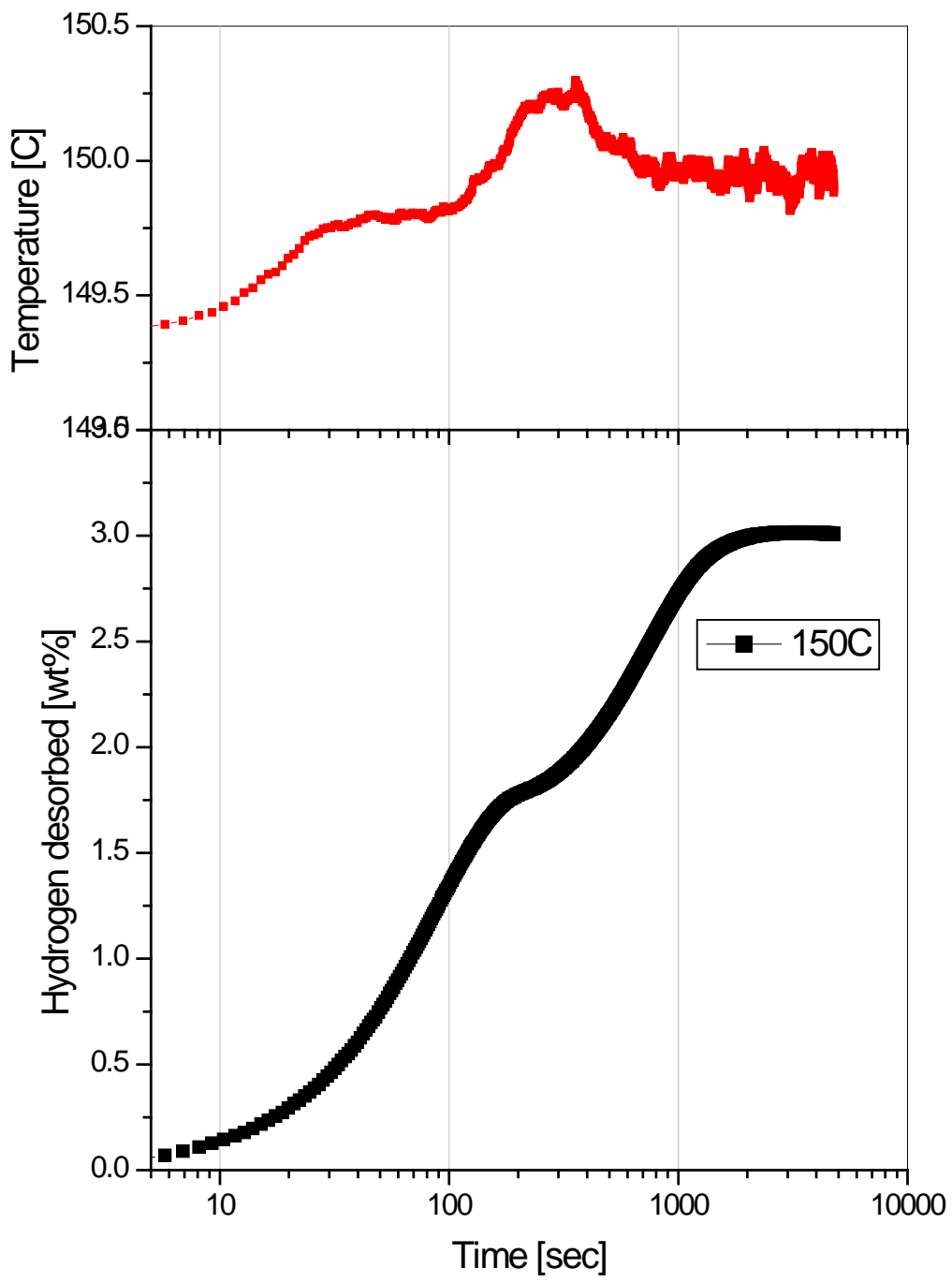


Figure 38 - 9NA kinetics at 150°C

8. DETAILED RESULTS PARTNER 10NA

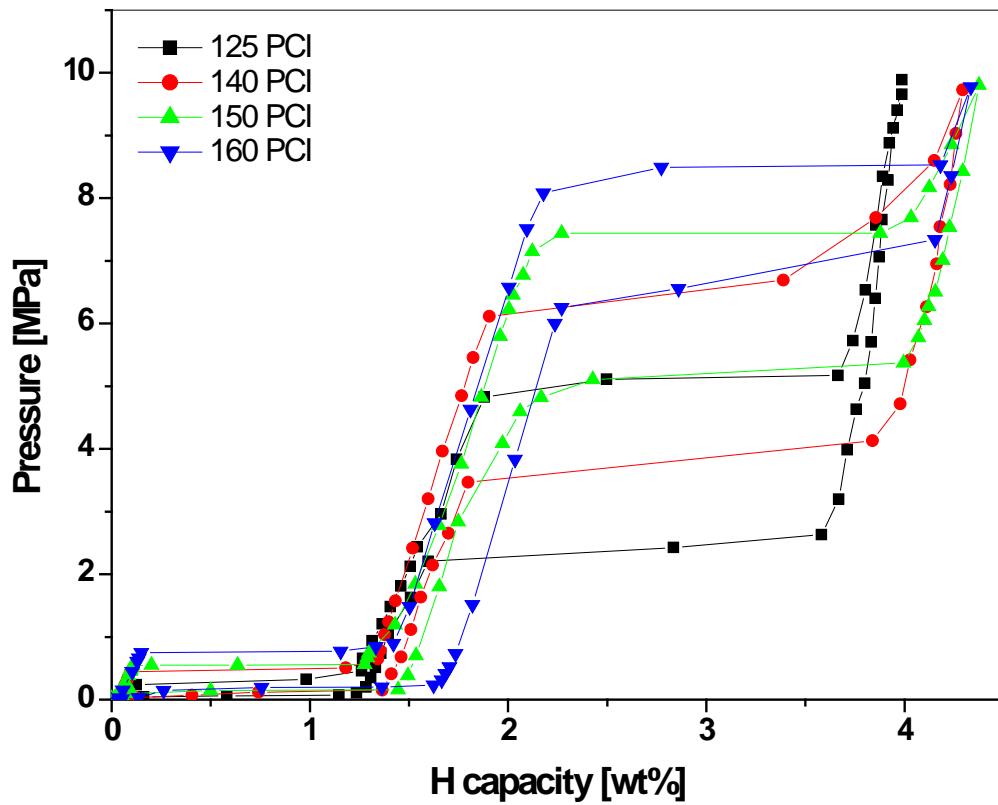


Figure 39 – Partner 10NA: ab- and desorption curves

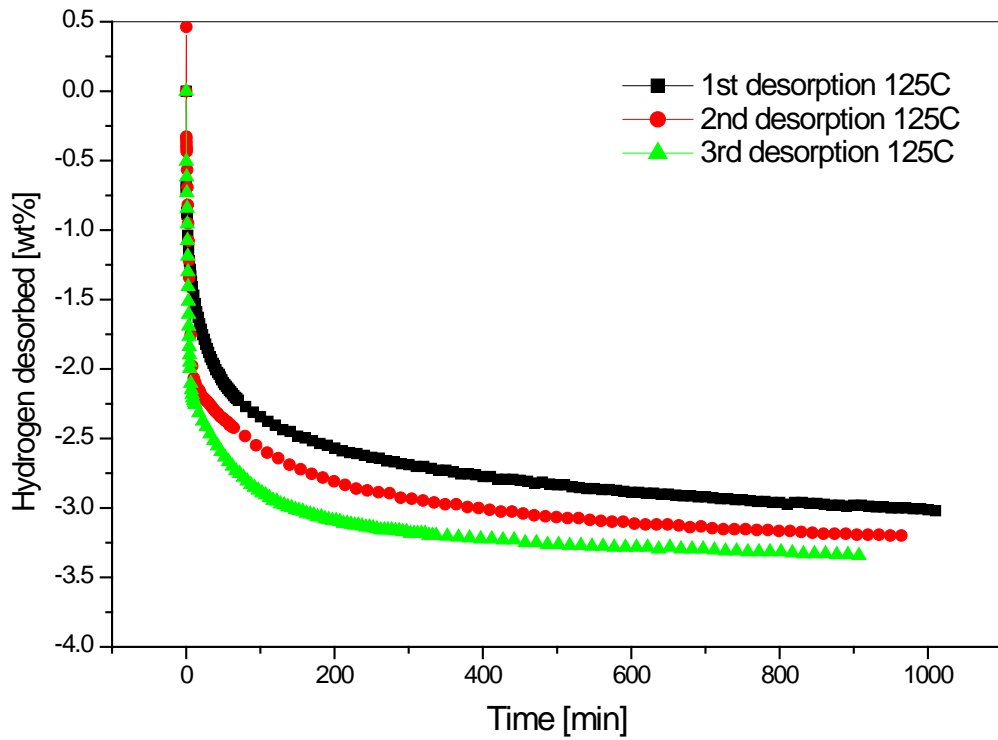


Figure 40 - Partner 10NA: activation procedure (desorption kinetic curves)

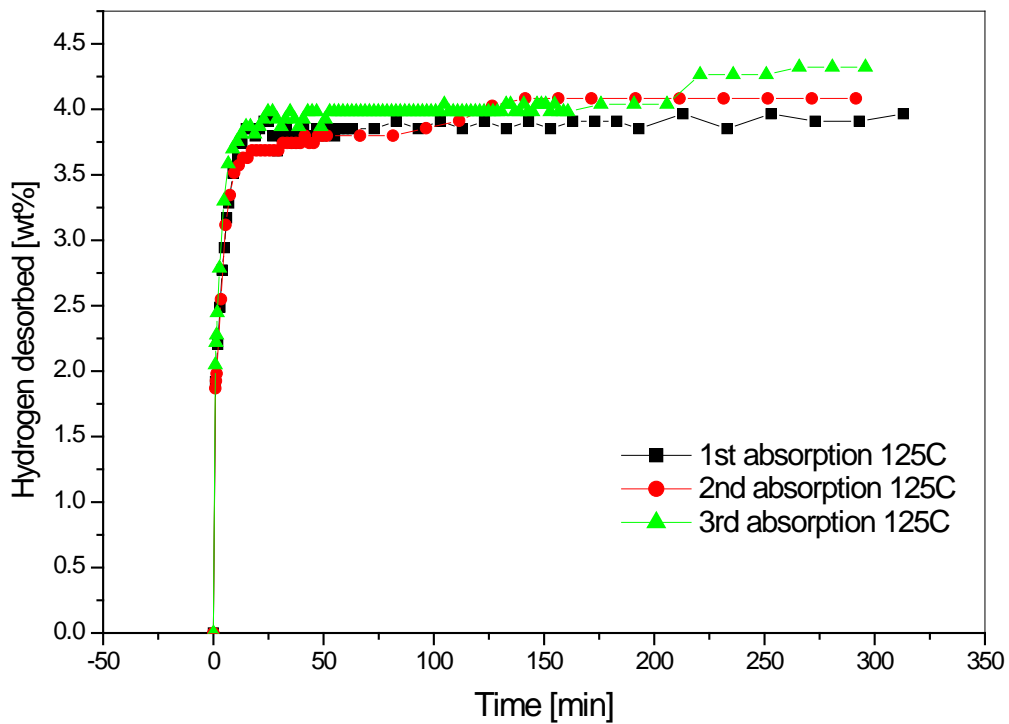


Figure 41 - Partner 10NA: activation procedure (absorption kinetic curves)

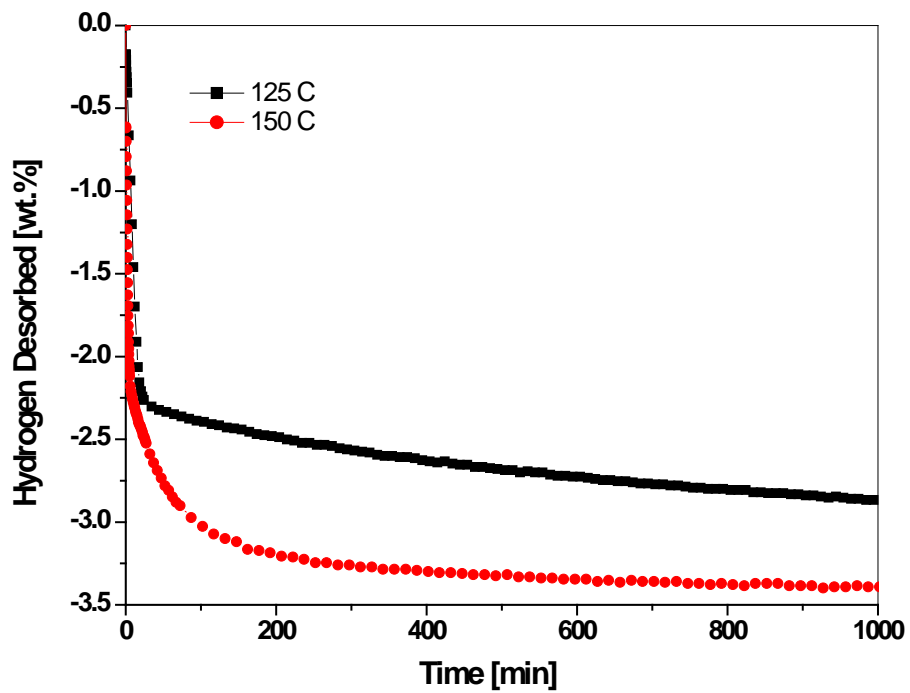


Figure 42 - Partner 10NA: kinetic curves.

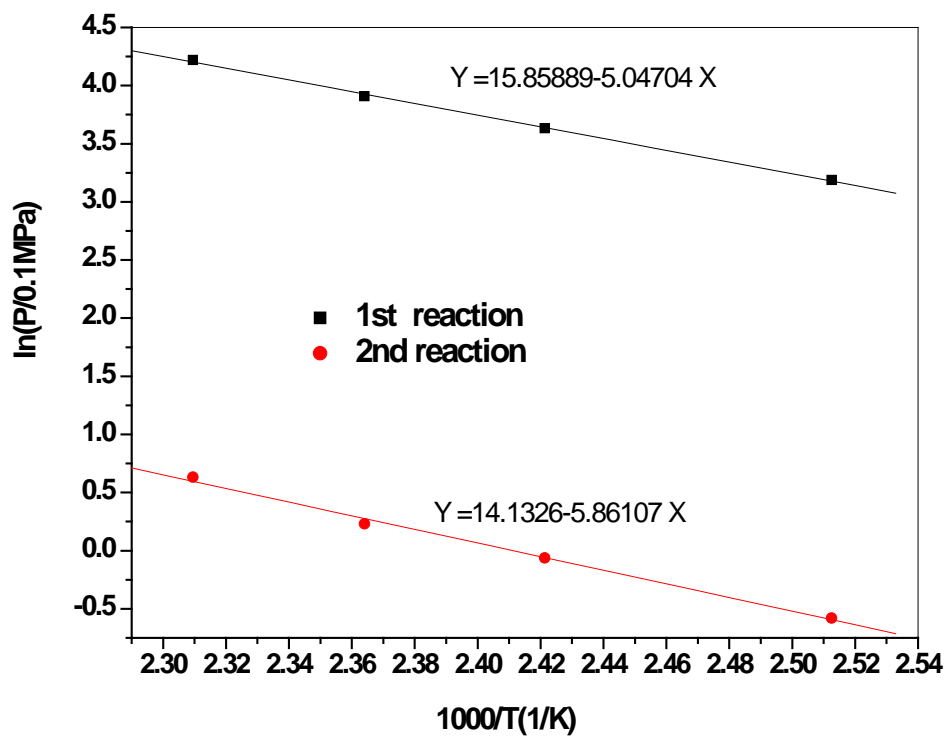


Figure 43 - Partner 10NA: van't Hoff plot

B

APPENDIX B (NREL REVIEW)

SOUTHWEST RESEARCH INSTITUTE®

6220 CULEBRA ROAD • POST OFFICE DRAWER 28510 • SAN ANTONIO, TEXAS, USA 78228-0510 • (210) 684-5111 • WWW.SWRI.ORG

Mechanical and Materials Engineering Division
March 1, 2004

Dr. Sunita Satyapal
Office of Hydrogen, Fuel Cells, and Infrastructure Technologies
U. S. Department of Energy, EE-2H
1000 Independence Avenue, SW
Washington, DC 20585

Subject: “*Carbon Nanotube Sorption Science - External Peer Review of NREL Activities*”
SwRI® Project No. 18.03.03.05064
Special Report (Revised)

Dear Sunita,

Please find enclosed a report, prepared in collaboration with Dr. Ray Gorte of U. Penn., which summarizes our review of research activities on hydrogen sorption of carbon nanotubes as directed by Dr. Michael Heben’s team at the National Renewable Energy Laboratory (NREL), Golden, CO. As you know, this external review was carried-out on location by Dr. Gorte and I, with you as a participant, during the week of January 19-23, 2004, and its outcome was presented subsequently to the FreedomCAR Technical Review Team on January 28th (slide presentation is attached).

We appreciate the opportunity to have been selected by DOE to participate in this important and challenging endeavor of national interest, and would like to express our sincere gratitude to the NREL team for their hospitality, enthusiastic participation, and scientific insights. They should be congratulated on a well organized and comprehensive plan of laboratory activities, which afforded these reviewers unrestricted oversight of the analytical methodologies and processing steps presently under scrutiny by the hydrogen storage community. It is gratifying to know that the business of science will now move forward with fervor by this and other research teams in a most dedicated effort to elucidate the materials-related factors that contribute to the variances reported for hydrogen uptake in carbon nanotubes.

Should you or your colleagues have any questions concerning the outcome of the external review, please do not hesitate to direct those to me or to Dr. Gorte at your convenience. I look forward to assisting DOE and its program partners in any way I can.

MAM/lls
C:\Data\Miller\Projects\SR05064.doc

Enclosures

cc: Record Copy A, B

Sincerely,

Michael A. Miller
Manager-R&D
Materials Characterization & Development Section



SAN ANTONIO (210) 684-5111 • HOUSTON, TEXAS (713) 9771377 • WASHINGTON, DC (301) 881-0289

CARBON NANOTUBE SORPTION SCIENCE

EXTERNAL PEER REVIEW OF NREL ACTIVITIES

Special Report (Revised)
SwRI[®] Project No. 18.03.03.05064

prepared by

Michael A. Miller
Southwest Research Institute[®]
San Antonio, Texas

Ray Gorte
University of Pennsylvania

prepared for

U.S. Department of Energy
Office of Hydrogen, Fuel Cells, and Infrastructure Technologies
Washington, DC 20585

March 1, 2004



SOUTHWEST RESEARCH INSTITUTE[®]
SAN ANTONIO HOUSTON WASHINGTON, DC

CARBON NANOTUBE SORPTION SCIENCE

EXTERNAL PEER REVIEW OF NREL ACTIVITIES

Special Report (Revised)
SwRI® Project No. 18.03.03.05064

prepared by

Michael A. Miller
Southwest Research Institute®
San Antonio, Texas


Ray Gorte
University of Pennsylvania

prepared for

U.S. Department of Energy
Office of Hydrogen, Fuel Cells, and Infrastructure Technologies
Washington, DC 20585

March 1, 2004

Approved:



James Lankford, Ph.D., Director
Materials Engineering Department

TABLE OF CONTENTS

	<i>Page</i>
1.0 INTRODUCTION	1
2.0 OBJECTIVES	4
3.0 APPROACH	4
4.0 ISSUES AND CONCERNS	5
5.0 OBSERVATIONS	9
6.0 CONCLUSIONS	12
7.0 RECOMMENDATIONS	12
PRESENTATION TO THE FREEDOMCAR TECHNICAL REVIEW TEAM.....	14
ADDENDUM	36

LIST OF TABLE AND FIGURES

	<i>Page</i>
Table 1 Hydrogen Sorption Results Obtained From The NREL External Review.....	9
Figure 1 Scatter plot of hydrogen content versus alloy content experimentally measured for alloy-doped SWNTs. Solid lines denote the theoretical boundaries for hydrogen capacity on the alloy fraction (lower line) and on the SWNT fraction (upper line). Hydrogen capacities measured for the alloy alone are indicated on the right margin. Data published by Heben et al. ⁶ and Hirscher et al. (2002).....	2
Figure 2 Elements of external review.....	5
Figure 3 Issues, concerns and observations pertinent to the methods and procedures used to quantify hydrogen sorption in SWNTs.....	6
Figure 4 Issues, concerns and observations pertinent to the characterization steps used to quantify the alloy content in doped SWNTs and to validate the structural morphology of sonicated SWNTs.	7
Figure 5 Issues, concerns and observations pertinent to the processing steps used to synthesize, purify and dope SWNTs.	7
Figure 6 TPD desorption thermogram obtained for alloyed and pure SWNTs.....	10

1.0 INTRODUCTION

The storage and delivery of hydrogen under practical and safe conditions of temperature and pressure is arguably one of the greatest challenges facing the acceptance of hydrogen as an alternative fuel source for automotive propulsion, distributive energy, and industrial applications in the future. Among the various technologies currently under development either privately or through governmental initiatives, reversible solid-state storage technologies embody both historical precedence as well as seemingly beneficial attributes in performance with respect to the need for practical operating conditions, particularly for automotive applications, and for potentially high storage energy densities on the basis of volume and mass. In particular, the employment of a material substrate in the solid state as a means of absorbing hydrogen reversibly provides a potentially practical venue for low-pressure, high-capacity storage, and for regeneration (desorption) into the gas phase at practical temperatures.

In the field of reversible solid-state hydrogen storage materials, significant strides toward improving storage capacity and kinetics have occurred along parallel fronts with the development of new materials and the catalyzation of existing ones. Catalyzation of a solid-state substrate is the common denominator across various forms of candidate material technologies. For example, the seminal investigation by Bogdanovic and Schwickardi¹ led to the identification of a new class of alkali metal hydride that, when doped with a catalyst such as TiCl, significantly enhances the kinetics of molecular hydrogen desorption and renders the dehydriding process reversible under moderate conditions. These new catalytically enhanced hydride materials, based on the aluminum hydride complex (AlH_4^-) and any alkali metal (Na, Li, Mg, Zr), are light-weight, store upwards of 5% H_2 by mass,² and release it below 200°C, thereby overcoming the limitations of conventional metallic (interstitial) hydrides.

Along similar lines, remarkable gains in storage capacities appear to be within our grasp with the advent of catalyzed nano-scale materials.³ As the single most important material of recent times with the potential for commodity availability, carbon single wall nanotubes (SWNTs) have been hypothesized to exhibit high intrinsic hydrogen storage capacities approaching a theoretical limit of approximately 8 wt.% for chemisorption uptake and, perhaps, even higher uptake at cryogenic temperatures (80 K) for molecular physisorption.⁴

Notably, the experimental investigations by Dillon and Heben et al.^{5,6} [National Renewable Energy Laboratory (NREL)] on catalyzed forms of SWNTs, wherein SWNTs are doped with a catalytic metal alloy, have suggested that storage capacities approaching the

¹ Bogdanovic, B. and Schwickardi, M., (1997), *J. Alloys and Compounds*, 1-9:253.

² Sandrock, G., Gross, K. J., Thomas, G.J., (2002), *J. Alloys and Compounds*, 299-308:339.

³ Rodriguez, N. and Baker, T., (1998), *J. Phys. Chem. B*, 4253:108.

⁴ Li, J. and Yip, S., (2003), *J. Chem. Phys.*, 2376-2385:119(4).

⁵ Dillon, A.C., Jones, K.M., Bekkedahl, T.A., Kiang, C.H., Bethune, D.S., and Heben, M.J., (1997), *Nature*, 377:386.

⁶ Heben, M.J., Dillon, A.C., Alleman, J.L., Gilbert, K.E.H., Jones, K.M., Parilla, P.A., Gennett, T., and Grigorian, L., (2001), *Materials Research Society Fall Meeting Symposium*, Z10.2.

chemisorption theoretical limit can be realized at room temperature. Moreover, these measured capacities were reported to exceed that for which can be accounted by the metal dopant alone (2.5 wt.%). For the purposes of the present and subsequent discussion, it is useful to show in Figure 1 the NREL results as a scatter plot of many of the measured values obtained to date, comparing also the results of one other investigator (Hirscher et al., 2002).

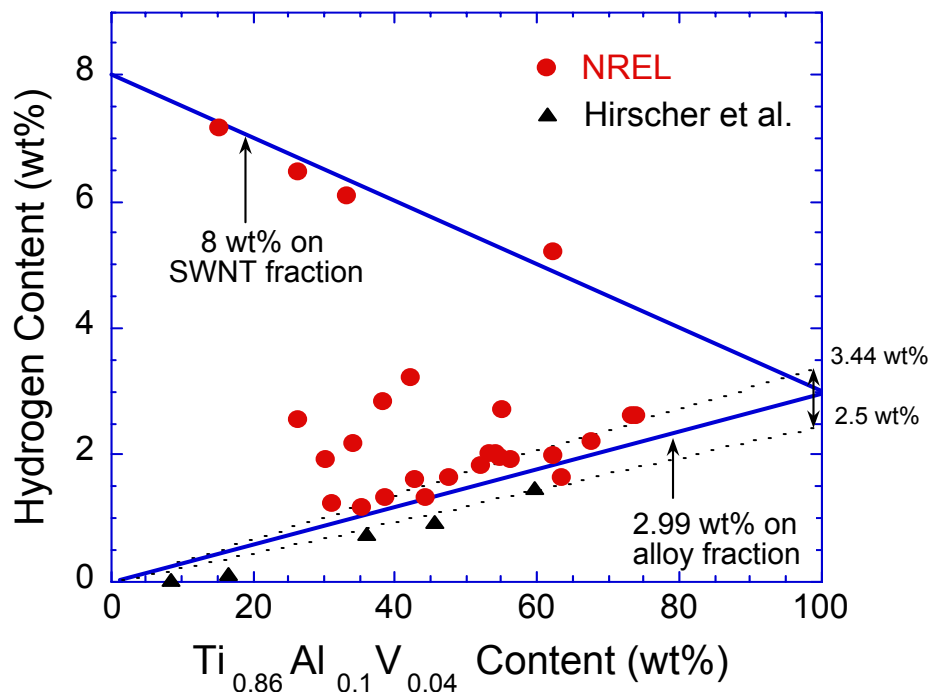


Figure 1. Scatter plot of hydrogen content versus alloy content experimentally measured for alloy-doped SWNTs. Solid lines denote the theoretical boundaries for hydrogen capacity on the alloy fraction (lower line) and on the SWNT fraction (upper line). Hydrogen capacities measured for the alloy alone are indicated on the right margin. Data published by Heben et al.⁶ and Hirscher et al. (2002).

A plausible, though speculative, mechanism that may conveniently explain the enhanced hydrogen uptake in catalyzed SWNTs is one borrowed from the mature field of heterogeneous catalysis, in particular that which concerns supported metal catalysts for hydrogenation. It has long been known that supported metal catalysts, such as Pt or Pd finely dispersed on transition metal oxide (*e.g.*, Al₂O₃, WO₃) or carbon supports used in the hydrogenation reactions of organic molecules, reversibly activate the dissociation of molecular hydrogen on the surface of the metal crystallite to yield atomic hydrogen chemically bound to the surface atoms of the metal crystallite. The desired hydrogenation reaction occurs as these weakly bound hydrogen atoms migrate on the surface and collide with a surface-adsorbed chemical species. Augmenting this mechanism, Khoobiar (1964)⁷ first reported an additional

⁷ Khoobiar, S., (1964), *J. Phys. Chem.*, 411:68.

phenomenon in which hydrogen spills over from the catalyst particle to the support through a process of surface interphase migration that today its mechanism still remains to be properly elucidated; yet its end-effect has been canonized as “hydrogen spillover”.⁸ Recently, hydrogen spillover on carbon supports has been experimentally validated much to the credit of advances in incoherent inelastic neutron scattering (INS) experiments.⁹

The landmark results of the NREL team (Figure 1) have not emerged without controversy, and have been the focus of intense scrutiny among the scientific community. Much of this controversy stems from the fact that independent laboratories have not been successful in reproducing the high hydrogen capacities reported for alloyed SWNTs by the NREL team. While some attempts have been made,^{10,11} it is evident that the analytical requirements for making accurate and precise measurements of hydrogen capacity for these sorts of materials are quite rigorous, and the variables associated with the synthesis and preparation of materials suitable for study are convoluted. Therefore, the potential for drawing erroneous conclusions from experiment – either contradictory or corroboratory with what is already reported – is very high unless careful steps are taken to ensure that the analytical methodologies employed provide sufficient precision and accuracy and, in particular, that the variables inherent in the processing of materials are clearly understood.

In considering the analytical methodologies conventionally practiced for hydrogen sorption measurements, the most suitable technique has been a topic of considerable debate.¹² There are, in general, at least four measurement principles from which to choose: 1) volumetric analysis (Sievert-type apparatus); 2) temperature programmed thermal desorption mass spectrometry (TPD); 3) thermo gravimetric analysis; and, 4) microcalorimetry. A sizeable body of literature has been amassed on each of these techniques over the past several decades for a broad spectrum of different materials.^{13,14,15} While the merits of each measurement principle relative to sorption studies on SWNT materials can be argued, the complementarity among these choices can be demonstrated as long as the constraint boundaries, such as mass, volume, and thermal resolution, are not ignored.

The important point to be made here is that once any two or more techniques can be demonstrated to be accurate, precise, and correlative for a given material class, the credibility of the measured results is no longer at issue. Emphasis can then be placed on further understanding the materials chemistry and processing variables that should be the focus of experimental research in solid-state hydrogen storage. It was the goal of this external review panel to specifically address these characteristics in relation to the analytical and, to a lesser extent, processing methodologies employed by the NREL team.

⁸ Sermon, P.A. and Bond, G.C., (1973), *Cat. Rev.*, 211:8(2).

⁹ Mitchell, P.C.H., Ramirez-Cuesta, A.J., Parker, S.F., and Tomkinson, J., (2003), *J. Phys. Chem. B*, 6838-6845:107.

¹⁰ Hirscher, M., Becher, M., Haluska, M., *et al.* (2001), *Appl. Phys. A.: Mater. Sci. Process*, 129:72.

¹¹ Hirscher, M., Becher, M., Haluska, M., *et al.* (2002), *J. Alloys Compd.*, 330-332:654.

¹² Checchetto, R., Trettel, G., and Miotello, A., (2004), *Meas. Sci. Technol.*, 127-130:15.

¹³ Sudibandriyo, M., Pan, Z., Fitzgerald, J., *et al.* (2003), *Langmuir*, 5323-5331:19(13).

¹⁴ Dhoots, S.N. and Freeman, B.D., (2003), *Rev. Sci. Inst.*, 5173-5178:74(12).

¹⁵ Pinkerton, F.E., Wicke, B.G., Olk, C.H., *et al.*, (2000), *J. Phys. Chem. B*, 9460-9467:104(40).

Hence, under the direction of the U.S. Department of Energy (DOE), Office of Hydrogen, Fuel Cells, and Infrastructure Technologies, the overarching goal of the present effort was to assemble an independent, external review panel with relevant expertise in sorption science to examine and assess the methods and procedures that are employed by the NREL team to determine hydrogen storage capacities in SWNTs. The outcome of this external review was presented subsequently to the FreedomCAR Technical Review Team on January 28, 2004 (slide presentation is attached). As a consequence of that presentation and the discussions that followed, additional slides have been appended to the presentation that bring to light certain aspects of the methods and results of the experiments which were unclear to various members of that team. The following sections examine the key facets of the review and provide an account of the most salient findings consistent with the stated objectives.

2.0 OBJECTIVES

The objectives of the external review constituted the following elements:

1. Perform a thorough peer review of NREL experimental activities pertaining to hydrogen sorption on SWNTs.
2. Review and witness analytical methods employed by NREL for the determination of hydrogen sorption.
3. Review and witness the material processes employed by NREL for the preparation of doped SWNTs.
4. Determine whether or not the appropriate control experiments and calibration steps have been properly executed.
5. Identify strengths and weaknesses in the methods.
6. Assess the degree of confidence that can be assigned to the accuracy and repeatability of the sorption measurements.

3.0 APPROACH

In order to accomplish the foregoing objectives, a multitude of actual laboratory experiments had to be carefully planned by the NREL team to the extent possible so that the essential details of the experimental methods could be witnessed and evaluated by the external reviewers over the course of approximately five days. Emphasis was directed towards 1) understanding clearly the operating principles associated with each of the analytical sorption apparatuses (volumetric and TPD) as well as other related analytical equipment, 2) comparing the precision and accuracy of each sorption technique by using a reference standard of known hydrogen composition (TiH_2), 3) reviewing the calibration methods for quantification of hydrogen in unknown samples (TiH_2 and SWNTs), 4) performing the necessary control experiments (*i.e.*, blank experiment) to demonstrate background levels of intrinsic hydrogen in the analytical apparatuses, and 5) witnessing the materials processing steps associated with the preparation and characterization of SWNT samples.

The overall scope of the external review encompassed several elements that can be categorized into three distinct tiers, below which underlie specific concerns of importance to the validation and credibility of the reported hydrogen capacities for alloyed SWNTs. These elements are shown diagrammatically in Figure 2.

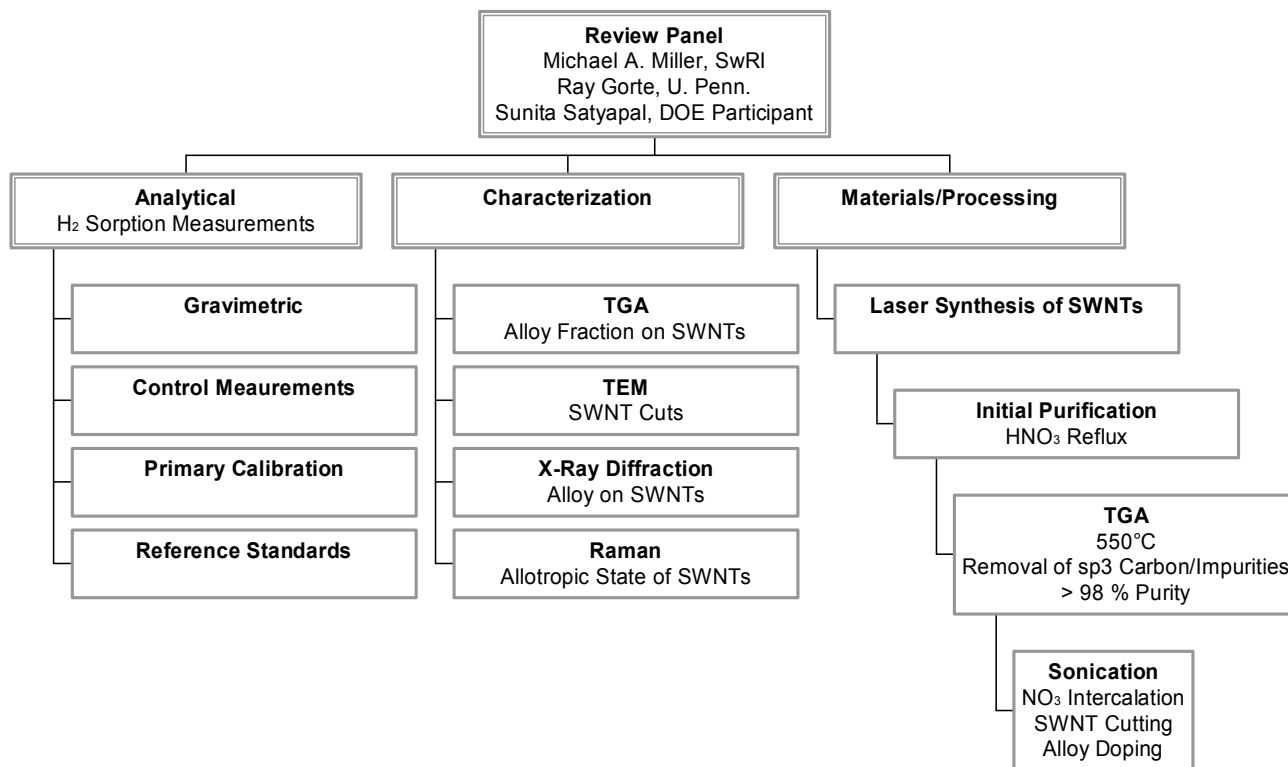


Figure 2. Elements of external review.

It is important to note that while materials processing can be a dominating factor in the distribution of the measured results from the viewpoint that synthesis and purification control the lot-to-lot sorption behavior of alloyed SWNT samples, this tier was not the central focus of the external review process. However, this aspect of the methods and procedures will be shown to have significant implications on the final assessment of this effort.

4.0 ISSUES AND CONCERNS

The issues and concerns to which each element of the external review in Figure 2 is assigned can be broken down into specific terms. In an attempt to shed light on these concerns from the perspective of the external reviewers, the relationships between the issues in question and the measures taken to address them are, for convenience, illustrated in tabular form in Figures 3-5 for each tier. The observations noted in these figures in most instances come from direct, on-site experimental validation, which is discussed in further detail in the subsequent section.

The major concern in our analysis regarded the use of TPD methods for analyzing adsorbed hydrogen. The procedure used at NREL involves dosing at room temperature, using approximately 500 torr of H₂, followed by cooling to liquid nitrogen temperature, before starting the temperature ramp. In addition to the usual concerns about calibration constants in TPD, we examined whether some of the desorption could come from the Pt foil used to carry the samples and the Cu leads used to heat the sample.

A related concern was whether a primary calibration of the analytical apparatuses for either technique, TPD or volumetric, was being performed to derive the response factors needed to obtain quantitative measures of hydrogen in terms of mass or moles. The importance of a primary calibration cannot be overemphasized for either technique because a reference material of theoretically known hydrogen content (*e.g.*, TiH₂) is not considered to be a suitable substitute as a primary calibration for absolute quantitation. However, subsequent to a primary calibration of the apparatus response, the use of a reference standard is quite appropriate for determining accuracy and precision of each technique, and for determining the correlation of measured values between the two techniques.

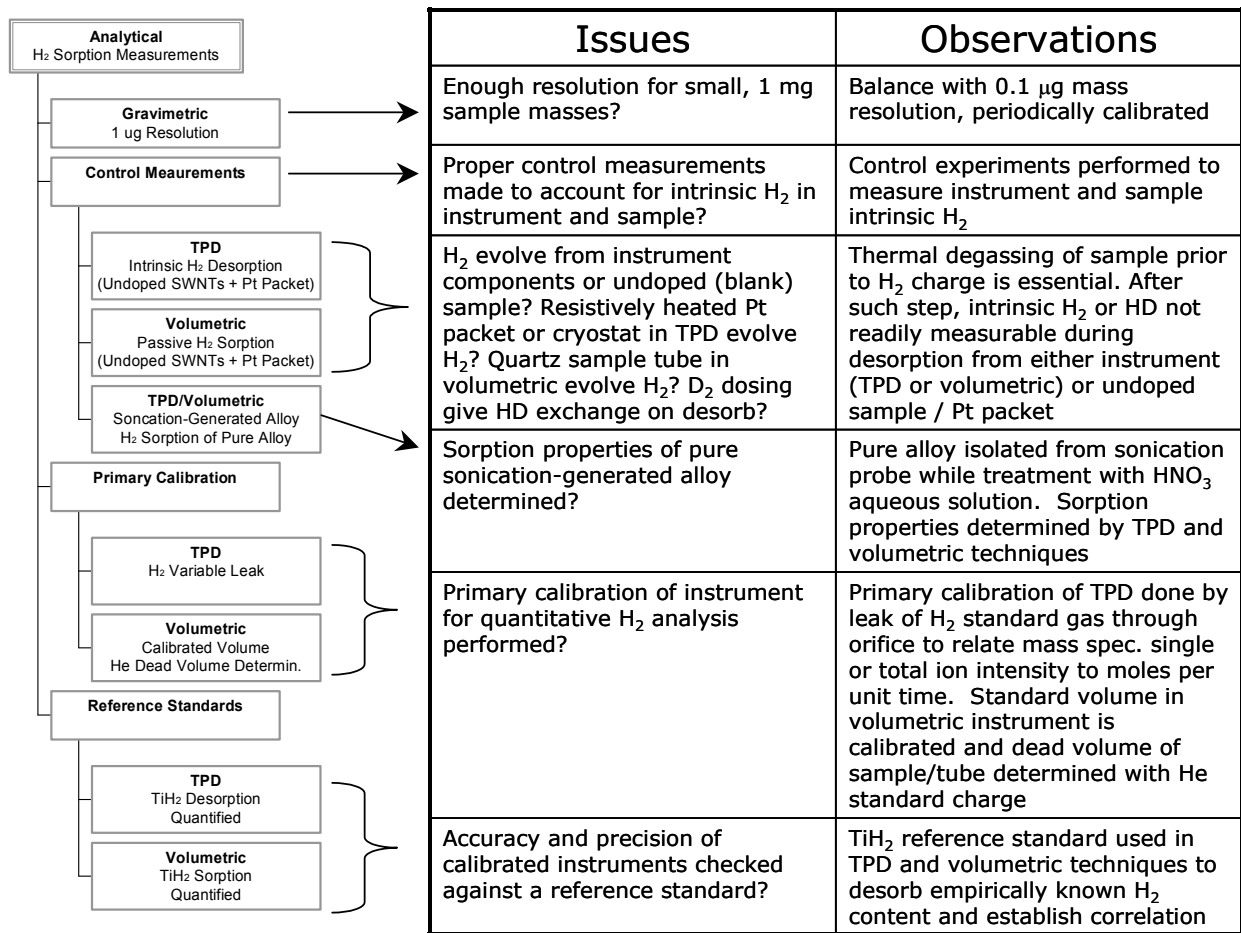


Figure 3. Issues, concerns and observations pertinent to the methods and procedures used to quantify hydrogen sorption in SWNTs.

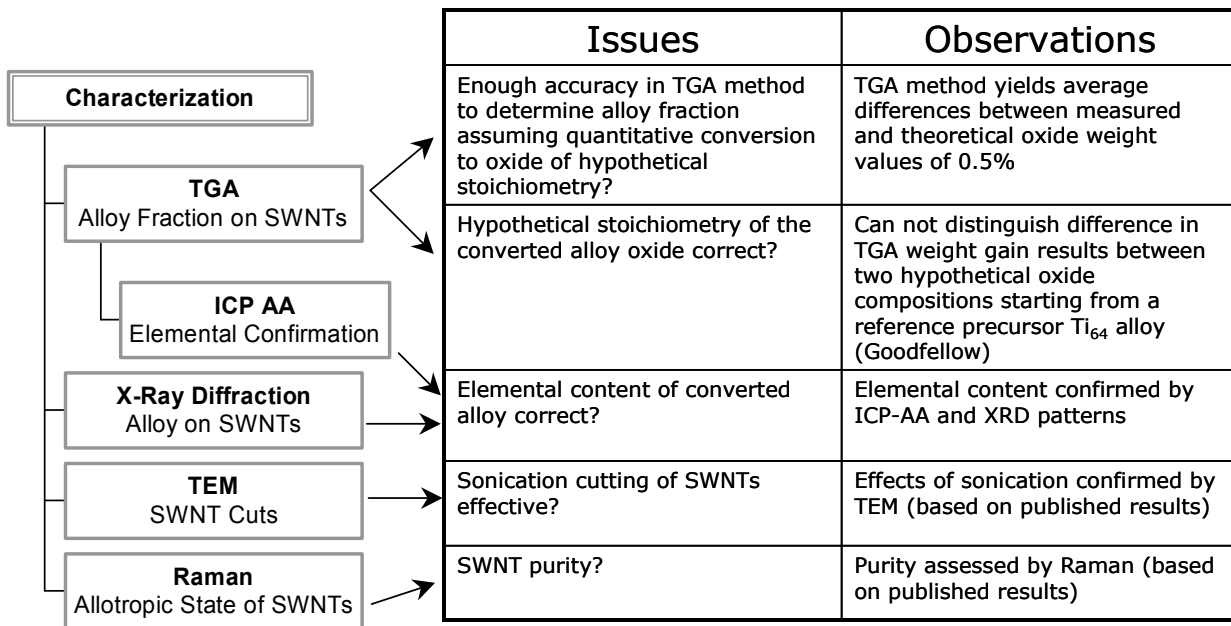


Figure 4. Issues, concerns and observations pertinent to the characterization steps used to quantify the alloy content in doped SWNTs and to validate the structural morphology of sonicated SWNTs.

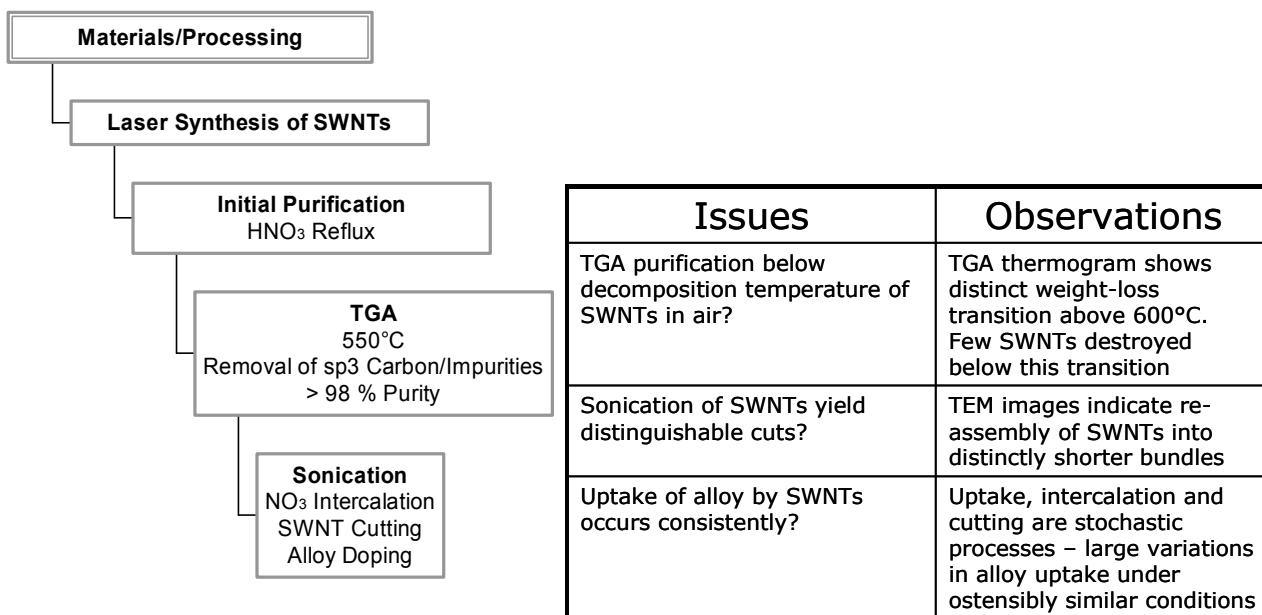


Figure 5. Issues, concerns and observations pertinent to the processing steps used to synthesize, purify and dope SWNTs.

We also looked for the possibility that impurities may affect the TPD results. Given that the samples in the TPD system were exposed to 500 torr of H₂ for 1 min, we thought it possible that some of the H₂ desorbing from the samples in the TPD might result from adsorption of impurities. For example, we considered the possibility that hydrocarbons could be introduced into the system during the adsorption due to ppm impurities in the source H₂, then decompose to H₂ during TPD, leaving carbon deposits within the sample. In a related issue, we questioned why adsorption was carried out at relatively high pressures and why the exposure was carried out at room temperature and liquid nitrogen.

In the opinion of one reviewer, volumetric adsorption measurements are much more straight-forward and do not have many of the impurity or calibration questions associated with TPD. We spent considerable time asking about why volumetric measurements were not used more extensively. We tried to establish whether the adsorbate coverages obtained using a volumetric apparatus would give identical results to the TPD system. We questioned whether any attempt had been made to obtain equilibrium adsorption isotherms.

Insofar as the characterization of SWNT materials is concerned, the use of reliable and accurate methods for determining the alloy content in SWNTs is a matter of extreme importance that could be readily overlooked. Accurate determination of the alloy content is a fundamental requirement for determining hydrogen capacity – whether one is interested in reporting the total capacity or the fraction residing on the SWNTs alone – because the differences between what would theoretically be absorbed by the alloy alone and any amount of hydrogen in excess of that can be small (points near the lower line of Figure 1). Therefore, uncertainties in the alloy mass fraction as determined by thermogravimetric analysis (TGA), uncertainties in the elemental purity and oxide form as determined by inductively coupled plasma atomic absorption (ICP-AA) and X-ray diffraction, respectively, or incorrect assumptions made about the stoichiometry of a hypothetical oxide for the probe-generated alloy, can compound the error associated with the calculated alloy fraction.

The concerns of the reviewers in regard to the synthesis and processing of SWNTs pertained to the purification and sonication steps. Prior to cutting SWNTs and doping them with alloy using a sonication probe, hydrocarbon impurities and other *sp*³-hybridized allotropic forms of carbon are removed (combusted) in a TGA apparatus under an air environment using a temperature-programmed cycle that plateaus at 550°C. From the viewpoint of the reviewers, this step was considered to be delicate, if not risky, because the onset for thermal decomposition of SWNTs (*sp*² carbon) occurs at approximately 600°C. If laser-based synthesis of SWNTs is an inherently variable process, the use of this delicate purification procedure brings into question whether thermally purified SWNTs will exhibit chemical instabilities upon subsequent thermal manipulation of the sample.

Related to the potential for inconsistencies in the stability of SWNTs as a consequence of the purification step, the reviewers acknowledged that the process of cutting SWNTs and doping them with alloy contains many difficult to control variables. Based upon the experience of one reviewer, the uptake of a transition metal complex by SWNTs from a known amount of that complex in solution can be shown to have an exponential rise to limit dependence. The variability in this limited uptake is thought to be related to the number of nucleation sites on the

graphene walls that are made accessible by the sonication-driven dispersion and cutting of SWNT bundles. In the case of the NREL methods, the situation appears to be significantly more complex because there is neither adequate control over the rate at which the alloy is generated from the sonication probe, nor control over the dissolution of alloy into solution. Therefore, it is apparent that these processes are by their nature stochastic, and that they are likely to manifest in highly variable hydrogen sorption properties.

5.0 OBSERVATIONS

Table 1 summarizes all results obtained from hydrogen sorption experiments prior to and during the course of the external review. The data listed in the top-half of the table correspond to control experiments that were designed to gauge the accuracy of each sorption technique as well as to determine the correlation between the two. In all instances, the weights of the reference standard (TiH₂) were determined by one of the reviewers and were not made known to the analyst making the sorption measurement. The data listed in the lower-half of the table correspond to sorption experiments conducted on doped and pure SWNTs, showing the date of synthesis and the purification cut.

Table 1. Hydrogen Sorption Results Obtained From The NREL External Review

Date	Method	Sample	Correct wt (mg)	Determined Wt (mg)		% Diff.
18-Jan	TPD	TiH2:run 1	1.540	1.560		1.30
		TiH2:run 2	1.730	1.760		1.73
Vloop= 15.56	Volumetric (closed end)	TiH2:run 1	11.400	11.107		-2.57
		TiH2:run 2	5.556	5.475		-1.46
Vloop= 16.04	Volumetric (closed end)	TiH2:run 1	11.400	11.450		0.44
		TiH2:run 2	5.556	5.644		1.58

Date	Method	Sample	Sample Identifier	Total H2 (wt%)	Alloy fraction (wt%)	wt% on SWNTs
01/11/2000	TPD	0	1/6/04, C#1	2.62	68.0	2.88
01/18/2000	TPD	1	1/6/04, C#1	2.39	66.4	2.17
01/19/2000	Vol, Abs	1	1/6/04, C#1	1.93	63.9	0.92
01/19/2000	Vol, Des	1	1/6/04, C#1	2.13	63.9	1.48
01/19/2000	TPD	2	1/12/04, P	0.01	0.0	0.01
01/19/2000	TPD	3	1/21/04, C#1	1.09	22.4	0.68
01/20/2000	Vol, Abs	4	1/21/04, C#2	1.51	45.8	0.67
01/20/2000	Vol, Des	4	1/21/04, C#2	1.50	45.8	0.65
01/20/2000	TPD	4	1/21/04, C#2	1.18	40.4	0.29
01/20/2000	TPD	5	probe alloy	2.40	100.0	na
01/21/2000	TPD	6	1/6/04, C#2	1.90	41.0	1.48
01/21/2000	Vol, Abs	7	4/15/03, C#1	0.87	35.7	0.00
01/21/2000	Vol, Des	7	4/15/03, C#1	1.19	35.7	0.46
01/22/2000	TPD	7	4/15/03, C#1	1.06	43.3	-0.04
01/22/2000	Vol, Abs	8	1/11/04, C	1.52	47.4	0.64
01/22/2000	Vol, Des	8	1/11/04, C	1.47	47.4	0.54
01/25/2000	Vol, Abs	2	1/12/04, P	0.01	0.0	0.01
01/25/2000	Vol, Des	2	1/12/04, P	0.00	0.0	0.00
01/25/2000	Vol, Abs	5	probe alloy	2.49	100.0	na
01/25/2000	Vol, Des	5	probe alloy	2.54	100.0	na

Note: C = cut
Note: P = pure SWNT
Note: assume alloy stores 2.5 wt% H2
Note: Volumetric desorption measurements are cooled to 75.6 K under H2 before evacuation
Note: Same sample cuts may have different alloy contents due to uncontrolled nature of alloy incorporation
Note: Subsequent & more rigorous calibration of Vloop provides closer predictions for TiH2 masses

Two important observations were made regarding TPD. First, TPD measurements performed without a sample showed no measurable adsorption, strongly implying that desorption from the leads provides negligible quantities to the quantification of adsorption (Figure 6). Second, TPD performed following adsorption of D_2 showed only desorption of D_2 , with negligible amounts of HD or H_2 leaving the sample. This result was viewed as crucial for ruling out the possibility that the H_2 could have been formed from decomposition of hydrocarbons, given that it is unlikely that deuterated hydrocarbons would be in the system, and that any significant levels of hydrogen intrinsic to the system contribute to the TPD signal.

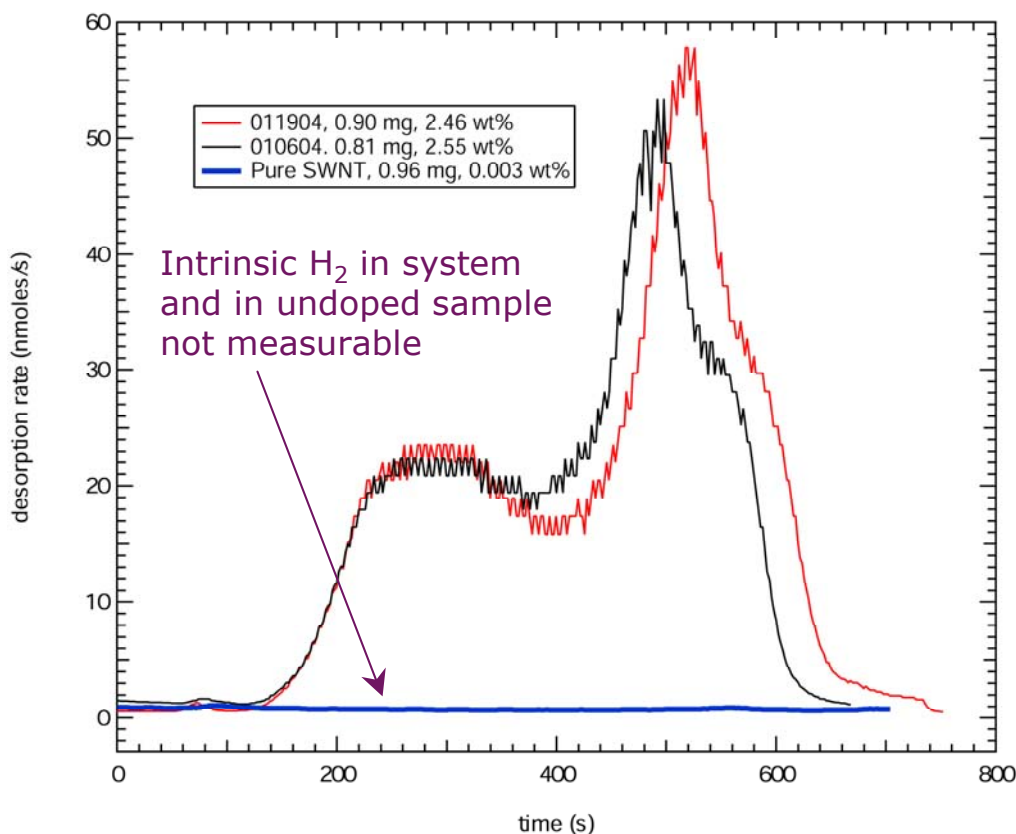


Figure 6. TPD desorption thermogram obtained for alloyed and pure SWNTs.

Results from the volumetric apparatus turned out to be more complicated. Volumetric measurements performed on well-behaved samples, like Pd, showed excellent agreement with the results from the TPD measurements. However, on the alloyed SWNT samples, we were told that past data gave adsorption quantities that were roughly $2/3^{\text{rds}}$ of that obtained on the TPD system. Acting on the hypothesis that the alloyed SWNT samples were being damaged during the initial outgassing measurements, we first examined the mass spectra of gases leaving the samples during outgassing. We then lowered the heating rate and attempted to improve the evacuation methods to determine whether better agreement might be obtained between the TPD and volumetric measurements.

The gases leaving the sample during outgassing in the volumetric system consisted largely of water and NO (from the nitric acid treatment.). It was also noted that the pressure over the sample rose to 30 mtorr by 200°C. At this point, we stopped the temperature ramp and did not continue to the normal outgassing temperature of 500°C. Since the peak desorption temperature during outgassing in the TPD apparatus occurred at 400°C and comparatively little desorption occurred at 200°C, it appears that the pressure above the sample in the volumetric apparatus could be significant during outgassing.

We had three samples examined in which a more thorough, gentler outgassing procedure was used in the volumetric apparatus. In two of these samples, we used a carrier gas to flush the gasses leaving the samples. In one, we used a second pump to provide additional evacuation. The agreement between the adsorption coverages obtained volumetrically and with TPD on those samples improved significantly, with the volumetric measurements showing coverages that were between 80% and 90% of the coverages obtained in TPD.

From a strict analytical viewpoint, both the TPD and the volumetric systems were shown to provide accurate measurements of hydrogen capacity for the reference standard (TiH₂), giving average differences of only 1.8%. Primary calibrations for each technique, which included a calibrated hydrogen leak through an orifice for the TPD technique and a pre-calibrated volume for the volumetric analyzer, were also tested with known weights of TiH₂. In each case, the measured values were within 1-2% of the known values. These results also indicated that the two measurement techniques were highly correlative.

As discussed earlier, the ability to delineate between excess hydrogen capacity on alloyed SWNTs and the amount of hydrogen that would be theoretically absorbed by the alloy alone requires that the alloy fraction be quantified accurately and reliably for each sample. In this regard, it was observed that the average differences between the measured and theoretical weights of the converted alloy oxide as determined by TGA was only 0.5%. It was further noted that in making an alternate assumption about the stoichiometry of the converted alloy oxide, the differences among the theoretical weight gains for the two different hypothetical stoichiometric formulas and the measured values was insignificant.

Finally, it is noteworthy that the hydrogen capacities for alloyed SWNT samples, which were compared by TPD and volumetric methods, varied significantly. The fact that the volumetric and TPD quantities corresponded extremely well on the basis of a reference standard (TiH₂) lent significant credibility to the results for alloyed SWNTs as reported by the NREL team (refer to Figure 1). Therefore, the large variances reported for hydrogen capacities of SWNTs cannot be attributed to the analytical methodologies employed. Instead, these variances are most likely due to the materials processes used to prepare samples for study, whose effect appear to be stochastic and convoluted. The apparent susceptibility of purified SWNTs to degradation upon thermal cycling (e.g., initial degassing of sample) may also contribute to these variances.

6.0 CONCLUSIONS

In summary, this external review has examined and assessed the methods and procedures that have been employed by the NREL team to determine hydrogen storage capacities in SWNTs. While a number of issues and concerns were initially raised about various aspects of the methods and procedures, the majority of these concerns have been addressed with favorable results. The most salient conclusions of this external review can be summarized as follows.

1. Hydrogen capacities for alloyed SWNTs as reported by the NREL team appear to be credible. This conclusion is tempered slightly by the fact that the high capacities near the chemisorption theoretical limit reported by the NREL team, which heretofore has been the focus of much controversy, were not observed in the present instance. However, one experiment did yield a hydrogen capacity of 2.39 wt.%, which falls comfortably above the lower boundary line demarcating the capacity of the alloy fraction (Figure 1).
2. The analytical methodologies employed for the determination of hydrogen capacities and for the characterization of alloyed SWNTs are well established and appropriate for their intended purpose.
3. The TPD and volumetric techniques were demonstrated to be accurate, repeatable, and correlative based upon measurements on a reference standard (TiH₂).
4. The large variances reported for hydrogen capacities of SWNTs cannot be attributed to the analytical methodologies employed. Instead, these variances are most likely due to the materials processes used to prepare samples for study, whose effect appear to be stochastic and convoluted. It is further suspected that the apparent susceptibility of purified SWNTs to degradation upon thermal cycling may also contribute to these variances.

7.0 RECOMMENDATIONS

- In the opinion of the reviewers, the hydrogen capacities obtained from TPD measurements by the NREL group are reliable. However, to help convince the community, the NREL team should improve their volumetric adsorption apparatus to allow a more vigorous evacuation procedure, more similar to what is used in the TPD apparatus. Assuming that the NREL team can demonstrate identical results for the two techniques for a number of samples, it is believed that the community will have significantly more confidence in the reliability of their analytical techniques.
- To further validate and gain confidence in the method presently employed by the NREL team to calibrate the TPD apparatus for quantitative measurements of hydrogen, the primary calibration of the instrument should be compared with that

obtained from NIST-traceable, calibrated leak devices, spanning at least three decades in leak rate and positioned such that the leak outlet is in close proximity to the sample cryostat.

- Given the apparent sensitivity of the alloyed SWNTs to pretreatment conditions, it would be helpful to establish the conditions necessary for avoiding sample damage. This will be critical for other groups to be able to reproduce the NREL data.
- The procedure currently employed by the NREL team to prepare undoped, pure SWNTs for determining the intrinsic sorption of hydrogen does not exactly duplicate the conditions under which alloyed SWNTs are formed. Without an alternative approach, this characteristic of the procedure is unavoidable, yet it raises the question whether, for example, the allotropic state and packing structure of alloyed SWNTs are effectively mimicked in the sorption studies for pure SWNTs. Ideally, it would be desirable to duplicate every characteristic that distinguishes alloyed SWNTs, minus the alloy itself, so that the sorption behaviors can be accurately compared between the two. A viable approach toward this goal is to modify the surface of the Ti-6Al-4V sonication probe such that the dissolution of alloy does not occur during the cutting process, while retaining the sonic efficiency and amplitude of the original probe. In this regard, diamond-like carbon and silicon carbide coatings may be suitable candidates to try.
- A single batch of well-characterized SWNTs, alloyed and pristine, should be prepared by the NREL team and distributed to other well-qualified teams for analysis. This form of testing will provide additional insights into the hydrogen sorption characteristics of these interesting materials, and will enable the scientific community to add credence to the growing dataset of measured hydrogen capacities.

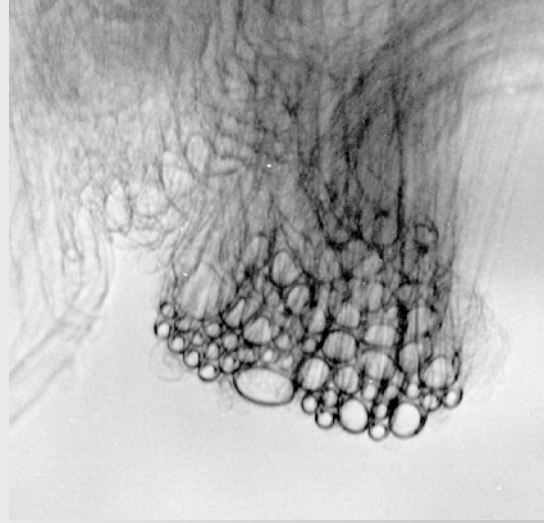
PRESENTATION TO THE FREEDOMCAR TECHNICAL REVIEW TEAM

January 28, 2004



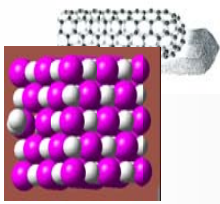
Carbon Nanotube Sorption Science External Peer Review of NREL Activities

January 19 – 23, 2004



Michael A. Miller
Southwest Research Institute
Ray Gorte
U. Penn
Sunita Satyapal
DOE Participant

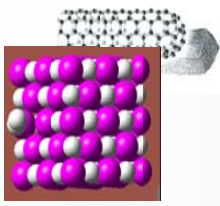




Objectives for External Reviewers



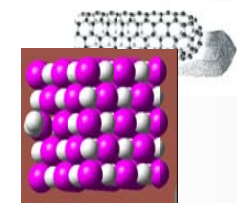
- Perform a thorough peer review of NREL experimental activities pertaining to hydrogen sorption on carbon single wall nanotubes (SWNTs)
- Review and witness analytical methods employed by NREL for the determination of hydrogen sorption
- Review and witness material processes employed by NREL for the preparation of doped SWNTs
- Determine whether or not the appropriate control experiments and calibration steps have been properly executed
- Identify strengths and weaknesses in methods
- Assess the degree of confidence that can be assigned to the accuracy and repeatability of the sorption measurements



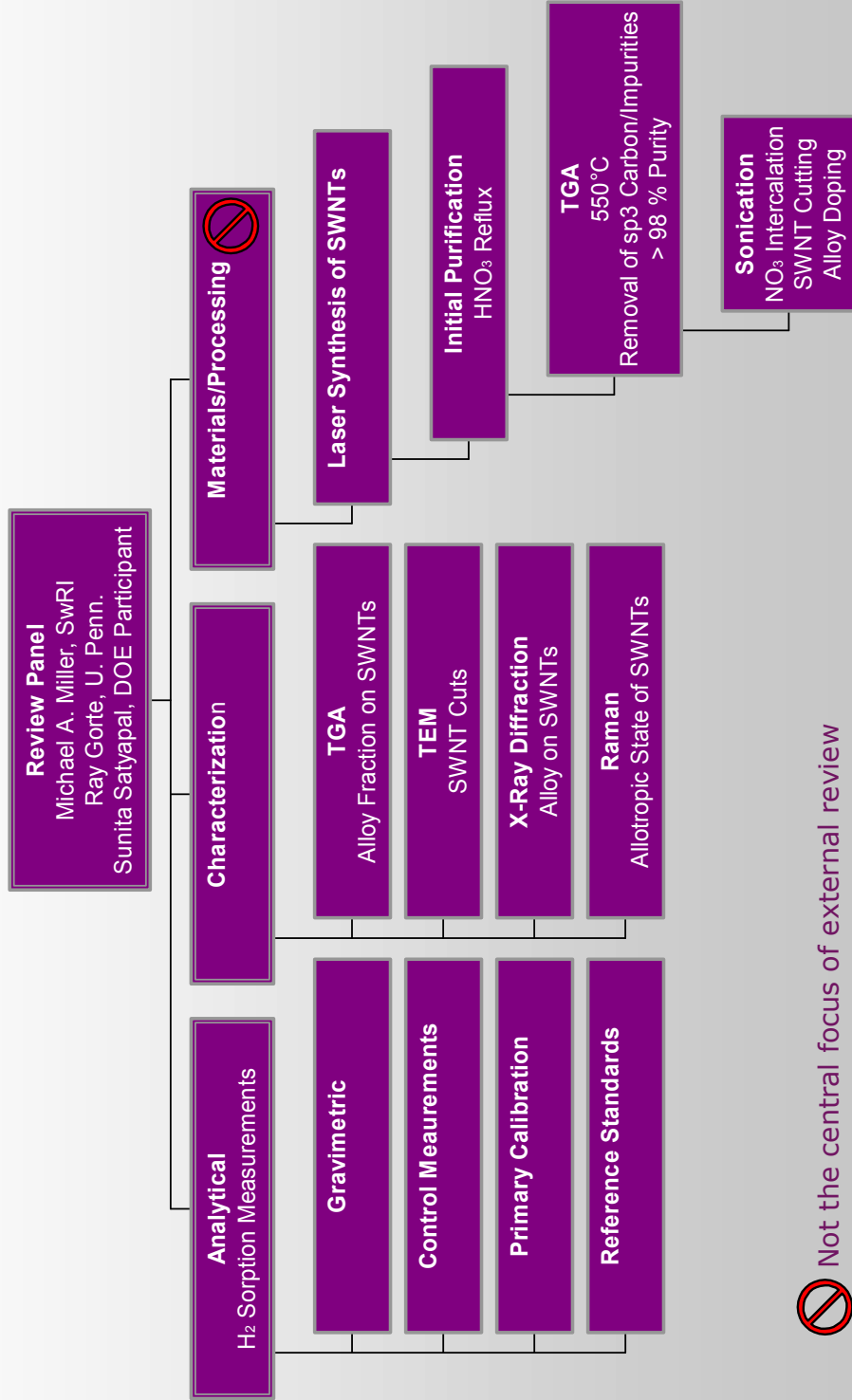
Objectives for NREL Team

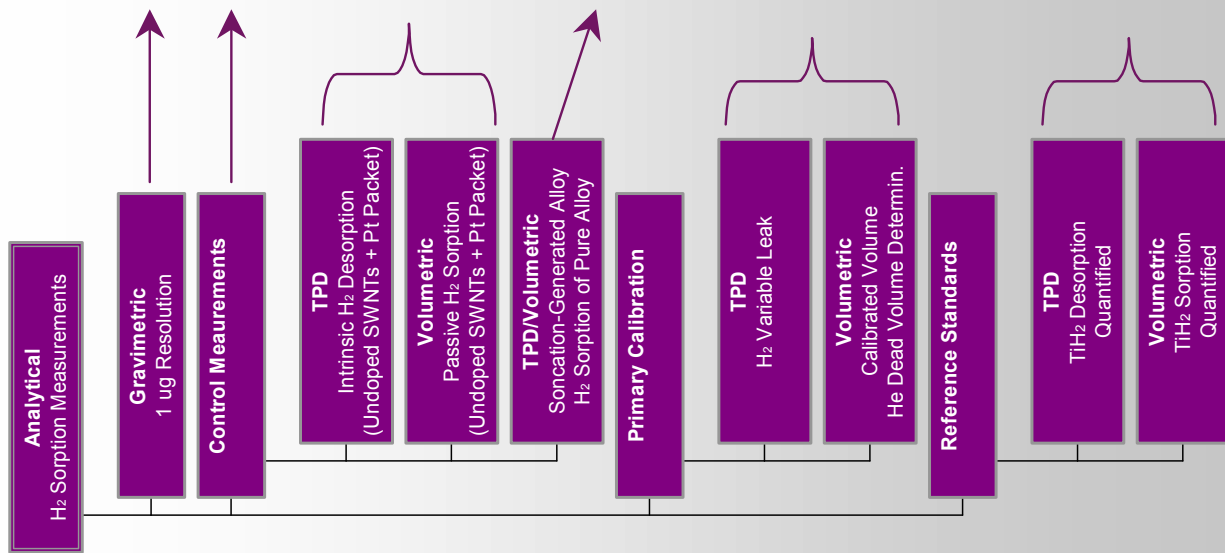


- Showcase operating principles of measurement apparatuses
 - Temperature programmed desorption mass spectrometer (TPD)
 - Volumetric analyzer (Sievert)
- Describe and demonstrate analysis of reference sample
- Describe and demonstrate methods of calibration for quantification of H₂ ⇔ both apparatuses
- Showcase determination of reference standard of unknown mass by both techniques
 - TiH₂ reference standard
 - Blind (unknown) sample mass (weighed-out by Miller)
 - Accuracy and repeatability
 - Correlation between techniques
- Demonstrate results of “blank” sample analysis ⇔ both apparatuses
 - Pure, undoped SWNTs
 - Maximum background levels of H₂ produced by undoped SWNTs and apparatus
- Showcase determination of H₂ storage capacity in doped (activated) SWNTs
 - TPD ⇔ desorption
 - Volumetric ⇔ desorption and adsorption
- Describe and demonstrate SWNT activation
- Describe and demonstrate SWNT characterization
 - Determination of total alloy dopant in SWNTs



Elements of External Review

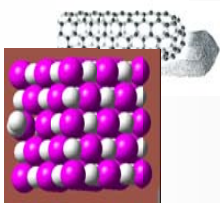




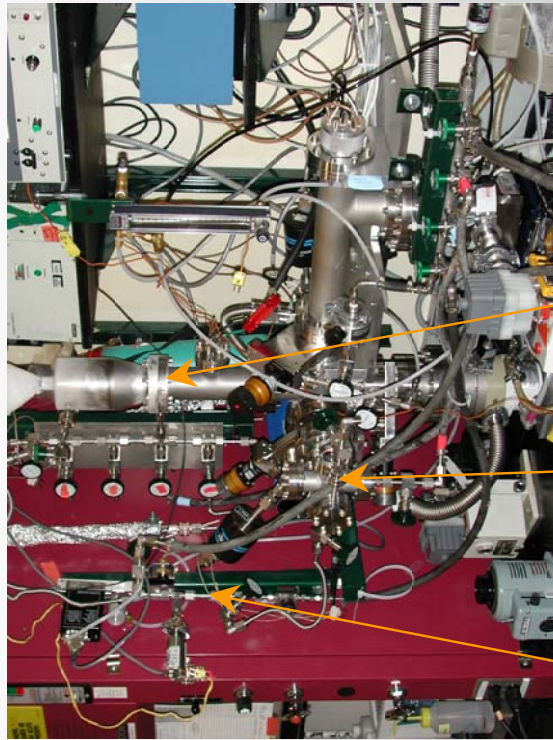
Issues	Observations
Enough resolution for small, 1 mg sample masses?	Balance with 0.1 μg mass resolution, periodically calibrated
Proper control measurements made to account for intrinsic H_2 in instrument and sample?	Control experiments performed to measure instrument and sample intrinsic H_2
H_2 evolve from instrument components or undoped (blank) sample? Resistively heated Pt packet or cryostat in TPD evolve H_2 ? Quartz sample tube in volumetric evolve H_2 ? D_2 dosing give HD exchange on desorb?	Thermal degassing of sample prior to H_2 charge is essential. After such step, intrinsic H_2 or HD not readily measurable during desorption from either instrument (TPD or volumetric) or undoped sample / Pt packet
Sorption properties of pure sonication-generated alloy determined?	Pure alloy isolated from sonication probe while treatment with HNO_3 aqueous solution. Sorption properties determined by TPD and volumetric techniques
Primary calibration of instrument for quantitative H_2 analysis performed?	Primary calibration of TPD done by leak of H_2 standard gas through orifice to relate mass spec. single or total ion intensity to moles per unit time. Standard volume in volumetric instrument is calibrated and dead volume of sample/tube determined with He standard charge
Accuracy and precision of calibrated instruments checked against a reference standard?	TiH_2 reference standard used in TPD and volumetric techniques to desorb empirically known H_2 content and establish correlation



Sorption Apparatuses

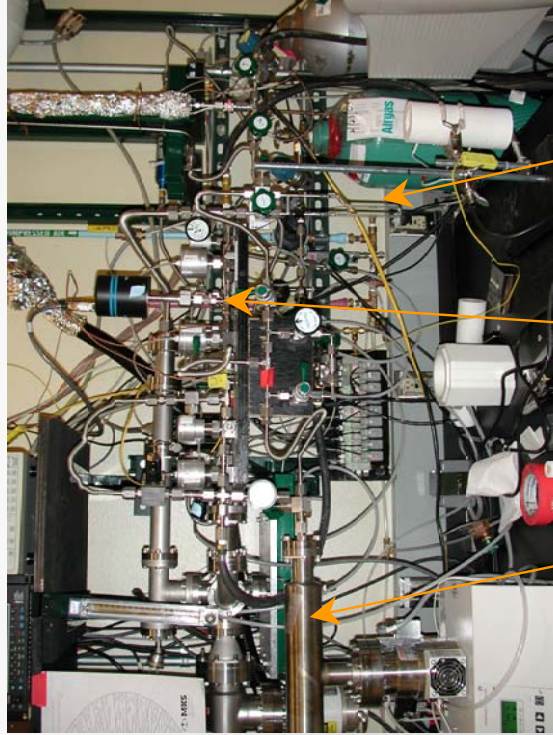


TPD

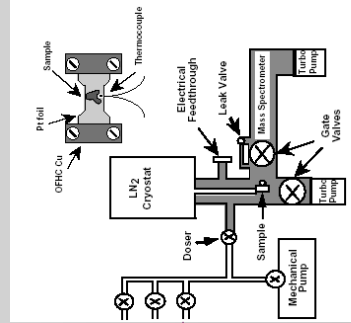


Calibrated Orifice Leak
 Cryostat / Pt-Packet Resistive Heater
 Prechamber & External Desorption Inlet

Volumetric

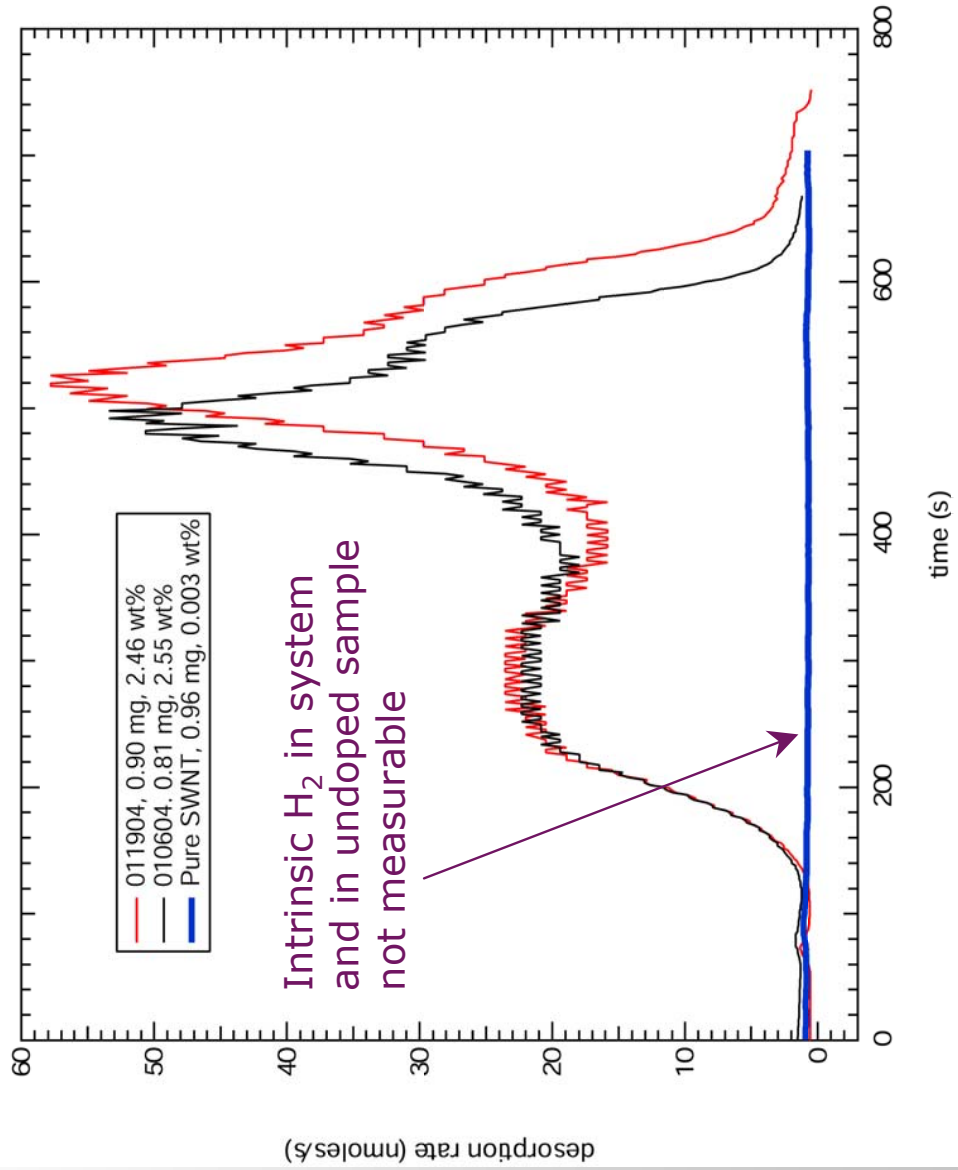
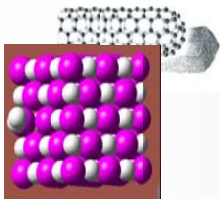


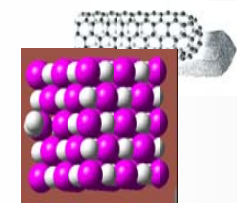
Mass Spec.
 Calibrated Volume
 Sample Tube (Flow-Through)



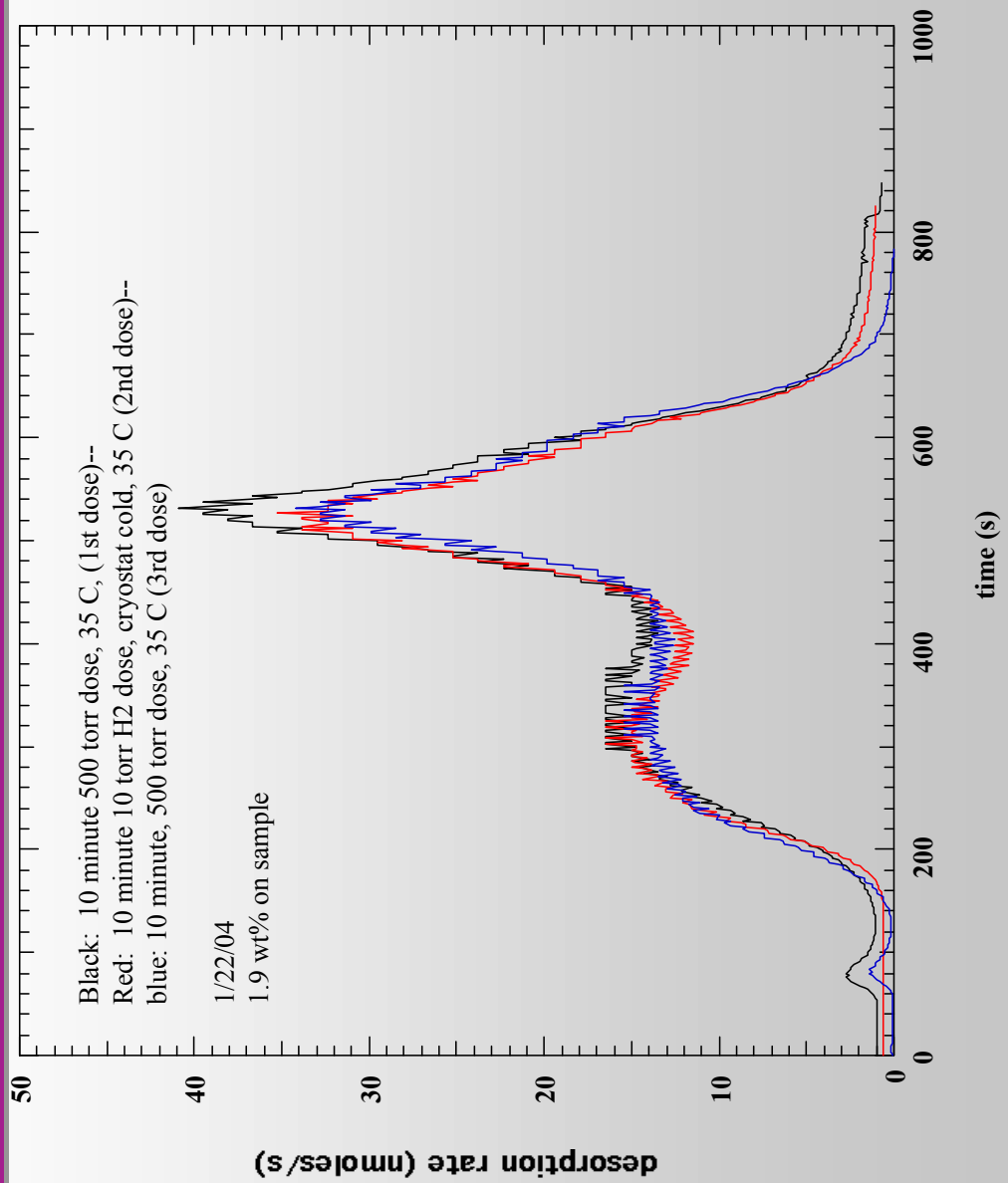


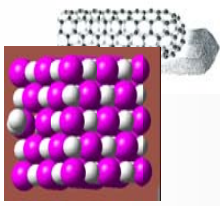
TPD Control Experiment





TPD Control Experiment





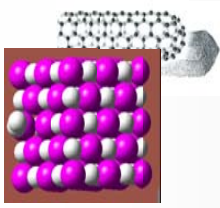
TPD Control Experiment



- D₂ dosing of undoped SWNT sample (blank)
- Does exchange occur with intrinsic H₂ within system to yield HD upon desorption?
- Is H₂ formed from the decomposition of hydrocarbons in SWNT sample?

Results

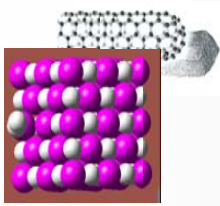
No measurable levels of HD observed in the desorption thermogram



Repeatability



- Within Batch Results
- Same synthesis, purification, cutting, filtering
 - SWNT#1: 2.39 wt% H₂ vs. 2.62 wt% H₂ in SWNT
 - Samples measured 1 week apart by TPD
 - Minimal degradation of material (stored in vacuum)



Accuracy

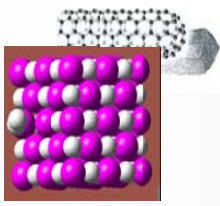


H₂ Mass Recovered from TiH₂ Reference Standard for Each Technique

	Volumetric	Measured ^a	Unknown ^b
		11.107 mg	11.400 mg
		5.475 mg	5.5564 mg
TPD	1.56 mg		1.54 mg
	1.76 mg		1.73 mg

^a Determined via H₂ evolved

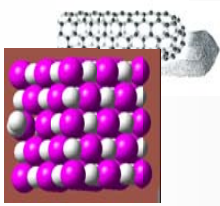
^b TiH₂ weights measured by M. Miller



Calibration



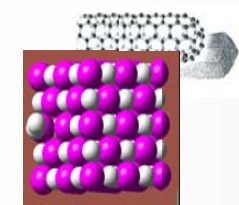
- Primary Calibration – H₂ leak through orifice
- Tested calibration with known weights of TiH₂
 - Sample weights- 1- 10 mg
 - TPD and volumetric
 - Results obtained to within 1-2%



Unknown Sample Analysis



- Tested calibration with unknown weights of TiH_2
 - 2 Different samples
 - Sample weights- 1- 10 mg (weighed by M.A. Miller)
 - TPD and volumetric
 - Results obtained to within 1-2%



Comparison of Sorption Results (wt. % H₂) for Doped SWNTs

Analysis Date	1/19/04	1/20/04	1/21/04	1/22/04	1/23/04
Synthesis Date	1/6/04	1/12/04	1/12/04	1/6/04	1/21/04
SWNT Cut	C1	C1	C2	C2	C1
<u>TPD</u>	2.62 (1/12/04) 2.39	1.09	1.18	1.9	1.06
<u>Volumetric</u>					
(Ads)	1.93				
(Des)	2.13		0.87		
(Ads)					
(Des)			1.19		
			1.51		
			1.50		

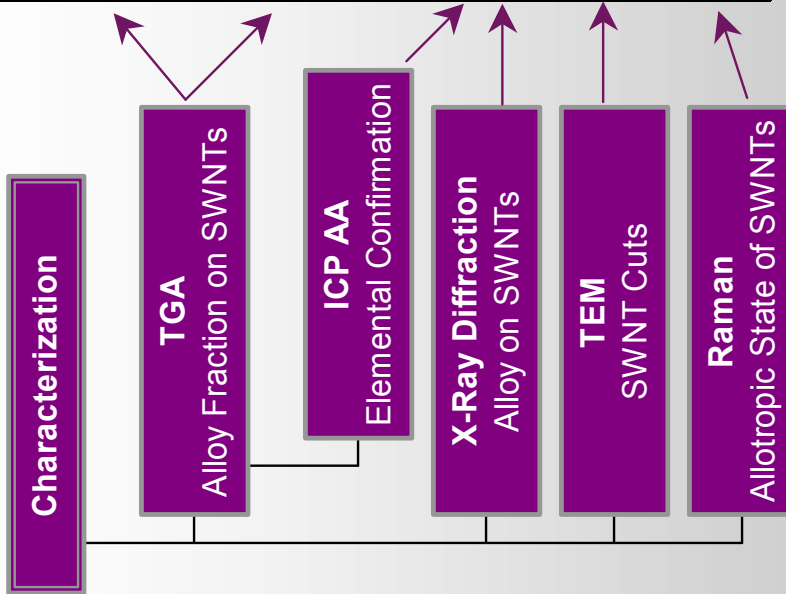
He flow for volumetric
Flow-through sample tube
Ramp to 500 C
Quench w/ LN2 for Desorption

He flow, evacuate at 500°C

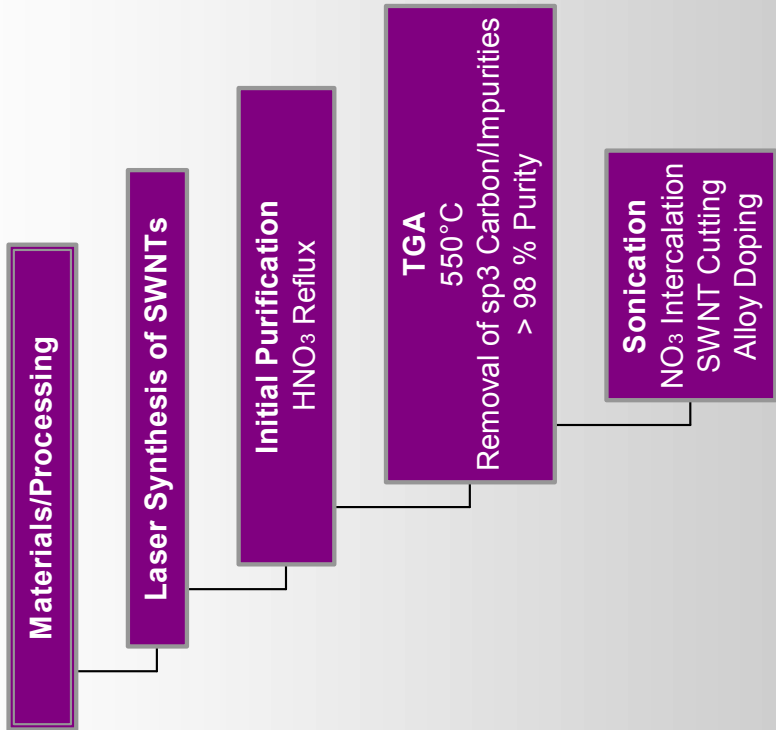
He flow, cool in flow

No flow, hold at 300°C, ramp to 500°C

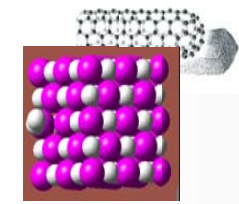
Issues	Observations
Enough accuracy in TGA method to determine alloy fraction assuming quantitative conversion to oxide of hypothetical stoichiometry?	TGA method yields average differences between measured and theoretical oxide weight values of 0.5%
Hypothetical stoichiometry of the converted alloy oxide correct?	Can not distinguish difference in TGA weight gain results between two hypothetical oxide compositions starting from a reference precursor Ti ₆₄ alloy (Goodfellow)
Elemental content of converted alloy correct?	Elemental content confirmed by ICP-AA and XRD patterns
Sonication cutting of SWNTs effective?	Effects of sonication confirmed by TEM (based on published results)
SWNT purity?	Purity assessed by Raman (based on published results)



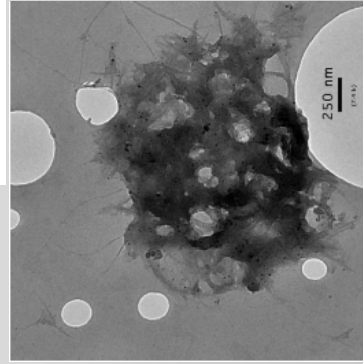
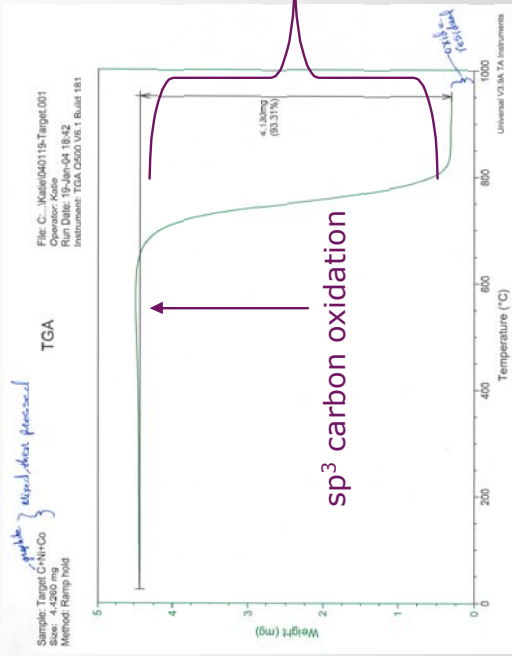
Inaccuracies in TGA measurements, elemental purity, or hypothetical stoichiometry of oxide can compound inaccuracy of alloy fraction



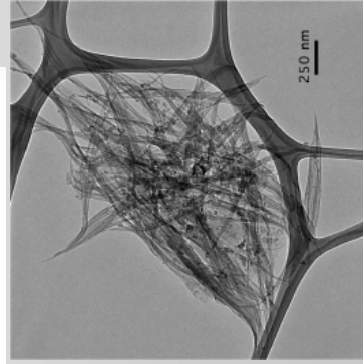
Issues	Observations
TGA purification below decomposition temperature of SWNTs in air?	TGA thermogram shows distinct weight-loss transition above 600°C. Few SWNTs destroyed below this transition
Sonication of SWNTs yield distinguishable cuts?	TEM images indicate re-assembly of SWNTs into distinctly shorter bundles
Uptake of alloy by SWNTs occurs consistently?	Uptake, intercalation and cutting are stochastic processes – large variations in alloy uptake under ostensibly similar conditions



TGA and Sonic-Probe Purification

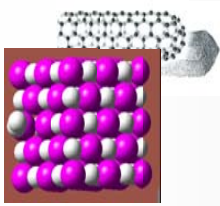


Crude Laser-Generated SWNTs
 HCl:H₂SO₄:HNO₃ Acid Cutting



SWNTs After Sonic-Probe Cutting
 in HNO₃

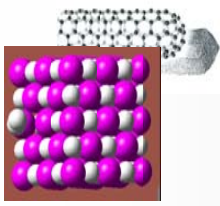
- Distinctly shorter bundles
- Cutting, intercalation, and alloy uptake are stochastic processes



Other Related Issues



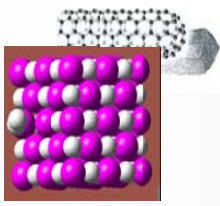
- Doped SWNTs appear to be sensitive to degradation, affecting the sorption reversibility
 - Hypothesis: Doped SWNTs may be damaged upon initial degassing cycle as a consequence of local exposure of sample to reactive species
 - Mass spectral analysis shows out-gassing of water and NO (from HNO_3 cutting procedure)
- Pressure above sample in volumetric system upon degassing was measured to be 30 mtorr @ 200°C
 - Substantiates flow-through sample tube design
 - Slower heating rates during degassing cycle also useful in mitigating “stagnation” of reactive species



Conclusions



- H₂ uptake values for alloyed SWNTs as reported by the NREL team are credible
- Analytical methodologies are well established
- TPD and volumetric techniques were demonstrated to be accurate and repeatable based on reference standard
- Excellent correlation between techniques using similar samples
- Large variances in H₂ uptake for SWNT materials not related to analytical methodologies
 - Likely attributed to the stochastic nature of sample processing (synthesis, purification, cutting, dopant uptake)
 - Sensitivity of samples to degradation during degas cycle



Recommendations



- NREL primary calibration of TPD (orifice leak) should be compared with NIST-traceable calibrated leaks (3-decade leak rate) near position of sample/cryostat
- Establish conditions to mitigate sample degradation during degassing cycle in volumetric system
 - Higher conductance for evacuation
 - He flow-through
- Submit samples to other labs for evaluation (single batch)
- Convince community by reporting volumetric sorption data
- Establish method to exactly duplicate SWNT cutting by sonication probe without incorporating alloy, suggest
 - DLC coat Ti₆₄ probe tip
 - Validate that sonic efficiency is preserved without erosion
- Move forward to understanding further the materials science!

* Summary report will be submitted to DOE

Acknowledgements

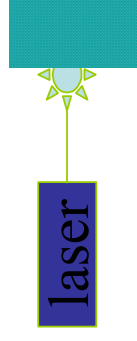


Front to back: Anne Dillon, Katherine Gilbert, Phil Parilla, Mike Heben (NREL), Michael Miller (SwRI), Ray Gorte (U. Penn.), Sunita Satyapal (DOE). Not pictured, Tom Gennett (RIT visiting scientist).

ADDENDUM

Ultrasonication-based Sample Preparation

Step 1: laser generation of SWNTs

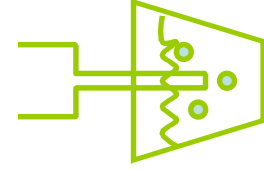


produces a synthesis batch

Co:Ni:C target

Step 2: purification of SWNTs

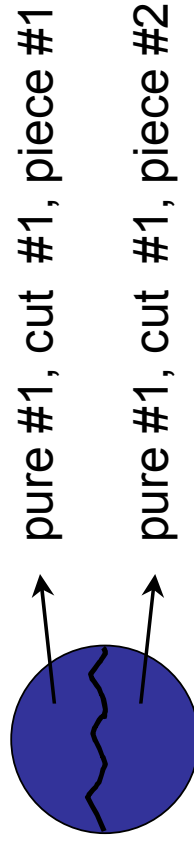
Reflux in HNO_3 , collect on filter, oxidize in air
produces a purification batch (e.g. pure #1)



Step 3: Ultrasonic cutting

produces a “cut” batch, introduces metal
(e.g. cut #1)

Step 4: Collect by filtration



Calculating Hydrogen Capacity on SWNT Fraction

$$(1) \quad X_{\text{alloy}} + X_{\text{SWNT}} = 1$$

$$(2) \quad (\text{wt}\% H_{\text{SWNT}} * X_{\text{SWNT}}) + (\text{wt}\% H_{\text{alloy}} * X_{\text{alloy}}) = \text{wt}\% H_{\text{sample}}$$

Where X_{alloy} and X_{SWNT} are weight fractions

$$\text{wt}\% H_{\text{SWNT}} = \frac{\text{wt}\% H_{\text{sample}} - (X_{\text{alloy}} * \text{wt}\% H_{\text{alloy}})}{(1 - X_{\text{alloy}})}$$

Requires accurate measurement of:

- ✓ Weight of sample
- ✓ Total amount of hydrogen adsorbed
- ✓ Weight of alloy in sample
- ✓ Hydrogen capacity of alloy

Results Obtained During the Review for Different Samples of Doped SWNTs

Sample	Technique	Wt% H ₂ total	Wt% alloy	Wt% H ₂ tubes
Pure #1, cut #1, piece #1	TPD	2.62	68.0	2.88
Pure #1, cut #1, piece #2	TPD	2.39	66.4	2.17
Pure #1, cut #1, piece #3	Vol (abs)	1.93	63.9	0.92
Pure #1, cut #1, piece #3	Vol (des)	2.13	63.9	1.48
Pure #1, cut #2, piece #1	TPD	1.90	41.0	1.48
Pure #2, cut #1, piece #1	TPD	1.09	22.4	0.68
Pure #2, cut #2, piece #1	Vol (abs)	1.51	45.8	0.67
Pure #2, cut #2, piece #1	Vol (des)	1.50	45.8	0.65
Pure #2, cut #2, piece #2	TPD	1.18	40.4	0.29
Pure #3, cut #1, piece #1	TPD	1.06	43.3	-0.04
Pure #3, cut #1, piece #2	Vol (abs)	0.87	35.7	0.00
Pure #3, cut #1, piece #2	Vol (des)	1.19	35.7	0.46

Comparison of the Adsorption/Desorption Volumetric Results

Sample	Direction	Wt% H ₂ total
Pure #1, cut #1, piece #3	abs	1.93
	des	2.13
Pure #2, cut #2, piece #1	abs	1.51
	des	1.50
Pure #3, cut #1, piece #2	abs	0.87
	des	1.19
Pure #4, cut #1, piece #1	abs	1.52
	des	1.57
Pure #2, no cut, piece #1 (blank)	abs	0.01
	des	0.00
Probe alloy #1, piece #1	abs	2.49
	des	2.54

Differences in degas methods lead to discrepancies in a few cases - focus of future milestone

Summary of the Adsorption/Desorption Volumetric Results

- Adsorption amount is determined by equilibrium adsorption at RT. Desorption amount is determined after cooling sample to 75.6 K in H₂, evacuating, and warming the sample
- 6 data sets can be compared; 4 ads/des pairs are in good agreement (within ~ 3%), 2 data sets show ads/des values that differ by 10 % or more
- Previous volumetric measurements with closed-end tubes always yielded a lower capacity than was found by TPD
- Flow-through tubes permitted a degas that yielded a larger volumetrically-determined capacity than was determined by TPD
- Research focus: Optimization of degas will lead to better agreement between ads & des measurements, and bring TPD and ads/des volumetric measurements into better agreement .

Variation in Uptake for Different Pieces from Same Purification and Cut

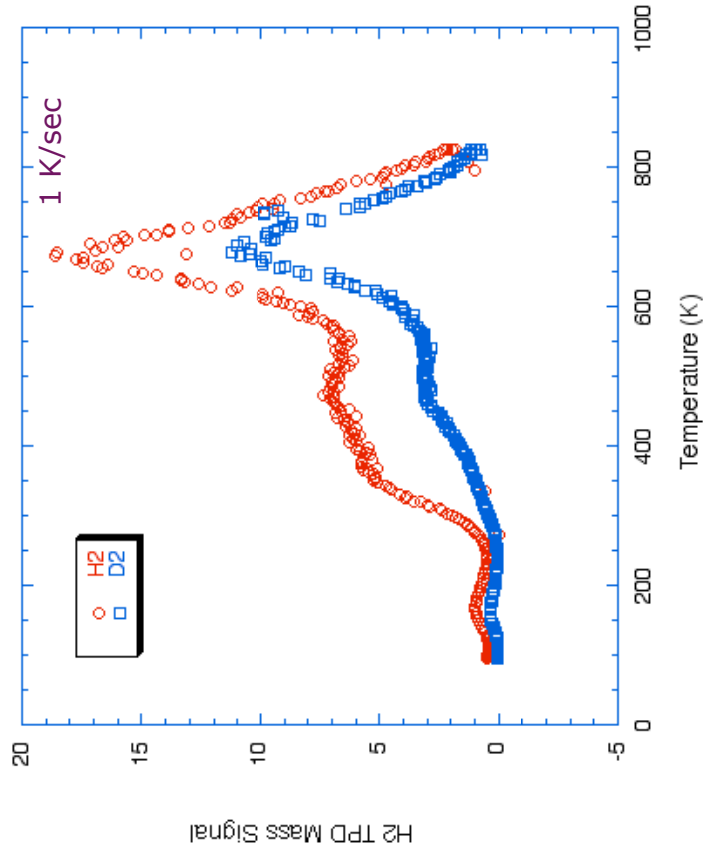
Sample	Technique	Wt% H ₂ alloy	Wt% H ₂ total	Wt% H ₂ tubes
Pure #1, cut #1:				
piece #1	TPD	68.0	2.62	2.88
piece #2	TPD	66.4	2.39	2.17
piece #3	Vol (abs)	63.9	1.93	0.92
piece #3	Vol (des)	63.9	2.13	1.48
Pure #2, cut #2:				
piece #1	Vol (abs)	45.8	1.51	0.67
piece #1	Vol (des)	45.8	1.50	0.65
piece #2	TPD	40.4	1.18	0.29
Pure #3, cut #1:				
piece #1	TPD	43.3	1.06	-0.04
piece #2	Vol (abs)	35.7	0.87	0.00
piece #2	Vol (des)	35.7	1.19	0.46

Variation in uptake not simply due to
variation in metal content

D₂ TPD Control Experiment on doped SWNT

TPD spectra after two separate doses with H₂ and D₂

- No measurable levels of HD or H₂ observed in the desorption thermogram after a D₂ dose
- No contribution to desorption signal from decomposition of hydrogen containing impurities



C

APPENDIX C (BEOS & SLD MODEL)

C.1 Bender Equation of State

The Bender equation of state (BEOS) is given by

$$P(\rho, T) = \rho T \left[R + B\rho + C\rho^2 + D\rho^3 + E\rho^4 + F\rho^5 + (G + H\rho^2)\rho^2 \exp(-a_{20}\rho^2) \right] \quad (\text{A.1})$$

where P is the gas pressure as a function of the gas density, ρ , and temperature, T . The coefficients of Eq. A.1 are expanded as follows:

$$\begin{aligned} B &= a_1 - a_2/T - a_3/T^2 - a_4/T^3 - a_5/T^4 \\ C &= a_6 + a_7/T + a_8/T^2 \\ D &= a_9 + a_{10}/T \\ E &= a_{11} + a_{12}/T \\ F &= a_{13}/T \\ G &= a_{14}/T^3 + a_{15}/T^4 + a_{16}/T^5 \\ H &= a_{17}/T^3 + a_{18}/T^4 + a_{19}/T^5 \\ R &= 4.12436 \text{ J/g} \cdot \text{K} \end{aligned}$$

The fugacity equation for the bulk gas in A.1 is written as:

$$\ln \frac{f(\rho, T)}{RT\rho} = \frac{1}{RT} \left\{ \begin{aligned} &2B\rho + \frac{3}{2}C\rho^2 + \frac{4}{3}D\rho^3 + \frac{5}{4}E\rho^4 + \frac{6}{5}F\rho^5 + \frac{1}{2a_{20}} \left(G + \frac{H}{a_{20}} \right) + \\ &\left[G \left(\rho^2 - \frac{1}{2a_{20}} \right) + H \left(\rho^4 - \frac{\rho^2}{2a_{20}} - \frac{1}{2a_{20}^2} \right) \right] \exp(-a_{20}\rho^2) \end{aligned} \right\} \quad (\text{A.2})$$

A list of the coefficients a_n used in Eq. A.1 and A.2 for hydrogen is provided in Table A1. In a sorption isotherm experiment, the experimentally accessible parameters in Eq. A.1 are pressure and temperature. Therefore, the bulk-gas density, $\rho(P, T)$, is determined by solving the roots of Eq. A.1 at the measured pressure and temperature.

Table C.1: Coefficients used in the BEOS (Eq. A.1 and A.2) for hydrogen.

a_n	Hydrogen Value
1	3.996218032E+01
2	2.051873895E+03
3	2.616700857E+05
4	-4.908661819E+06
5	3.040449501E+07
6	8.414021008E+01
7	1.549870652E+04
8	-2.498914344E+05
9	1.310058224E+04
10	-7.258581160E+05
11	-1.224315455E+05
12	2.045796918E+07
13	-1.330602191E+07
14	1.797997237E+08
15	-5.139989863E+09
16	3.890142315E+10
17	8.831790280E+10
18	-1.937659071E+12
19	1.285759712E+13
20	7.400000000E+02

C.2 Derivation of Fitting Function for Gravimetric Buoyancy Correction

The chemical potential at equilibrium describing the relation between the bulk gas and its interaction with the potential of a heterogeneous surface is

$$\mu_{ad} = \mu_b + U \quad (\text{A.3})$$

where μ_{ad} is the chemical potential of the adsorbed fluid in a field of the surface potential, U , and μ_b is the chemical potential of the bulk gas. For non-ideal bulk and adsorbed fluids, the chemical potential is related to the fugacity according to:

$$\mu_b = \mu_0 + RT \ln\left(\frac{f_b}{f_0}\right) \quad (\text{A.4})$$

$$\mu_{ad} = \mu_0 + RT \ln\left(\frac{f_{ad}}{f_0}\right) \quad (\text{A.5})$$

From Eq. A.4 and A.5, the relation between the fugacity of the adsorbed fluid and that of the bulk-fluid then becomes

$$f_{ad} = f_b \exp\left(\frac{-U}{RT}\right) \quad (\text{A.6})$$

Recalling the definition of the Gibbs excess adsorption in terms of a gravimetric measurement:

$$W_a - W_{sb} \left(1 - \frac{\rho_b}{\rho_{sb}}\right) - W_s \left(1 - \frac{\rho_b}{\rho_s}\right) = V_{ad} (\rho_{ad} - \rho_b) \equiv \Gamma$$

W_a = Apparent Weight

W_{sb} = Weight of Sample Basket

W_s = Weight of Sample

V_{ad} = Volume of Adsorbed Phase

Γ = Gibbs Excess Adsorption

ρ_b = Density of Bulk - Phase Gas

ρ_{sb} = Density of Sample Basket

ρ_s = Density of Sample

ρ_{ad} = Density of Adsorbed Phase

(A.7)

Eq. A.7 can be rearranged in terms of the density of the adsorbed fluid, ρ_{ad} , thus allowing a master equation for the non-ideal bulk gas under isothermal conditions to be derived from the fugacity (Eq. A.2) and its relation to the adsorbed phase (Eq. A.6), as a function of the apparent weight, W_a , and the bulk-gas density, ρ_b . The volume of the adsorbed phase, V_{ad} , the density of the sample, ρ_s , and the adsorption potential, U , are used as fitting parameters in a Levenberg-Marquardt surface fitting algorithm (Systat Software, Inc., San Jose, CA). The fitting function is thus given by:

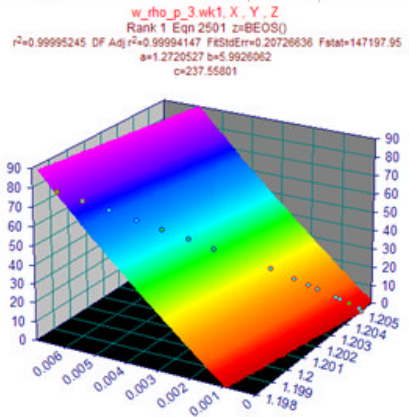
$$f_b \Rightarrow f_b(W_a, \rho_b)_T = RT\rho_{ad} \exp\left\{\xi + \frac{U}{RT}\right\} \quad (\text{A.8})$$

where ξ is equal to all the terms on the right-hand-side of Eq. A.2, and

$$\rho_{ad} = \left\{ \frac{\left[W_a - W_{sb} \left(1 - \frac{\rho_b}{\rho_{sb}} \right) - W_s \left(1 - \frac{\rho_b}{\rho_s} \right) \right]}{V_{ad}} \right\} + \rho_b \quad (\text{A.9})$$

C.3 Example Dataset for Gravimetric Sorption Buoyancy Correction

			rho Sample (g/cc):	1.2720527	Adsorbed Volume (cc):	5.993
			Basket (g/cc):	0.627452	Adsorption Potential (J/g):	237.6
			Basket (g):	0.668432		
Apparent Weight (g)	BEOS	Measured				
	Roots	Equilibrium Pressure (bar)	Corrected Excess (g)	Corrected Excess (wt.%)		
rho (g/cc)						
1.205204	0.0000000000	0.000	0	0		
1.205252	0.0001087986	1.341	0.000267027	0.022151234		
1.205084	0.0003243869	4.005	0.000532392	0.044154948		
1.204815	0.0006451004	7.983	0.000909095	0.075373896		
1.204428	0.0010707341	13.293	0.001379197	0.114305997		
1.203369	0.0021147638	26.459	0.002421165	0.200489755		
1.201908	0.0032442015	40.936	0.003233184	0.26755084		
1.200645	0.0042662089	54.251	0.004028052	0.333108196		
1.199349	0.0052666524	67.488	0.004744826	0.392150921		
1.198709	0.0057456219	73.892	0.005069081	0.418837679		
1.198074	0.0062158262	80.229	0.005380342	0.444441632		
1.200031	0.0047434224	60.527	0.004374402	0.361646741		
1.201288	0.0037485441	47.470	0.003628297	0.30014889		
1.203900	0.0015992697	19.928	0.001914677	0.158615427		
1.204216	0.0012802837	15.916	0.001589135	0.131682469		
1.204893	0.0005378650	6.650	0.00077098	0.06393		
1.205250	0.0000864719	1.066	0.000219704	0.018226308		



***D* APPENDIX D (STANDARD OPERATING PROCEDURES)**

Standard Operating Procedure

Master Protocol Index & Facility Overview (Small Scale Analysis)

Document No. 05064-0001
Rev. 1

Prepared By: _____
Michael A. Miller, Manager-R&D

Date: 02/06/2006

Approved By: _____

Date: _____

1. PURPOSE

- 1.1 This document provides a master guide to all protocols associated with the maintenance, operation, and small-scale scientific and analytical activities of the National Testing Laboratory for Solid-State Hydrogen Storage Technologies (a U.S. Department of Energy Sponsored Laboratory designed, managed and operated by Southwest Research Institute[®]).
- 1.2 The primary objectives of the protocols are to:
 - 1.2.1 Assure that laboratory operations are performed in a safe manner.
 - 1.2.2 Provide for precise and accurate measurements of hydrogen sorption in a repeatable manner.
 - 1.2.3 Provide a clear understanding of the methods used within the laboratory facility.

2. SCOPE

- 2.1 The Master Protocol Index provides a guide to all protocols (Standard Operating Procedures) of the most current revision that define the operational functions of the laboratory facility and its sub-elements.
- 2.2 This index may be used to identify the appropriate document and its most current revision. It also assigns the general responsibilities of trained personnel, lists all references contained in the master group of protocols, and provides an illustrative overview of the laboratory facility, including the facility's sub-assemblies, equipment and instrumentation.

3. RESPONSIBILITIES

- 3.1 It is the responsibility of the Technical Manager to train the appropriate technical staff and certify competency in the procedures of this master guide and to make certain trained technical staff are following all procedure properly.
- 3.2 It is the responsibility of the trained technical staff to comply with the procedures of each protocol when conducting laboratory studies.

4. MASTER PROTOCOL INDEX

- 4.1 The Master Protocol Index is shown in Scheme 1, referencing the SwRI document numbers and most current revision of each standard operating procedure (SOP). Four primary tiers comprise this Master Protocol Index: Laboratory Facility, Sample Handling and Activation, Sorption Analysis, and Sample Characterization.
- 4.2 The Laboratory Facility tier pertains to all activities or functions that are required to operate and maintain the source gas and safety services of the laboratory facility, including emergency procedures for gas leak and fire scenarios. It excludes protocols that pertain to custodial, scientific and analytical activities.

- 4.3 The Sample Handling and Activation tier pertains to material sample (test article) login, storage, and custody. It also includes protocols that provide general guidance on the activation of materials, when required, and specific procedures on the husbandry of glove boxes.
- 4.4 The Sorption Analysis tier pertains to all scientific and analytical functions of the laboratory. It contains specific SOPs on quantitative and qualitative sorption measurements.

5. LABORATORY FACILITY

- 5.1 The physical layout of the laboratory facility is shown in Scheme 2. Not shown in detail or to scale is a revetment area in which tube trailers of hydrogen and helium gases are stationed.
- 5.2 Tube trailers (separate hydrogen and helium) are replenished on-site as needed from a mobile (trucked) delivery source. Nominal gas pressures of each gas in the respective tube trailer range 2500-3000 psig and nominal purity from the mobile delivery source is 99.9995% for each gas.
- 5.3 A flow-loop and manifold station is located in proximity of the tube trailers to enable replenishment of tube containers as noted above and to purge the connection points with gas while the transmission lines are isolated. Purging of the flow loop maximizes gas purity and minimizes potential contamination of the transmission lines. SOPs pertaining to gas service are described in SwRI Document No. 05064-0002.
- 5.4 Source gases from the revetment area at the flow-loop and manifold station are transmitted to connection inlets of an ultra-high purity (UHP) central gas manifold via 0.5 inch OD high-purity stainless steel lines (semiconductor grade as defined below).
- 5.5 The UHP central gas manifold is located inside the laboratory facility and is illustrated separately in Scheme 3. This manifold is used to distribute each gas (hydrogen and helium) to the appropriate analytical or process station. It is also used to manage and control gas conditions such as pressure regulation, flow restriction, and purity. SOPs pertaining to the husbandry of the central gas manifold are described in SwRI Document No. 05064-0003.
- 5.6 The UHP central gas manifold and any other associated tubulation as applicable conforms to the specifications for material quality, surface finish, and inert fabrication and assembly as outlined in REF. (heretofore designated as “semiconductor-grade”).
- 5.7 A central console (PC-based user interface) is used to control, manage, and log the operating conditions of the UHP central gas manifold, including the remote actuation of valves, the safety system interlocks, and safety sensors (gas-leak detection). It is also used to monitor and log the laboratory environmental conditions (temperature, barometric pressure, and relative humidity).
- 5.8 The central console is the user interface to a PLC system from which all control and monitoring operations of the UHP central manifold and laboratory sensors are processed

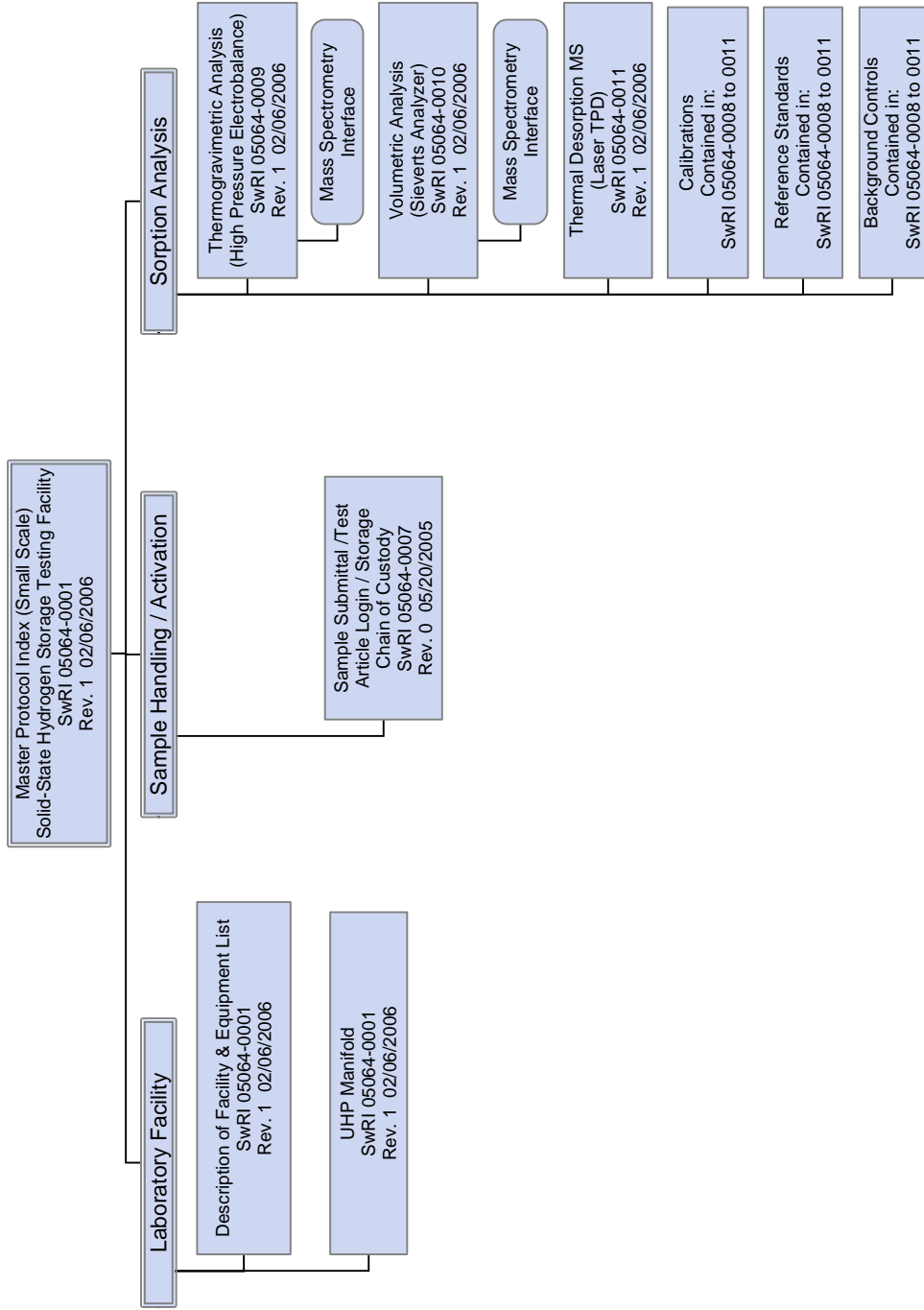
and executed. The PLC system can also be operated independently of the central console user interface.

- 5.9 A 20kVA uninterruptible power supply (UPS) is used to provide conditioned and uninterrupted power to critical systems and analytical instrumentation. The transition from grid power to sustained UPS battery power is of such duration to permit a diesel generator located adjacent to the facility to complete its startup and power regulation sequence (~8 sec).
- 5.10 Hydrogen leak detection is afforded at two levels by two independent systems: a high-sensitivity hydrogen-specific leak detector with distributed sampling of the UHP gas manifold or portable on-site surveys (handheld wand), and a central facility detector coupled to emergency shut-off master valve and rapid ventilation system. SOPs pertaining to laboratory facility safety, including hydrogen leak detection and emergency procedures, are described in SwRI Document No. 05064-0004.

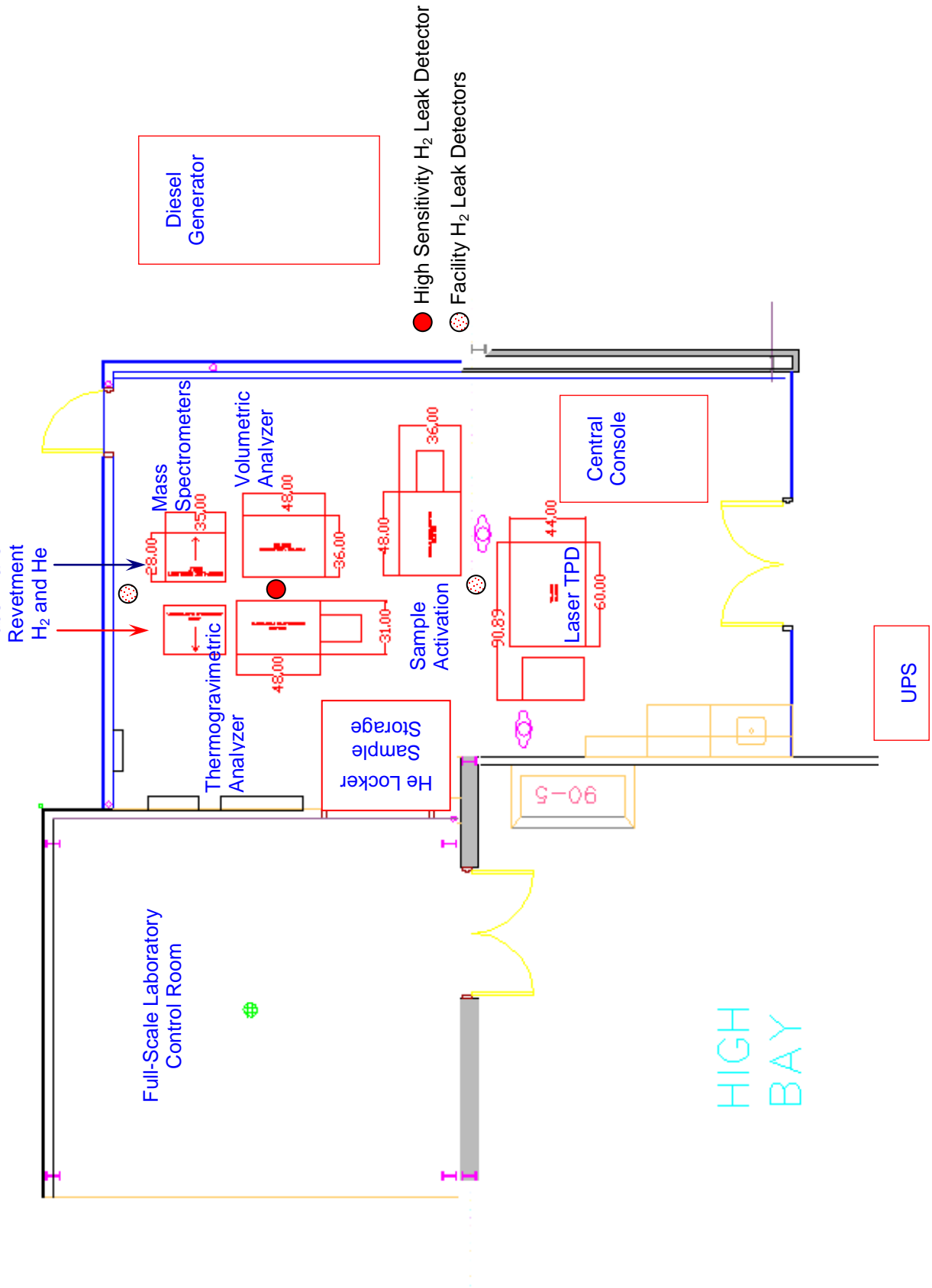
6. EQUIPMENT AND INSTRUMENTATION

- 6.1 A list of equipment and instrumentation for the laboratory facility is given in Table 1.

Scheme 1. Master Protocol Index.



Scheme 2. Laboratory Facility Layout



Scheme 3. UHP Gas Handling Manifold

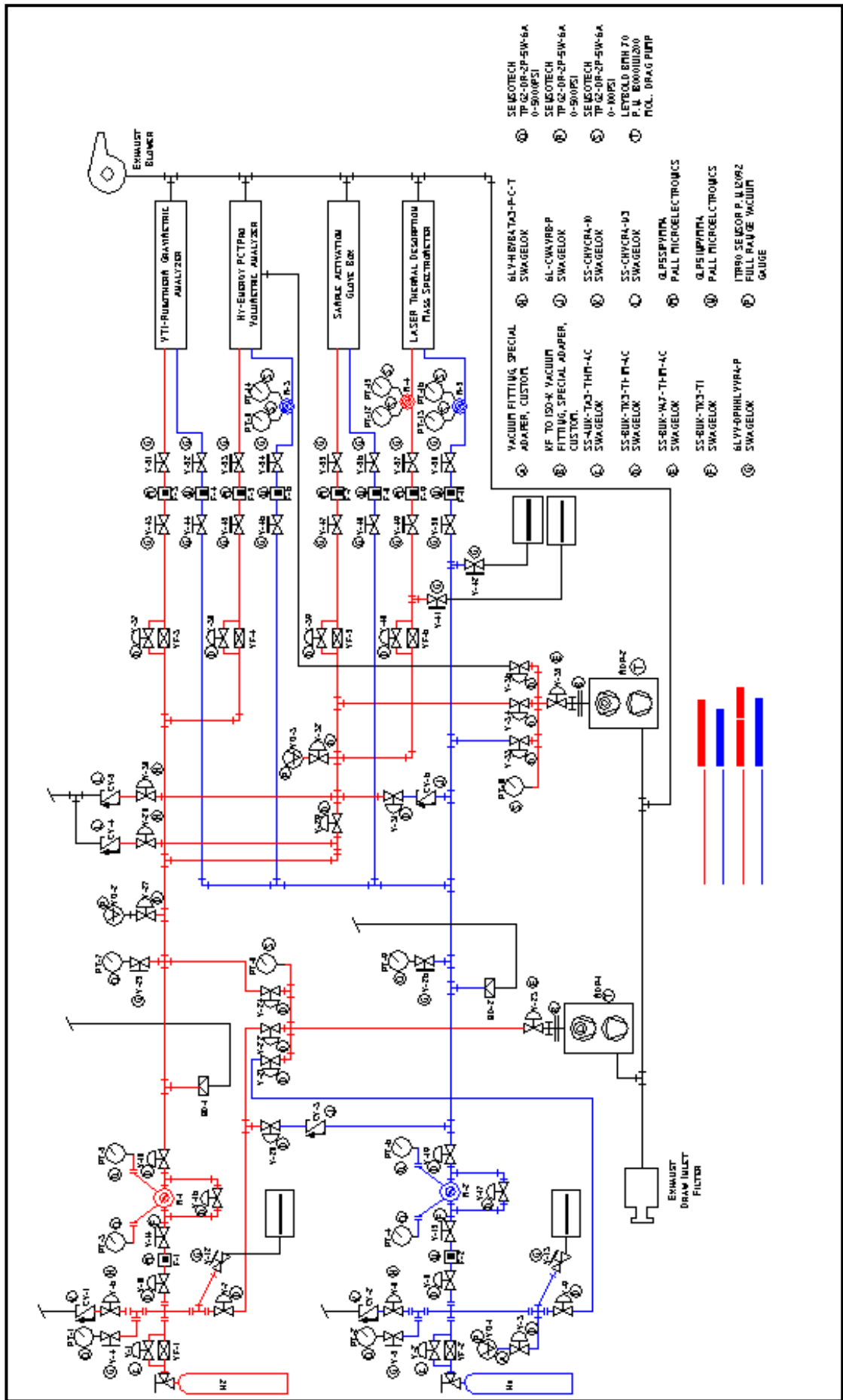


Table 1. Equipment and Instrumentation

Equipment Item (Number of Replicates)	Description
Thermogravimetric Analyzer, VTI, Inc. / SwRI Microbalance: Magnetic Suspension (Rubotherm)	All metal; UHV to 150 bar; contactless vertical force measurements; controlled environment housing for microbalance, sample chamber, and gas manifolds; connections to system through leak-tight feed ports; < 1 ppm H ₂ O and O ₂ mol. sieve and Cu catalyst
Volumetric Analyzer, Hy-Energy LLC, PCTPro-2000	All metal; UHV to 200 bar; PED controlled; low dead-volume; 5 calibrated reservoir volumes; compatible with full-size system testing
Laser Thermal Desorption Mass Spectrometer (TPD), SwRI	Quadrupole mass spectrometer (1-400 amu); 90° off-axis SEM; gas-tight ion source; ultra-clean analyzer chamber and Ytterbium fiber laser sample heating device with direct diode control, motorized neutral density filter, and acousto-optic modulation for closed-loop power control
Quadrupole Mass Spectrometer, Thermostar, Pfeiffer, Inc. for Gravimetric Analyzer MS Interface	Mass Spec. System; 1-300 amu mass range; gas-tight ion source; SEM/Faraday detectors; integrated turbo pumping station; heated quartz capillary interface (1 atm maximum inlet pressure)
Hydrogen Leak Detector / Sampling System, Sensistor Technologies, H2000	Microelectronic, H ₂ -specific sensor, 0.02 – 5 x 10 ⁻⁷ mbar•L/s sensitivity, portable wand sensor for on-site leak detection, and stationary sensor with pneumatic sampling unit for distributed low leak-rate detection of UHP central gas manifold
High Vacuum System (Leybold) for Sample Activation Reactor & UHP Facility Gas Manifold (3)	Turbo-drag pump; dry diaphragm backing pump; 60 L/s; 10 ⁻⁸ mbar

Table 1 (Cont.)

Equipment Item	Description
<p>Quadrupole Mass Spectrometer, Omnistar, Pfeiffer, Inc. with GSS-300 (6-Channel Gas Stream Select) Multisampling Unit for UHP Manifold Sampling and Volumetric Analyzer MS Interface</p>	<p>Mass Spec. System; 1-300 amu mass range; gas-tight ion source; SEM/Faraday detectors; integrated turbo pumping station; automated 6-channel gas stream selection module (1 atm maximum inlet pressure each channel); one channel dedicated to volumetric analyzer MS interface</p>
<p>MS Interface for Volumetric Analyzer, SwRI</p>	<p>Thermally regulated dual rotary valve system; low dead volume; capillary tubing connections between valves and to reactor vessel of volumetric analyzer</p>
<p>Sample Activation Reactor System and Glove Box, Parr Instruments, Inc. / SwRI</p>	<p>SS High-Pressure Reactor Vessel with heating unit and PID controller for high-pressure H₂ activation of sample materials in controlled environment glove box</p>
<p>Microbalance, Mettler-Toledo, UMX-2, (2)</p>	<p>Load cell microbalance; 2 g capacity; 0.1 µg resolution</p>
<p>Hydrogen Detector</p>	<p>Hydrogen detector; centrally located in laboratory facility and interfaced with central alarm unit and emergency vent system</p>

Revision Number	Effective Date	Description of Changes
0	09/13/2004	Initial document. Labeled "Draft".
1	02/06/2006	Expanded purpose. Revised Scheme 2.

Standard Operating Procedure

Sample Submittal, Login, Storage, & Chain of Custody

Document No. 05064.0007
Rev. 0

Prepared By:



Michael A. Miller, Manager-R&D

Date: 05/20/2005

Approved By:

Date: _____

1. PURPOSE

- 1.1 Provide a standard procedure by which government or commercial research laboratories (Client) may package test articles (samples), applicable to the function of the above entitled laboratory, and ship them to SwRI for analysis in compliance with all applicable local, state, Federal, and international laws and regulations on the transport of hazardous materials or articles.
- 1.2 Provide a standard procedure by which samples are accepted by SwRI for analysis in accordance with established analytical procedures, are logged into a central register (database), and are stored until the time of analysis.
- 1.3 Provide a standard procedure by which SwRI conducts chain of custody procedures for samples, during the time that such samples are stored, analyzed, and either returned to Client or properly disposed.

2. SCOPE

- 2.1 This SOP describes the procedures to be followed by the Client for requesting hydrogen sorption analyses of Client's samples and for submitting such samples to SwRI for analysis. It also provides general guidelines to the Client for assigning a hazard classification to the sample, and for selecting the appropriate shipping materials and procedures for safe shipment of sample(s).
- 2.2 The procedures to be followed by SwRI for accepting custody of Client's samples are also described in this SOP.

3. RESPONSIBILITIES & INDEMNIFICATIONS

- 3.1 It is the responsibility of the Client to train the appropriate technical staff and certify competency in the applicable procedures of this SOP, and to comply with all applicable local, state, Federal, and international laws and regulations on the transport of hazardous materials or test articles.
- 3.2 It is the responsibility of SwRI trained technical staff to comply with this procedure when receiving, logging, and storing test articles, and when conducting custodial procedures for the same.
- 3.3 Indemnification: Client agrees to indemnify and hold harmless SwRI, its agents and employees, from any and all liability, loss, damage and expense sustained by reason of Client's failure to exercise due care in the packaging, labeling, and shipment of samples.
- 3.4 Client warrants that the materials or structure of matter that constitute samples received by SwRI for analysis do not infringe any patent or other property right that would otherwise prohibit the use of such samples for investigational purposes.

4. REFERENCES

- 4.1 U.S. Department of Transportation, Pipeline and Hazardous Materials Safety Administration (PHMSA), Office of Hazardous Materials Safety (<http://hazmat.dot.gov>).
- 4.2 Hazardous Materials Regulations, 49 CFR Parts 100-185.

5. SAMPLES

- 5.1 Samples can be of solid or liquid state, and may exhibit a propensity to absorb hydrogen, or may chemically decompose to yield hydrogen as a desirable product along with other byproducts. In the case of solid-state materials, samples can be granular or a fine powder in morphology and, in many instances, may be labile in the presence of air or moisture to the extent that they may be classified as pyrophoric (will ignite spontaneously in air or moisture). Liquid-state samples may be volatile or labile (or both) in the presence of air or moisture, and may also be classified as pyrophoric.
- 5.2 Samples can be in the hydride, activated state (containing hydrogen) or in the dehydride (hydrogen removed) state, the latter either being an activated material pre-conditioned to absorb hydrogen or a non-activated material not yet pre-conditioned for chemical activity.
- 5.3 Sample aliquots ranging from milligram (> 1 mg) to multi-gram (< 500 g) quantities will be pre-weighed by Client and transferred to a suitable container for shipment. The conditions under which samples will be packaged and the packaging materials used therein, including the container, will be chosen based upon the class of material being submitted for analysis and the applicable regulations for shipment as outlined in this SOP.

6. MATERIALS AND EQUIPMENT

- 6.1 Flame-seal glass vial.
- 6.2 Glass vial with septum screw cap.
- 6.3 Stainless steel container vessel with face-seal or compression fittings.
- 6.4 Vermiculite.
- 6.5 Dry nitrogen or dry argon.
- 6.6 Inert, dry storage locker for samples (SwRI).

7. PROCEDURE

7.1 Material Designation and Hazard Communication (from References 4.1 and 4.2) – Client’s Responsibility

- 7.1.1 Hazardous materials' regulations are subdivided by function into four basic areas:

Procedures and/or Policies 49 CFR Parts 101, 106, and 107

Material Designations 49 CFR Part 172

Packaging Requirements 49 CFR Parts 173, 178, 179, and 180

Operational Rules 49 CFR Parts 171, 173, 174, 175, 176, and 177.

7.1.2 The Hazardous Materials Table (49 CFR Part 172.101) designates specific materials as hazardous for the purpose of transportation. It also classifies each material and specifies requirements pertaining to its packaging, labeling, and transportation. Hazard communication consists of documentation and identification of packaging and vehicles. This information is communicated in the following formats:

Shipping papers (Part 172, Subpart C)

Package marking (Part 172, Subpart D)

Package labeling (Part 172, Subpart E)

Vehicle placarding (Part 172, Subpart F).

7.1.3 Based upon the information contained in 7.1.1 and 7.1.2, determine the shipping name and hazard classification of the sample that most closely matches that listed in the Hazardous Materials Table (Section 172.101).

7.2 Packaging Requirements for Shipment – Client’s Responsibility

7.2.1 Hazardous materials' packaging regulations were formulated to meet two criteria:

- Packaging of hazardous material must be adequate in strength and quality to withstand normal transportation.
- Packaging used must be compatible with the hazardous material and adequate considering the level of risk presented by the material.

7.2.2 Determine from Part 173 of Section 172.101 of the Hazardous Materials Table the correct packaging required to transport the sample. Packaging authorized for the transportation of hazardous materials is either manufactured to DOT standards (Parts 178 and 179) or does not meet DOT standards, but is approved for shipments of less hazardous materials and limited quantities. The shipper (Client or SwRI) is responsible for determining the shipping name. The shipper must also ascertain the hazard class, United Nations Identification number (if required), labels, packaging requirements, and quantity limitations.

7.2.3 If the packaging requirement for the sample is not clear from the codes referenced above, consult with the following administrations for further guidance:

7.2.3.1 Research and Special Programs Administration (RSPA). Responsible for container manufacturers, reconditioners, and retesters and shares authority over shippers of hazardous materials.

7.2.3.2 Federal Highway Administration (FHA). Enforces all regulations pertaining to motor carriers.

7.2.3.3 Federal Railroad Administration (FRA). Enforces all regulations pertaining to rail carriers.

7.2.3.4 Federal Aviation Administration (FAA). Enforces all regulations pertaining to air carriers.

7.2.3.5 Coast Guard. Enforces all regulations pertaining to shipments by water.

7.3 Sample Container – Client’s Responsibility

7.3.1 Depending on the chemical sensitivity of the sample, care should be taken to choose an appropriate working environment that will enable the sample to be handled safely and that will ensure that it is not contaminated. Therefore, the following steps will most typically be performed in an inert, dry environment such as an argon atmosphere glove box.

7.3.2 Weigh and record the sample aliquot to be shipped for analysis under an inert and dry atmosphere.

7.3.3 Transfer the sample aliquot to an appropriate glass, flame-seal or septum screw-top vial and seal in the manner specified for the sample container. In some instances, it may be necessary or desirable to have set up a vacuum manifold that can be configured to evacuate the sample and purge it with nitrogen or argon over several cycles prior to sealing the sample container.

7.3.4 Apply a label to the sample container written or typed with indelible ink that clearly indicates the sample identification, the weight contained, and the date packaged, along with other pertinent information as deemed appropriate (*e.g.*, lot number and date prepared).

7.4 Sample Submittal Form – Client’s Responsibility

7.4.1 Before a sample is packaged and shipped, a Sample Submittal Form must be prepared and transmitted to SwRI for authorization. This step will ensure that SwRI staff are aware of the shipment and can be available to accept custody of it. The form is contained in the Appendix of this SOP. Note that the form must include the attachments indicated on it.

7.4.2 Enter as many fields of the Sample Submittal Form as information is available and transmit the form via facsimile or electronic mail using the following information:

Facsimile Number: 210.522.6220

e-Mail: mmiller@swri.org

7.4.3 After transmitting the form, a return authorization number and a suggested shipping date shall be assigned by SwRI and transmitted to Client by facsimile or e-mail. This authorization number must be assigned to Client’s request before sample is shipped.

7.4.4 A copy of the return authorization shall be retained for Client’s records and an exact duplicate shall be placed in the shipping package (serves as original manifest).

- 7.4.5 Once a return authorization has been received from SwRI along with a suggested shipping date, the sample container shall be packaged and shipped in accordance with the requirements established in 7.2. The following physical address and contact information shall be used to ship samples:

Southwest Research Institute
National Testing Laboratory for
Solid-State Hydrogen Storage Technologies

Building 90

6220 Culebra Road

San Antonio, TX 78238-5166

Attn: Michael A. Miller

7.5 Return Authorization of Sample Submittal Form – SwRI’s Responsibility

- 7.5.1 Sample Submittal Forms received from Client shall be reviewed and a schedule shall be assigned to the request indicating the approximate start and completion dates of the analyses.
- 7.5.2 A return authorization number shall be assigned to the Sample Submittal Form along with a suggested shipping date and the form shall be transmitted to Client.

7.6 Sample Login and Storage Procedures

- 7.6.1 Client-supplied samples shall be logged into a central Sample Control Record.
- 7.6.2 Client-supplied items shall be identified from the initial receipt inspection up to and including sample analysis and disposition (disposal or return of sample to client).
- 7.6.3 The sample shall be given a unique SwRI control number, which will be located on the sample container to provide traceability between the item and applicable documentation. This control number along with the date of sample receipt, the original Client-provided identifiers, and the quantities received shall be entered into the Sample Control Record.
- 7.6.4 Once entered into the Sample Control Record, a sample receipt confirmation shall be transmitted to Client.
- 7.6.5 A dry, inert storage locker shall be used for sample storage. This locker shall be periodically purged with dry helium to remove air and shall contain an appropriate quantity of desiccant to maintain moisture levels below 1 ppm.
- 7.6.6 Following sample login, labeled sample containers shall be immediately placed in a designated area of the dry storage locker. The locker must be purged with laboratory-

supplied dry helium upon opening and closing the doors providing access to the designated storage areas.

7.7 Chain of Custody Procedure

- 7.7.1 Sample containers removed from storage for complete or partial analysis shall be logged-out of the Sample Control Record.
- 7.7.2 The date and time a sample container is removed from storage and the person who takes custody of the sample shall be entered into the log.
- 7.7.3 Any mass aliquot of sample removed from a sample container for analysis shall be indicated in the Sample Control Record.
- 7.7.4 The date and time the original sample container is returned to storage shall be entered into the log.

SwRI® National Testing Laboratory for Solid-State Hydrogen Storage Technologies

Sample Submittal Form

Client Information

Contact Name:

Organization:

Address:

Phone:

Fax:

DOE Contract Number
(If Applicable)

Sample Information (Attach MSDS)

Sample ID	Chemical Classification / Chemical Formula	Activation State	Amount	Analyses and Conditions Required

SwRI Authorization No.:

Date:

SwRI Signature:

Revision Number	Effective Date	Description of Changes
0	5/20/05	Initial Revision.

Standard Operating Procedure

Volumetric Analysis

Document No. 05064-0010

Rev. 1

Prepared By:

Michael A. Miller, Manager-R&D

Date: 02/06/2006

Approved By:

Date: _____

1. PURPOSE

- 1.1 To provide a standard procedure by which the uptake (adsorption or absorption) and release (desorption) of hydrogen in solid-state materials can be quantitatively determined under precisely known thermodynamic conditions of temperature and pressure using a volumetric-monometry technique.
- 1.2 To derive intrinsic sorption properties of solid-state materials (test samples) from the uptake and release of hydrogen under precisely known thermodynamic conditions, which include: 1) the uptake capacity; 2) the kinetics associated with the uptake and release of hydrogen; 3) the hysteresis, if any, between the isothermal uptake and release cycle; and, 4) the sorption enthalpy.

2. SCOPE

- 2.1 Quantify the sorption properties of the sample, as noted above, using a high-pressure volumetric analyzer (Sieverts apparatus) in accordance with the following analytical requirements:
 - 2.1.1 Calibrate to determine free volume (void volume) of the system and sample volume.
 - 2.1.2 Calibrate to correct isotherm sorption curves for the effects of temperature gradients between the gas dosing reservoirs of the instrument and the sample.
 - 2.1.3 Ensure that measurements are accurate and precise based upon reference standards.
- 2.2 This procedure assumes that the sample has undergone the necessary process steps to activate its chemical activity for hydrogen sorption in accordance with the requirements of the material. Should the sample require activation in accordance with the general procedure established under the present testing facility, SwRI Document No. 05064-0006 may be used for this purpose.

3. RESPONSIBILITIES

- 3.1 It is the responsibility of the Technical Manager to train the appropriate technical staff and certify competency in the procedures of this protocol and to make certain trained technical staff are following this procedure properly.
- 3.2 It is the responsibility of the trained technical staff to comply with this procedure when conducting laboratory studies.

4. REFERENCES

- 4.1 Puziy, A. M.; Herbst, A.; Poddubnaya, J.G.; and Harting, P., *Langmuir* **2003**, *19*, 314-320.
- 4.2 Rangarajan, B.; Lira, C.T.; Subramanian, R. *AIChE J.* **1995**, *41*, 838.
- 4.3 Benedict, M.; Webb, G.B.; Rubin, L.C. *J. Chem. Phys.* **1940**, *8*, 334.
- 4.4 Sircar, S. *AIChE J.* **2001**, *47*, 1169.

5. SAMPLES AND STANDARDS

- 5.1 Samples and standards will remain stored until time of analysis. The conditions under which the samples are stored are chosen based upon the class of material being evaluated. SwRI Document No. 05064-0007 will be followed to conform to the proper login, storage, and chain of custody of samples. At the time of analysis, samples will be handled in accordance with the procedures of this document.

6. EQUIPMENT

- 6.1 Volumetric analyzer (Hy-Energy, LLC, Model PCTPro-2000), all stainless-steel construction of tubing and reaction vessel, containing five reservoirs of calibrated volumes. Entire system is compatible to pressures ranging UHV to 200 bar. Schematic of system is shown in Scheme 1.
- 6.2 Gas inlets for hydrogen and helium are connected to the UHP manifold, which is terminated at the instrument's gas inlets by a point-of-use purifier for each gas.
- 6.3 Quadrupole mass spectrometer (QMS, Pfeiffer Model Omnistar) interfaced with gas sampling system (Model GSS-300). One gas inlet channel (heated) of gas sampling system is dedicated to a high-pressure sampling interface for the reaction vessel of the volumetric analyzer.
- 6.4 High-pressure mass spectrometer capillary interface for volumetric analyzer, consisting of dual, electrically actuated rotary valves of very low dead volume and capillary tubing interconnections. Interface system including rotary valves is thermally controlled.
- 6.5 Microbalance (Mettler-Toledo, Model UMX-2), 0.1 μg mass resolution, located inside sample activation glove box of laboratory facility.
- 6.6 Sample activation glove box.
- 6.7 Stainless steel, high-pressure reaction vessel for sample analysis, configured with an isolation valve and thermocouple well.
- 6.8 Stainless steel tweezers.
- 6.9 Stainless steel scoopula.
- 6.10 Aluminum weighing boats.
- 6.11 Stainless steel or sapphire sample inserts for the sample vessel of gravimetric analyzer (used to contain sample around thermocouple well of sample vessel, and to remove dead volume below sample).
- 6.12 Stainless steel extraction tool for sample inserts.
- 6.13 Stainless steel or sapphire spacers for the sample vessel of volumetric analyzer (used to remove dead volume above sample inserts).
- 6.14 Polished, stainless steel compaction tool (used to mechanically compact sample in sample insert or to make a compressed pellet of sample).

6.15 Fritted, stainless steel VCR gaskets (0.25 and 0.5 inch).

7. REAGENTS AND MATERIALS

7.1 Reference Standards

- 7.1.1 Silicon (Si), 99.999%, shards, cubes, or rod.
- 7.1.2 Germanium (Ge), 99.999%, shards, cubes, or rod.
- 7.1.3 Vanadium Hydride (VH₂), 99.998%, fine powder of known BET surface area.
- 7.1.4 Palladium Hydride (PdH_{0.6}), 99.998%, fine powder of known BET surface area.
- 7.1.5 Magnesium Hydride (MgH₂), 99.998%, fine powder of known BET surface area.
- 7.1.6 Titanium Hydride (TiH₂), 99.998%, fine powder of known BET surface area.
- 7.1.7 Calibrated leaks, hydrogen, 99.9998%, of predetermined leak rate.
- 7.1.8 Mass calibration leak.
- 7.1.9 All standards must be accompanied by a Certificate of Analysis (COA).

7.2 Source Gases

- 7.2.1 UHP hydrogen (from central gas manifold), < 1ppb of contaminant species, including water, oxygen, carbon monoxide, and carbon dioxide.
- 7.2.2 UHP helium (from central gas manifold), < 1ppb of contaminant species, including water, oxygen, carbon monoxide, and carbon dioxide.
- 7.2.3 UHP deuterium (D₂), < 1ppb of contaminant species, including water, oxygen, carbon monoxide, and carbon dioxide. Lecture bottle attached to auxiliary inlet tee at helium gas inlet of instrument.

8. PROCEDURE

- 8.1 Refer to SwRI Document No. 05064-0008 for proper procedures on weighing samples and materials.
- 8.2 Verify that the environment in the sample activation glove box is below the maximum moisture and oxygen level requirements of operation as described in SwRI Document No. 05064-0007.
- 8.3 Weigh-out a predetermined amount of each sample and reference standard(s) as needed into aluminum weighing boats using the UMX-2 microbalance located inside the sample activation glove box. Record the initial weight of each sample and enter value into the appropriate Laboratory Record Book (LRB).
- 8.4 Weigh the reference material into an aluminum boat using the UMX-2 microbalance located inside the sample activation glove box. Record the initial weight and enter into LRB.
- 8.5 Select an appropriately sized sample insert for the compacted volume of sample, and the correct number of spacers to fill the dead space above the sample. Place empty sample

insert and spacers inside the sample vessel, making certain that top-most spacer is nearly level with the rim of the VCR fitting on the sample vessel.

8.6 Assemble sample vessel by attaching the VCR fitting of the manual valve to the vessel using a fritted VCR gasket, then applying an appropriate amount of torque to the fitting.

8.7 Helium Purge and Evacuation of Volumetric Analyzer

8.7.1 Transfer a clean, empty sample vessel, including the sample insert and spacers, out of the sample activation glove box in accordance with SwRI Document No. 05064-0007 (Test Article Login/Storage and Chain of Custody), making certain that the isolation valve attached to the vessel is in the fully closed position.

8.7.2 Connect the clean, empty sample vessel to the sample port connection point (VCR fitting) of the volumetric analyzer. Use a new fritted (0.2 μm) gasket to make connection and tighten fitting to the required torque as specified in the instrument manual.

8.7.3 Initiate helium purge/vacuum cycles of instrument's internal reservoirs, tubing, and sample vessel as described in the instrument manual.

8.7.4 Following completion of the initial purge/vacuum cycles, open the manual valve of the sample vessel and begin to elevate the temperature of the vessel to 200°C using a ramp rate $\leq 5^\circ/\text{min}$. Note: Refer to Section 8.12.2 for instructions on heating the sample vessel.

8.7.5 While the temperature of the vessel is approaching its set point, initiate a second sequence of purge/vacuum cycles.

8.7.6 After the first helium purge/vacuum cycle of the second sequence is complete, open electro-pneumatic micro-valve at the tee of the MS interface (above the isolation valve) and activate MS interface to begin sampling, monitoring, and recording gas composition using the Omnistar/GSS QMS. Use the multiple scan-analog mode of the QMS for this procedure, setting the scan range to full width (m/z 0 to 200 amu). Enter filename of acquisition sequence into the LRB.

8.7.7 At a convenient point after helium purge/vacuum cycles, close the electro-pneumatic micro-valve at the tee of the MS interface and stop acquiring QMS spectra (closes acquisition file).

8.7.8 Change scan range on the QMS to monitor peaks between 0 and 50 amu, then re-start acquiring QMS spectra without recording to a file.

8.7.9 Monitor spectra until it is apparent that steady-state background levels have been achieved. Stop acquisitions and reset scan range to full width.

8.7.10 Acquire, and record to a new file, at least five averaged scans of background spectra. Enter filename of background acquisition into the LRB.

8.7.11 Recall the acquisition sequences by filename using the spectrum reprocessing module of the computer acquisition system. Analyze the acquired spectra according to the following general procedure:

8.7.11.1 Subtract the background spectrum from the helium spectra, then save subtracted spectra to new files. Enter filenames into the LRB.

8.7.11.2 Integrate subtracted helium spectra over the entire mass range. Enter values into LRB.

8.7.11.3 Integrate only the helium peak of each subtracted helium spectrum. Enter values into LRB.

- 8.7.11.4 Divide the integration values entered for the helium peak of the subtracted helium spectra by the integration values for the full spectrum of the same. Enter values into LRB.
- 8.7.11.5 Compare the integration ratios entered above to those previously determined for the analysis of gases in the UHP manifold. Refer to protocol SwRI 05064-0003 for the analysis of gases in the UHP manifold.
- 8.7.12 Continue purge/vacuum cycles while monitoring gas composition with the QMS until helium gas purity is greater than or equal to the UHP manifold source gas requirements for helium (internally purified UHP manifold gas). Note: Source gas from tube trailer is lower in purity than the internally purified UHP manifold gas.
- 8.7.13 Close electro-pneumatic micro-valve at the tee of the MS interface and de-activate MS interface.
- 8.7.14 Evacuate the sample vessel and allow pressure to equilibrate to vacuum base pressure ($\leq 5 \times 10^{-5}$ torr).
- 8.7.15 Allow the sample vessel to cool to 25°C while under vacuum.

8.8 Absolute Calibration of QMS

- 8.8.1 Open valve to calibrated leak and permit hydrogen to leak into the capillary inlet of MS interface. Electro-pneumatic valve at tee of the MS interface must be closed before opening valve to calibrated leak.
- 8.8.2 Acquire and record multiple scans in the scan-analog mode (m/z ranging 0 to 5 amu) to calibrate hydrogen signal intensity at a constant leak rate. Enter leak rate (ϕ = mol/sec) of gas calibrator and acquisition filename into the LRB.
- 8.8.3 Close valve to calibrated leak.
- 8.8.4 After five minutes, acquire, and record to a new file, multiple scans to determine hydrogen background signal intensity generated from the MS interface. Enter filename into LRB.
- 8.8.5 Change acquisition mode of the MS to intensity versus time, monitoring molecular hydrogen (m/z = 2) and setting the total number of acquisition cycles to ≥ 100 .
- 8.8.6 Acquire, and record to a new file, intensity versus time data for approximately half the number of total acquisition cycles. Enter filename into LRB.
- 8.8.7 Open valve to calibrated leak and permit hydrogen to leak into the capillary inlet of the MS interface.
- 8.8.8 Continue to acquire and record intensity versus time data for the remainder of the acquisition cycles.
- 8.8.9 Close valve to calibrated leak and deactivate MS interface.
- 8.8.10 Recall the calibration sequences by filename using the spectrum reprocessing module of the computer acquisition system. Analyze the acquired spectra according to the following general procedure:
 - 8.8.10.1 Subtract the background spectrum from the hydrogen scan-analog spectra, then save subtracted spectra to new files. Enter filenames into the LRB.

- 8.8.10.2 Integrate the hydrogen peak for the molecular ion ($m/z = 2$) from each subtracted hydrogen spectrum. Enter integration values (A_{H_2}) into LRB.
- 8.8.10.3 Calculate a response factor (R_{fsa}) from the integration values of the subtracted spectra as follows: $R_{fsa} = \phi \text{ (mol/sec)} / A_{H_2} \text{ (Int.}\cdot\text{amu)}$. Enter values into LRB.
- 8.8.10.4 Recall the calibration files for the intensity vs. time scans.
- 8.8.10.5 Calculate the average signal intensity (I_{lk}) from the flat region of the profile at which time the calibrated leak was turned on. Enter the average value into the LRB.
- 8.8.10.6 Calculate the average signal intensity (I_{bkg}) from the flat region of the profile at which time the calibrated leak was turned off. Enter the average value into the LRB.
- 8.8.10.7 Calculate a response factor (R_{fit}) from the two average signal intensities as follows: $R_{fit} = \phi \text{ (mol/sec)} / [I_{lk} - I_{bkg}]$. Enter values into LRB.

8.9 Hydrogen Purge and Evacuation of Volumetric Analyzer

- 8.9.1 Close manual valve to sample vessel.
- 8.9.2 Initiate hydrogen purge/vacuum cycles of instrument's internal reservoirs and tubing, but not the sample vessel, as described in the instrument manual. Last sequence must leave internal reservoirs and tubing in an evacuated state.
- 8.9.3 After completing the hydrogen purge/vacuum sequence, program analyzer to set initial pressure of sample to 1 bar of hydrogen while leaving manual valve to sample vessel in the closed position. This procedure will effectively deliver gas to the MS interface valve for sampling, while maintaining the sample vessel isolated from the system.
- 8.9.4 Open the electro-pneumatic micro-valve at the tee of the MS interface and activate MS interface to begin sampling, monitoring, and recording gas composition using the Omnistar/GSS QMS. Use the multiple scan-analog mode of the QMS for this procedure, setting the scan range to full width (m/z 0 to 200 amu). Enter filename of acquisition sequence into the LRB.
- 8.9.5 Repeat steps 8.5.7 through 8.5.14, replacing helium with hydrogen where indicated.

8.10 Determination of Intrinsic Hydrogen (Optional)

- 8.10.1 Evacuate the sample vessel and allow pressure to equilibrate to vacuum base pressure.
- 8.10.2 Allow sample vessel to equilibrate to 25°C while under vacuum.
- 8.10.3 Isolate helium supply line to instrument helium gas inlet at valve Y-54 (manual valve immediately after gas purifier).
- 8.10.4 Evacuate the helium manifold of the instrument's internal gas delivery system starting from valve Y-54 (in the closed position) and allow system to equilibrate to the vacuum base pressure.
- 8.10.5 Open manual valve at helium inlet tee to deuterium cylinder and continue evacuation until vacuum base pressure is achieved.
- 8.10.6 Open valve to deuterium cylinder to pressurize system.
- 8.10.7 Dose the sample vessel with approximately 1 atm of deuterium, then close valve at helium inlet tee to deuterium cylinder.

- 8.10.8 Activate MS interface, then acquire, and record to a new file, multiple scan-analog spectra to analyze the background gas composition in the sample vessel, then deactivate MS interface. Enter background filename into the LRB.
- 8.10.9 Open the micro-valve at the tee of the MS interface. Activate MS interface, then acquire, and record to a new file, multiple scan-analog spectra to analyze gas composition in the sample vessel, then deactivate MS interface. Enter filename into the LRB.
- 8.10.10 Raise temperature of sample vessel to 200°C and allow pressure, and temperature to equilibrate. Note: Refer to Section 8.12.2 for instructions on heating the sample vessel.
- 8.10.11 Activate MS interface, then acquire, and record to a new file, multiple scan-analog spectra to analyze deuterium exchange in the reaction vessel, monitoring the signal intensity of $m/z = 2, 3, 4, 18, 19,$ and 20 amu. Enter filename into the LRB.
- 8.10.12 Recall the acquisition sequences by filename using the spectrum reprocessing module of the computer acquisition system. Analyze the acquired spectra according to the following general procedure:
- 8.10.12.1 Subtract the background spectrum from the deuterium spectra, then save subtracted spectra to new files. Enter filenames into the LRB.
- 8.10.12.2 Integrate subtracted deuterium spectra over the entire mass range. Enter values into the LRB.
- 8.10.12.3 Integrate the deuterium peak for the molecular ion (D_2 , $m/z = 4$ amu) of each subtracted deuterium spectrum. Enter values into the LRB.
- 8.10.12.4 Divide the integration values entered for the deuterium peak of the subtracted deuterium spectra by the integration values for the full spectrum of the same. Enter values into the LRB.
- 8.10.12.5 Integrate the HD peak ($m/z = 3$ amu), if present, of each subtracted deuterium spectrum. Enter values into LRB.
- 8.10.12.6 Integrate the D_2O ($m/z = 20$ amu) and HDO ($m/z = 19$) peaks, combined, of each subtracted deuterium spectrum. Enter values into the LRB.
- 8.10.12.7 Divide the integration values entered for each of the deuterium-exchanged ions by the integration values for the full spectrum of the same. Enter values into the LRB
- 8.10.13 Open helium supply line to instrument helium gas inlet at valve Y-54.
- 8.10.14 Initiate helium purge/vacuum cycles of instrument's internal reservoirs, tubing, and sample vessel as described in the instrument manual.
- 8.10.15 Cool the sample vessel to 25°C while under helium purge.
- 8.11 Vessel and Sample Void Volume (Helium Calibration)
- 8.11.1 This procedure may be conducted before or after PCT measurements of sample in hydrogen (see Section 8.12).
- 8.11.2 Program instrument parameters, as described in the instrument manual, to execute a helium volume determination of the empty sample vessel (V^e), including the sample insert and spacers, and perform this measurement at 25°C. Make at least four replicate measurements of the empty volume, each measured by an adsorption and desorption cycle. Enter the average value and standard deviation (SD) of V^e into the LRB.

8.11.3 Isolate sample vessel at manual valve (valve in closed position), then loosen and disconnect the vessel from its connection fitting.

8.11.4 Transfer the sample vessel to the sample activation glove box.

8.11.5 Sample Loading

8.11.5.1 Verify that the glove box environment is below the maximum moisture and oxygen level requirements of operation as described in SwRI Document No. 05064-0007.

8.11.5.2 Loosen and remove top fitting plus manual valve of sample vessel to gain access to the internal volume.

8.11.5.3 Extract the spacers and sample insert from the vessel.

8.11.5.4 Carefully transfer sample to be evaluated from the pre-weighed boat to the sample insert until approximately half of the insert volume remains.

8.11.5.5 Reweigh sample boat and enter value into the LRB.

8.11.5.6 Compact the sample in the insert using the polished end of the compaction tool. Alternatively, make a compacted pellet from the sample using a pelletizing tool, weight the pellet, and then place it in the sample insert. (Note: It is important that the free volume of the system, which is the interstitial volume of the sample plus the dead volume above the sample in the sample vessel, be minimized as much as possible so that the free-to-sample volume ratio determined in step 8.11.8 is also small. This step to compact or pelletize the sample plus the addition of spacers above the sample insert is done to minimize the ratio. However, it is also important to ensure that the compaction forces used in this step are not so great that the microstructure of the sample is inadvertently damaged).

8.11.5.7 Repeat steps 8.11.5.4 – 8.11.5.6 until the entire volume of the sample insert is filled with compacted sample. Obtain a final weight of the sample boat and enter value into the LRB.

8.11.5.8 Replace spacers over top of sample, making certain that top-most spacer is nearly level with the rim of the VCR fitting on the sample vessel.

8.11.5.9 Reassemble top fitting with a new, fritted VCR gasket, secure and tighten the fitting to the required torque as specified in the instrument manual. Make certain manual valve is in the closed position.

8.11.5.10 Transfer the loaded sample vessel out of the sample activation glove box, and then mount the vessel to the sample port connection point (VCR fitting) of the analyzer. Use a new fritted (0.2 μm) gasket to make connection and tighten fitting to the required torque as specified in the instrument manual.

8.11.5.11 *Sample Drying and Conditioning.* (Note: Proceed with the following steps only if sample requires further drying, conditioning, or dehydriding, or if the intent of the experiment is to evaluate hydrogen uptake from a dehydridated state):

8.11.5.11.1 Slip heating jacket over copper sleeve of sample vessel, fasten snugly, and then insert sample thermocouple (TC) into the TC well at bottom of sample vessel. Connect power line of heating jacket to the temperature controller.

8.11.5.11.2 Insert control and limit TCs into opposing cavities at top (or bottom) of the copper sleeve of sample vessel. Connect TCs to the corresponding receptacles on the temperature controller.

- 8.11.5.11.3 Program temperature controller to ramp at a rate not to exceed 10°/min. Set the thermal soak such that the highest soak temperature set-point is below the onset of thermal decomposition of sample, and does not exceed 400°C.
- 8.11.5.11.4 Initiate a sample and reservoir evacuation sequence at the instrument, as described in the manual of the analyzer, and set evacuation time to not less than 480 min. Note: The actual evacuation and heating time will depend on the specific conditions of the sample.
- 8.11.5.11.5 Initiate thermal ramp. Make certain manual valve on the sample vessel is in the open position.
- 8.11.5.11.6 Open manual micro-valve at the tee of the MS interface (Optional).
- 8.11.5.11.7 Activate MS interface, then acquire, and record to a file, multiple scan-analog spectra to analyze and monitor degas composition of the sample in the reaction vessel (Optional). Enter filename into the LRB.
- 8.11.5.11.8 Continue evacuating the sample until equilibrium vacuum base pressure is achieved ($\leq 5 \times 10^{-5}$ torr).
- 8.11.5.11.9 Deactivate MS interface and close manual micro-valve to the MS interface (Optional).
- 8.11.5.11.10 Enter into the LRB the total conditioning time, temperature, and final base pressure to which the sample was subjected.
- 8.11.6 Cool the reaction vessel and sample to 25°C.
- 8.11.7 Program instrument parameters, as described in the instrument manual, to execute helium volume determination of the loaded sample vessel at 25°C. Make at least four replicate measurements of the void volume (V^0), each measured by an adsorption and desorption cycle. Enter average value and SD of V^0 into the LRB.
- 8.11.8 Calculate the free-to-sample volume ratio (V_s^0) as follows: $V_s^0 = V^0/(V^e - V^0)$. Enter value into the LRB.
- 8.11.9 Upon completion of the helium calibration, initiate evacuation cycle of sample vessel.
- 8.11.10 Heat the sample vessel to 50°C while evacuating the sample vessel and allow pressure to equilibrate to vacuum base pressure ($\leq 5 \times 10^{-5}$ torr). This procedure should be done for not less than 1 hour.
- 8.11.11 Cool the sample vessel to 25°C while under vacuum.
- 8.12 Pressure-Composition-Isotherm (PCT) Measurements of Sample
- 8.12.1 A minimum of three (3) replicate PCT measurements must be performed on each sample. **Important:** Additional replicate runs should be performed as necessary in order to ensure that the sorption behavior of the sample reaches steady-state and, thereby, the isotherm curves are repeatable.
- 8.12.2 Program instrument parameters, as described in the instrument manual, to execute PCT measurements for hydrogen in either the forward or reverse direction, or both, of the desired pressure path and the desired temperature (isothermal) regime.

- 8.12.3 Proceed with the following steps if PCT experiments are to be done at greater than or equal to room temperature:
- 8.12.3.1 Ensure that manual valve on sample vessel is in the closed position.
 - 8.12.3.2 Slip heating jacket over copper sleeve of sample vessel, fasten snugly, and then insert sample thermocouple (TC) into the TC well at bottom of sample vessel. Connect power line of heating jacket to the temperature controller.
 - 8.12.3.3 Insert control and limit TCs into opposing cavities at top (or bottom) of the copper sleeve of sample vessel. Connect TCs to the corresponding receptacles on the temperature controller.
 - 8.12.3.4 Program temperature controller to ramp to the desired isothermal temperature of the PCT experiment at a rate not to exceed 10°/min.
 - 8.12.3.5 Allow the sample to reach thermal equilibrium as determined by the sample TC.
- 8.12.4 Proceed with the following steps if PCT experiment is to be done at 77 K:
- 8.12.4.1 Ensure that manual valve on sample vessel is in the closed position.
 - 8.12.4.2 Place a level mark, readily visible to the naked eye, 1 cm below the top edge of the copper sleeve of the sample vessel.
 - 8.12.4.3 Insert sample vessel in a double-wall glass dewar by elevating the dewar with a lab jack so that its rim is above the copper sleeve of the sample vessel and approximately even with the reduced neck of the manual valve (below the body of the valve).
 - 8.12.4.4 Insert sample TC into one of the cavities of the copper sleeve and secure tightly.
 - 8.12.4.5 Wrap polypropylene pipe insulation (or other high R-value flexible material) around body of manual valve so that the lower edge of the insulation extends down to the reduced neck of the sample vessel. Secure insulation tightly with plastic tie wraps.
 - 8.12.4.6 Initiate a sample evacuation sequence, setting the time long enough so that the internal tubing is under dynamic vacuum throughout the time that is required for the sample to reach thermal equilibrium at 77 K. (Note: This step is designed to prevent cryopumping and condensation of species in the section of tubing between the manual valve and the internal dosing valves).
 - 8.12.4.7 Begin filling the dewar with liquid nitrogen (LN₂) at a slow rate until thermal equilibrium is achieved.
 - 8.12.4.8 Adjust liquid level of LN₂ so that it remains parallel with the level mark on the copper sleeve.
 - 8.12.4.9 Cover the opening of the dewar using a removable insulation cap and adjust its position such that it surrounds the reduced neck of the sample vessel, mating with the lower edge of the insulation that was placed around the body of the manual valve.
 - 8.12.4.10 After the PCT experiment has been initiated (subsequent steps), the LN₂ level should be checked periodically and, if needed, carefully replenished to the level mark. Important: The first aliquot of gas delivered to a fully dehydrated sample will be the most exothermic, after which time the dewar will require attention to ensure that the LN₂ level is adjusted to the mark before subsequent gas aliquots. However, level adjustments should only be done when the instrument is filling a calibrated volume with a gas aliquot and not during the period in which the pressure is equilibrating after a gas aliquot has been delivered to, or from, the sample vessel.

- 8.12.5 At the MS computer console, program select times, if any, at which to activate the MS interface. Enter parameters to acquire and record multiple scan-analog spectra of the sample in the reaction vessel (Optional).
- 8.12.6 Initiate PCT run and activate MS interface for timed sequence if applicable.
- 8.12.7 Open manual micro-valve at the tee of the MS interface if applicable.
- 8.12.8 Continue PCT measurements for the remaining isotherms in conformance with the objectives of the experiment.
- 8.12.9 Record to file equilibrium pressures and temperatures for each isotherm and, if applicable, kinetics data. Enter filename into LRB.
- 8.12.10 Upon completion of all PCT measurements, initiate evacuation cycle of the sample vessel.
- 8.12.11 Isolate sample vessel at manual valve (valve in closed position), then loosen and disconnect the sample vessel from its connection fitting. Remove heating jacket or dewar, as applicable, and TCs before disconnecting the sample vessel.
- 8.12.12 Transfer the sample vessel to the sample activation glove box.
- 8.13 Thermal Gradient Correction for Low- or High Temperature PCT Experiments
- 8.13.1 Proceed with the following steps if the difference between the isothermal temperature of the desired PCT experiment and the internal calibration volumes is greater than or equal to 20°.
- 8.13.2 While the sample vessel is in the sample activation glove box, disassemble it and carefully extract the spacers and sample insert with the appropriate tools.
- 8.13.3 Carefully transfer the sample from the insert to a pre-labeled vial. Seal the vial and set it aside in the glove box.
- 8.13.4 Using the microbalance, tare a weighing boat and weigh a mass aliquot (m_s) of high purity silicon or germanium of known density (ρ_{cal}) that equates to the same volume as that of the test sample. The relationship is given by: $m_s = (V^e - V^0) \times \rho_{cal}$. Enter the aliquot mass (m_s) of this calibration sample into the LRB.
- 8.13.5 Transfer the aliquot to the sample insert and reassemble the vessel using the same spacers as were used for the sample and a new fritted VCR gasket.
- 8.13.6 Reweigh the empty boat and enter the empty weight (m_e) into the LRB. The actual volume (V^s) of the calibration sample transferred to the sample insert and its calculated void volume are given by: $V^s = (m_s - m_e) / \rho_{cal}$ and $(V^e - V^s)$, respectively.
- 8.13.7 Ensure that the manual valve on the sample vessel is in the closed position, remove the vessel from the glove box, and reconnect it to the sample vessel port using a new VCR gasket.
- 8.13.8 Initiate a sample evacuation sequence at the instrument, as described in the manual of the analyzer, and set evacuation time to not less than 30 min.
- 8.13.9 Repeat steps 8.11.1 and 8.11.2. Enter void volume and SD of calibration sample into the LRB.
- 8.13.10 Compare the measured void volume of the calibration sample with the calculated one from step 8.13.6. If the difference between the two values is significant (> 3% relative difference), repeat the void volume determination. If significant differences persist, repeat from step 8.13.1.

8.13.11 Initiate a sample evacuation sequence at the instrument, as described in the manual of the analyzer, and set evacuation time to not less than 30 min.

8.13.12 Repeat steps in section 8.12.

8.14 Data Processing

8.14.1 The actual uptake, or desorption, of hydrogen in the sample is determined from the apparent (measured) values by calculating the Gibbs excess for hydrogen. A simple equation of state (SEOS) derived from the helium calibration sequence for the sample is used by the analyzer to determine void volume (V^0) and a correction term from Henry's Law.

8.14.2 Gibbs Excess Simple Equation of State (SEOS)

The relationship between the gas densities measured by the instrument and the apparent Gibbs excess [4.1 – 4.3] can be described as follows:

$$\begin{aligned}
 V^C(\rho^C - \rho_a) - V^0 \rho_a &= V_{ad}(\rho_{ad} - \rho_b) \equiv G_{ex}^a \\
 V^C &= \text{Calibrated Volume} \\
 \rho^C &= \text{Density of Gas in Calibrated Volume} \\
 \rho_a &= \text{Apparent Gas Density} \\
 V^0 &= \text{Total Void Volume} \\
 V_{ad} &= \text{Volume of Adsorbed Phase} \\
 \rho_b &= \text{Density of Bulk - Phase Gas} \\
 \rho_{ad} &= \text{Density of Adsorbed Phase} \\
 G_{ex}^a &= \text{Apparent Gibbs Excess Adsorption}
 \end{aligned} \tag{1}$$

where the void volume of the sample and system from the helium calibration sequence is given by,

$$\begin{aligned}
 V^0 &= V^C \left(\frac{\rho_{He}^C - \rho_{He}}{\rho_{He}} \right) \\
 \rho_{He}^C &= \text{Density of Helium in Calibrated Volume} \\
 \rho_{He} &= \text{Final Density of Helium}
 \end{aligned} \tag{2}$$

The apparent Gibbs excess for hydrogen measured from the PCT experiment of the sample (Eq. 1) is corrected using the following equation:

$$G_{ex} = G_{ex}^a + \left(|m_{He}| \times P_s \times \frac{M_{H_2}}{M_{He}} \right)$$

G_{ex} = Gibbs Excess Adsorption
 m_{He} = Slope of Helium Isotherm (Henry's Constant)
 P_s = Pressure
 M = Molecular Weight

(3)

8.14.3 At a computer console in which the post-processing macro HydataAnalysis V1.1.7 resides, running under Igor[®] Pro, recall PCT acquisition data by filename, then make certain the instrument parameter entries (under Set Instrument Parameters) are properly set to: Instrument Low Pressure Limit = 5 bar; Displacement Volume of Valve 1 = 0.039 mL; and, Volume of Low Pressure Transducer = 3.58 mL.

8.14.4 Proceed with the following steps if the PCT experiment was done at low or high isothermal temperatures:

8.14.4.1 To account for the temperature gradient that arises when making sorption isotherm measurements above or below the regulated temperature of the calibrated dosing volumes, a temperature correction factor (C_f) is derived from the calibration experiments of Section 8.12, which measured the gradient effects on the free-volume gas space that resides between the dosing valve and the sample vessel. The effect is illustrated in Figure 1. This factor is used to correct the hydrogen sorption isotherm of the test sample. It is derived by adjusting the free volume of the calibration sample to the effective free volume according to the following relationship:

$$V_{s,eff} = \left[C_f \left(\frac{T_c}{T_s} - 1 \right) + 1 \right] \cdot V_s$$
(4)

where T_c and T_s are the isothermal temperatures of the calibrated volume and sample vessel, respectively, V_s is the actual free volume of the sample vessel, $V_{s,eff}$ is the effective free volume of the sample vessel, and C_f is a correction factor to be adjusted from the adsorption isotherm of the inert sample. The form of this equation as a function of sample temperature is illustrated in Figure 2 for different values of C_f and fixed temperature of the calibrated volume.

8.14.4.2 Recall the PCT data for the calibration sample, and then go to the “Recalculate PCT” dialogue to make interactive parameter adjustments of C_f , which is entered as the “ratio” parameter in this dialogue. (Note: Make certain that all other parameters appearing in this dialogue are set to their correct values according to the desired hardware and experiment parameters).

8.14.4.3 Interactively adjust the C_f parameter as a fractional constant such that the pressure versus concentration isotherm curve approaches a vertical line (i.e., slope approaches infinity), but not to such an extent that the calibration points for low pressures fall in the negative quadrant of the plot. For each adjustment, the temperature averaging parameter must be set to “yes”. Expand scale as necessary to determine where the intercept points fall with each adjustment. A typical example of the effect of this parameter adjustment is shown in Figure 3. Enter the final value of C_f into the LRB.

- 8.14.5 Recall the PCT data for the sample analysis, and then go to the “Recalculate PCT” dialogue. Enter the C_f parameter, if applicable, as the “ratio”, set temperature averaging to “yes”, and recalculate concentrations to obtain the corrected PCT isotherm. Save corrected isotherm values as a new file and then enter filename into the LRB.
- 8.14.6 Transfer numerical values of the corrected isotherms to a spreadsheet template for reporting and include isotherm plots as needed. Example of reporting format is shown in Figures 4 and 5.
- 8.14.7 Proceed with the following steps if sample material is of a type in which hydrogen uptake is dominated by physisorption (e.g., carbon materials).
- 8.14.7.1 Using a non-linear numerical fitting algorithm, fit the corrected data for the hydrogen adsorption isotherm of the sample to either the Langmuir or Langmuir-Freundlich model equations, or both, given by:

$$\theta_q = q_{sat} \left(\frac{K_q P_{eq}}{1 + K_q P_{eq}} \right) \quad \text{Langmuir} \quad (5)$$

$$\theta_q = q_{sat} \left(\frac{K_q P_{eq}^\beta}{1 + K_q P_{eq}^\beta} \right) \quad \text{Langmuir – Freundlich} \quad (6)$$

where θ_q is the hydrogen concentration for excess adsorption, q_{sat} is the saturation concentration, P_{eq} is the equilibrium pressure, K_q is the equilibrium constant for non-dissociative sorption, and β is a correction term used to account for the tortuosity of the material.

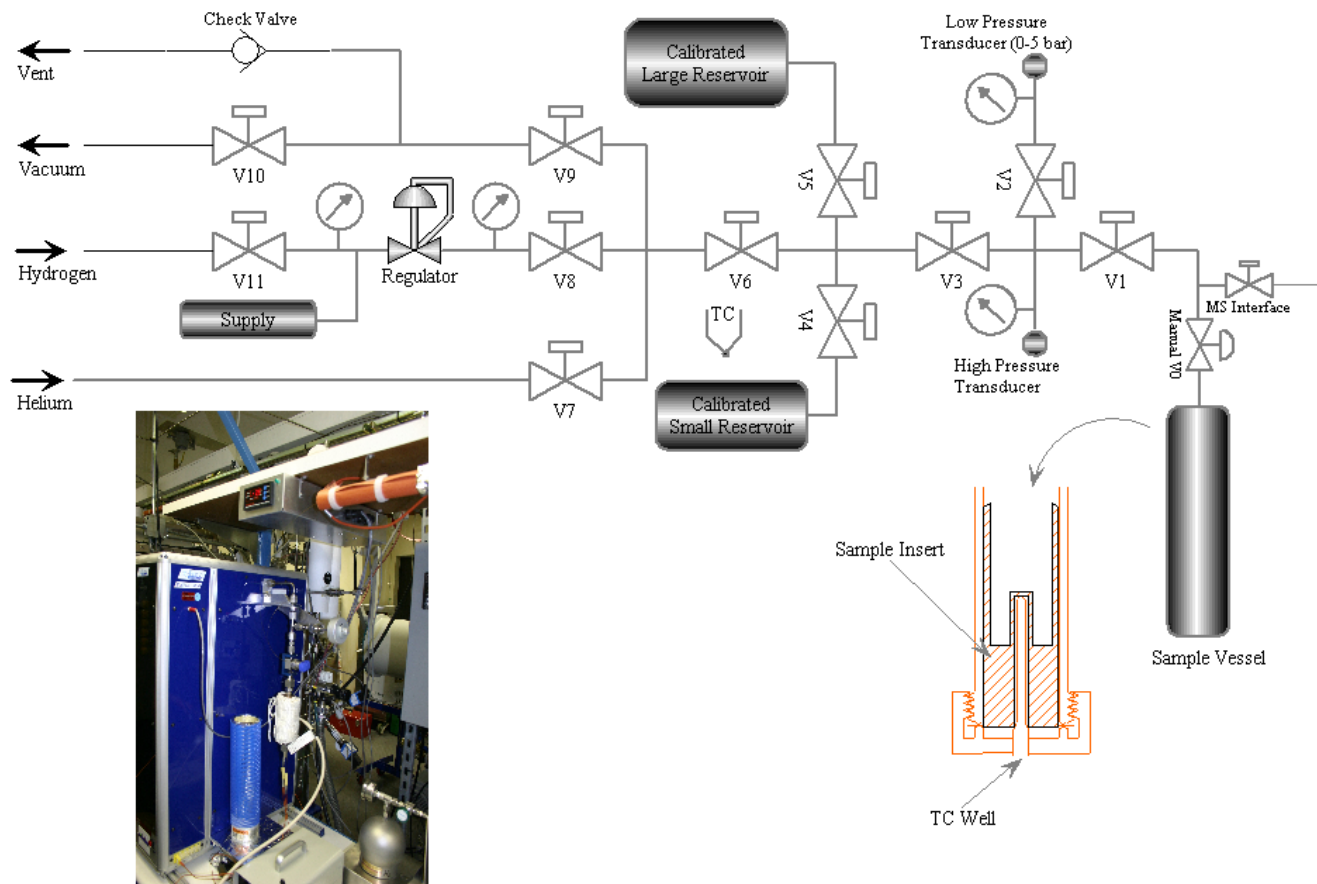
- 8.14.7.2 Transfer the predicted values to the spreadsheet template along with the parameter estimates and correlation coefficient (r^2). Replot both the measured and predicted values for reporting. Example plot is shown in Figure 6.

8.15 Determination of Accuracy and Precision (Reference Standards)

- 8.15.1 This procedure may be conducted at any time to check or verify the accuracy of volumetric measurement.
- 8.15.2 Evacuate residual gas from the sample vessel as needed.
- 8.15.3 Isolate sample vessel at manual valve (valve in closed position), then loosen and disconnect the vessel from its connection fitting.
- 8.15.4 Transfer the sample vessel to the sample activation glove box.
- 8.15.5 Verify that the glove box environment is below the maximum moisture and oxygen level requirements of operation as described in SwRI Document No. 05064-0007.
- 8.15.5.1 Loosen and remove top fitting plus manual valve of sample vessel to gain access to the internal volume.
- 8.15.5.2 Extract the spacers and sample insert from the vessel.

- 8.15.5.3 Select an appropriately sized sample insert for the compacted volume of the reference sample, and the correct number of spacers to fill the dead space above the reference sample. Place empty sample insert and spacers inside the sample vessel, making certain that top-most spacer is nearly level with the rim of the VCR fitting on the sample vessel.
- 8.15.5.4 Carefully transfer reference sample to be evaluated from the pre-weighed boat to the sample insert until approximately half of the insert volume remains.
- 8.15.5.5 Reweigh sample boat and enter value into the LRB.
- 8.15.6 Compact the reference sample in the insert using the polished end of the compaction tool. Alternatively, make a compacted pellet from the sample using a compact-pellet tool, weight the pellet, and then place it in the sample insert. (Note: It is important that the free volume of the system, which is the interstitial volume of the sample plus the dead volume above the sample in the sample vessel, be minimized as much as possible so that the free-to-sample volume ratio determined in step 8.11.8 is also small. This step to compact or pelletize the sample plus the addition of spacers above the sample insert is used to minimize the ratio. However, it is also important to ensure that the compaction forces used in this step are not so great that the microstructure of the sample is inadvertently damaged).
- 8.15.6.1 Repeat steps 8.15.5.4 – 8.15.5.6 until the entire volume of the sample insert is filled with compacted reference sample. Obtain a final weight of the sample boat and enter value into the LRB.
- 8.15.6.2 Replace spacers over top of sample, making certain that top-most spacer is nearly level with the rim of the VCR fitting on the sample vessel.
- 8.15.6.3 Reassemble top fitting with a new, fritted VCR gasket, secure and tighten the fitting to the required torque as specified in the instrument manual. Make certain manual valve is in the closed position.
- 8.15.7 Transfer the loaded sample vessel out of the sample activation glove box, and then mount the vessel to the sample port connection point (VCR fitting) of the analyzer. Use a new fritted (0.2 μm) gasket to make connection and tighten fitting to the required torque as specified in the instrument manual.
- 8.15.8 Repeat steps described in Section 8.11.5.11, and in 8.12 through 8.14.
- 8.15.9 Compare the hydrogen capacity measured for the reference standard to the known value and calculate the relative difference. Enter the measured and known values along with the percent relative difference into the LRB.
- 8.15.10 Plot the desorbed capacity measured for the reference standard and indicated known value. Example result is shown in Figure 7.
- 8.15.11 Repeat this procedure as necessary with additional reference standards.

Scheme 1. Schematic of high-pressure volumetric analyzer.



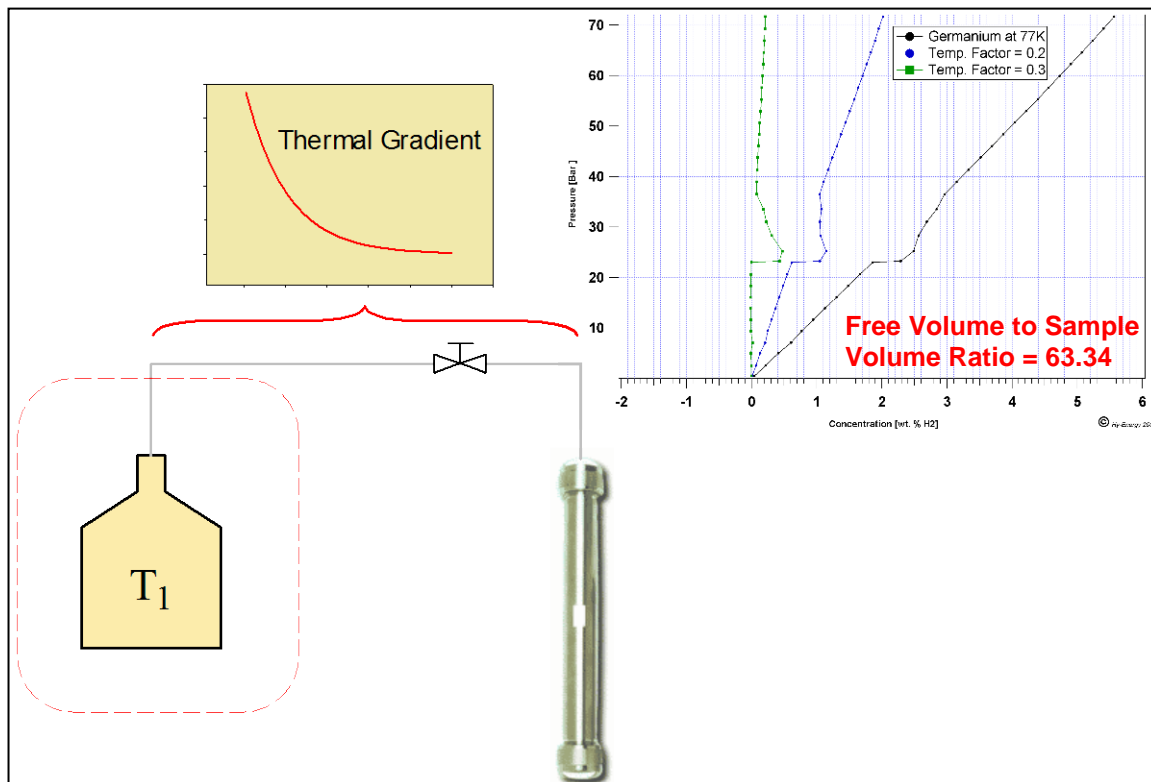


Figure 1. Illustration of the thermal gradient arising from the difference between the regulated temperature, T_1 , of the calibrated volume and that of the sample vessel. The free volume includes that which is contained in the sample vessel and the tubing connection between the valve of the calibrated volume and the sample vessel. Inset shows a typical calibration isotherm for an inert material (germanium in the present case) for the uncorrected data (black curve) and the effects of adjusting C_f (from Equation 4).

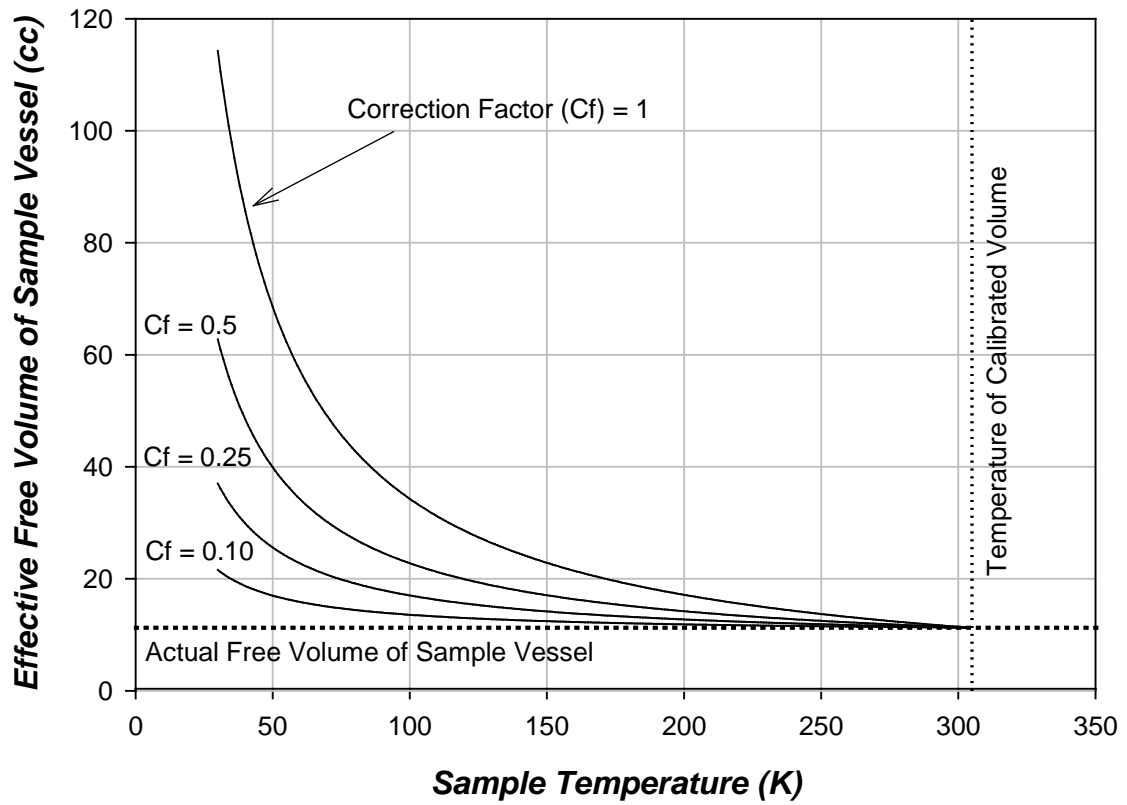
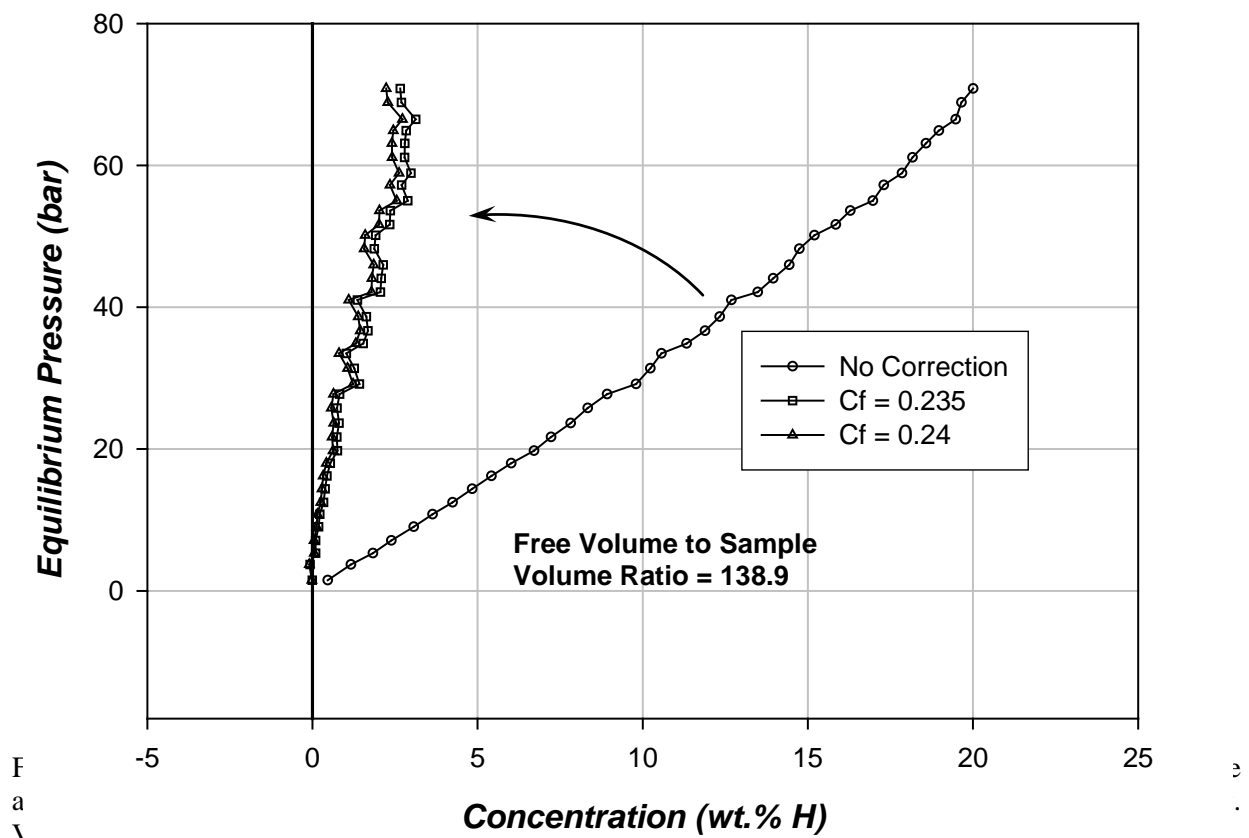


Figure 2. Dependence of the effective free volume of the sample vessel, $V_{s,eff}$, with sample temperature for different values of C_f . Reference lines indicate the actual free volume of the sample vessel (as determined by helium calibration below 5 bar) and the regulated (isothermal) temperature of the calibrated volume.

Silicon Temperature Correction at 77 K




 Southwest Research Institute					Equilibrium Pressure (bar)	Concentration (wt.% H)	Sample Temp. (C)
		Volumetric Analysis					
Sample Analysis		Adsorption Data			2.314	0.0305	25.8
Sample ID:	ABC123	Aliquot Mass for Measurement (mg):	414.869	4.148	0.0534	25.8	
Date Received:	6-May-2005	Void Volume (cc):	11.275	4.208	0.0542	25.8	
Amount Received (mg):	1354	Void Volume SD (cc):	0.0301	4.944	0.0631	25.8	
Total Mass After Equilibration in He Glovebox (mg):	1354	Measured Sample Volume (cc):	0.2066	6.303	0.0790	25.8	
		Apparent Sample Density (g/cc):	2.008	6.411	0.0803	25.8	
		Free-to-Sample Volume Ratio:	54.6	7.382	0.0913	25.8	
		Number of Test Runs:	3	8.861	0.1076	25.8	
		Temp. Factor (25C):	0.13	8.907	0.1081	25.8	
		Temp. Factor (-196C):	0.3	9.666	0.1163	25.8	
				11.318	0.1335	25.8	
				11.406	0.1344	25.8	
				12.071	0.1411	25.8	
				13.723	0.1574	25.8	
				13.785	0.1580	25.8	
				14.365	0.1636	25.8	
				16.082	0.1796	25.8	
				16.271	0.1813	25.8	
				16.691	0.1851	25.8	
				18.506	0.2012	25.8	
				18.611	0.2021	25.8	
				18.963	0.2052	25.8	
				20.810	0.2207	25.8	

Figure 4. Example of format for reporting numerical values of PCT results.

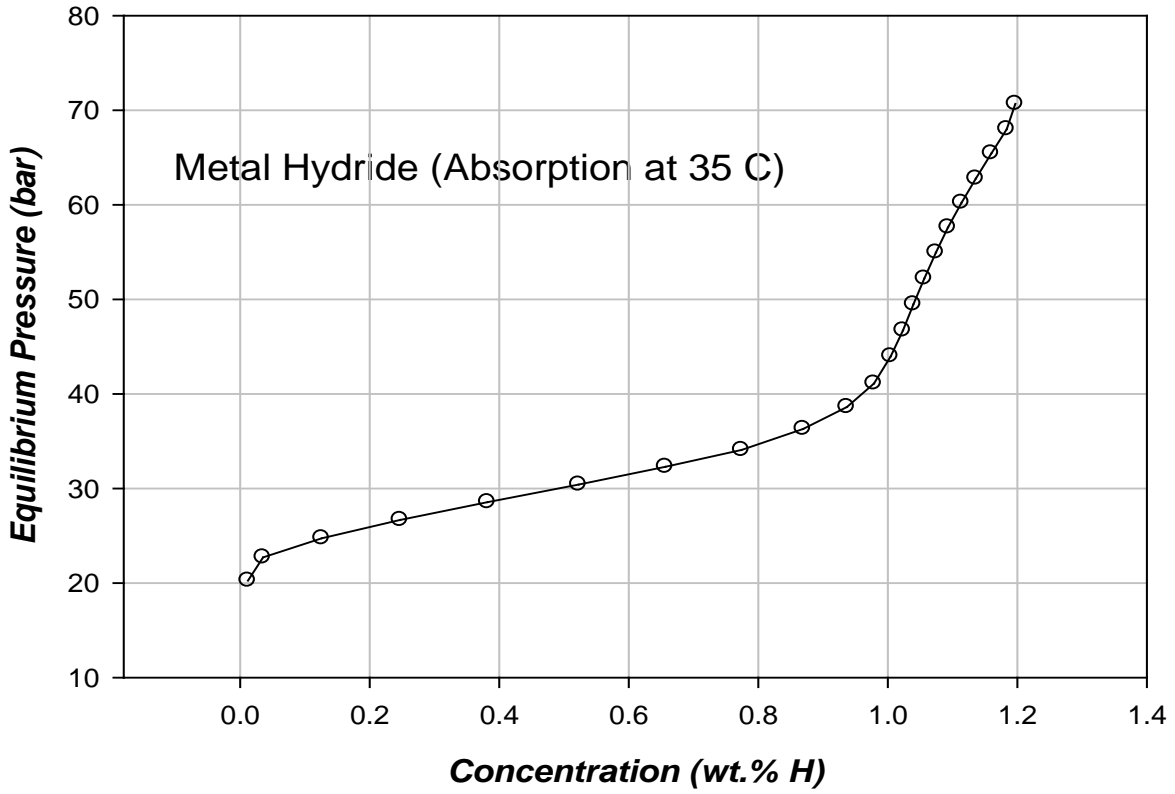


Figure 5. Example of reporting PCT isotherm plot for a metal hydride.

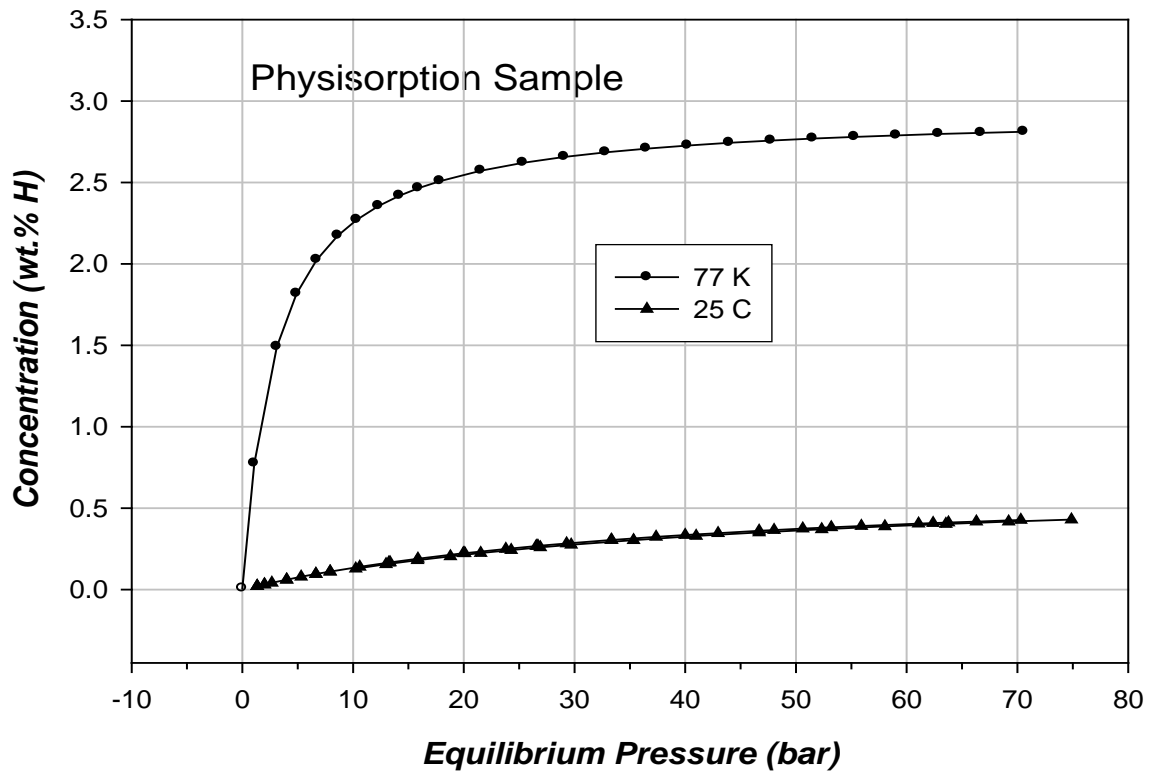


Figure 6. Example of reporting adsorption isotherm plots for a physisorption sample.

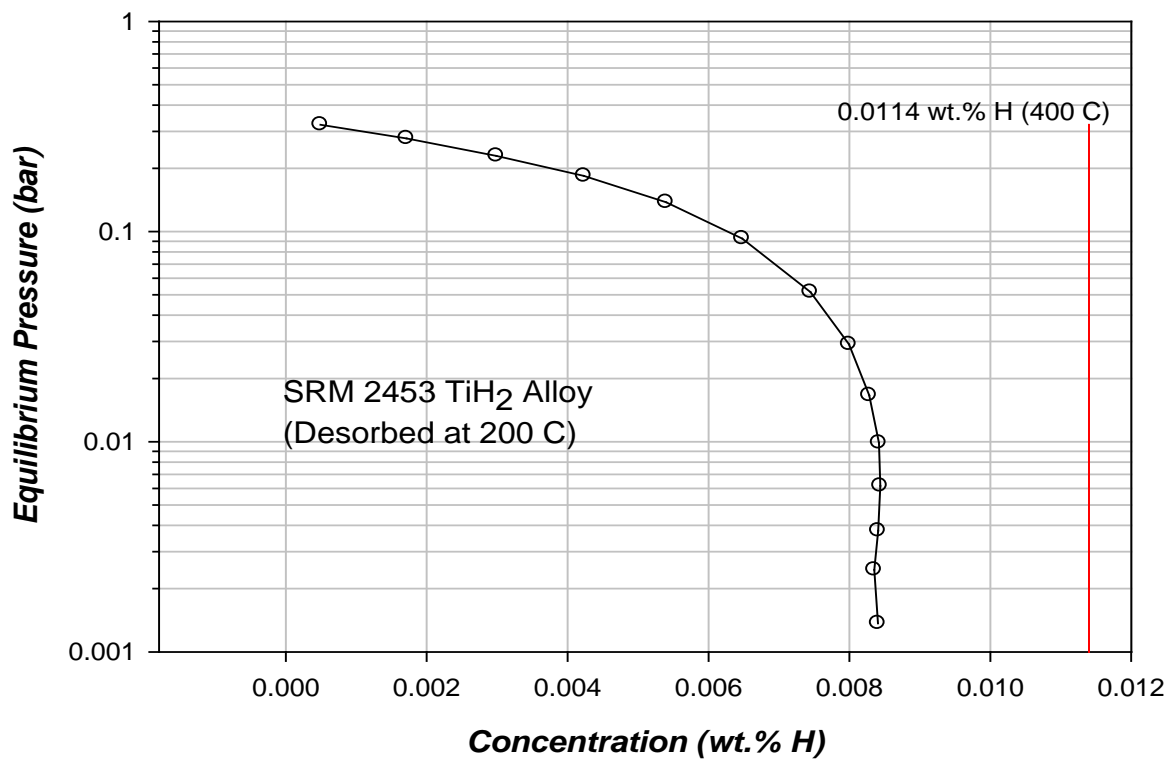


Figure 7. Example of reporting the desorbed capacity plot of a reference standard.

Revision Number	Effective Date	Description of Changes
0	6/16/04	Initial Revision.
1	02/06/06	Expanded details of procedures for sample loading, conditioning, analysis, and reprocessing of data; values and conditions to record manually in the LRB are noted; added illustrations to support procedures and data reporting.

Standard Operating Procedure

High-Pressure Thermogravimetric Analysis

Document No. 05064-0009

Rev. 1

Prepared By: _____ Date: 09/13/2004
Michael A. Miller, Manager-R&D

Approved By: _____ Date: _____

1. PURPOSE

- 1.1 To establish a standard procedure to study and quantitatively determine the intrinsic sorption properties of solid-state materials for the storage and release of hydrogen under precise thermodynamic conditions of temperature and pressure.
- 1.2 To derive the intrinsic hydrogen sorption properties of solid-state materials (test samples) from the adsorption and desorption isotherms, the uptake capacity, the kinetics for isothermal adsorption and desorption, the hysteresis in the isothermal adsorption and desorption cycle, and the enthalpy for adsorption.

2. SCOPE

- 2.1 Quantify the sorption properties of the sample, as noted above, using high-pressure thermogravimetric analysis techniques in accordance with necessary calibrations of instrument response; accounting for intrinsic hydrogen in sample and system, correcting for deviations from ideal gas behavior and buoyancy effects, and ensuring that the measurements are accurate and precise based upon reference standards.
- 2.2 This procedure assumes that the sample has undergone the necessary process steps to activate its chemical activity for hydrogen sorption in accordance with the requirements of the material. Should the sample require activation in accordance with the general procedure established under the present testing facility, SwRI Document No. 05064-0006 may be used for this purpose.

3. RESPONSIBILITIES

- 3.1 It is the responsibility of the Technical Manager to train the appropriate technical staff and certify competency in the procedures of this protocol and to make certain trained technical staff are following this procedure properly.
- 3.2 It is the responsibility of the trained technical staff to comply with this procedure when conducting laboratory studies.

4. REFERENCES

- 4.1 Puziy, A. M.; Herbst, A.; Poddubnaya, J.G.; and Harting, P., *Langmuir* **2003**, *19*, 314-320.
- 4.2 Rangarajan, B.; Lira, C.T.; Subramanian, R. *AIChE J.* **1995**, *41*, 838.
- 4.3 Benedict, M.; Webb, G.B.; Rubin, L.C. *J. Chem. Phys.* **1940**, *8*, 334.
- 4.4 Sircar, S. *AIChE J.* **2001**, *47*, 1169.

5. SAMPLES AND STANDARDS

- 5.1 Samples and standards will remain stored until time of analysis. The conditions under which the samples are stored are chosen based upon the class of material being evaluated. SwRI Document No. 05064-0007 will be followed to conform to the proper login,

storage, and chain of custody of samples. At the time of analysis, samples will be handled in accordance with the procedures of this document.

6. EQUIPMENT

- 6.1 Thermogravimetric analyzer (VTI, Inc / Rubotherm) enclosed in a controlled environment housing (glove box) consisting of a magnetically suspended electrobalance with 1 μg mass resolution and a 316 stainless steel reaction vessel. Sample and environment in reaction vessel are physically isolated from the microbalance components using a contactless magnetic coupling for vertical force measurements. Reaction vessel is compatible to pressures ranging UHV to 150 bar. Schematic of system is shown in Scheme 1.
- 6.2 Gas inlets for hydrogen and helium are connected to the UHP manifold, which is terminated at the instrument's gas inlets by a point-of-use purifier for each gas.
- 6.3 Quadrupole mass spectrometer (QMS, Pfeiffer Model ThermoStar) with heated fused silica capillary inlet.
- 6.4 High-pressure mass spectrometer capillary interface for thermogravimetric analyzer.
- 6.5 Microbalance (Mettler-Toledo, Model UMX-2), 0.1 μg mass resolution, located inside sample activation glove box of laboratory facility.
- 6.6 Sample activation glove box.
- 6.7 Sealable stainless steel transfer pig for transferring samples, standards, and sample baskets between glove box enclosures.
- 6.8 Stainless steel tweezers.
- 6.9 Stainless steel scoopula.
- 6.10 Aluminum weighing boats.

7. REAGENTS AND MATERIALS

7.1 Standards

- 7.1.1 Vanadium Hydride (VH_2), 99.998%, fine powder of known BET surface area.
- 7.1.2 Palladium Hydride ($\text{PdH}_{0.6}$), 99.998%, fine powder of known BET surface area.
- 7.1.3 Magnesium Hydride (MgH_2), 99.998%, fine powder of known BET surface area.
- 7.1.4 Titanium Hydride (TiH_2), 99.998%, fine powder of known BET surface area.
- 7.1.5 Calibrated leaks, hydrogen, 99.9998%, of predetermined leak rate.
- 7.1.6 Mass calibration leak.
- 7.1.7 All standards must be accompanied by a Certificate of Analysis (COA).

7.2 Reference Materials

7.2.1 Hyper-pure vapor grown silicon ingot, > 99.998%.

7.3 Source Gases

7.3.1 UHP hydrogen (from central gas manifold), < 1ppb of contaminant species, including water, oxygen, carbon monoxide, and carbon dioxide.

7.3.2 UHP helium (from central gas manifold), < 1ppb of contaminant species, including water, oxygen, carbon monoxide, and carbon dioxide.

7.3.3 UHP deuterium (D₂), < 1ppb of contaminant species, including water, oxygen, carbon monoxide, and carbon dioxide. Lecture bottle attached to auxiliary inlet tee at helium gas inlet of instrument.

7.4 Sample basket composed of a non-interacting, inert material (metal alloy, sapphire, quartz or glass) and of suitable dimensions.

8. **PROCEDURE**

8.1 Refer to SwRI Document No. 05064-0008 for proper procedures on weighing sample baskets and materials.

8.2 Weigh clean, empty sample baskets to 0.1 µg, as many as are needed, in the sample activation glove box enclosure using the UMX-2 microbalance. Record each weight.

8.3 Weigh-out a predetermined amount of each sample and reference standard(s) as needed onto a disposable aluminum weighing boat using the UMX-2 microbalance located inside the sample activation glove box. Record each weight.

8.4 Weigh the reference material ingot on a disposable aluminum weighing boat using the UMX-2 microbalance located inside the sample activation glove box. Record the weight.

8.5 Place pre-weighed sample baskets, samples, standards and reference material in the transfer pig.

8.6 Transfer the required samples, standards, reference material, sample baskets, tools and supplies into the glove box enclosure of the instrument as described in SwRI Document No. 05064-0007 (Test Article Login/Storage and Chain of Custody).

8.7 Verify that the glove box environment is below the maximum moisture and oxygen level requirements of operation as described in SwRI Document No. 05064-0007.

8.8 Purge and Evacuate (Helium)

8.8.1 Ensure that the electrobalance hanger is in the rest position before proceeding.

8.8.2 Mount the pre-weighed sample basket onto the electrobalance hanger and ensure that it meets the clearance requirements for the reaction vessel. Use tweezers for this procedure.

8.8.3 Carefully raise the reaction vessel over the basket to the connection point, secure and tighten the fitting to the required torque as specified in the instrument manual.

- 8.8.4 Determine the tare weight of the sample basket and zero the electrobalance.
- 8.8.5 Initiate helium purge/vacuum cycles of reaction vessel at elevated temperature (300°C) and at elevated static pressure soaks of 10 atm.
- 8.8.6 After the first helium purge/vacuum cycle, activate MS interface to begin sampling, monitoring, and recording gas composition using the Thermostar QMS. Use the multiple scan-analog mode of the QMS in this procedure.
- 8.8.7 Continue purge/vacuum cycles while monitoring gas composition with the QMS until helium gas purity is at least equal to the UHP source gas requirements for helium.
- 8.8.8 Deactivate MS interface.
- 8.8.9 Evacuate the reaction vessel and allow pressure to equilibrate to vacuum base pressure.
- 8.8.10 Cool the reaction vessel to 25°C while under vacuum and record weight changes of the sample basket during this procedure.
- 8.8.11 Open valve to calibrated leak and permit hydrogen to leak into the reaction vessel while under dynamic vacuum.
- 8.8.12 Activate MS interface.
- 8.8.13 Acquire and record multiple scans in the scan-analog mode to calibrate hydrogen signal intensity at a constant leak rate.
- 8.8.14 Close valve to calibrated leak.
- 8.8.15 Acquire and record multiple scans to determine hydrogen background signal intensity.
- 8.8.16 Change acquisition mode of the MS to intensity versus time, monitoring $m/z=2$ for hydrogen and setting the total number of acquisition cycles to > 100 .
- 8.8.17 Acquire and record intensity versus time data for approximately half the number of total acquisition cycles.
- 8.8.18 Open valve to calibrated leak and permit hydrogen to leak into the reaction vessel while under dynamic vacuum.
- 8.8.19 Continue to acquire and record intensity versus time data for the remainder of the acquisition cycles.
- 8.8.20 Close valve to calibrated leak.
- 8.8.21 Deactivate MS interface.
- 8.9 Purge and Evacuate (Hydrogen)
- 8.9.1 Repeat steps 8.8.5 through 8.8.10, using hydrogen source gas from the central manifold in place of helium.
- 8.10 Determination of Intrinsic Hydrogen (Optional)

- 8.10.1 Evacuate the reaction vessel and allow pressure to equilibrate to vacuum base pressure.
- 8.10.2 Cool the reaction vessel to 25°C while under vacuum and record weight changes of the sample basket during this procedure.
- 8.10.3 Isolate helium supply line to instrument helium gas inlet at valve Y-52 (manual valve immediately after gas purifier).
- 8.10.4 Evacuate the helium manifold of the instrument's internal gas delivery system starting from valve Y-52 (in the closed position) and allow system to equilibrate to the vacuum base pressure.
- 8.10.5 Open manual valve at helium inlet tee to deuterium cylinder and continue evacuation until vacuum base pressure is achieved.
- 8.10.6 Open valve to deuterium cylinder to pressurize system.
- 8.10.7 Dose reaction vessel with approximately 1 atm of deuterium, then close valve at helium inlet tee to deuterium cylinder.
- 8.10.8 Activate MS interface and acquire and record multiple scan-analog spectra to analyze gas composition in the reaction vessel, then deactivate MS interface.
- 8.10.9 Raise temperature of reaction vessel to 300°C and allow pressure, mass, and temperature to equilibrate.
- 8.10.10 Activate MS interface and acquire and record multiple scan-analog spectra to analyze deuterium exchange in the reaction vessel, monitoring the signal intensity of $m/z = 2, 3, 4, 18, 19,$ and 20.
- 8.10.11 Open helium supply line to instrument helium gas inlet at valve Y-52.
- 8.10.12 Repeat steps 8.8.5 through 8.8.9.
- 8.10.13 Cool the reaction vessel to 25°C while under helium purge.
- 8.11 Sample Buoyancy and Density Calibration (Helium Isotherm)
 - 8.11.1 This procedure may be conducted before or after PCT measurements of sample in hydrogen (see Section 8.10)
 - 8.11.2 Terminate helium purge and vent residual gas from the reaction vessel.
 - 8.11.3 Ensure that the electrobalance hanger and sample basket are in the rest position before proceeding.
 - 8.11.4 Unlock and lower reaction vessel from its connection fitting to expose sample basket.
 - 8.11.5 Remove sample basket from electrobalance hanger and place on a clean surface inside the glove box. Use tweezers for this procedure.
 - 8.11.6 Transfer the pre-weighed sample into the sample basket and remount sample basket onto electrobalance hanger using tweezers.

- 8.11.7 Carefully raise the reaction vessel over the basket to the connection point, secure and tighten the fitting to the required torque as specified in the instrument manual.
- 8.11.8 Determine the tare weight of the sample basket and sample combination, and zero the electrobalance.
- 8.11.9 Initiate evacuation cycle of reaction vessel.
- 8.11.10 Program a linear thermal ramp with a final thermal soak such that the highest soak temperature set-point is below the onset of thermal decomposition of sample, and does not exceed 400°C.
- 8.11.11 Initiate thermal ramp.
- 8.11.12 Activate MS interface and acquire and record multiple scan-analog spectra to analyze and monitor degas composition of the sample in the reaction vessel.
- 8.11.13 Continue evacuation of sample until equilibrium vacuum base pressure is achieved (a minimum of 4 hours).
- 8.11.14 Deactivate MS interface.
- 8.11.15 Cool the reaction vessel and sample to 25°C.
- 8.11.16 Program instrument parameters, as described in the instrument manual, to execute helium isotherm calibrations over the desired pressure and temperature (isothermal) regimes. This step may include a helium isotherm at 77 K to derive the density of the sample.
- 8.11.17 Initiate first helium isotherm calibration over the relevant pressure regime.
- 8.11.18 Continue helium calibration for the remaining isotherms in conformance with the objectives of the experiment.
- 8.11.19 Record mass changes as a function of time and pressure for each isotherm.
- 8.11.20 Upon completion of all helium calibration isotherms, initiate evacuation cycle of reaction vessel.
- 8.11.21 Evacuate the reaction vessel and allow pressure to equilibrate to vacuum base pressure.
- 8.11.22 Cool the reaction vessel to 25°C while under vacuum.
- 8.12 Pressure-Composition-Isotherm (PCT) Measurements of Sample
 - 8.12.1 Program instrument parameters, as described in the instrument manual, to execute PCT measurements for hydrogen in the forward and reverse direction of the desired pressure path and the desired temperature (isothermal) regime.
 - 8.12.2 At the MS computer console, program select times, if any, on which to activate the MS interface. Enter parameters to acquire and record multiple scan-analog spectra of the sample in the reaction vessel.

- 8.12.3 Initiate PCT run and activate MS interface for timed sequence if applicable.
- 8.12.4 Continue PCT measurements for the remaining isotherms in conformance with the objectives of the experiment.
- 8.12.5 Record mass changes as a function of time and pressure for each isotherm.
- 8.12.6 Upon completion of all PCT measurements, initiate evacuation cycle of the reaction vessel, then backfill reaction vessel with helium to atmosphere.
- 8.12.7 Terminate helium purge and vent residual gas from the reaction vessel.
- 8.12.8 Ensure that the electrobalance hanger and sample basket are in the rest position before proceeding.
- 8.12.9 Unlock and lower reaction vessel from its connection fitting to expose sample basket.
- 8.12.10 Remove sample basket from electrobalance hanger and place on a clean surface inside the glove box. Use tweezers for this procedure.
- 8.13 Helium Isotherm of Reference Material
 - 8.13.1 This procedure may be conducted before or after PCT measurements of sample in hydrogen.
 - 8.13.2 Repeat steps in Section 8.11 (inclusive of steps 8.11.2 through 8.11.20), substituting the reference material (pure silicon ingot) in place of the sample.
- 8.14 PCT Measurement of Reference Material
 - 8.14.1 This procedure should be conducted after the procedure described above (Section 8.13).
 - 8.14.2 Repeat steps in Section 8.12 (omitting step 8.12.2).
- 8.15 Data Processing
 - 8.15.1 The actual uptake of hydrogen in the sample is determined from the apparent measured uptake by one or more of three methods: 1) simple equation of state buoyancy correction from the helium isotherm for the sample; 2) determination of the Gibbs excess adsorption using the helium isotherm for the sample in combination with the Bender equation of state; and, 3) determination of the Gibbs excess adsorption using the low-temperature helium isotherm to determine the helium density of the sample, the hydrogen isotherm (PCT) for the sample, and the hydrogen isotherm for the reference material.
 - 8.15.2 Simple Equation of State (SEOS)
 - 8.15.2.1 Fit a first-order function (linear) to the weight versus pressure relationship for the helium isotherm data of the sample and derive the best-fit value for the slope this data.
 - 8.15.2.2 Correct the apparent weight of the PCT weight data for the sample using the following equation:

$$W_{corr} = W_a + \left(m_{He} \times P_s \times \frac{M_{H_2}}{M_{He}} \right)$$

W_{corr} = Corrected Weight
 W_a = Apparent Weight
 m_{He} = Slope of Helium Isotherm
 P_s = Pressure
 M = Molecular Weight

(1)

8.15.3 Gibbs Excess (Bender EOS)

8.15.3.1 The relationship between the mass measured by the instrument, corrected for the buoyancy of the gas, and the Gibbs excess adsorption of gas [4.1 – 4.3] can be described as follows:

$$W_a - W_{sb} \left(1 - \frac{\rho_b}{\rho_{sb}} \right) - W_s \left(1 - \frac{\rho_b}{\rho_s} \right) = V_{ad} (\rho_{ad} - \rho_b) \equiv G_{ex}$$

W_a = Apparent Weight
 W_{sb} = Weight of Sample Basket
 W_s = Weight of Sample
 V_{ad} = Volume of Adsorbed Phase
 G_{ex} = Gibbs Excess Adsorption
 ρ_b = Density of Bulk - Phase Gas
 ρ_{sb} = Density of Sample Basket
 ρ_s = Density of Sample
 ρ_{ad} = Density of Adsorbed Phase

(2)

8.15.3.2 Derive the density of the sample from the helium isotherm of the same. This value may also be treated as a fitting parameter in the subsequent fitting algorithm.

8.15.3.3 Calculate the bulk density of hydrogen for each pressure using the Bender EOS [4.1, 4.3]. In this equation, the coefficients entered into the equation are for hydrogen.

8.15.3.4 Determine the density of the adsorbed phase (ρ_a) by fitting the calculated Gibbs excess equation (from the fugacity relationship of the Bender EOS) to the experimentally measured Gibbs excess adsorption using nonlinear least-squares fitting algorithm. Adjust unknown parameters V_{ad} (the volume of the adsorbed phase), ρ_s (density of

sample), and U (the adsorption potential), so that algorithm converges to best-fit parameters.

8.15.3.5 Calculate the Gibbs excess adsorption from the fitting results.

8.15.4 Gibbs Excess (Reference Material)

8.15.4.1 Derive the density of the reference material from the helium isotherm of the same. For a pure reference material, the known chemical density of the material from literature data can be used in lieu of direct measurement.

8.15.4.2 Derive the density of the sample from the low-temperature (77 K) helium isotherm of the same.

8.15.4.3 The weight of the reference material that equates to the same volume as the adsorbent sample is given by the following equation:

$$W_s^R = W_s \frac{\rho_s^R}{\rho_s}$$
$$W_s^R = \text{Weight of Reference Material} \tag{3}$$
$$W_s = \text{Weight of Sample}$$
$$\rho_s^R = \text{Density of Reference Material}$$

8.15.4.4 The Gibbs excess adsorption (Equation 2) of gas in the sample is combined with the same for the reference material, wherein G_{ex} for the reference material is assumed to be zero, and Equation 3 is substituted into the result to give:

$$G_{ex} = W_a - W_s - W_a^R + W_s^R + \hat{K}_s^{He}$$
$$W_a^R = \text{Apparent Weight of Reference Material} \tag{4}$$
$$\hat{K}_s^{He} = \text{Correction Term (Henry's Law)}$$

8.15.4.5 Correction term in Equation 4 is not used if the real chemical density of the sample is known when used in Equation 3 [4.4].

8.15.4.6 Use correction term to account for the adsorption of helium in a porous sample and when the helium density of the sample is used in Equation 3.

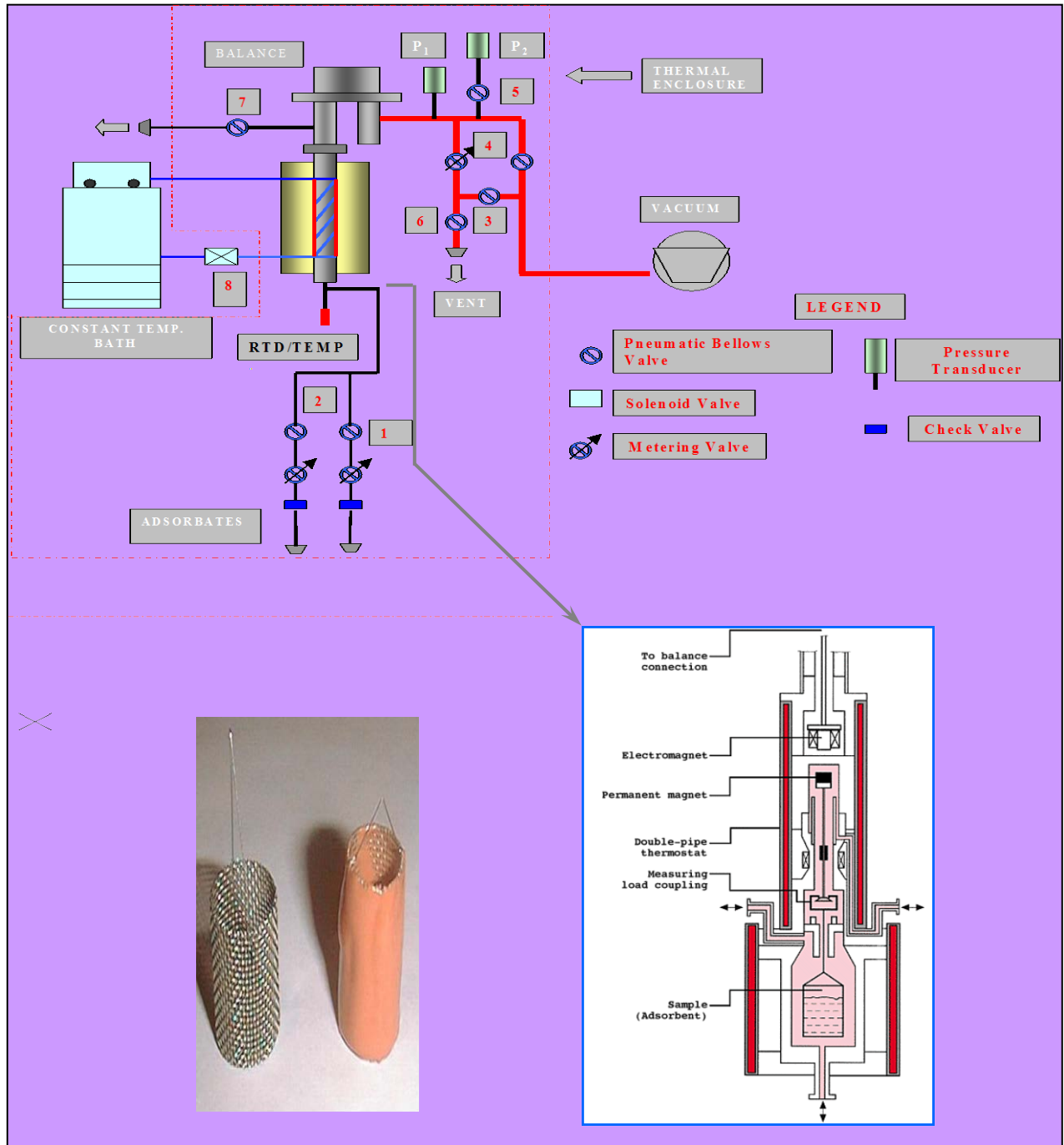
8.16 Determination of Accuracy and Precision (Reference Standards)

8.16.1 This procedure may be conducted at any time to check or verify the accuracy of gravimetric measurements.

8.16.2 Vent residual gas from the reaction vessel as needed.

8.16.3 Ensure that the electrobalance hanger and sample basket are in the rest position before proceeding.

- 8.16.4 Unlock and lower reaction vessel from its connection fitting to expose sample basket.
- 8.16.5 Remove sample basket from electrobalance hanger and place on a clean surface inside the glove box. Use tweezers for this procedure.
- 8.16.6 Transfer a pre-weighed reference sample into a clean sample basket and remount sample basket onto electrobalance hanger using tweezers.
- 8.16.7 Carefully raise the reaction vessel over the basket to the connection point, secure and tighten the fitting to the required torque as specified in the instrument manual.
- 8.16.8 Determine the tare weight of the sample basket and sample combination, and zero the electrobalance.
- 8.16.9 Initiate evacuation cycle of reaction vessel and allow system to reach equilibrium vacuum base pressure.
- 8.16.10 Program a linear thermal ramp with a final thermal soak such that the highest soak temperature set-point is below the onset of thermal decomposition of sample, and does not exceed 400°C.
- 8.16.11 Initiate thermal ramp.
- 8.16.12 Record mass changes as a function of time until absolute total mass readings reach steady-state conditions.
- 8.16.13 Calculate the total mass loss from the measured data and compare with the theoretical hydrogen content of the reference standard.
- 8.16.14 Repeat this procedure as necessary with additional reference standards.



Revision Number	Effective Date	Description of Changes
0	6/16/04	Initial Revision.
1	2/14/06	Removed requirement for low-temperature (77 K) helium isotherm to determine sample density (8.15).

Standard Operating Procedure

Laser Thermal Desorption Mass Spectrometry

Document No. 05064-0011

Rev. 1

Prepared By:

Michael A. Miller, Manager-R&D

Date: 09/13/2004

Approved By:

Date: _____

1. PURPOSE

- 1.1 To establish a standard procedure to study and quantitatively determine the intrinsic sorption properties of solid-state materials for the storage and release of hydrogen under precise thermodynamic conditions of temperature and pressure.
- 1.2 To quantify the intrinsic hydrogen storage capacity of nano-structured solid-state materials (test samples) using laser-induced thermal desorption mass spectrometry.

2. SCOPE

- 2.1 Quantify the hydrogen storage capacity of the sample, as noted above, in accordance with the necessary calibrations of instrument response; accounting for intrinsic hydrogen in sample and system, and ensuring that the measurements are accurate and precise based upon reference standards.
- 2.2 This procedure assumes that the sample has undergone the necessary process steps to activate its chemical activity for hydrogen sorption in accordance with the requirements of the material. Should the sample require activation in accordance with the general procedure established under the present testing facility, SwRI Document No. 05064-0006 may be used for this purpose.

3. RESPONSIBILITIES

- 3.1 It is the responsibility of the Technical Manager to train the appropriate technical staff and certify competency in the procedures of this protocol and to make certain trained technical staff are following this procedure properly.
- 3.2 It is the responsibility of the trained technical staff to comply with this procedure when conducting laboratory studies.

4. REFERENCES

- 4.1

5. SAMPLES AND STANDARDS

- 5.1 Samples and standards will remain stored until time of analysis. The conditions under which the samples are stored are chosen based upon the class of material being evaluated. SwRI Document No. 05064-0007 will be followed to conform to the proper login, storage, and chain of custody of samples. At the time of analysis, samples will be handled in accordance with the procedures of this document.

6. EQUIPMENT

- 6.1 Thermal Desorption Mass Spectrometer (SwRI) configured with a near-infrared (1080 nm) ytterbium fiber laser and optical bench for non-resistive, photon heating of sample. A quadrupole mass spectrometer (QMS) with a mass range of 1-400 amu, a 90° off-axis secondary electron multiplier detector, and a gas-tight electron impact ion source comprise the mass spectrometer sub-assembly of the system. An ultra-clean, Summa[®] passivated reaction vacuum chamber is coupled with the QMS system via a dual gate-valve interface with a selectable orifice for control of differential pressure. Turbomolecular pumps with dry backing pumps are used to maintain chamber and QMS sub-assemblies of system under high vacuum. Cryosorption pumps are used to achieve roughing pressures upon initial pump-down sequence. The laser heating sub-assembly provides three levels of thermal-feedback control depending on the combination of temperature regime and thermal resolution desired: 1) direct control of laser power; 2) secondary control of output beam via a motorized neutral density filter wheel; and, 3) secondary control via acousto-optic modulation of laser output beam. Low-temperature control of sample is afforded by a solenoid-actuated LN₂ cooling loop (cryo-cooler). An image of the system is shown in Figure 1.
- 6.2 Gas inlets for hydrogen and helium are connected to the UHP manifold, which is terminated at the instrument's gas inlets by a point-of-use purifier and a sub-atmospheric regulator for each gas.
- 6.3 Quartz crystal dosing valve to precisely control dosing gas leak rate.
- 6.4 Sample crucible consisting of high-purity quartz.
- 6.5 Internal laser beam-steering mirror assembly for sample crucible of reaction vacuum chamber (selected when sample volume is very small).
- 6.6 Internal hyperbolic laser mirror assembly for sample crucible of reaction vacuum chamber (selected when sample volume is > 200 μL).
- 6.7 Ultra-thin thermocouple for sample crucible assembly.
- 6.8 Microbalance (Mettler-Toledo, Model UMX-2), 0.1 μg mass resolution, located inside sample activation glove box of laboratory facility.
- 6.9 Sample activation glove box.
- 6.10 Sealable stainless steel transfer pig for transferring samples, standards, and sample crucibles between glove box and instrument.
- 6.11 Stainless steel tweezers.

6.12 Stainless steel scoopula.

7. REAGENTS AND MATERIALS

7.1 Standards

- 7.1.1 Vanadium Hydride (VH_2), 99.998%, fine powder of known BET surface area.
- 7.1.2 Palladium Hydride ($\text{PdH}_{0.6}$), 99.998%, fine powder of known BET surface area.
- 7.1.3 Magnesium Hydride (MgH_2), 99.998%, fine powder of known BET surface area.
- 7.1.4 Titanium Hydride (TiH_2), 99.998%, fine powder of known BET surface area.
- 7.1.5 Calibrated leaks, hydrogen, 99.9998%, of predetermined leak rate.
- 7.1.6 Mass calibration leak
- 7.1.7 All standards must be accompanied by a Certificate of Analysis (COA).

7.2 Source Gases

- 7.2.1 UHP hydrogen (from central gas manifold), < 1ppb of contaminant species, including water, oxygen, carbon monoxide, and carbon dioxide.
- 7.2.2 UHP helium (from central gas manifold), < 1ppb of contaminant species, including water, oxygen, carbon monoxide, and carbon dioxide.
- 7.2.3 UHP deuterium (D_2), < 1ppb of contaminant species, including water, oxygen, carbon monoxide, and carbon dioxide. Lecture bottle attached to auxiliary inlet tee at helium gas inlet of instrument.

8. PROCEDURE

- 8.1 Refer to SwRI Document No. 05064-0008 for proper procedures on weighing samples and materials.
- 8.2 Verify that the environment in the sample activation glove box is below the maximum moisture and oxygen level requirements of operation as described in SwRI Document No. 05064-0007.
- 8.3 Weigh-out a predetermined amount of each sample and reference standard(s) as needed into clean (thermally desorbed) quartz crucibles using the UMX-2 microbalance located inside the sample activation glove box. Record each weight.

- 8.4 Embed ultra-thin thermocouple into sample.
- 8.5 Place pre-weighed quartz sample crucibles, samples, standards and reference material in the transfer pig.
- 8.6 Transfer the required sample crucibles, samples, standards, and reference material from the glove box enclosure to the instrument as described in SwRI Document No. 05064-0007 (Test Article Login/Storage and Chain of Custody).
- 8.7 Chamber Evacuation and Thermal Desorption of Intrinsic Matter
- 8.7.1 This procedure assumes that the QMS system is already under vacuum and isolated from the reaction vacuum chamber via the dual gate-valve interface (both gates in the closed position).
- 8.7.2 Mount a clean, empty quartz sample crucible onto the optical heating assembly of the reaction vacuum chamber of the instrument.
- 8.7.3 Select and mount the appropriate internal laser mirror assembly depending on the sample volume to be analyzed in subsequent steps.
- 8.7.4 Align internal laser mirror assembly such that incident beam of Ytterbium fiber laser impinges on empty sample crucible. Use the safe laser-pointing device of laser system to accomplish this step.
- 8.7.5 Attach the thermocouple to the feedthrough connection.
- 8.7.6 Clean sealing surface of reaction vacuum chamber with low-particulate wipe and 2-propanol. Do the same to the gasket of the chamber lid, and then close the reaction vacuum chamber with the chamber lid. Make certain that lid is centered on sealing surface of chamber.
- 8.7.7 If turbo-pump servicing the reaction vacuum chamber is rotating (previously isolated from chamber by gate valve), achieve rough pressure ($\sim 10^{-3}$ Torr) in chamber using cryosorption pumps, then slowly open gate valve to turbo-pump. Otherwise, start turbo-pump sequence from the stopped state by first opening the gate valve to the chamber.
- 8.7.8 Continue evacuation of the reaction chamber until equilibrium high-vacuum base pressure ($< 10^{-6}$ Torr) is achieved (typically an overnight process).
- 8.7.9 Energize RF power, ion source, and SEM detector of QMS and adjust ion source and detector parameters as needed in accordance with instrument manual.
- 8.7.10 Open both gates of the dual gate-valve interface to QMS.

- 8.7.11 Acquire and record multiple scans in the scan-analog mode to obtain representative background spectra.
- 8.7.12 Program laser heating controller to execute a linear thermal ramp from room temperature to 400°C (or greater as needed) at an initial target rate of 2°/min (adjust rate as needed depending on the rate of intrinsic matter desorption) with a final soak of approximately 5 min as needed.
- 8.7.13 Initiate thermal ramp.
- 8.7.14 Acquire and record multiple scans in the scan-analog mode to obtain representative intrinsic desorption spectra at discrete times throughout the thermal ramp and at the thermal soak.
- 8.7.15 Terminate thermal ramp and allow sample crucible to cool to 25°C while under vacuum.

8.8 QMS Calibration

- 8.8.1 This procedure must be conducted after the steps described in Section 8.6 above.
- 8.8.2 Set acquisition mode of the QMS to multi-ion intensity versus time, monitoring $m/z=2, 4, 14, 18, 28,$ and 32 and setting the total number of acquisition cycles to 100.
- 8.8.3 Open valve to calibrated leak and permit hydrogen to leak into the reaction vacuum chamber while under dynamic vacuum.
- 8.8.4 Acquire and record intensity versus time data for approximately half the number of total acquisition cycles.
- 8.8.5 Close valve to calibrated leak.
- 8.8.6 Continue to acquire and record intensity versus time data for the remainder of the acquisition cycles.
- 8.8.7 Lower gate valve of the QMS interface configured with leak orifice (left side) into position.
- 8.8.8 Repeat steps 8.7.2 through 8.7.6.
- 8.8.9 Open gate valve configured with leak orifice (left side).
- 8.8.10 Manually set the laser heating controller to 150°C and allow sample crucible to reach thermal equilibrium.

- 8.8.11 Repeat steps 8.7.2 through 8.7.9.
- 8.8.12 Manually set the laser heating controller to 300°C and allow sample crucible to reach thermal equilibrium.
- 8.8.13 Repeat steps 8.7.2 through 8.7.9.

8.9 Determination of Intrinsic Hydrogen (Optional)

- 8.9.1 This procedure may be performed for an empty crucible or for a sample crucible, or both.
- 8.9.2 Cool the sample crucible to 25°C while under vacuum and allow system to reach vacuum base pressure.
- 8.9.3 Close both gate valves of QMS interface.
- 8.9.4 Open valve to deuterium cylinder.
- 8.9.5 Leak deuterium into the chamber using quartz crystal leak valve.
- 8.9.6 Lower gate valve to turbo-pump to achieve static base pressure.
- 8.9.7 Dose reaction vacuum chamber with approximately 1 millitorr of deuterium, then close valve quartz crystal leak valve and valve at deuterium cylinder.
- 8.9.8 Open gate valve of QMS interface (right side), and leave gate valve configured with leak orifice (left side) in place.
- 8.9.9 Acquire and record multiple scans in the scan-analog mode to obtain representative initial spectra.
- 8.9.10 Lower gate valve of QMS interface (right side).
- 8.9.11 Manually set the laser heating controller to 300°C and allow sample crucible to reach thermal equilibrium.
- 8.9.12 Open gate valve of QMS interface (right side), and leave gate valve configured with leak orifice (left side) in place.
- 8.9.13 Acquire and record multiple scan-analog spectra to analyze deuterium exchange in the reaction vacuum chamber, monitoring the signal intensity of $m/z = 2, 3, 4, 18, 19,$ and 20 .

- 8.9.14 Open gate valve to turbo-pump and allow system to reach dynamic vacuum base pressure.
- 8.9.15 Open both gate valves of QMS interface.
- 8.9.16 Acquire and record multiple scan-analog spectra to analyze deuterium exchange in the reaction vacuum chamber, monitoring the signal intensity of $m/z = 2, 3, 4, 18, 19,$ and 20.
- 8.9.17 Lower both gate valves of QMS interface.
- 8.9.18 Allow the sample crucible to cool to 25°C while under dynamic vacuum.

8.10 Thermal Desorption of Sample

- 8.10.1 Lower gate valve to turbo-pump and backfill the reaction chamber with UHP helium until chamber reaches atmospheric pressure.
- 8.10.2 Apply a thin film of 2-propanol to external crevice between the chamber lid gasket and the chamber, and then apply manual force to chamber lid to remove it.
- 8.10.3 Remove the empty quartz sample crucible from the optical heating assembly of the reaction vacuum chamber and replace it with a pre-weighed sample crucible.
- 8.10.4 Align internal laser mirror assembly such that incident beam of Ytterbium fiber laser impinges on center of sample. Use the safe laser-pointing device of laser system to accomplish this step.
- 8.10.5 Attach thermocouple to feedthrough connection.
- 8.10.6 Clean sealing surface of reaction vacuum chamber with low-particulate wipe and 2-propanol. Do the same to the gasket of the chamber lid, and then close the reaction vacuum chamber with the chamber lid. Make certain that lid is centered on sealing surface of chamber.
- 8.10.7 If turbo-pump servicing the reaction vacuum chamber is rotating (previously isolated from chamber by gate valve), achieve rough pressure ($\sim 10^{-3}$ Torr) in chamber using cryosorption pumps, then slowly open gate valve to turbo-pump. Otherwise, start turbo-pump sequence from the stopped state by first opening the gate valve to the chamber.
- 8.10.8 If sample has been pre-dosed (adsorbed) with gas in a separate step, start cryo-cooling sequence of sample immediately after achieving rough vacuum.

- 8.10.9 Continue evacuation of the reaction chamber until equilibrium high-vacuum base pressure ($< 10^{-6}$ Torr) is achieved (typically an overnight process).
- 8.10.10 Energize RF power, ion source, and SEM detector of QMS and adjust ion source and detector parameters as needed in accordance with instrument manual.
- 8.10.11 Open both gates of the dual gate-valve interface to QMS. If the rate of gas evolution from the thermal desorption run is expected to exceed the maximum set limits for total pressure of QMS, lower gate valve of the QMS interface configured with leak orifice (left side) into position.
- 8.10.12 Acquire and record multiple scans in the scan-analog mode to obtain representative background spectra.
- 8.10.13 Program laser heating controller to execute a linear thermal ramp from room temperature to 400°C (or greater as needed) at an initial target rate of 2°/min (adjust rate as needed depending on the rate of intrinsic matter desorption) with a final soak of approximately 5 min as needed.
- 8.10.14 Change acquisition mode of QMS to multi-ion intensity versus time mode and enter the appropriate number of total cycles (~5000 at 1 Hz). Set ion monitoring to $m/z=2, 4, 14, 18, 28,$ and 32, and other masses as needed.
- 8.10.15 Initiate thermal ramp.
- 8.10.16 Acquire and record multi-ion intensity versus time data.
- 8.10.17 Terminate thermal ramp and allow sample crucible to cool to a desired temperature while under vacuum.
- 8.10.18 Close both gate valves of QMS interface.
- 8.10.19 Leak UHP hydrogen into the chamber using quartz crystal leak valve.
- 8.10.20 Lower gate valve to turbo-pump to achieve static base pressure.
- 8.10.21 Dose sample in chamber with approximately 700 Torr of hydrogen, then close valve quartz crystal leak valve.
- 8.10.22 Start cryo-cooling sequence to rapidly lower temperature to ~77 K.
- 8.10.23 Achieve rough pressure ($\sim 10^{-3}$ Torr) in chamber using cryosorption pumps, then slowly open gate valve to turbo-pump to reach equilibrium vacuum base pressure.

- 8.10.24 Open gate valve of QMS interface (right side), and either leave gate valve configured with leak orifice (left side) in place or open depending on the expected rate of gas desorption.
- 8.10.25 Initiate thermal ramp.
- 8.10.26 Acquire and record multi-ion intensity versus time data.
- 8.10.27 Terminate thermal ramp and allow sample crucible to cool to to 25°C while under vacuum.
- 8.10.28 Close both gate valves of QMS interface.
- 8.10.29 Lower gate valve to turbo-pump and backfill the reaction chamber with UHP helium until chamber reaches atmospheric pressure.
- 8.10.30 Apply a thin film of 2-propanol to external crevice between the chamber lid gasket and the chamber, and then apply manual force to chamber lid to remove it.
- 8.10.31 Remove the sample crucible from the optical heating assembly of the reaction vacuum chamber.

8.11 Data Processing

- 8.11.1 For each calibration run of known leak rate, subtract the average background signal intensity ($m/z=2$) from the average signal intensity of the leak.
- 8.11.2 Calculate a calibration factor from the step above as follows:

$$CF = \frac{L_{H_2}}{(I_{H_2} - I_0)}$$

$$L_{H_2} = \text{Calibrated Leak Rate (moles/sec)} \quad (1)$$

$$I_{H_2} = \text{Average QMS Signal Intensity During Leak}$$

$$I_0 = \text{Average QMS Background Signal (no leak)}$$

- 8.11.3 Apply calibration factor to each measurement point of the desorption thermogram to generate a calibrated desorption thermogram in terms of desorption rate.
- 8.11.4 Integrate calibrated desorption thermogram to determine total hydrogen desorbed.

8.12 Determination of Accuracy and Precision (Reference Standards)

- 8.12.1 This procedure may be conducted at any time to check or verify the accuracy of thermal desorption mass spectrometry measurements.
- 8.12.2 Repeat steps in Section 8.10 starting from 8.10.3 to 8.10.18, omitting step 8.10.8.
- 8.12.3 Close both gate valves of QMS interface.
- 8.12.4 Lower gate valve to turbo-pump and backfill the reaction chamber with UHP helium until chamber reaches atmospheric pressure.
- 8.12.5 Apply a thin film of 2-propanol to external crevice between the chamber lid gasket and the chamber, and then apply manual force to chamber lid to remove it.
- 8.12.6 Remove the sample crucible from the optical heating assembly of the reaction vacuum chamber.
- 8.12.7 Calculate the total mass loss from the integrated pressure versus time data and compare with the theoretical hydrogen content of the reference standard.
- 8.12.8 Repeat this procedure as necessary with additional reference standards.

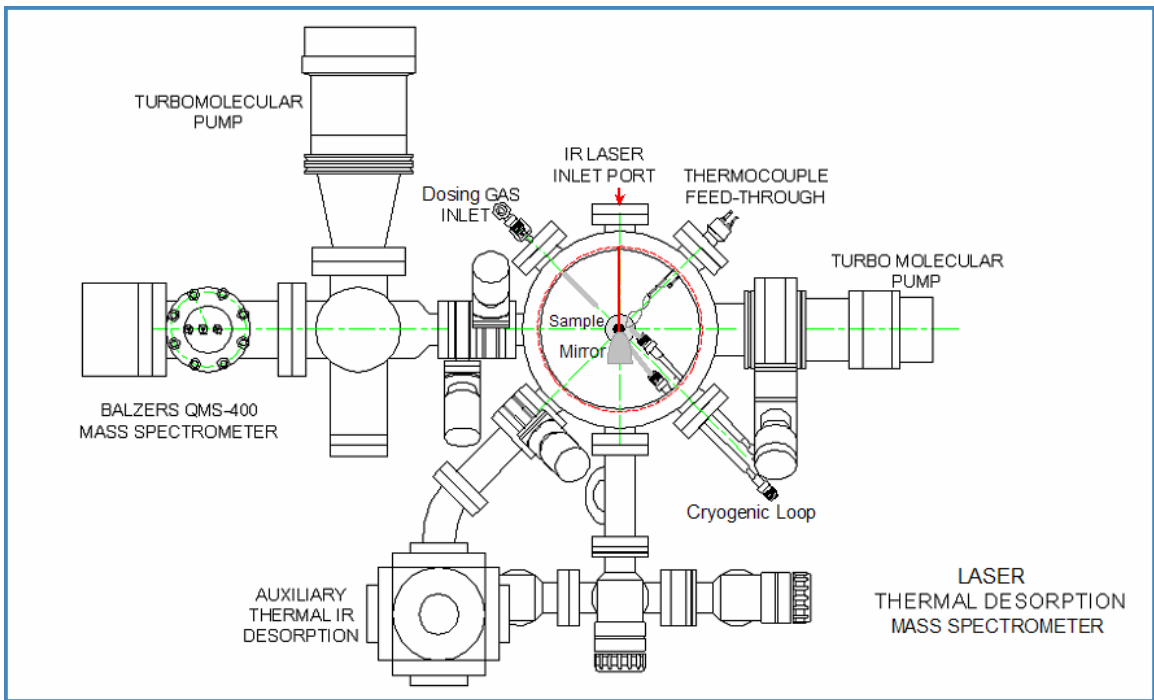


Figure 1a. Schematic of Laser-Induced Thermal Desorption Mass Spectrometer System.

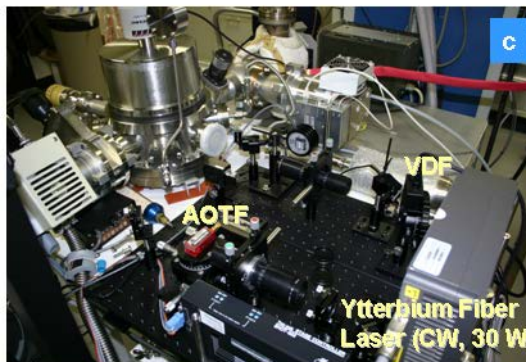
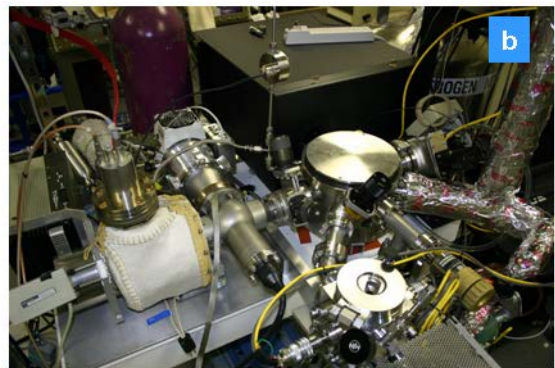
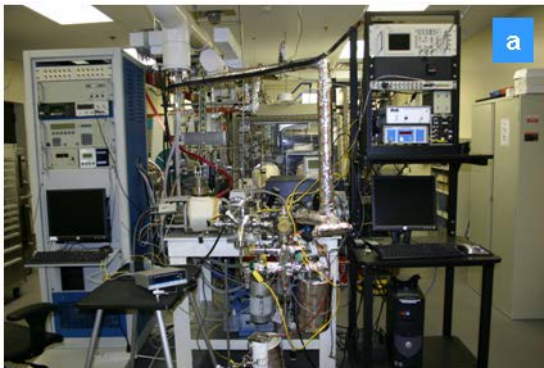


Figure 1b. Complete spectrometer system attached to an ultra-high purity gas manifold and electronic controls (a); vacuum chamber, QMS analyzer, and laser driver (b); optical bench for steering beam of laser through a variable density filter (VDF), acousto-optic tunable filter (AOTF), and collimating lenses before entering the sample chamber (c).

Revision Number	Effective Date	Description of Changes
0	6/16/04	Initial Revision.
1	2/14/06	Updated details of spectrometer system.